REGULATION OF Ca^{2+} INFLUX BY CELL SHAPE IN SWISS 3T3 CELLS

Thesis submitted in accordance with the requirements of the University of Liverpool for the degree of Doctor in Philosophy

Ying Shen

November 2010

DECLARATION

This thesis is the result of my own work. The material contained within this thesis has not been presented, nor is currently being presented, either wholly or in part for any other degree or qualification.

Ying Shen

Regulation of Ca^{2+} Influx by Cell Shape in Swiss 3T3 Cells

Abstract

It has been found that cell shape and Ca^{2+} influx are both important elements in regulating cell proliferation. When cells are prevented from spreading on a substrate, mitogen-stimulation is no longer able to promote proliferation and the influx component of the mitogen (bombesin)-evoked $[Ca^{2+}]_i$ response is lost (SOCE; Pennington et al., 2007). Since cell-shape-dependent Ca^{2+} influx plays an important role in the regulation of cell cycle, the regulation of this influx has been investigated.

In fura-2 loaded Swiss 3T3 cells, using large (ø45μm) and small (ø22μm) adhesive islands to control cell shape and the presence of cell-shape-dependent Ca^{2+} influx was confirmed. Influx occurred in cells on the large adhesive islands, but not in the cells on the small adhesive islands.

Also in fura-2-loaded fibroblasts, by substituting extracellular Ca^{2+} for Sr^{2+} and Ba^{2+}, it was suggested that the bombesin-evoked Ca^{2+} influx pathway shared Sr^{2+} and Ba^{2+} permeability characteristics that were most similar to those of ETYA, an arachidonic acid (AA) analogue, rather than to thapsigargin, an agonist evokes store-operated Ca^{2+} entry (SOCE; Foster, 2005). Due to the variability in the behavior of Ba^{2+} and Sr^{2+} fluxes, it was difficult to further characterize non-store operated Ca^{2+} entry (NSOCE) and SOCE using this approach. As a result, the involvement of AA in the mitogen-evoked Ca^{2+} influx is first studied. Cytoplasmic phospholipase A_2 ($cPLA_2$) is a Ca^{2+}-dependent enzyme that mediates agonist-dependent AA release in many cell types. The activation of $cPLA_2$ involves Ca^{2+}-dependent translocation of the enzyme from the cytosol to intracellular membranes and phosphorylation of the Ser^{505} residue (de Carvalho *et al.*, 1996). Immunofluorescence was used to determine whether changes in cell shape affect the distribution of phosphorylated $cPLA_2$ (phospho-$cPLA_2$; the activated form of $cPLA_2$) in 3T3 fibroblasts. In addition, mitogen-activated protein (MAP) kinases inhibitors (FR180204 & PD98059) which inhibit the phosphorylation of $cPLA_2$ were also used to examine the role of $cPLA_2$ in the bombesin-evoked Ca^{2+} influx pathway. The distribution of phospho-$cPLA_2$ was examined using a Leica AOBS scanning confocal microscope (excitation 488nm and emission 510-525nm). The results showed that there is a significant increase in the intensity of phospho-$cPLA_2$

immunofluorescence after the stimulation by bombesin (100nM) in normal spreading Swiss 3T3 cells. This increase in the intensity of phospho-$cPLA_2$ immunofluorescence was not affected when the cell spreading was restricted using small adhesive islands (ø22μM). Both FR180204 and PD98059 showed little inhibition on the increase in the intensity of phospho-$cPLA_2$ immunofluorescence. Additionally, they failed to inhibit the bombesin-evoked Ca^{2+} influx when the $[Ca^{2+}]_i$ responses were monitored using a PTI Ca^{2+} imaging system or a Flexstation plate reader. These findings suggest that $cPLA_2$ may not be required to activate the bombesin-evoked Ca^{2+} influx. Instead of $cPLA_2$, $iPLA_2$ may be important to this Ca^{2+} influx pathway since bromoenol lactone (BEL), an $iPLA_2$ inhibitor, effectively blocked the bombesin-evoked Ca^{2+} influx. Ca^{2+}-independent phospholipase A_2 is reported to generate AA (Atsumi *et al.*, 1998), but may also have other action that are critical to Ca^{2+} entry. It is believed to be a key component in the activation of SOCEs associated with (Ca^{2+} influx factor) CIF and stromal interacting molecule 1 (STIM1)-Orai (reviewed by Bolotina, 2008).

The participation of AA in the bombesin-evoked Ca^{2+} influx is further studied using AA inhibitors including two $cPLA_2$ inhibitors ($cPLA_2\alpha$ inhibitor & AACOCF3) and one DAG inhibitor (RHC80267). The results suggested that AA may still be involved in this Ca^{2+} entry. However, rather than $cPLA_2$, it may be generated through the DAG pathway.

The involvement of SOCEs is investigated. The use of a widely applied SOCEs inhibitor, SK&F96365, indicated that SOCEs play a role in this bombesin-evoked Ca^{2+} influx. The effect of cell shape on the activity of STIM1, a key component in SOCEs activation (Liou *et al.*, 2005), was then examined using mCherry- /YFP-STIM1 plasmids. Bombesin is able to induce the STIM1 puncta formation in unrestricted HeLa and Swiss 3T3 cells. However, bombesin is not as effective as thapsigargin in evoking STIM1 puncta. No clear bombesin-induced STIM1 puncta was observed in the shape-restricted Swiss 3T3 cells. The results indicated that the thapsigargin-induced STIM1 puncta formation is not cell-shape dependent. Thapsigargin is effective in promoting STIM1 puncta formation in shape-restricted cells. It remains a possibility that attenuation of puncta formation after stimulation by bombesin in the cell spreading-restricted cells underlines cell-shape-dependent Ca^{2+} influx.

Acknowledgements

I would like to firstly thank my supervisor, Dr Alec Simpson for all his help and support over the last 3 years. He gave a great help not just in the study but in adapting to the life abroad.

I would like also to thank Dr Helen Burrell and Dr Alex Laude. Helen helped me a lot during my PhD study, especially at the beginning of the research. Helen trained me to use the PTI Ca^{2+} imaging system and immunofluorescence techniques. Thanks to Alex for practical training, especially plasmid preparation, transfection and Flexstation operation.

I want to thank all the other members in the research group and staff in the Human Anatomy and Cell Biology department, for their kindness and help during my study.

Finally, a great thanks to my family for their support for my study in UK. I do appreciate my parents, without their help, I could not have finished the thesis.

Contents:

List of abbreviations:

2-APB	2-Aminoethoxydiphenylborne
AA	Arachidonic Acid
AACOCF3	Arachidonyl Trifluoromethyl Ketone
ACh	Acetylcholine
ADP	Adenosine Diphosphate
ARC channel	Arachidonic Acid-regulated Ca^{2+} Channel
ATM	ataxia-telangiectasia-mutated
ATP	Adenosine Triphosphate
ATR	ATM and Rad3-related
AVP	Arginine Vasopressin
Ba^{2+}	Barium ions
$[Ba^{2+}]_i$	Intracellular free Ba^{2+} Concentration
$BaCl_2$	Barium Chloride
BEL	Bromoenol Lactone
Ca^{2+}	Calcium ions
$CaCl_2$	Calcium Chloride
$[Ca^{2+}]_i$	Intracellular free Ca^{2+} Concentration
$[Ca^{2+}]_c$	cytosolic free Ca^{2+} Concentration
CAD	CRAC Activating Domain
cADPR	Cyclic Adenosine Diphosphate Ribose
CaLB domain	Ca^{2+}-dependent phospholipid binding domain
CaM	Calmodulin
CaMKII	Ca^{2+}/CaM-dependent Kinase II
CaMKs	Ca^{2+}/CaM-dependent Protein Kinases
cAMP	Adenosine 3',5'-cyclic Monophosphate
CBP/300	CREB Binding Protein/p300
CCE	Capacitative Ca^{2+} Entry (also termed SOCE)

CCh	Carbachol
CCK	Cholecystokinin
CDKs	Cyclin-dependent Kinases
CICR	Ca^{2+}-induced Ca^{2+} Release
cGMP	Cyclic Guanosine 3,5-monophosphate
ChK	Human Checkpoint Kinase
CHO cells	Chinese Hamster Ovary Cells
CIF	Ca^{2+} Influx Factor
CKIs	CDK Inhibitors
CO_2	Carbon Dioxide
COX	Cyclooxygenase
$cPLA_2$	Cytosolic Phospholipase A_2
CRAC	Ca^{2+} Release-activated Current
CRACM	Ca^{2+} Release-activated Ca^{2+} Channel Protein
CREB	cAMP Response Element-binding Protein
CSF	Colony-stimulating Factor
CYP450	Cytochrome P450
DAG	Diacylglycerol
DHP	1,4-dihydropyridine
DMEM	Dulbecco's modified Eagle's medium
DMSO	Dimethyl Sulfoxide
DNA	Deoxyribonucleic Acid
DREAM	Downstream Regulatory Element Antagonist Modulator
DT40 cells	Chicken DT40 B Lymphoma Cells
ECM	Extracellular Matrix
EDTA	Ethylenediaminetetraacetic Acid
EETs	Epoxyeicosatrienoic Acids
EGTA	Ethylene glycol Tetraacetic Acid
ER	Endoplasmic Reticulum

ERKs	Extracellular-regulated Kinases
ERM coiled-coil region	Ezrin/Radixin/Moesin Coiled-coil Region
ERM-like domain	Ezrin/Radixin/Moesin-like Domain
ETYA	5,8,11,14-eicosatetraynoic acid
FAs	Focal Adhesions
FCS	Fetal Calf Serum
FKBPs	FK506-binding Proteins
FN	Fibronection
Fura-2 AM	Fura-2-acetoxymethyl Ester
GFP	Green Fluorescent Protein
H^+	Hydrogen Ions
HBS	HEPES Buffered Saline
HEK293 cells	Human Embryonic Kidney 293 cells
HEPES	4-(2-hydroxyethyl)-1-piperazineethanesulfonic Acid
HVA	High-voltage Activated
I_{ARC}	Arachidonic Acid Regulated Ca^{2+} Current
I_{CRAC}	Ca^{2+}-release Activated Current
IFNγ	$Interferon_{\gamma}$
IP_3	Inositol 1,4,5-trisphosphate
IP_3Rs	Inositol 1,4,5-trisphosphate receptors
$iPLA_2$	Ca^{2+}-independent Phospholipase A_2
JNK	c-Jun N-terminal Kinases
KCl	Potassium Chloride
Kd	Dissociation Constant
kDa	KiloDalton
KH_2PO_4	Potassium Dihydrogen Phosphate
La^{3+}	Lanthanum Ions
LOE 908	(R,S)-(3,4-dihydro 6,7-dimethoxy-isoquinoline- i-yl)-2-phenyl-N,N-di-[2- (2,3,4-trimethoxy phenyl)ethyl]-acetamide

LOX	Lipoxygenase
LRD	Lipid Raft Domain
LVA	Low-voltage-activated
MAP kinase	Mitogen-activated Protein Kinases
MAPK	Mitogen-activated Protein Kinases
MEK	MAPK/ERK kinase
Mg^{2+}	Magnesium Ions
MgSO4	Magnesium Sulphate
Mn^{2+}	Manganese Ions
MOCCs	Mechanically-operated Ca^{2+} Channels
Na^{+}	Sodium Ions
NAD	Nicotinamide Adenine Dinucleotide
NAADP	Nicotinic Acid Adenine Dinucleotide Phosphate
NaCl	Sodium Chloride
NaH_2PO_4	Sodium Dihydrogen Phosphate
NCCE	Non-capacitative Ca^{2+} Entry (also termed NSOCE)
NFAT	Nuclear Factor of Activated T Cells
NFκB	Nuclear Factor kappa B
NSOCE	Non Store-operated Ca^{2+} Entry (also termed NCCE)
NSCCs	Non Selective Ca^{2+} Channels
OASF	Orai Activating Small Fragment
Orai	Ca^{2+} release-activated Ca^{2+} Channel Protein
PA	Phosphatidic Acid
PAF-AH	Platelet-activating Factor Acetlhydrolases
PBS	Phosphate Buffered Saline
PC-PLC	Phosphatidylcholine Specific-PLC
PGs	Prostaglandins
PI3K	Phosphoinositide 3-kinase
PIP_2	Phosphatidylinositolbisphosphate

PI-PLC	Phosphoinositide Specific-PLC
PKA	cAMP-dependent Protein Kinase
PKC	Protein Kinase C
PKG	cGMP-dependent Protein Kinase
PLA_2	Phospholipase A_2
PLC	Phospholipase C
PLD	Phospholipase D
PMCA	Plasma Membrane Ca^{2+} ATPase
polyHEMA	poly (2-hydroxyethyl methylacrylte)
PTKs	Protein Tyrosine Kinases
Rb protein	Retinoblastoma Protein
RBL cells	Rat Basophilic Leukemia Cells
RHC80267	1,6-di(O-(carbamoyl)cyclohexanoneoxime)hexane
R_{max}	Fura-2 Ratio 340/380 in Zero Ca^{2+}
R_{min}	Fura-2 Ratio 340/380 in Saturating Ca^{2+}
ROCCs	Receptor-operated Ca^{2+} Channels
ROCE	Receptor-operated Ca^{2+} Entry
RTK	Receptor Tyrosine Kinases
RyRs	Ryanodine Receptors
SERCA	Sarcoplasmic/Endoplasmic Reticulum Ca^{2+} ATPase
Sf9 cells	Spodoptera Frugiperda Cells
SF-DMEM	Serum Free-DMEM
SK&F96365	1-{beta-[3-(4-methoxyphenyl)propoxyl]-4-methoxyphenethyl}-1H-imida-zole
SOAR	STIM1 Orai Activating Region
SOCCs	Store-operated Ca^{2+} Channels
SOCE	Store-operated Ca^{2+} Entry (also term CCE)
SPCA	Secretory pathway Ca^{2+} ATPase
$sPLA_2$	Secreted PLA_2s

SPZN	Sulphinpyrazone
SR	Sarcoplasmic reticulum
Sr^{2+}	Strontium Ions
$SrCl_2$	Strontium Chloride
STIM	Stromal interacting molecule
TNF	Tumor Necrosis Factor
TPCs	Two-Pore Channels
TRP	Transient Receptor Potential
Trp3 protein	Transient Receptor Potential3 Protein
TRPC	Transient Receptor Potential Canonical
TRPM	Transient Receptor Potential Melastatin
TRPV	Transient Receptor Potential Vanilloid
$VO_3(OH)_2$	Orthovanadate
VOCCs	Voltage-operated Ca^{2+} Channels
VOCE	Voltage-operated/gated Ca^{2+} Entry

Chapter 1

General introduction

Contents: **page**

Figures:

1.1 Introduction

Cell proliferation is necessary for controlled growth, development, tissue maintenance and tissue repair. This involves the faithful replication of genome, organellogenesis and highly coordinated partitioning of the chromosome and organelles. Regulation of cell proliferation is essential to allow appropriate growth and development. Extracellular signals (*e.g.* growth factors) and environmental events serve to regulate this process. Deregulation of cell cycle is a key event in the development of various diseases, such as cancer, cardiovascular diseases and hyperplasias. Hence, it is important to study the mechanisms of cell cycle regulation.

1.2 The cell cycle

The cell cycle is the series of events that lead to cell replication. In eukaryotes cells, the cell cycle consists of two consecutive processes: interphase and mitosis (M) phase. During the interphase, cells grow in size, accumulate the nutrients needed for the mitosis and duplicate their DNA. This interphase stage is made up of 3 phases: G_1, S and G_2 (Figure 1.1, page 8). Cells increase in size in G_1 phase and prepare for the DNA replication during S phase, while the G_2 phase is a gap for the cell to prepare for mitosis (reviewed by Norbury and Nurse, 1992). Following the transition through G_2 phase, cell undergoes the M phase, which begins with mitosis. Mitosis is traditionally divided into four distinct phases, sequentially known as prophase, metaphase, anaphase and telophase. During the mitosis, the duplicated DNA is distributed to a pair of identical daughter nuclei. Once mitosis is completed, the second major process of M phase-cytokinesis splits the cell into two daughter cells, each with one nucleus. Cells that have temporarily or reversibly stopped dividing are said to have entered a state of quiescence called the G_0 phase (reviewed by Norbury and Nurse, 1992). The cell cycle is tightly regulated by series of checkpoints, such as DNA damage checkpoints and spindle checkpoints to detect possible defects. Once defects are detected, the cell cycle is arrested so that repair can take place (reviewed by Vermeulen *et al.*, 2003). Various extracellular signals also play an important role in coordinating the cell cycle progression. The mechanisms of cell cycle regulation are explained in sections 1.2.1-1.2.5.

1.2.1 Regulation of the cell cycle by intracellular checkpoints

The transition from one cell cycle phase to another occurs in a precise order and is regulated by

different cellular proteins. The key regulatory molecules are the cyclin-dependent kinases (CDKs). CDKs are serine/threonine protein kinases that are activated when associated with cyclins. Cyclins are a family of proteins that function as regulators of cell cycle progression (reviewed by Nigg, 1995; Murray, 2004). Multiple cyclins and CDKs have been identified. There are three interphase CDKs (CDK2, CDK4 and CDK6), a mitotic CDK (CDK1) and four main types of cyclins (cyclin A, cyclin B, cyclin D and cyclin E). When activated by a bound cyclin, CDKs activate or inactivate target proteins by phosphorylation to coordinate entry into the next phase of the cell cycle (Morgan, 1995). CDKs are constitutively expressed in cells whereas the concentration of cyclins varies at specific stages of the cell cycle, in response to various molecular signals (Figure 1.2, page 9). When the concentration is low, the cyclins disassociate from the CDKs, which inhibits the enzymatic function of CDKs.

Different cyclin-CDK complexes function at different phases and they are negatively regulated by various CDK inhibitors (CKIs) to ensure the correct timing and sequence of key steps required for cell division (Figure 1.1. page 8). When a defect is detected at a checkpoint of the cell cycle, CKIs can arrest the cell cycle through different signaling pathways. They bind to the CDK alone or the cyclin-CDK complex to regulate CDK activities. Two CKI families have been discovered: the INK4 family and the Cip/Kip family (reviewed by Sherr and Roberts, 1995). The INK4 family includes $p16^{INK4a}$ (p16), $p15^{INK4b}$ (p15), $p18^{INK4c}$ (p18), and $p19^{INK4d}$ (p19). The cip/kip family in contrast, includes the gene products from $p21^{Cip1/Waf1/Sdi1}$ (p21), $p27^{Kip1}$ (p27) and $p57^{Kip2}$ (p57). The INK4 family inhibits CDK4 and CDK6 activity during G1 phase specifically, whereas the Cip/Kip family can inhibit CDK activity during all phases of the cell cycle (reviewed by Sherr and Roberts, 1999).

After stimulation by a mitogenic signal, cyclin D is expressed and preferentially activates CDK4 and CDK6. This enables cells to enter the G_1 phase from G_0, starting the cell cycle progression. The cyclinD-CDK4/6 complex then enables the cell to pass the checkpoint in G_1 phase by phosphorylating and inactivating the retinoblastoma protein (Rb) (reviewed by Sherr, 1994). The Rb is a tumor suppressor pocket protein that is dysfunctional in many types of cancer. It prevents the cell from replicating damaged DNA by preventing progression through the cell cycle from G_1 into S (reviewed by Massague, 2004). When Rb is in an activated state (unphosphorylated), it

binds and inhibits transcription factors of the E2F family, and the resulting Rb–E2F interaction blocks the transcriptional activities of many important genes necessary for S phase (Dyson, 1998). Once Rb is phosphorylated by cyclinD-CDK4/6, it disassociates from E2F and enables the E2F dependent transcription of the cyclin E gene along with other components that support DNA replication (reviewed by Stevaux and Dyson, 2002). Cyclin E then activates CDK2 in late G_1. In addition, the cyclinE-CDK2 complex can further phosphorylate Rb, leading to the expression of additional genes necessary for DNA synthesis (Ohtani *et al.*, 1995; Harbour *et al.*, 1999). Both families of CKIs were reported to have a role in the G_1-S checkpoint. For instance, p16 can arrest the cell cycle at the G_1 phase by binding and inhibiting CDK4 and CDK6 to prevent the Rb phosphorylation (McConnell *et al.*, 1999; Thullberg *et al.*, 2000). P21 can arrest the cell cycle at the G_1 checkpoints when activated through the ataxia-telangiectasia-mutated (ATM)-p53 pathway triggered by damaged DNA. The ATM is one of a number of protein kinases that can recognize damaged DNA. Activated ATM phosphorylates p53, a tumor suppressor protein, which further leads to the activity of p21 (Siliciano *et al.*, 1997; Gartel and Tyner, 1999). Another Cip/Kip protein p27 is found to be effective in antagonizing the activity of cyclinE–CDK2 which may not be present in quiescent cells or in early G_1 phase (Coats *et al.*, 1996).

After the cell cycle enters S phase, cyclin E is degraded and cyclin A accumulates, which leads to an exchange of cyclin E with cyclin A in the CDK2 complexes (Girard *et al.*, 1991). Following S phase, cyclin A separates from CDK2 and associates with CDK1 promoting the entry into mitosis. The mechanism of S phase checkpoint is still poorly understand, while in the G_2/M phase, the cell cycle can be arrested by the ATM-dependent and other damaged DNA sensing manners, such as ATR (ATM and Rad3-related)-dependent pathway. For example, the human checkpoint kinase 2 (Chk2) and Chk1 which are activated by ATM and ATR respectively can phosphorylate and inhibit cdc25. Cdc25, a specific tyrosine phosphatase, its dysfunction can lead to the suppression of cyclin A/B-CDK1 complex and restraint of cell cycle in G_2/M phase (Karlsson-Rosenthal and Millar, 2006) In addition, the ATM-p53-p21 pathway is also capable of arresting the G_2 phase by sequestrating CDK1 in the cytoplasm and by inactivating cyclinB–CDK1 complexes, respectively (reviewed by Stewart *et al.*, 2003).

Finally, mitosis is regulated by cyclin B in complex with CDK1 (King *et al.*, 1994; Wheeler *et al.*, 2008). There is a spindle checkpoint during M phase which monitors the microtubule structure and chromosome attachments of the mitotic spindle and delays chromosome segregation during anaphase until defects in the mitotic spindle apparatus are corrected. More details on the spindle checkpoint is reviewed by Musacchio and Hardwick (2002).

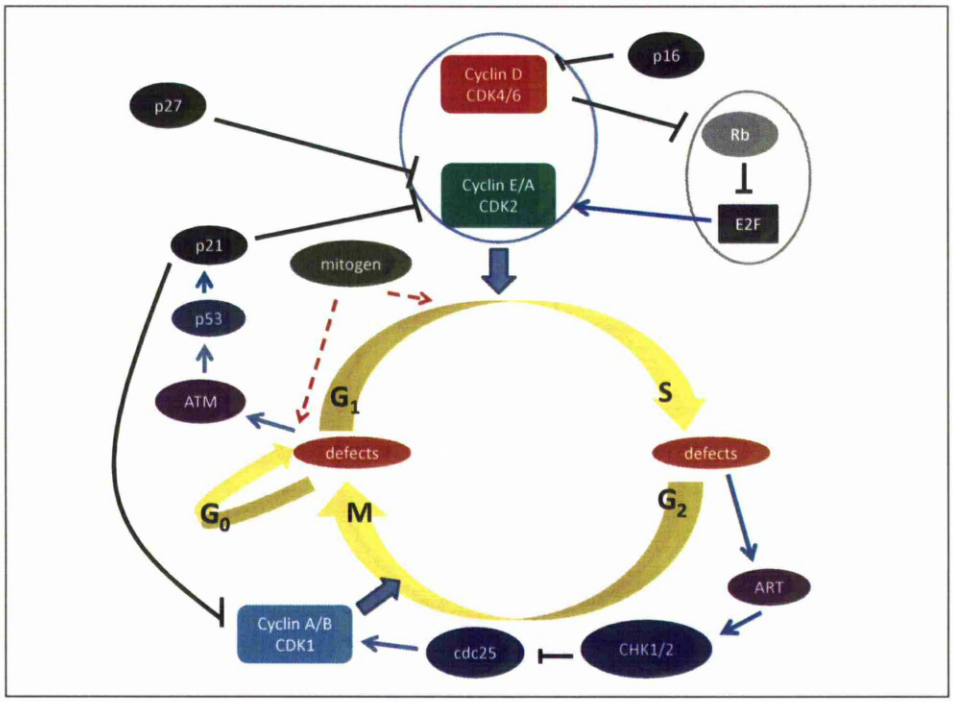

Figure 1.1-Regulation of checkpoints during cell cycle

The cell cycle progress of four distinct phases: G_1, S, G_2 and M phases. Cells that have temporarily or reversibly stopped dividing are said to have entered a state of quiescence called G_0 phase. Various positive and negative regulators are presented in this figure.

The figure is modified from 'G1 cell-cycle control and cancer' (Massague, 2004).

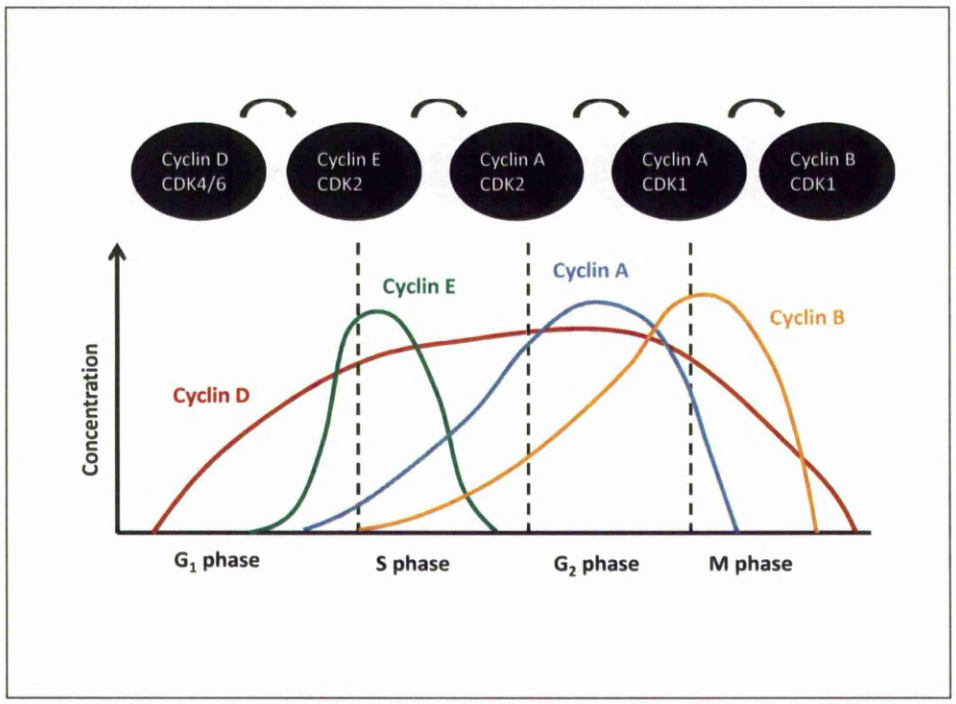

Figure 1.2-Expression levels of cyclins during cell cycle

Expression levels of 4 main cyclins (cyclin A, cyclin B, cyclin D and cyclin E) change during the cell cycle progression are shown in the figure. Different cyclin/CDK complexes function in different cell cycle phases.

1.2.2 The cell cycle and MAP kinase

Intracellular regulators are not sufficient to fully control cell cycle progression. Extracellular signals, which trigger and mediate these regulators, are required. Many cells remain in G_0 phase for long periods of time. The commencement of a cell cycle is triggered by mitogens which activate intracellular signaling cascades. These mitogens act to overcome the intrinsic inhibition of the restriction points in the G_1 phase (reviewed by Kahl and Means, 2003; Lipskaia and Lompre, 2004). Mitogens include a wide range of substances, such as growth factors, cytokines and many hormones (reviewed by Munaron *et al.*, 2004). They induce a series of intracellular signals either by binding to membrane or intracellular receptors and activate protein kinase C (PKC) via G protein-coupled receptors, receptor tyrosine kinases (RTK), or Raf kinases via the mitogen-activated protein (MAP) kinases (Figure 1.3, page 11). MAP Kinases, also described as extracellular-regulated kinases (ERKs), belong to a family of serine/threonine protein kinases. In mammalian cells, there are mainly two highly homologous MAP Kinases: p42 and p44, also called ERK2 and ERK1 respectively. As shown in figure 1.3, the RTK activated by the mitogen activates a GDP binding protein called Ras, which subsequently associates with the serine-threonine kinase Raf. Raf kinase phosphorylates and activates MAP kinase kinase kinases and MAP kinase kinases generally referred as MEKs. MEKs downstream phosphorylate and activate MAP Kinases. Phosphorylated MAP Kinases could translocate into the nucleus and there interact with different transcription factors (Avruch *et al.*, 2001). Previous works have shown that the Ras-regulated Raf-MEK-MAPK/ERK protein kinase cascade plays an important role in the control of cell proliferation and differentiation in both G_0/G_1 and G_1/S transitions (Lenormand *et al.*, 1993; Pages *et al.*, 1993). Ras itself induced several changes that promote G_1 arrest, including induction of p21, p15 and p16 (Dajee *et al.*, 2003). In addition, Ras was reported to induce nuclear factor (NF)-kB activity, a transcription factor which can suppress CDK4 in G_1 phase, through a pathway involving phosphoinositide 3-kinase (PI3K), Akt or PKC (Shirakawa and Mizel, 1989; Pan *et al.*, 1999; Madrid *et al.*, 2001; Dajee *et al.*, 2003) (Figure 1.3, page 11).

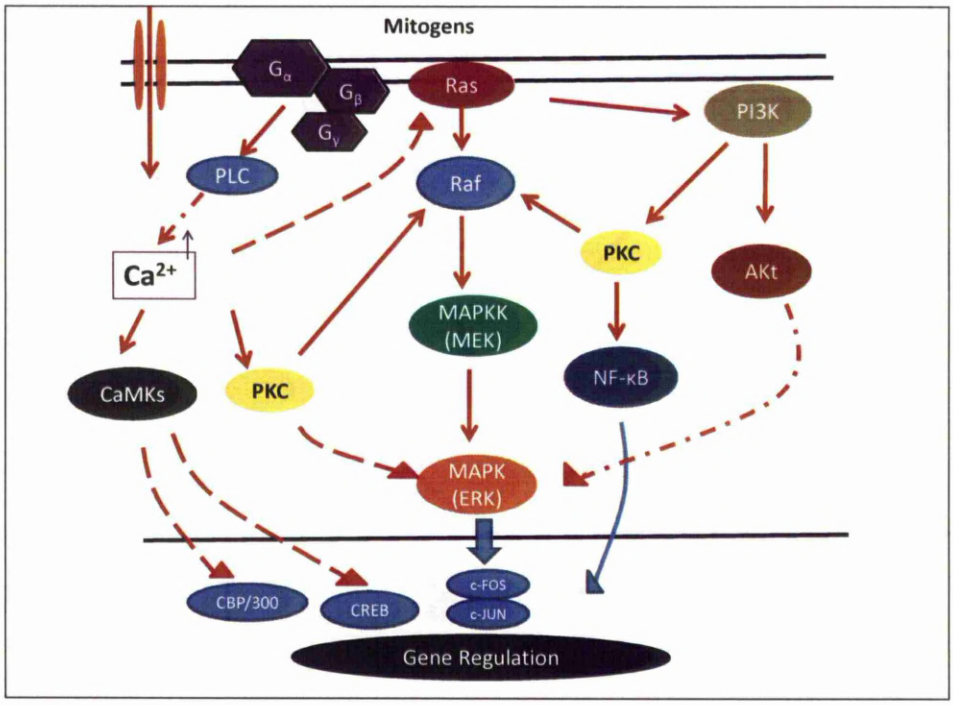

Figure 1.3- MAPK signaling pathways

Main MAPK signaling pathways, including Ras-MEK/MAPK pathway and MAPK-PI3K-AKt pathway, are shown in the figure. The downstream of these signal cascades results in the activation of various transcription factors, such as c-Fos, c-JUN, CREB which in turn regulate the cell cycle progression.

The figure is modified from '3-Hydroxyanthranilic acid inhibits PDK1 activation and suppresses experimental asthma by inducing T cell apoptosis'(Hayashi *et al.*, 2007)

1.2.2.1 Bombesin as a mitogen

Bombesin is an amphibian teradecapeptide first isolated from the skin of the European frog Bombina Bombina (Anastasi et al., 1971). The peptides of the bombesin family including gastrin-releasing peptide (GRP) and neuromedins are potent mitogens for a variety of cells (Wang *et al.*, 1996; Burdakov *et al.*, 2001). The function of bombesin was widely studied, especially in Swiss 3T3 cells (Rozengurt and Sinnett-Smith, 1983; Rozengurt and Sinnett Smith, 1987; Battey *et al.*, 1991). The mitogenic response induced by bombesin depends on its binding to specific, high-affinity G protein receptors, which distinguish bombesin from other growth factors.

Bombesin plays a role in the regulation of cell proliferation. A complex set of events can be triggered by bombesin. It induces the activation of both mitogen-activated protein (MAP) kinase pathway and epidermal growth factor (EGF) receptor (Igishi and Gutkind, 1998; Santiskulvong *et al.*, 2001). Bombesin evokes rapid activation of p42 and p44 in Swiss 3T3 cells (Withers *et al.*, 1995), that is completely dependent on PKC (Pang *et al.*, 1993) It also activates p42 and p74 through a PKC-independent pathway in Rat-1 cells (Charlesworth and Rozengurt, 1997). In addition, bombesin is able to stimulate DNA synthesis and cell division without the presence of other mitogens (Rozengurt and Sinnett-Smith, 1983). It can induce the expression of the nuclear transcription factors c-fos and c-myc (Rozengurt and Sinnett Smith, 1987).

It was reported that bombesin coupled with a G_q-like G proteins to elicit phospholipase C (PLC) mediated hydrolysis of phosphatidylinositolbisphosphate (PIP_2). This leads to a Ca^{2+} release from intracellular stores and the activation of PKC (Wang *et al.*, 1996; Rozengurt, 2007). The RyR receptors are also involved in bombesin-evoked Ca^{2+} response and may be required to produce cytosolic Ca^{2+} spiking (Burdakov *et al.*, 2001). It was suggested that, along with cholecysokinin (CCK), bombesin shares the ability to transfer a local Ca^{2+} signal to a global Ca^{2+} transients (Takahashi et al., 2000).

1.2.3 The cell cycle and Ca^{2+} signaling

One of the critical cascades of these mitogen evoked signaling pathways is the increase of

intracellular free Ca^{2+} ($[Ca^{2+}]_i$) which as a key second messenger further regulates the cell cycle progression. The increase of $[Ca^{2+}]_i$ is due to both the Ca^{2+} release from intracellular stores and the influx of extracellular Ca^{2+} through the plasma membrane. While the Ca^{2+} release is transient, the mitogen-induced Ca^{2+} influx is sustained and can last for 1 hour (Barbiero *et al.*, 1995). Many reports support the essential role of Ca^{2+} in cell cycle (Takuwa *et al.*, 1995; Whitaker and Larman, 2001). It is reported that G_0/G_1 and G_1/S transitions are sensitive to the Ca^{2+} pool depletion (Means, 1994). On the other hand, the presence of extracellular Ca^{2+} is required during the cell cycle progression, especially at some critical points, such as the G_0/G_1, G_1/S and G_2/M phases (Barbiero *et al.*, 1995; Bodding, 2001; Santella *et al.*, 2005). For instance, when proliferating fibroblasts are cultured in medium containing a low Ca^{2+} concentration media, they cease cellular division at the G_1 phase (Kahl and Means, 2003). It was also observed that blocking the Ca^{2+} influx with SK&F96365 results in the accumulation of cells in the G_2/M phases (Barbiero *et al.*, 1995).

Ca^{2+} elevation is transduced into cellular effects by either directly binding to target effectors or by binding to Ca^{2+} binding proteins, such as calmodulin (CaM). In mammalian cells, CaM is a highly conserved Ca^{2+} binding protein that contains four EF-hand Ca^{2+} binding motifs. The intracellular CaM level varies following cell cycle progression, and this affects the proliferative capacity of cells. It has been shown that CaM is required at two points of cell cycle: early after mitogen stimulation and near the G_1/S boundary (Chafouleas *et al.*, 1982; Rasmussen and Means, 1987). There are numerous enzymes which are targets of the Ca^{2+}/CaM complex which broadens the function of Ca^{2+}. Among them, the Ca^{2+}/CaM-dependent protein kinases (CaMKs) and the Ca^{2+}/CaM-dependent protein phosphatase 2B, calcineurin are two identified essential enzymes that mediate cell proliferation. In the early G_1 phase, inhibition of both CaMKs and calcineurin results in the accumulation of cells before the activation of cyclinD-CDK4. While at G_1/S boundary, CaMKs or calcineurin inhibitors could lead to p27 and p21 accumulation respectively, which arrests cell progression by blocking the expression of CDK2 (Kahl and Means, 2003). The mechanisms by which CaMKs and calcineurin regulate the cell cycle are complex and differ among cell types. So far, it has been demonstrated that the transcription factor adenosine 3',5'-monophosphate (cAMP) response element-binding protein (CREB) and CREB binding protein/p300 (CBP/300) signaling pathway is one of the models through which CaMKs participate

in mediating proliferation. Following the increase of $[Ca^{2+}]_i$, the activated CaMKs phosphorylate CREB and CBP/300 which promotes the transcription activity of p53 and p21 expression. On the other hand, calcineurin is most well characterized in term of its function in nuclear factor of activated T cells (NFAT) signaling. NFAT translocates into nucleus and regulates the transcription of cell cycle-related genes such as cyclin A, cyclin D, CDK4 and Rb (Baksh *et al.*, 2002; Caetano *et al.*, 2002; Neal and Clipstone, 2003). The translocation of NFAT is mediated by calcineurin and is dependent on the increase of $[Ca^{2+}]_i$. Besides, CaMKs and calcineurin have been reported to participate in the Ca^{2+} dependent MAPK-NFκB pathway which controls the cell cycle through transcriptional regulation of cyclin D1 during G_0/G_1 phase (See *et al.*, 2004). In addition to CaM, other Ca^{2+} sensors have been identified including downstream regulatory element antagonist modulator (DREAM) and S100B which can directly modulate transcription through interaction with a DNA promoter element or a transcription factor (Ikura *et al.*, 2002). For example, S100B, a Ca^{2+}-binding peptide, is suggested to interact with the p53 and inhibits both p53 by PKC (Delphin *et al.*, 1999). DREAM is an EF-hand Ca^{2+}-binding protein that represses transcription of c-fos genes (Mellström and Naranjo, 2001).

Despite a great deal of research into how Ca^{2+} controls the cell cycle, the bigger picture remain unknown. It is no doubt that Ca^{2+} is involved in more than one cell cycle regulation pathway since the mechanisms vary at different cell cycle transitions. Moreover, different cell types may have distinct Ca^{2+} dependent mechanisms.

1.2.4 The cell cycle and cell adhesion

In addition to mitogens and Ca^{2+}, cell adhesion to the extracellular matrix (ECM) is another equally important regulator for normal cell cycling. It is known that most normal mammalian cells start to proliferate only when they are attached to a substrate (Folkman and Moscona, 1978). For instance, the ECM has been proved to play a key role in modulating capillary endothelial (CE) cell sensitivity to soluble mitogens and, thereby, trigger and control their cell proliferation (Ingber, 1990).

The molecular mechanism of this adhesion-dependent growth control is still unclear. The

interaction of cells with the ECM is a dynamic process. The primary subcellular structures that mediate the regulatory effects of ECM adhesion on cell behaviour are the focal adhesions (FAs) (Chen *et al.*, 2003). Focal adhesions are macromolecular complexes that form regions where the surface of the cells come closest to the substrate. They regulate cell adhesion to the ECM by coupling integrins to the actin cytoskeleton. Integrins represent a family of heterodimeric cell surface proteins receptors that bind to ECM proteins, such as fibronection (FN; Ruoslahti, 1991). Cells have been observed to lose the ability to hyperphosphorylate Rb when they are coated on low FN density substrates (Ingber, 1990).

The key function of integrins is to promote cell adhesion and to transduce signals to the nucleus and enable gene expression by activating the intracellular pathways (Schwartz and Ingber, 1994). It was found that integrins could stimulate multiple early mitogen-induced events associated with transition from G_0 to G_1 phase of the cell cycle. These include expression of immediate early growth response genes (Huang and Ingber, 1999). Such adhesion-dependent control on the cell cycle process is believed to occur through the integrin-mediated activation of MAPK/ERK pathway which regulates the cell cycle (Morino *et al.*, 1995). The integrin binding appears to promote the transferring and propagation of signals to ERK pathways (Clark and Hynes, 1996; Lin *et al.*, 1997).

Studies using fibroblasts revealed that the adhesion to ECM controls entry into S phase as well. Unanchored fibroblasts remain arrested in mid-G_1 phase, whereas the same cells pass through this restriction point and enter S phase when allowed to reattach and spread on an ECM substrate. A decrease of the level of cyclin E or cyclin D and an increase of CDK inhibitor p27 and p21 was observed in different studies (Zhu *et al.*, 1996; Resnitzky, 1997; Huang and Ingber, 1999).

1.2.5 The cell cycle and cell spreading

Along with adhesion to the ECM, changes in cell spreading are also essential to cell cycle. The maintenance of cell shape and its spread relies on the attachment of integrins and the arrangement of the cytoskeleton. The cytoskeleton is composed of three major types of protein filaments, including microfilaments, microtubules and intermediate filaments. The

microfilaments are polymers of actin. They constitute the actin cytoskeleton together with a large number of actin-binding and associated proteins. The actin cytoskeleton is essential for the modulation of cell shape (Hay, 2005).

There are mainly two ways to manipulate the cell shape and control the spreading in studies on cell shape. One method is to restrict spreading using a non-adhesive polymer called poly (2-hydroxyethyl methylacrylate) (polyHEMA). Varying concentrations of polyHEMA have been used (Folkman and Moscona, 1978). Cells attached but did not spread on thick layers of high concentration polyHEMA while they attached and spread on a thin layer of low concentration polyHEMA. This method has been modified by growing cells on a defined area of palladium-substratum surrounded by non-adhesive polyHEMA over which the cells cannot spread (Ireland *et al.*, 1987). These areas of palladium-substratum are called adhesive islands. Another widely used method to prevent cell spreading is to disrupt the actin cytoskeleton using drugs, such as cytochalasins and jasplakinolide (Huang and Ingber, 2002).

It has been shown that restricting cell spreading with adhesive islands of ø22μm and ø45μm prevents S phase entry (Ireland *et al.*, 1987; Pennington *et al.*, 2007). While ECM and growth factor signals trigger the cell to pass through the G_0/G_1 phase, they are not sufficient to promote the progression to S phase when the actin cytoskeleton is disrupted (Huang and Ingber, 1999).

In summary, restricting the cell spreading by culturing the cells on small adhesive islands or disrupting the cell cytoskeleton by drugs prevent S phase entry, but how cell shape controls the cell growth remains obscure. So far, it has been found that preventing cell spreading failed to increase cyclin D levels or down-regulation of p27 and the cells are arrested in late G_1 before Rb checkpoint (Huang *et al.*, 1998).

1.3 Ca^{2+} signaling

The intracellular Ca^{2+} ($[Ca^{2+}]_i$) is a critical signal that regulates various cellular activities from the rapid responses such as contraction and secretion to long-term regulation of transcription, growth, and cell division, as reviewed by Potier and Trebak (2008). Changes of $[Ca^{2+}]_i$ level are

tightly controlled by complex interactions among ion channels, transporters, pumps and binding proteins. The resting level of $[Ca^{2+}]_i$ is normally maintained in the range of around 100nM. To maintain this low concentration, Ca^{2+} is actively pumped from the cytosol and accumulated in the intracellular stores, such as the endoplasmic reticulum (ER) or sarcoplasmic reticulum (SR), and sinks such as mitochondria. Signaling occurs when Ca^{2+} is stimulated to enter from the outside through the plasma membrane or to be released from the ER/SR. The level of $[Ca^{2+}]_i$ normally rises to 500–1,000nM after the stimuli. Most of the increased $[Ca^{2+}]_i$ binds to buffers, whereas a small proportion binds to the effectors that activate and mediate a large number of cellular processes (Berridge *et al.*, 2003).

The properties of Ca^{2+} signals are quite diverse and can be local or global, transient or sustained. Local Ca^{2+} signals occur when the Ca^{2+} concentration is elevated within restricted microdomains at the mouth of channels or when larger subcellular Ca^{2+} signals span several micrometers (Bootman *et al.*, 2001). They can be generated by opening the channels located either in the plasma membrane or in the Ca^{2+} store membrane as long as the stimulus is sufficiently small (Cancela *et al.*, 2002). For instance, Ca^{2+} "blips" are signals that are caused by the opening of the inositol 1,4,5-trisphosphate receptors (IP_3Rs) while "quarks" are the result of the opening of ryanodine receptors (RyRs) (reviewed by Webb and Miller, 2003). More details of the IP_3Rs and RyRs are described in section 1.4. Local Ca^{2+} signals can last for up to 200ms and have an amplitude less than 30nM depending upon the cytosolic environment, spread for no more than a couple of micrometers (reviewed by Laude and Simpson, 2009). The amplitude of Ca^{2+} signaling events including Ca^{2+} "puffs" or "sparks" form from the coordinated Ca^{2+} release from a population of IP_3Rs or RYRs respectively. These two events can spread no more than 6μm, possess a typical amplitude of up to 200nM and last for no longer than 500ms (reviewed by Laude and Simpson, 2009). Since such signals can remain localized and activate effectors within a particular region, it is believed that local Ca^{2+} signals serve to activate specific targets to regulate different events via Ca^{2+} passage through different channels (Bootman *et al.*, 2001; Taylor *et al.*, 2009).

Local Ca^{2+} signals can transform into global Ca^{2+} signals in different ways. A higher agonist

concentration is one of the causes. For example, low concentration of acetylcholine (ACh) or CCK generates local Ca^{2+} signals whereas higher concentration causes global Ca^{2+} signals (Cancela *et al.*, 2002). In addition, Ca^{2+}-induced Ca^{2+} release (CICR) is another way to transform a local Ca^{2+} signal into a global wave (Cancela *et al.*, 2002). One of the global Ca^{2+} signals, a Ca^{2+} wave, was observed to be generated by the recruitment of various local Ca^{2+} signals, starting from a restricted region of the cell. This then propagates, leading to a global Ca^{2+} wave (Boittin *et al.*, 1999; Dumollard *et al.*, 2002). Ca^{2+} waves can then pass through the cell and spread to other cells if they are connected.

Ca^{2+} oscillations are another well studied global Ca^{2+} signal which has been seen in many, if not all, types of cells (Fewtrell, 1993). The term oscillation refers to all fluctuations in Ca^{2+} whether these appear as regular fluctuations about a mean value (sinusoidal oscillations) or occur as discrete transients arising from a constant resting level (transient oscillations; Berridge, 1990). There are numerous speculations about the role of oscillations, especially in the non-excitable cells. A widespread theory is that oscillations permit a smoothly graded input to be translated into a digital all-or nothing signal in which the information is robustly encoded in the timing rather than the amplitude of pulses. Oscillations allow Ca^{2+} signals to regulate various processes via timing and frequency in different patterns (Lewis and Cahalan, 1989; Bhakta *et al.*, 2005).

The generation and modulation mechanisms of oscillations have been extensively studied. In the excitable cells, oscillations usually arise from the Ca^{2+} entry from outside through the voltage-gated channels. In non-excitable cells, oscillations can be generated in receptor-controlled models mainly relying on the IP_3Rs (Berridge, 1990).

All these Ca^{2+} signals are important parts of the Ca^{2+} homeostasis system, which is sustained by extracellular Ca^{2+} influx along with Ca^{2+} release from intracellular stores. They will be discussed in section 1.4 to 1.6.

1.4 Intracellular Ca^{2+} release

1.4.1 Ca^{2+} stores

Various intracellular Ca^{2+} stores play both a structural and dynamic role in Ca^{2+} homeostasis. Due to a large number of immobile Ca^{2+} binding sites in the cytosol, the diffusion of cytosolic Ca^{2+} ($[Ca^{2+}]_c$) is slower than other second messengers. The elevation of $[Ca^{2+}]_c$ by the influx from the outside is insufficient to fulfill all its diverse functions. The existence of widely distributed and rapid by mobilizable intracellular Ca^{2+} stores facilitate the diffusion of Ca^{2+} and, moreover, permit the generation of local Ca^{2+} signals. These may be initiated at a distance from the plasma membrane. More importantly, the Ca^{2+} stores sequester Ca^{2+} to keep a low level of $[Ca^{2+}]_c$ after the Ca^{2+} transient has occurred (Pozzan *et al.*, 1994). So far, the most prevalent Ca^{2+} stores or sinks are ER/SR, mitochondria and Golgi.

The ER contains the rapidly exchanging Ca^{2+} pools in non-excitable cells while the SR functions in muscle cells (Pozzan *et al.*, 1994). They accumulate Ca^{2+} via the sarcoplasmic/endoplasmic reticulum Ca^{2+} ATPase (SERCA) pumps and release it through IP_3Rs and RyRs. The ER/SR is physically continuous and spatially and functionally heterogeneous. Many Ca^{2+} binding proteins are unevenly distributed in ER. These include calsequestrin and calretiulin which function as major Ca^{2+} buffers. The concentration of Ca^{2+} inside the ER varies from micromolar to near millimolar concentration. Generally values of at least 100μm are seen when the store is Ca^{2+} loaded and a number of reports suggest that concentration of Ca^{2+} inside the ER is between 400 and 800μm (reviewed by Laude and Simpson, 2009).

Mitochondria sequester Ca^{2+} via a low-affinity, high-speed uniporter powered by the mitochondrial membrane potential. It was reported that the mitochondrial Ca^{2+} uptake was stimulated by IP_3-evoked Ca^{2+} release, capacitative Ca^{2+} entry (Section 1.6), and Ca^{2+} leaking from the ER. The amplitude of $[Ca^{2+}]_i$ signals is also a determinant of mitochondria Ca^{2+} accumulation (Collins *et al.*, 2001). Due to these special properties, mitochondria can dampen and prolong the $[Ca^{2+}]_i$ responses (reviewed by Laude and Simpson, 2009).

The Golgi is another IP_3-sensitive Ca^{2+} store. This IP_3-mediated Ca^{2+} release is slower than that

from the ER (Pinton *et al.*, 1998). It accumulates Ca^{2+} via SERCA pumps and also the secretory pathway Ca^{2+}ATPase (SPCA; Pinton *et al.*, 1998). In addition (reviewed by Rizzuto and Pozzan, 2006), other various compartments such as acidic endosomes, lysosomes and secretory granules can accumulate Ca^{2+} as well.

1.4.2 Different Ca^{2+} release mechanisms

It has been revealed that ER/SR can release Ca^{2+} through various different membrane channels. The IP_3Rs and RyRs are two major Ca^{2+} channels regulating Ca^{2+} release from ER/SR. These two receptors are sensitive to different messengers. For example, IP_3Rs can be activated by IP_3 while the RyRs can be triggered by cyclic adenosine diphosphate ribose (cADPR). Significantly both also operate by Ca^{2+}-induced Ca^{2+} release (CICR). This is the primary trigger of Ca^{2+} release via RyRs (Endo, 1977). In addition, nicotinic acid adenine dinucleotide phosphate (NAADP) has been reported to cause Ca^{2+} release in a distinct way. All these multiple messengers modulate Ca^{2+} release in different ways and produce specific Ca^{2+} signals responding to different stimuli. There is also believed to be a hierarchy of Ca^{2+} release in which trigger events initiate further release (Bootman *et al.*, 1997; Huser and Blatter, 1997).

1.4.2.1 IP_3 sensitive Ca^{2+} release

IP_3R is a tetramer of about 260 kilodalton (kDa) subunits. The receptor is expressed in abundance in the ER (reviewed by Tsien and Tsien, 1990). At least three different isoforms have been identified in mammalian cells, and there may exist in heterotetramers (Dawson, 1997).

The IP_3R enables Ca^{2+} influx due to its sensitivity to IP_3. The role of IP_3 on Ca^{2+} release was first reported in 1980s (Streb *et al.*, 1983). Since then, many cell types were observed to demonstrate IP_3-induced Ca^{2+} release. IP_3 is generated as a consequence of an agonist binding to cell surface receptors resulting in activation of G-proteins or certain tyrosine kinases. They in turn activates enzyme PLC, which catalyzes the hydrolysis of PIP_2 into IP_3 and diacylglycerol (DAG; Lee and Rhee, 1995) (Figure 1.5, page 41). IP_3 triggers the Ca^{2+} release by activating the IP_3Rs in ER. In addition, IP_3 can cause Ca^{2+} release from the Golgi and some other secretory granules as well (Pinton *et al.*, 1998).

IP_3R as a Ca^{2+} release channel in the ER Ca^{2+} store is regulated by a number of ligands, including the most important ones IP_3 and Ca^{2+}. These ligands regulate the IP_3R activity mainly by modifying the sensitivity of the channels to Ca^{2+} regulation.

The IP_3-gated Ca^{2+} release plays a crucial role in the generation of Ca^{2+} signals including oscillations and waves (Berridge, 1990). IP_3R exhibits very complicated properties. Generally, Ca^{2+} regulates steady-state IP_3R channel gating with a biphasic concentration-dependence: Ca^{2+} at low concentrations activates the channel, whereas at higher concentrations, Ca^{2+} inhibits the channel (reviewed by Foskett *et al.*, 2007). This biphasic effect of $[Ca^{2+}]_c$ on IP_3Rs provides the key to understanding the oscillatory behaviour. Most IP_3Rs become more sensitive to IP_3 as the $[Ca^{2+}]_c$ is modestly increased, which leads to CICR. While the $[Ca^{2+}]_c$ increases further, IP_3Rs are then inhibited. It is argued that IP_3Rs are ideal for CICR, since in the presence of IP_3, a small increase of $[Ca^{2+}]_c$ is able to trigger Ca^{2+} release via the IP_3Rs (Foskett *et al.*, 2007). A possible mechanism for these effects is that: a IP_3R is inhibited by Ca^{2+} without IP_3 bound, but after IP_3 binding the inhibitory Ca^{2+}-binding site is concealed and a stimulatory Ca^{2+}-binding site is exposed, allowing Ca^{2+} to promote channel opening (Adkins and Taylor, 1999; Taylor and Laude, 2002).

IP_3Rs work in a complex way. In addition to ligands, they are also regulated by phosphorylation by various kinases. As reviewed by Foskett *et al.* (2007), these kinases include cAMP-dependent protein kinase (PKA), cyclic guanosine 3,5-monophosphate (cGMP)-dependent protein kinase (PKG), Ca^{2+}/CaM-dependent kinase II (CaMKII), PKC and various protein tyrosine kinases (PTKs).

1.4.2.2 RyRs sensitive Ca^{2+} release

The RyRs were first identified in skeletal muscle cells (Endo, 1977). So far, three mammalian RyRs subtypes have been defined (RyR1, RyR2 and RyR3). The RyRs are expressed in a variety of tissues (Fill and Copello, 2002). The RyR1 protein is the predominant isoform in skeletal muscle cells while the RyR2 protein is the most abundant isoform in cardiac muscle cells and the RyR3 is expressed more widely, but especially in the brain (Zucchi and Ronca-Testoni, 1997; Fill and Copello, 2002). They may co-exist with IP_3Rs in the same cells.

The study of the RyRs has focused on its role in muscle cells. In striated muscles, RyRs are responsible for regulating Ca^{2+} release from the SR in order to trigger contraction. this occurs through a mechanism called "excitation-contraction coupling" (Rossi and Sorrentino, 2002). RyRs are also thought to be involved in CICR with a bell-shaped relationship with Ca^{2+} (Chen *et al.*, 1992), which will be discussed in the next paragraph.

Evidence shows that the RyR channels are poor Ca^{2+} selective channels with high conductance, which can be activated by various endogenous and exogenous regulators. For instance, it is found that cADPR and caffeine can activate RyR channels, while, ruthenium red is a well known RyR channel inhibitor (Rossi and Sorrentino, 2002). In addition, other regulators, such as Ca^{2+} itself, CaM and ryanodine have biphasic effect on RyR channel activity at different concentrations (Rossi and Sorrentino, 2002). Like Ca^{2+}, the RyR channels are activated by low $[Ca^{2+}]_c$ (nM-μM) and inhibited by high $[Ca^{2+}]_c$ (μM-mM).

Among these modulators, cADPR plays an important role in regulating RyRs to induce CICR in many cell types (Galione *et al.*, 1991). Cyclic adenosine diphosphate ribose is a metabolite of nicotinamide adenine dinucleotide (NAD). It was first found to act as a powerful intracellular Ca^{2+} release agent in sea urchin eggs (reviewed by Churchill *et al.*, 2002). The cADPR-induced Ca^{2+} release can by blocked by chemical analogues, such as 8-amino- cADPR or 8-bromo- cADPR (Galione and Churchill, 2002). The precise mechanism of how cADPR activates RyRs is still unclear. It may bind directly to RyRs or through a separate cADPR-binding protein, such as FK506-binding proteins (FKBPs) (Galione and Churchill, 2002). The cADPR elevated $[Ca^{2+}]_i$ during activation lasts longer that IP_3 elevated. Hence, it is suggested that IP_3 may induce a short-term Ca^{2+} signaling while the major role of cADPR may be the generation of more prolonged Ca^{2+} signals (Galione and Churchill, 2002).

1.4.2.3 NAADP sensitive Ca^{2+} release

NAADP is another Ca^{2+} mobilizing messenger discovered in sea urchin eggs (Chini *et al.*, 1995; Aarhus *et al.*, 1996). It is believed to induce Ca^{2+} release distinct from that activated by IP_3 or

cADPR. It is found that the NAADP-sensitive Ca^{2+} release is unaffected by pharmacological agents of all known Ca^{2+} release mechanisms that affect either IP_3Rs or cADPR receptors, including heparin, ruthenium red, procaine and 8-NH2-cADPR (Aarhus *et al.*, 1996; Yamasaki *et al.*, 2005). Nevertheless, NAADP-induced Ca^{2+} release can be selectively blocked by a disparate group of channel blockers, such as D600, verapamil, and SK&F96365 (Galione and Ruas, 2005). In addition, studies showed that the NAADP-evoked Ca^{2+} release from unique stores which are distinct from those sensitive to IP_3 and cADPR in sea urchin eggs (Lee and Aarhus, 2000). The NAADP-sensitive stores can still persist under the stimulation of thapsigargin, a SERCA pump inhibitor (Thastrup *et al.*, 1990), while both IP_3 and cADPR sensitive stores are discharged (Genazzani and Galione, 1996). Some data suggests that the NAADP-sensitive Ca^{2+} store was probably an acidic organelle or lysososome-related (Galione and Ruas, 2005). However, there are reports that NAADP might also activate ryanodine receptors on the ER (Dammermann and Guse, 2005). All these findings remain controversial. More studies are required to identify the NAADP receptors and their location. Recently, it was found that two-pore channels (TPCs), novel members of the superfamily of voltage-gated ion channels, comprise a family of NAADP receptors, with TPC1 and TPC3 being expressed on endosomal and TPC2 on lysosomal membranes (Calcraft *et al.*, 2009).

NAADP is a very potent messenger. In mammalian cells, it is able to induce Ca^{2+} release at nM level whereas μM concentrations of IP_3 or cADPR are needed to evoke such responses in the same cell. Curiously, increasing the NAADP produces no further Ca^{2+} response. Conversely, NAADP in the μM range is highly effective in desensitizing the NAADP-sensitive Ca^{2+} release mechanism. This "bell-shaped" concentration response curve for NAADP appears to be a hallmark of NAADP-mediated Ca^{2+} release in mammalian cells (Galione and Ruas, 2005). Sub-threshold concentrations of NAADP for Ca^{2+} release are able to fully inactivate NAADP-evoked Ca^{2+} release to a subsequent challenge by a higher, normally effective concentration (Galione and Churchill, 2002).

Studies show that NAADP can evoke localized signals, which may be amplified into global signals by recruiting $InsP_3Rs$ and RyRs through CICR mechanisms (Cancela *et al.*, 2000; Churchill and Galione, 2001; Yamasaki *et al.*, 2005). The existence and interaction of the diverse Ca^{2+} mobilizing

messengers, including IP_3, cADPR and NAADP, in a single cell system ensures that cells can respond to given extracellular signals. In addition, those multi messengers permit local Ca^{2+} signal occurs in different regions within the cell and with different characteristics (da Silva and Guse, 2000).

1.5 Ca^{2+} sequestration and efflux

After stimulation, the $[Ca^{2+}]_i$ needs to return to resting level and then be kept at this low level when the cell is at rest. This can be achieved by either pumping Ca^{2+} to the external environment or sequestering the Ca^{2+} into the intracellular stores.

Ca^{2+} is transferred across the plasma membrane mainly through the plasma membrane Ca^{2+} pump (PMCA pump). PMCA pump belongs to the P-type class of ion-motive ATPase. This type of pump forms a phosphorylated intermediate during the reaction cycle. In the high-affinity conformation (E1), Ca^{2+} binds to the cytosolic domain of the enzyme, followed by the phosphorylation of the catalytic aspartic acid by adenosine triphosphate (ATP). The phosphorylated enzyme changes the E1 conformation to a low Ca^{2+} affinity conformation E2, which exposes Ca^{2+} to the extracellular side and promotes Ca^{2+} release prior to the hydrolytic cleavage of the phosphorylated intermediate. After the cleavage of the intermediate, the pump returns to the E1 conformation (Carafoli and Brini, 2000). In addition, Na^+/Ca^{2+} exchangers also eject Ca^{2+} and these do so with a higher transport capacity particularly in excitable cells (Di Leva *et al.*, 2008). The distribution of PMCA pump varies among different cell types. In some cell types, the pump is located in small plasma membrane invaginations called caveolae. While in other cell types, the pump is distributed diffusely throughout the plasma membrane (Monteith *et al.*, 1998). Two of the basic PMCA isoforms, PMCA1 and PMCA4 are distributed ubiquitously in animal tissues and other two PMAC2 and PMCA3 isoforms are mainly restricted to nervous cells (Carafoli and Brini, 2000).

The PMCA pump can be inhibited by orthovanadate ($VO_3(OH)_2$) and by La^{3+}. It has a low affinity to Ca^{2+} at the μM $[Ca^{2+}]_c$ level. It was found that the affinity of the pump for Ca^{2+} can be increased through a number of mechanisms, for example, by lowering its Kd to values as low as about

200nM. CaM is also one of the activators for PMCA pump. Technically, Ca^{2+}/CaM relieves an auto inhibition of the pump. In addition, PMCA pump can be regulated by various kinases, such as the PKC, cAMP-dependent protein kinase, and cGMP-dependent protein kinase (Monteith *et al.*, 1998). On the other hand, most of the $[Ca^{2+}]_i$ is sequestered in the intracellular stores. After the Ca^{2+} stores are depleted, they can be replenished by extracellular Ca^{2+} via different uptake pathways, such as the capacitative Ca^{2+} influx pathway (Putney *et al.*, 2001). Furthermore, the repeated Ca^{2+} release and refill from ER/SR directly results in Ca^{2+} oscillation.

ER/SR reuptakes Ca^{2+} through the SERCA pumps which are widely distributed in ER/SR. SERCA pump belongs to the P-type pump as well. The activation of SERCA pump requires the chemical energy produced from the conversion of ATP into adenosine diphosphate (ADP) as does the PMCA. It transports Ca^{2+} ions across the membrane from the cytosol to the ER, against a concentration gradient (Higgins *et al.*, 2006). Besides the function of transporting Ca^{2+} into stores, it is also found that due to the delay in the binding and release of Ca^{2+}, the SERCA pump contributes in buffering Ca^{2+} (Higgins *et al.*, 2006).

Apart from ER/SR, mitochondria and other intracellular organelles buffer Ca^{2+} as well. It has been found that mitochondria and some acidic organelles uptake Ca^{2+} through the H^+ electrochemical gradient created by H^+-ATPases as the driving force for Ca^{2+} accumulation (Pozzan *et al.*, 1994). Moreover, it was reported that mitochondria can also recycle Ca^{2+} to ER/SR and prevent the depletion of neighbouring ER regions (Arnaudeau *et al.*, 2001).

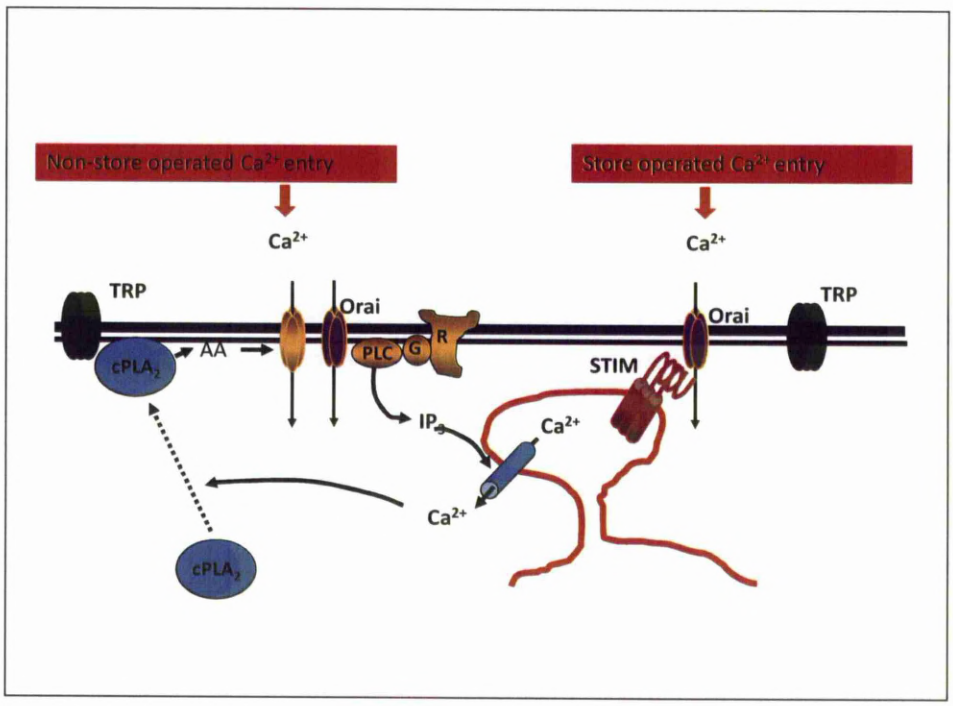

Figure 1.4-Two major Ca^{2+} entry pathways in non-excitable cells

Common models for two major Ca^{2+} entry pathways in non-excitable cells are shown in the figure. One is called SOCE, which involves the activation of STIM and Orai proteins. TRP channels are likely to participants in SOCE. Another pathway is the NSOCE. The most characterized NSOCE is the AA-regulated Ca^{2+} entry pathway. STIM, Orai and TRP proteins may also play a role in this pathway.

1.6 Diverse Ca^{2+} entry pathways

Resting cells generally have a low plasma membrane permeability to Ca^{2+}. An increase in membrane permeability to Ca^{2+} can be achieved by opening Ca^{2+} permeable ion channels. A variety of different Ca^{2+} permeable channels have been found located in the plasma membrane. Cell Ca^{2+} entry has been given various and sometimes confusing different names. For a long time, there has been no universal admitted classification of these Ca^{2+} entry pathways. This was due to the lack of precise knowledge about the activation mechanisms of Ca^{2+} influx and in some cases the absence of information on their molecular identity.

Ca^{2+} channels have either been characterized by how they are activated or by the electrophysiology characteristics of Ca^{2+} entry. The most clear defined one is the voltage-operated/gated Ca^{2+} entry (VOCE) pathways, which are found, mostly, in excitable cells. The voltage-operated Ca^{2+} channels (VOCCs) have been extensively studied (reviewed by Lacinova, 2005). Furthermore, there are many other voltage-independent Ca^{2+} entry pathways that exist in both excitable and non-excitable cells. They are opened in response to different external signals, majority of which are agonist dependent. These voltage-independent, agonist-dependent Ca^{2+} entry pathways can be further divided into two broad defined categories. (i) The store-operated Ca^{2+} entry (SOCE) is also called capacitative Ca^{2+} entry (CCE) and is triggered by the emptying of the intracellular Ca^{2+} stores. The Ca^{2+} channels activated in this entry pathway are so called store-operated Ca^{2+} channels (SOCCs) (figure 1.4, page 26). (ii) The non store-operated Ca^{2+} entry (NSOCE) or non-capacitative Ca^{2+} entry (NCCE). This type of pathway is named opposite to SOCE, since it was first noticed as a kind of Ca^{2+} influx that was independent on store depletion (Shuttleworth and Thompson, 1996). The most characterized and typical NSOCE is the one mediated by the activation of arachidonic acid (AA) which has been observed in a variety of different cell types (Mignen and Shuttleworth, 2000) (figure 1.4, page 26). The channels are normally named as arachidonic acid-regulated Ca^{2+} (ARC) channels.

SOCE and NSOCE are sweeping definitions. These Ca^{2+} entry pathways have other names according to different classification criteria. For instance, the AA-induced Ca^{2+} entry is referred to as a type of receptor-operated Ca^{2+} entry (ROCE), in which a group of channels activated by

agonists acting on a range of receptors. On the other hand, owing to the growing understanding on the mechanisms of SOCE, there is emerging evidence that the receptor-operated Ca^{2+} channels (ROCCs) and SOCCs may be closely related (reviewed by McFadzean and Gibson, 2002). There has been a controversy about the identification of SOCE, which will be discussed in section 1.6.2. In addition to those widely distributed voltage-gated or agonist-operated Ca^{2+} entry channels described above, there are other Ca^{2+} channels presented in some cell types such as mechanically-operated Ca^{2+} channels (MOCCs) or the tonically-actived Ca^{2+} channels (reviewed by Tsien and Tsien, 1990).

Many of these channels have been demonstrated to belong to the large transient receptor potential (TRP) ion-channel family (reviewed by Berridge *et al.*, 2003). This family consists of three groups: the transient receptor potential canonical (TRPC) family, the transient receptor potential vanilloid (TRPV) family and the transient receptor potential melastatin (TRPM) family. It is reported that the TRP channels tend to have low conductance and therefore can operate over much longer time scales without swamping the cell with too much Ca^{2+}. They are essentially important in controlling slow cellular processes such as smooth-muscle contractility and cell proliferation (reviewed by Venkatachalam and Montell, 2007). In the following paragraphs, primary types of Ca^{2+} entry pathways which play a vital role in cellular progresses will be discussed.

1.6.1 Voltage-operated Ca^{2+} entry

Voltage-operated Ca^{2+} channles are the ion channels that are activated by changes in membrane potential. At physiological or resting membrane potential, VOCCs are normally closed. They are then opened at depolarized membrane potentials.

They are mostly present in excitable cells including nerves and muscle. Activation of particular VOCCs enables a rapid Ca^{2+} entry into the cell, which depending on the cell type, results in muscular contraction, excitation of neurons, up-regulation of gene expression, or release of hormones or neurotransmitters (reviewed by Lacinova, 2005).

VOCCs are formed as a complex of several different subunits: α1, α2δ, β1-4, and γ (reviewed by Tsien and Tsien, 1990; Jagannathan *et al.*, 2002). The α1 subunit forms the ion conducting pore while the associated subunits have several functions including modulation of gating. There are several different classifications of VOCCs. The most widely used one is to divide them into two subgroups regarding their activation threshold, low-voltage-activated (LVA) and high-voltage activated (HVA). LVA Ca^{2+} channels, which are also called T-types, are activated with relatively small depolarisation (between −80 and−60 mV). The T-type Ca^{2+} channels are characterized by their low voltage of activation, rapid inactivation, and slow deactivation. In contrast to LVA, the HVA Ca^{2+} channels are activated at relatively depolarized potentials (>−40mV) and have slow kinetics of current decay. They can be further classified into L-type, N-type, P/Q type, and R types (reviewed by Tsien and Tsien, 1990; Jagannathan *et al.*, 2002; Lacinova, 2005).

The L-type is the first defined and most characterized HVA Ca^{2+} channel, which is widely expressed in diverse cell types, especially in the excitable cells. They are responsible for Ca^{2+} entry in the heart and also play a significant role in neurons, smooth muscle cells and certain endocrine cells. They have quite high conductance and slow time- or voltage-dependent inactivation (reviewed by Treinys and Jurevicius, 2008). One hallmark of all L-type channels is their sensitivity to 1,4-dihydropyridine (DHP) which encompasses a wide class of drugs that either have an inhibitory (*e.g.* nifedipine, nisoldipine, isradipine) or activatory (*e.g.* Bay K 8644) action on this L-type channel (Hess and Tsien, 1984; Belkacemi *et al.*, 2005).

The other three types of HVA Ca^{2+} channels differ significantly from L-type channels in their sensitivity to ω-conotoxin which is one of a group of neurotoxic peptides isolated from the venom of the marine cone snail and spiders. The channel sensitive to ω-conotoxin, kept the name N-type channel, while the channel sensitive to ω-Aga toxin was named P/Q-type Ca^{2+} channel. The channel resistant to these toxins were named R-type Ca^{2+} channel (reviewed by Lacinova, 2005).

1.6.2 Store-operated Ca^{2+} entry

SOCE is primarily responsible for the refilling of the Ca^{2+} stores such as ER/SR and the maintenance of the stable Ca^{2+} level inside the ER/SR (Putney, 2001). In contrast to the transient increase of $[Ca^{2+}]_i$ resulting from the discharge of ER/SR, the Ca^{2+} that enters the cells via SOCE supplies a sustained elevation of $[Ca^{2+}]_i$ level. This is crucial for specific signaling events (Smyth *et al.*, 2006), especially those in non-excitable cells. Since SOCE can affect many aspects of cell biology, it is vital to understand the molecular aspects of SOCE. As a result, we may fully appreciate its contribution to normal physiological as well as pathophysiological states.

The existence of SOCE was first proposed by Jim Putney (1986). Since then, numerous studies have been carried out to investigate the mechanisms of SOCE. The first SOCC to be well characterized was from mast cells and its characteristic Ca^{2+} current was named as Ca^{2+} release-activated current (CRAC; Hoth and Penner, 1992). Initially, because of its extremely small conductance, the CRAC current (I_{CRAC}) could not be resolved on the single channel level, but the whole-cell I_{CRAC} was recorded in non-excitable cells (Bolotina and Csutora, 2005). I_{CRAC} is not the only store-operated current, yet it is the most well studied SOCE. CRAC channels are remarkably selective for Ca^{2+} although they can conduct Ba^{2+} and Sr^{2+} as well (Parekh and Putney, 2005). Whilst I_{CRAC} remained characteristic archetypal SOCE pathways, other non-selective forms of SOCE were also observed.

The study on SOCE was once mired in difficulties. The key feature of SOCE is that it is the fall in Ca^{2+} content within the ER/SR and not the subsequent rise in $[Ca^{2+}]_i$, such as Ca^{2+} itself or other downstream signals, that activates the channels. It was difficult to distinguish the SOCE from other types of Ca^{2+} entry pathways. The application of some specific pharmacological inhibitors of SERCA pumps, which are responsible for pumping Ca^{2+} into the lumen of the ER/SR from the cytoplasm, has been invaluable in the study of SOCE function and regulation. Thapsigargin is the most common used agent to induce SOCE in experimentation, since it triggers store-depletion without direct activation of cell signaling pathways. Several agents are known to inhibit this thapsigargin-evoked Ca^{2+} influx, such as econazole, SK&F96365, 2-aminoethoxydiphenylborne (2-APB) and the vanilloid capsaicin. Like all Ca^{2+} influx pathways, store-operated channels are

inhibited by divalent and trivalent cations, probably via a block by slow permeation. Trivalent cations like La^{3+} and Gd^{3+} are particularly effective, blocking the channels fully in a low concentration range (Parekh and Putney, 2005). After more than 20 years' study, two major questions about SOCE questions remained enigmatic: (i) how does the ER/SR inform the SOCCs located in the plasma membrane of its emptying and (ii) the molecular identity of the SOCCs.

1.6.2.1 Models of SOCEs

There were two general hypotheses for the communication between internal ER/SR and the plasma membrane SOCCs. The first involved the action of a diffusible messenger or a Ca^{2+} influx factor (CIF) that is released from the ER/SR to trigger the SOCCs in the plasma membrane upon ER/SR Ca^{2+} depletion. This diffusible messenger model was first put forward by Putney and colleagues in 1989 (Takemura *et al.*, 1989). Later, evidence for the existence of such a factor was demonstrated by Randriamampita and Tsien (1993), who isolated CIF an acid-extractable factor from thapsigargin-treated lymphocytes. The ability of CIF in activating Ca^{2+} influx has been demonstrated in several different cell types. The mechanism by which CIF triggers Ca^{2+} influx remains unclear, although more recent work suggested an important role of Ca^{2+}-independent phospholipase A_2 ($iPLA_2$) in this CIF model. It has been found that $iPLA_2$ is required for the activation of SOCE in various cell types (Smani *et al.*, 2003). Then, CIF is demonstrated to be able to activate $iPLA_2$ by the displacement of inhibitory CaM from $iPLA_2$ and that the lysophospholipid generated by $iPLA_2$ is then responsible for directly activating SOCCs (Bolotina and Csutora, 2005). Based on these important findings, a novel model CIF-$iPLA_2$-SOCE was proposed (reviewed by Bolotina, 2008). Despite these studies, the exact mechanism by which CIF activates SOCE is still an enigma. It remains uncertain whether CIF or other diffusion messengers is necessary for some types of SOCEs.

The second hypothesis was originally referred to as conformational coupling model. This idea was first introduced by Irivne (1990) and further developed by Berridge (1990) involved protein-protein interaction. This model suggested that the IP_3Rs located on the ER membrane are physically attached to the store operated Ca^{2+} channels in the plasma membrane, and that a conformational change of the IP_3Rs upon ER Ca^{2+} depletion opens SOCCs. This hypothesis was

revised by Patterson *et al.* (1999) and has became known as the secretion-like coupling model that suggested that the IP_3Rs are separated from SOCCs when the stores are full and that they move close to SOCCs in response to the store depletion (Patterson *et al.*, 1999). However, other research provided strong evidence that the interaction of Ca^{2+} influx channels with the IP_3Rs is not required for the activation of I_{CRAC} (Sugawara *et al.*, 1997). Though the function of IP_3Rs in conformation coupling was challenged, it does not exclude the idea that there may be other proteins that act as a link between ER and SOCCs.

1.6.2.2 STIM and Orai in SOCEs

Recently, the advent of large scale RNAi-based screens brought a great breakthrough in identifying the molecular constituents of SOCE that identified the functional role of two proteins in SOCE (Liou *et al.*, 2005). The first one is stromal interacting molecule (STIM) that was first found in Drosophila S2 cells (Roos *et al.*, 2005). Mammals have two STIM proteins, STIM1 and STIM2, whose knockdown reduced SOCE (Liou *et al.*, 2005). It is now clear that STIM1 is a necessary component of I_{CRAC}-activation and SOCE while some research indicates that STIM2 may also participate in the SOCE (Parvez *et al.*, 2008). STIM1 is a single-pass transmembrane protein residing primarily in the ER (Manji *et al.*, 2000). It contains several conserved regions, including an EF-hand and a sterile alpha motif (SAM) domain in the N-terminus directed towards the lumen of the ER. In the cytosolic STIM1 C-terminus, there are two coiled-coil regions overlapping with the ezrin-radixin-moesin (ERM)-like domain, and a lysine-rich region are essential for I_{CRAC} activation (Frischauf *et al.*, 2009).

Although it is clear that STIM1 is required for the I_{CRAC} and other store-operated entries, the mechanism by which it acts is still being elucidated. So far, the most accepted model involves a marked change in the distribution of STIM1 in the ER membrane, from a generally diffuse distribution to the formation of clusters of the proteins at sites either within or immediately adjacent to the plasma membrane (Zhang *et al.*, 2005). When the ER Ca^{2+} stores are filled, the EF-hand domain which is suggested as the sensor of ER Ca^{2+} has bound Ca^{2+} while STIM1 is a dimer stabilized by the coiled-coiled interactions. Once the ER Ca^{2+} store is depleted, the EF-hand domain releases bound Ca^{2+} which leads to quick STIM1 oligomerization mediated by the SAM

domain. These clustered STIM1 proteins immediately translocate to form puncta, close to the plasma membrane (Wu *et al.*, 2006). This conveys the message that ER store has been depleted. Some studies indicate that this ER-resident STIM1 migration might be guided by the microtubules (Smyth *et al.*, 2007). Further investigation needs to be carried out on this possibility.

Another functional protein component identified in SOCE was named as Ca^{2+} release-activated Ca^{2+} channel protein 1 (Orai or CRACM). There are three member types in the Orai family: Orai1, Orai2 and Orai3 all of which are expressed in mammalian cells. They are predicted to be membrane spanning proteins with 4 transmembrane domains located in the plasma membrane with their C and N termini located in the cytoplasm. All three Orai proteins possess a conserved putative coiled-coil domain in the C-terminus while only the N-terminus of Orai1 consists of a proline/arginine-rich region (Frischauf *et al.*, 2009). Orai1 is suggested to be the major regulator of SOCE, whereas Orai3 can complement partially and Orai2 has a lesser role (Gwack *et al.*, 2007). Orai1 is regarded as the pore-forming subunits of CRAC channels (Prakriya *et al.*, 2006). Upon store-depletion, Orai1 proteins require STIM1 co-expression to form a clustered localization in the plasma-membrane at sites in close proximity to STIM1 puncta. The STIM1 and Orai1 complex has been identified during the SOCE by co-immunoprecipitation and by Forster resonance energy transfer (Yeromin *et al.*, 2006). Several reports have demonstrated a remarkable amplification of I_{CRAC} when Orai1 is coexpressed with STIM1 (Peinelt *et al.*, 2006). However, either Orai1 or STIM1 expressed alone cannot result in an increase of SOCE (Xu *et al.*, 2006). Hence, this interaction between STIM1 and Orai1 is necessary for the activation of I_{CRAC}. The two other members of the Orai family, Orai2 and Orai3, display similar, but smaller store-operated Ca^{2+} influx currents after co-expression with STIM1 (DeHaven *et al.*, 2007; Lis *et al.*, 2007).

The question as to the molecular interaction of STIM1 and Orai1 is still unclear. Evidence suggests that the C terminus of STIM1 contains the domain that is responsible for the opening of Orai channels. Recently, this domain has been found to be seated in the ezrin/radixin/moesin (ERM) coiled-coil region, which was named by three independent teams as STIM1 Orai activating Region (SOAR)(Yuan *et al.*, 2009) or CRAC Activating Domain (CAD) (Park *et al.*, 2009) or Orai Activating Small Fragment (OASF)(Muik *et al.*, 2009). According to these findings, this Orai activating region

has been narrowed down to approximately 100 amino acids from STIM1 in the region of 344 to 442. Strong evidence demonstrates that it is this fragment in STIM1 that binds directly to Orai and triggers Orai protein clusters. Moreover, either the C terminus of STIM1 or this short fragment alone has been proven sufficient to constitutively activate I_{CRAC} independently of store-depletion (Zhang *et al.*, 2008). In turn, the domain of Orai protein is responsible for the binding with STIM1 has been generated. Orai1 deletion mutants devoid in their whole N or C terminus have been conducted (Muik *et al.*, 2008; Frischauf *et al.*, 2009). Deletion of either terminal failed to induce Ca^{2+} influx. Hence, both N and C terminus of Orai are necessary for the activation of I_{CRAC} channels. However, mutation of the Orai1 C terminus completely abrogates the coupling with STIM1. This observation suggests that the C terminus of Orai protein plays a dominant role in coupling to STIM1 independently of the N terminus. Presently, it has been revealed that a conserved putative coiled-coil region in the C terminus of Orai proteins mediates the coupling with STIM1 (Muik *et al.*, 2008; Frischauf *et al.*, 2009). This putative coiled-coil domain is a common motif involved in homo-as well as heteromeric protein-protein interactions (Woolfson, 2005; Muik *et al.*, 2008). Mutation at this coiled-coil region of Orai1 with point mutations from leucine to serine (Orai1 L273S), which is expected to destabilize coiled-coil structure, was observed to fully disrupt the interaction with STIM1 in HEK293 cells (Muik *et al.*, 2008). The same single mutation in Orai2 or Orai3 proteins resulted in similar inhibition of binding with STIM1, though this was not completely abolished (Frischauf *et al.*, 2009). In conclusion, STIM1 and Orai protein directly interact with each other at their C terminus coiled-coil domains.

Now we understand how the protein STIM can bind with Orai, then follows the question of how many STIM and Orai molecules are required to activate SOCE. The understanding of Orai stoichiometry differs based on different research approaches. In biochemical experiments, it is suggested that the Orai complex is a dimer in both resting and in SOCE, while in functional measurements of expressed tandem Orai multimers, it is indicated that Orai exists in a tetramer during SOCE (Penna *et al.*, 2008). Recently, a newly developed method has been utilized to investigate the structure of Orai protein, which can detect the number of GFP (green fluorescent protein)-tagged Orai subunits per channel by counting the number of photobleaching steps (Ji *et*

al., 2008; Penna *et al.*, 2008). Collectively, these experiments show that Orai is present stably as dimer in the plasma membrane in resting cells, but when the SOCE is induced, Orai is found predominantly as a tetramer forming active channels. Similar photobleaching approach reveals that two STIM1 molecules are required to activate the tetrameric Orai channel (Ji *et al.*, 2008).

1.6.2.3 TRPC in SOCEs

Apart from STIM and Orai proteins, the mammalian TRP superfamily, particularly those from TRPC family, have long been proposed as the candidates for the conduction of SOCE. TRPC channels are non-selective, Ca^{2+} permeable cation channels containing six transmembrane domains. There are seven types of TRPCs named from TRPC1 to TRPC7. All TRPC channels are activated by receptor stimulation and conduct receptor operated cation currents while several TRPCs have been suggested to function as SOCCs. Among these TRPCs, the case for TRPC1 as a subunit of SOCCs is the most widely investigated one (Liu *et al.*, 2003; DeHaven *et al.*, 2009; Salido *et al.*, 2009).

The functional role of TRPC1 in SOCE is supported by a series of studies. It has been observed in different cells, such as HEK293 cells, that overexpression of TRPC1 enhances thapsigargin- or DAG-induced SOCEs, while overexpression of TRPC mutations or TRPC knockouts results in a reduced SOCE current (Ambudkar *et al.*, 2007; Ong *et al.*, 2007; Liao *et al.*, 2009). This evidence is further upheld since overexpression of Orai is reported to increase SOCE current in the cells stably expressing TRPC but not in the control cells. This suggests an interaction between TRPCs and Orai proteins in SOCE (Liao *et al.*, 2009). On the other hand, STIM1 has shown the ability to regulate all TRPC channels, except TRPC7 (Yuan *et al.*, 2007). The interaction of STIM1 with TRPCs requires the ERM domain to bind TRPCs directly as well as the polybasic lysine (K)-rich domain to open the channels, which both located at the C terminus of STIM1 (Huang *et al.*, 2006).

Despite numerous supporting findings, the involvement of TRPCs in SOCEs is still a controversy challenged by other research reports. For instance, several investigators have failed to observe store-operated behaviour of TRPCs even in the same cellular models mentioned above (Salido *et al.*, 2009). However, owing to a series of recent results, these discrepancies between studies in

favour and against the participation of TRPCs in SOCEs may be reconciled. First, it is validated that some TRPCs can function in a STIM1-dependent and STIM1-independent manner as different types of ion channels. It was shown that TRPC1, TRPC4 and TRPC5 when regulated directly by STIM1 performed as SOCCs under all conditions. In comparison, TRPC3 and TRPC6 function as SOCC function mediated by STIM1 indirectly through the heteromultimerization with other TRPCs when they are expressed at low level (Zeng *et al.*, 2008). The STIM1 mediated heteromultimerization is suggested to be necessary for TRPCs to form SOCCs. Besides, this STIM1 indirectly regulates TRPCs. It is reported that translocation of TRPC1 to the plasma membrane does not occur in the absence of other TRPC isoforms, such as TRPC4 or TRPC5 (Zeng *et al.*, 2008; Salido *et al.*, 2009). Thus, investigations may fail to assess the role of TRPCs in SOCE when they were overexpressed or when other TRPC isoforms were absent.

As with TRPCs ion channel subunits, Orai proteins have recently been implicated to also possess the ability to conduct ion current in different manners not restricted to SOCEs. It was observed that mutation Orai1 not only inhibited SOCE but also ROCE. Moreover, Orai1 is suggested to heteromerize with Orai2 or Orai3 to form the SOCCs under the regulation of STIM1 (Frischauf *et al.*, 2009).

Collectively, though STIM1 is not the only factor to activate TRPC or `Orai channels, it is obligatory for TRPCs and Orai proteins to perform as SOCCs. Respecting the additional finding that TRPCs and Orais can conduct SOCE current independently of each other, discrete store operated Ca^{2+} signals could be generated depending on whether STIM1 couples to TRPCs or Orai channels or to the TRPCs and Orai channel complexes (Zeng *et al.*, 2008). SOCCs formed as a heteromultimeric complex by different combination modes among TRPC and Orai isoforms with STIM molecules is suggested to meet the diverse demands of various ion currents in different cells. The SOCCs formed by TRPCs are suggested to be less selective Ca^{2+} channels while the Orai formed channels or the TRPC-Orai complex channels are believed to conduct highly selective Ca^{2+} currents, such as I_{CRAC}. Receptors may also independently activate the TRPCs and Orai channels to tune their Ca^{2+} signals and it is possible that STIM1 determines which type of Ca^{2+} influx pathway ROCE or SOCE mediates Ca^{2+} entry (Zeng *et al.*, 2008).

A recent report proposed a STIM regulated heteromeric Orai/TRPC model to explain how STIM1 convert TRPCs from ROCs to SOCCs. It is implicated that upon the stimulation-induced SOCE, Orai molecules rapidly release from TRPCs with the concomitant activation of TRPC channels to conduct ROCE. As the intracellular Ca^{2+} store is depleted, the aggregated STIM1 forms puncta and triggers the migration of both Orai and TRPC to the same microdomains. This then causes complexes of Orai, TRPC and STIM1 to form which acts as SOCCs located in lipid draft domain (LRD) (Alicia *et al.*, 2008; Liao *et al.*, 2009). Plasma membrane LRDs are domains containing high concentration of cholesterol and sphingolipids known to function as centers for the assembly of signaling complexes. This facilitates both specificity and efficiency of signaling events by positioning functionally associated molecules in close proximity to each other (Gajate *et al.*, 2009). It has been shown that LRDs are required for activation of TRPC1-mediated SOCE. Disruption of LRD inhibits both TRPC1 and STIM1 translocation leading to the decrease of SOCE (Gajate *et al.*, 2009). Hence, the proposed role of LRDs is to bring STIM molecules in the ER and TRPCs in the plasma membrane, along with Orai, sufficiently close to each other to activate Ca^{2+} influx. Further studies will be required to establish the function of LRDs in SOCE.

Although there has been rapid and significant progress since the initial discovery of STIM and Orai's role in SOCE, what we have known is only part of the regulation mechanism of SOCE. Other than STIM, Orai and TRPCs, there may be additional molecular components to the mechanism. The CIF pathway is suggested to co-exist with the STIM-Orai protein-protein coupling model. This assumption is derived from the report that knockdown or overexpression of STIM1 results in corresponding impairment or amplification of CIF production (Potier and Trebak, 2008).

1.6.3 Arachidonic acid activated Ca^{2+} entry

As it is mentioned above, there are alternative, non store-operated Ca^{2+} entry pathways that co-exist mostly in non-excitable cells. These have been argued to provide the predominant route of Ca^{2+} entry particularly at lower, more physiologically relevant levels of stimulation. In particular, the activation of these NSOCEs was observed, under most conditions, to result in Ca^{2+} oscillations (Shuttleworth and Thompson, 1996; reviewed by Shuttleworth, 2009). In virtue of the properties

of the oscillatory Ca^{2+} signals, the function of the non-store operated Ca^{2+} signals is believed to enable cells to regulate a diverse range of effects and responses in more precise and appropriate manners, and therefore represent the relevant responses to a range of different agonists (reviewed by Shuttleworth, 2009).

The most classic NSOCE, AA regulated Ca^{2+} entry, was first discovered in the 1990s (Shuttleworth, 1996). The ARC channels have a highly Ca^{2+}-selective conductance whose activation is specifically dependent on the receptor-mediated generation of low levels of intracellular AA. They display conductance values similar to CRAC channels and are inhibited by external La^{3+} and Gd^{3+}. Nevertheless, I_{ARC} can be distinguished from I_{CRAC} by the absence of any fast-inactivation during brief pulses to negative potentials, insensitivity to low external pH and to 2-APB, and a significantly higher monovalent (Na^{+}) to Ca^{2+} current ratio (reviewed by Shuttleworth *et al.*, 2007).

1.6.3.1 STIM and Orai in arachidonic acid activated Ca^{2+} entry

Although the ARC currents have been demonstrated in various cell lines such as HEK293 and HeLa cells (Mignen and Shuttleworth, 2000; Mignen *et al.*, 2007), further insight into the nature of the ARC channels was impeded by the lack of any clear indication of their molecular identity. This situation lasted until the very recent when, unexpectedly, it was found that STIM and Orai proteins are not limited to SOCEs but play a key role in regulation of ARC channels as well (Mignen *et al.*, 2007; Mignen *et al.*, 2008). These studies revealed that STIM and Orai proteins mediate ARC channels in a completely distinct model from that regulates SOCCs.

It is reported that the mobilization of STIM1 in the ER to sites close to the plasma membrane is not required for the activation of ARC channels. Moreover, instead of the heavily studied ER STIM1 being responsible for the modulation of SOCCs, the pool of STIM1 residing in the plasma membrane has been suggested be responsible for the regulation of ARC channels (Mignen *et al.*, 2007). The plasma membrane STIM1 is orientated with its N-terminal domain which exposed to the extracellular medium. Exposure of intact cells to an N-terminal STIM1 antibody markedly reduced currents through the ARC channels by almost 70% (reviewed by Shuttleworth *et al.*,

2007). Based on the similar biophysical properties of the conductance represented by the ARC channels and the CRAC channels and the finding that they are both mediated by STIM1, the possibility of the involvement of Orai proteins in I_{ARC} was examined. The results showed that both Orai1 and Orai3 appear to contribute to the ARC channels pore whilst the formation of CRAC channel pore only requires Orai1 (Mignen *et al.*, 2008).

Consequently, these findings suggest that the ARC channel could be considered as a STIM1 mediated Orai-based channel like CRAC channels but that they are regulated in a different manner. The precise mechanism of how plasma membrane STIM1 regulates the ARC channels is still unclear. Given that the presence of low concentrations of AA is predicted to activate ARC channels, two possibilities arise to explain the action of STIM1 on the ARC channels. Firstly, STIM1 may be the target of AA. The interaction between STIM1 and AA could somehow enable STIM1 to activate the ARC channels. Secondly, AA could open ARC channels directly when the channels are associated with STIM1 (reviewed by Shuttleworth *et al.*, 2007).

Although AA has been revealed to directly regulate various ion channels, no consistent sequence has been identified to be a possible candidate domain for binding with Orai channels (Meves, 2008). Besides, there is no further evidence of the interaction of AA and plasma membrane STIM1. On the other hand, the ARC channels are proposed to be formed by Orai1 and Orai3 (reviewed by Shuttleworth, 2009). Studies of the structure of Orai3 reveal that Orai3 possesses an extended extracellular loop that is not seen in either Orai1 or Orai2. In addition, compared with Orai1, Orai3 lacks both the arginine-rich domain and the two flanking porline-rich sequences. Moreover, Orai3 has a much high probability of the putative coiled-coil domain in the C-terminus. The function of all these unique features of Orai3 remain to be investigated, but they may explain ARC channels regulation (reviewed by Shuttleworth, 2009). Far more questions need to be solved before we could understand how ARC channels works.

1.6.3.2 Arachidonic acid

AA is a 20-carbon polyunsaturated fatty acid in mammalian cells. It cannot be synthesized by mammalian cells and is absorbed from the diet. After AA biosynthesis, it is esterified into the

phospholipids located on the cell membranes (Sigal, 1991). Evidence indicate that the ARC channel is specifically dependent on AA for activation rather than any of the AA metabolism products called eicosanoids (Mignen *et al.*, 2008). It was demonstrated that concentrations of AA at 2 to 10μM could lead to the activation of ARC channel (Mignen *et al.*, 2008). There are three major pathways that lead to the release of AA through the activation of phospholipases, including phospholipase A_2 (PLA_2), PLC/DAG lipase and phospholipase D (PLD) (Figure 1.5, page 41). Among them, only PLA_2 is able to cleave AA from the sn-2 position (Balsinde *et al.*, 1999). Therefore, the PLA_2 activation is regarded as the primary pathway through which AA is liberated from phospholipids.

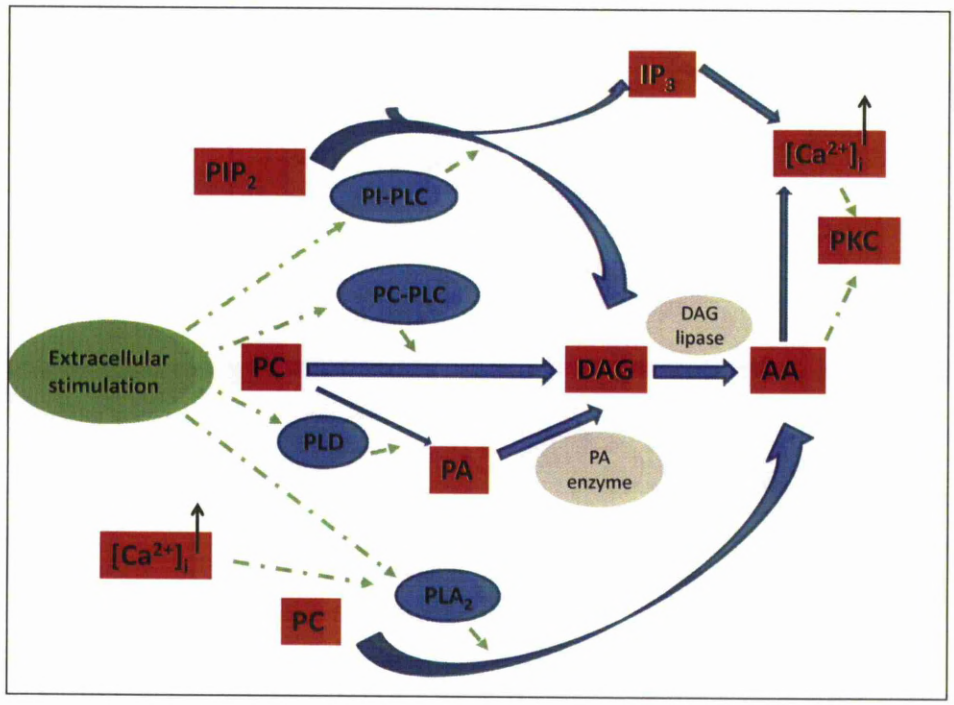

Figure 1.5-AA generation pathways

Various extracellular stimulation can active PI-PLC, PC-PLC, PLD or PLA_2 enzymes, which further trigger four AA production pathways respectively, as shown in the figure.

This figure is modified from 'Contribution of different phospholipases and arachidonic acid metabolites in the response of gallbladder smooth muscle to cholecystokinin' (Alcón et al., 2002).

1.6.3.3 Release arachidonic acid by PLA_2

1.6.3.3.1 PLA_2 superfamily

The PLA_2s are a large enzyme superfamily that plays diverse functional roles and undoubtedly many of them can participate in the release of AA. The superfamily of PLA_2s currently consists of 15 groups and many subgroups and includes five distinct types of enzymes, namely the cytosolic PLA_2s ($cPLA_2$), the secreted PLA_2s ($sPLA_2$), the Ca^{2+}-independent PLA_2s ($iPLA_2$), the platelet-activating factor acetlhydrolases (PAF-AH), and the lysosomal PLA_2s (reviewed by Gijon and Leslie, 1999). The PLA_2 superfamily has grown continuously since it was classified in 1994. These five types of enzymes are assigned based on different catalytic mechanisms as well as functional and structural features.

The $cPLA_2$s are large cytosolic proteins with variable sizes from 61-114 kDa. The 85-kDa cytosolic $cPLA_2\alpha$ has been extensively studied for its dominant role in regulation the agonist-induced AA release (reviewed by Kudo and Murakami, 2002). So far, $cPLA_2\alpha$ is the only PLA_2 identified which is specific for the phospholipid bearing AA. The $cPLA_2\alpha$ has an N-terminal C2 domain or called Ca^{2+}-dependent phospholipid binding (CaLB) domain, which is critical for Ca^{2+}-dependent association with phospholipids membranes (reviewed by Burke and Dennis, 2009). The catalytic domain of $cPLA_2\alpha$ contains many active site residues including Ser^{228}, Ser^{505},Asp^{549}, and Asp^{200} (reviewed by Burke and Dennis, 2009). The mechanism of $cPLA_2$ activation and regulation will be discussed later.

Although $cPLA_2$ is primarily responsible for AA release, both $iPLA_2$ and $sPLA_2$ have demonstrated the capacity to mobilize AA (reviewed by Schaloske and Dennis, 2006). The $sPLA_2$s are small secreted proteins. They are characterized by their low molecular weight (13-15 kDa), histidine in the catalytic site, Ca^{2+} bound in the active site, as well as 6 conserved disulfide bonds, with 1 or 2 variable disulfide bonds (reviewed by Lambeau and Gelb, 2008). All of these $sPLA_2$s have experimentally observed phospholipolysis enzymatic activity at sn-2 position (Murakami *et al.*, 1999). Studies show that some of them have the capacity to regulate the release of AA in distinct ways (Schievella *et al.*, 1995).

The $iPLA_2$ enzymes are characterized by not requiring Ca^{2+} for catalytic activity. The classical $iPLA_2$ exists in an aggregated form and occurs in several splice variants (reviewed by Burke and Dennis, 2009). This enzyme, similar to the $cPLA_2$, uses a serine in the active site to catalyze the cleavage of the sn-2 ester bond. However, it does not show AA specificity (Lambeau and Gelb, 2008). The function of $iPLA_2$ in the cell physiology processes has been shown to be very complex. So far, it is suggested that this $iPLA_2$ enzyme plays a role in phospholipid remodeling, AA-release resulting in eicosanoid formation, protein expression, acetylcholine-mediated endothelium-dependent relaxation of the vasculature, secretion, cell apoptosis and cell proliferation (Gijon and Leslie, 1999). Additionally, as mentioned above, $iPLA_2$ might participate in the SOCEs through co-operating with CIF (Smani *et al.*, 2003). Recently, it is argued that CIF- $iPLA_2$ may play an important role in SOCEs as an essential compound of signal conduction between STIM1 and Orai channels in SOCEs (Bolotina, 2008).

1.6.3.3.2 Regulation of $cPLA_2$

The $cPLA_2$ is a widely distributed enzyme that is ubiquitously expressed in most cells and tissues. It is no doubt that the 85-kDa cytosolic $cPLA_2\alpha$ is the primary regulator in agonist-induced AA liberation from phospholipids (Qiu *et al.*, 1998; Gijon and Leslie, 1999). The $cPLA_2$ activity is stimulated by a wide variety of cytokines and mitogens such as interleukin-1, tumor necrosis factor (TNF), macrophage colony-stimulating factor (CSF), epidermal growth factor, ATP, interferon$_\gamma$ (IFN_γ), and endothelin (reviewed by Leslie, 1997). It is subject to complex mechanisms of regulation at both the transcriptional and post-transcriptional levels.

At the transcriptional level, cytokines and growth factors can increase $cPLA_2$ messenger RNA and protein in a variety of cell types (Sigal, 1991; Shimizu *et al.*, 2008). The main regulation of $cPLA_2$ in the posttranslational level is by the increase of $[Ca^{2+}]_i$ level and phosphorylation following various stimuli. Both of the two mechanisms are required for the activation of $cPLA_2$ to release AA.

The $cPLA_2$ is cytosolic in resting cells but it is translocated to the intracellular membranes when the $[Ca^{2+}]_i$ increases. Micromolar Ca^{2+} binding to the $cPLA_2$ C2 domain increases its affinity for membranes allowing access to the AA containing phospholipids substrates. It has been identified

that the C2 domain of $cPLA_2$ contains four acidic groups including Asp^{37}, Asp^{43}, Asp^{93}, Glu^{100} that are required for binding with Ca^{2+} (reviewed by Leslie, 1997).

It is documented that Ca^{2+} plays a role in delivering the catalytic domain of $cPLA_2$ to interact with the membrane through a hydrophobic mechanism. Studies discovered a tryptophan (W464) on the membrane binding face of the catalytic domain that stabilizes $cPLA_2$ and prolongs membrane binding even after the decrease of $[Ca^{2+}]_i$ (reviewed by Murakami and Kudo, 2002). A patch of basic residues (K488, K541, K543, K544) in the $cPLA_2$ catalytic domain has been identified as the sites to interact with PIP_2, which increases catalytic activity *in vitro* (reviewed by Tucker *et al.*, 2009).

The exact site of $cPLA_2$ relocation remains unknown although it has been studied for decades. It appears to be cell specific. In the majority of studies, $cPLA_2$ has been reported to translocate to the nuclear envelope, endoplasmic reticulum and Golgi (Leslie, 1997). How $cPLA_2$ is selectively transferred to these sites is not known. It is observed that the subcellular localization of $cPLA_2$ can be effected by cell density (Zhao *et al.*, 2002). Ca^{2+}-dependent translocation of $cPLA_2$ to the plasma membrane has not been observed in most cells. However, $cPLA_2$ localizes to cell-cell junctions in confluent endothelial cells and is transiently recruited to the plasma membrane by NADPH oxidase in the caveolae (Shimizu *et al.*, 2008). It has been demonstrated that in the human monocytes, $cPLA_2$ and AA is required for the regulation of NADPH oxidase which normally located in the caveolae of the plasma membranes (reviewed by Murakami and Kudo, 2002). Interaction of $cPLA_2$ with plasma membrane microdomains such as caveolae should be explored further as a possible regulatory mechanism in $cPLA_2$ activation (reviewed by Burke and Dennis, 2009).

Although important, the Ca^{2+} dependent $cPLA_2$ relocation is not sufficient for full activation of $cPLA_2$. Agonist induced phosphorylation is another necessary element. Several functionally important phosphorylation sites including Ser^{505}, Ser^{727}, Ser^{515} Ser^{437} and $Ser4^{54}$, in the catalytic domain of $cPLA_2$ have been identified (reviewed by Tucker *et al.*, 2009).

Residue Ser^{505} is identified as a consensus site for phosphorylation by MAPKs including ERKs, p38 MAPK and JNK (Lin *et al.*, 1993). *In vitro*, MAPKs mediated phosphorylation of Ser^{505} of $cPLA_2$ resulting in an up to 2 to 3-fold increase in the catalytic activity (reviewed by Kudo and Murakami, 2002). In addition, Ser^{727} can be phosphorylated by MAPK-activated protein kinase MNK1 or another related kinase (reviewed by Burke and Dennis, 2009). Ser^{515} is another important phosphorylation site on $cPLA_2$. Several studies suggest that CaMKII prefers to phosphorylate Ser^{515} of $cPLA_2$ to induce the AA release (Sigal, 1991; Farooqui and Horrocks, 2005). Another two sites, Ser^{437} and Ser^{454} of $cPLA_2$ are also phosphorylated in spodoptera frugiperda (Sf9) cells (Börsch-Haubold et al., 1998). However, it is not clear whether they are important for the $cPLA_2$ activation and which types of kinases are involved in this phosphorylation event (reviewed by Kudo and Murakami, 2002). In general, however, phosphorylation *per se* is insufficient for, but rather plays an augmentative role in $cPLA_2$ mediated cellular AA release, since it was demonstrated that phosphorylated $cPLA_2$ fails to release AA in the absence of an increase in $[Ca^{2+}]_i$ (reviewed by Kudo and Murakami, 2002).

1.6.3.4 Release arachidonic acid by PLC or PLD

Two other main phospholipase enzymes, PLC and PLD, participate in the generation of AA from phospholipids (Balsinde *et al.*, 1999) (Figure 1.5, page 41). Rather than cleave the phospholipid directly to release AA like PLA_2, the phosphoinositide specific PLC (PI-PLC) first splits membrane phospholipid PIP_2 into two second messages including DAG and IP_3 (Smrcka *et al.*, 1991). DAG can then be cleaved to generate AA via a DAG-lipase (Kennerly *et al.*, 1979). Besides, another PLC the phosphatidylcholine specific PLC (PC-PLC) can generate DAG directly from PC (Alcón *et al.*, 2002).

In a similar way, PLD can hydrolyze PC to phosphatidic acid (PA) and choline. PA can then be acted upon by phosphatidic acid phosphohydrolase to yield DAG which can produce AA (reviewed by Nakanishi and Rosenberg, 2006; Hyde and Missailidis, 2009). On the other hand, both PLC and PLD have been reported to facilitate AA release through a PLA_2 pathway. For example, studies show that the PLC reaction substrate, PIP_2, is able to promote the binding of $cPLA_2$ to lipid vesicles in a Ca^{2+} independent manner, which dramatically increases the $cPLA_2$ activity (Mosior *et al.*, 1998). Similarly, PLD has been reported to facilitate the $cPLA_2$ activation as well (Ueno *et al.*,

2000).

1.6.3.5 Arachidonic acid metabolism

AA is the precursor in the production of eicosanoids. Eicosanoids are important cell signaling molecules play a central role in the cellular signaling cascades. They exert complex control in essential functions such as inflammation and immunity. It has recently been identified that their abnormal activation is associated with some cancers (reviewed by Nakanishi and Rosenberg, 2006). Given these findings, understanding the cascades of AA metabolism is critical to the study of cancer and inflammatory disease (Mignen *et al.*, 2003).

AA can be metabolized to eicosanoids via three pathways, namely the cyclooxygenase (COX) pathway, the lipoxygenase (LOX) pathway and the cytochrome P450 (CYP450) pathway. So far, three isoforms of the membrane bound enzyme COX have been identified, COX-1, COX-2 and COX-3. In the COX pathway, AA is converted into three main products: prostaglandins (PGs), prostacyclin I_2 and thromboxane A_2 (reviewed by Nakanishi and Rosenberg, 2006). There are nine PGs that have been identified. PGA_2, PGD_2, PGE_2 and PGF_2 are the major products in this AA metabolism. They bind a subfamily of cell surface seven-transmembrane receptors, G-protein-coupled receptors, performing variety of functions in different types of cells (reviewed by Tucker *et al.*, 2009). Another important product of COX pathway is the generation of thromboxane. It is a vasoconstrictor and a potent hypertensive agent, and it facilitates platelet aggregation.

In the LOX pathway, AA leads to the formation of the leukotrienes, lipoxins and hepoxilins. Leukotrienes act principally on a subfamily of G protein coupled receptors. They function in various physiological processes including asthmatic, allergic reactions and inflammatory responses. The enzyme CYP450 converts AA into epoxyeicosatrienoic acids (EETs). EETs are signaling molecules that act as short-range hormones in cardiovascular system and kidney. They cause Ca^{2+} release from the intracellular stores and increase the cell proliferation (reviewed by Watanabe *et al.*, 2003).

1.7 Ca^{2+} signaling and cell spreading

Among the cell cycle regulatory elements, what caught our attention is an interaction between Ca^{2+} and the cell shape. The Ca^{2+} signal is affected by the state of the actin cytoskeleton, as mitogen-induced Ca^{2+} mobilisation in NIH 3T3 cells is abolished by cytochalasin D. This agent disrupts the actin cytoskeleton (Ribeiro *et al.*, 1997). However, the SOCE in NIH 3T3 cells was reduced by actin cytoskeleton disruption (Ribeiro *et al.*, 1997). Another drug, jasplakinolide, which can induce polymerization of monomeric actin, was observed to prevents SOCE but has little effect on the receptor activated Ca^{2+} store depletion (Patterson *et al.*, 1999). Thus, the actin cytoskeleton does not appear to play an obligate role *per se* in the SOCE pathway. The role of the microtubule cytoskeleton in SOCE has also been investigated as well. However, several studies have reported that nocodazole, a drug which causes depolymerization of the microtubular cytoskeleton, fails to inhibit SOCE or I_{CRAC} in rat basophilic leukemia (RBL) and chicken DT40 B lymphoma (DT40) cells (Bakowski *et al.*, 2001; Baba *et al.*, 2006). Nevertheless, microtubules are reported to play a facilitatory role in organizing STIM1 for optimal Ca^{2+} sensing and/or communication with Orai channels (Smyth *et al.*, 2007). Recent research has also shown that restricting cell spreading in Swiss 3T3 cells, by using adhesive islands to control cell shape, blocks the mitogen-evoked Ca^{2+} influx (Pennington et al., 2007).

1.8 Objectives of the research

The strict control of the cell cycle progression is the key guarantee of normal cell physiology activities. The cell cycle phase to phase transitions are mainly regulated by different cyclin-CDK combinations and CKIs (Brooks, 2005). In addition, mitogenic stimuli are required for the transition of G_0 to G_1 phase and also for the G_1 progressing to S phase. Mitogens function through various intracellular signal pathways, such as the MAPKs or ERKs pathway plays a critical role in G_1 progression (Pages *et al.*, 1993).

Moreover, it was found that the $[Ca^{2+}]_i$ response which could be evoked by mitogens is another key regulator in the cell cycle control. For example, both the intracellular Ca^{2+} store depletion and the presence of extracellular Ca^{2+} are necessary for the transitions between G_0/G_1 and G_1/S phases (Takuwa *et al.*, 1995; Santella *et al.*, 2005). Ca^{2+} with its binding proteins mediates the cell

cycle by affecting various regulators, such as p27, p21, CDK2 and CDK4 at different transitions (Rasmussen and Means, 1987).

In addition to the Ca^{2+} signaling, cell adhesion and cell spreading are influential to the cell cycle regulation as well. Cell adhesion to ECM permits the entry from G_0 to G_1 (Folkman and Moscona, 1978). The adhesion facilitates the signal transferring from the ECM proteins to the intracellular pathways, such as MAPK pathway, which fulfils the regulation of the cell cycle (Zhu and Assoian, 1995). On the other hand, the normal spreading cell shape and intact cytoskeleton are suggested to be the critical regulators in the transition from G_1 to S phase (Huang and Ingber, 1999). It was reported that restriction of the CE cell spreading prevents the increase of cyclin D and the down regulation of p27 arresting in G_1 phase (Huang *et al.*, 1998).

Although it has been widely accepted that both Ca^{2+} signaling and cell shape can mediate cell cycle progression, the regulation mechanisms are not fully understood. A relationship between these two elements, Ca^{2+} signaling and cell shape has been reported. For instance, it was observed that disruption the actin cytoskeleton by cytochalasin D result in the inhibition of ATP or platelet-derived growth factor evoked $[Ca^{2+}]_i$ responses in NIH 3T3 cells (Ribeiro *et al.*, 1997), while jasplakinolide was observed to prevent SOCE in A7r5 cells (Patterson *et al.*, 1999). More importantly, a recent study revealed that, in Swiss 3T3 cells, restricting the cell spreading with polyHEMA adhesive islands not only prevents the cell cycle progression but also blocks the mitogen (bombesin)-evoked Ca^{2+} influx (Pennington et al., 2007). Such findings imply a possible role of Ca^{2+} that accounts for the cell shape regulation of cell cycle progression.

Based on these findings, the aim of this study is to identify the mechanism of this cell shape-dependent and bombesin-evoked Ca^{2+} influx. PolyHEMA islands (ø22μm and ø45μm) have been used to restrict the spreading of Swiss 3T3 cells (Ireland *et al.*, 1987; Pennington *et al.*, 2007). It is well known that there are two major Ca^{2+} entry pathways existed in non-excitable cells. These include SOCEs and AA regulated Ca^{2+} influx. A previous study in our laboratory has suggested that this bombesin-induced Ca^{2+} influx is more likely to be activated through the regulation of AA, since it was observed that bombesin acted like 5,8,11,14-eicosatetraynoic acid

(ETYA), a non-metabolizable analogue of AA, but not thapsigargin in Ba^{2+} and Sr^{2+} influxes (Foster, 2005). Therefore, the AA-induced Ca^{2+} influx has been studied first.

As described in section 1.3.8.3, the $cPLA_2$ pathway is the primary way to generate AA. Since the translocation of $cPLA_2$ to intracellular membranes with the increase of $[Ca^{2+}]_i$ is suggested to rely on the actin cytoskeleton (Cybulsky *et al.*, 2004), altering the cell spreading by adhesive islands is likely to affect the activation of $cPLA_2$ which may account for the absence of Ca^{2+} influx in restricted cells. As a result, the involvement of $cPLA_2$ activation in the bombesin-evoked Ca^{2+} influx was studied. The study focused on the phosphorylation of $cPLA_2$, as it is another key prerequisite for the $cPLA_2$ activation. Immunofluorescence was utilized as the main approach.

On the other hand, the possible role of SOCEs in this bombesin-evoked shape dependent Ca^{2+} influx pathway cannot be ruled out. Referring to the various models of SOCEs described in section 1.3.7, alteration of the cell shape might affect the link between ER and SOCCs. Furthermore, STIM1, as the pivotal molecular component in SOCEs, is guided by microtubules to translocate to puncta (Smyth *et al.*, 2007). Hence, the involvement of SOCEs was investigated using SOCE inhibitors. In addition, the formation of STIM1 puncta was examined to identify SOCEs.

Once the mechanism of this cell shape required Ca^{2+} influx is revealed, it might be possible to explain how the cell shape inhibits the bombesin-induced Ca^{2+} influx in the cell on small islands and why the cell failed to enter S phase in the cell cycle.

Chapter 2

Material & Methods

Contents:

Part 1: Methods

2.1 Cell culture

2.1.1 Cell culture in flasks

Swiss 3T3 cells were cultured in Dulbecco's modified Eagle's medium containing 10% fetal calf serum (FCS) and 1% antibiotic/mycotic (10% FCS-DMEM) and maintained in a humidified carbon dioxide (CO_2) incubator at 37°C. The media was replenished 2-3 times per week and the cells were passaged when they were approximately 80% confluent. When passaging, the media was removed and the cells were washed with 5ml PBS (136.8mM NaCl, 2.68mM KCl, 6.21mM Na_2HPO_4 and 1.47mM KH_2PO_4). In order to remove the cells from the surface of the flask, they were treated for 5 minutes (at 37°C) with 0.05% trypsin-0.02% EDTA using 1 and 3 ml volume for a $25cm^3$ and $75cm^3$ flask respectively. Subsequently, the flasks were gently tapped in order to dislodge the cells. Then, each flask was supplemented with 5-10ml 10% FCS-DMEM to stop the digestion by 0.05% trypsin-0.02% EDTA. The cell suspension was centrifuged at 140xg for 5 minutes. The supernatant was removed and the cell pellet was resuspended in 5 or 10ml 10% FCS-DMEM and divided into flasks. Cells were cultured in 25ml 10% FCS-DMEM for a $75cm^3$ flask and 5ml for a $25cm^3$ flask.

2.1.2 Plating cells onto coverslips/ islands

To plate the cells on coverslips, cells were removed from the surface of the flasks and centrifuged as described in section 2.1.1. Cells were resuspened in 15ml 10% FCS-DMEM. The cell suspension was then plated into a UV sterilized 6-well plate containing one coverslip in each well. Each coverslip was covered with 1ml of this cell suspension and 1ml of FCS-DMEM media.

To restrict the cell shape, 3-4 days old Swiss 3T3 cells were plated onto sterilized coverslips coated with either small or large palladium islands that were placed in 6-well plates in 10% FCS-DMEM following the same protocol as described above. The density of cells added to the coverslips need to be controlled. For the small islands, it was approximately 4×10^5 cells/ml, while for the large island it was 2×10^5 cells/ml.

Cells on coverslips or islands were allowed to attach in the presence of serum for 3-4 hours until attached and then kept in serum free (SF)-DMEM for 16 hours before each experiment.

2.1.3 Cryopreservation of cells

After the Swiss 3T3 cells were cultured in flasks for 3 to 4 days, they were removed from the surface of the flasks and centrifuged following the protocol described in section 2.1.1. The cell pellet was resuspended with fresh made freezing medium made up with 10% DMSO and 90% FCS. Subsequently, the cell suspension was divided into cryovial tube (1ml each tube). All the cryovial tubes were placed into a Mr. Frosty and kept in a -80°C freezer. Cells were left in the -80°C freezer overnight and were then transferred to the liquid nitrogen dewar.

To re-grow the cells that were kept in liquid nitrogen, cells were thawed using a water bath pre-heated to 37°C. The thawed cells were placed into a $25cm^3$ flask contained 5ml pre-warmed FCS-DMEM. The media was changed with fresh FCS-DMEM when the cells had adhered to the flask.

2.2 Coverslip preparation

2.2.1 Preparation of adhesive islands

Round glass coverslips (ø22μm) were first cleaned. They were immersed in chromic acid for about 15 minutes and rinsed under fast flowing water. After that, the coverslips were placed into racks and immersed in distilled water for 1.5 hours while the water was changed every half an hour. After the washing, they were dried at 60°C.

2.2.2 PolyHEMA coating

A 12% (w/v) polyHEMA stock in 95% ethanol was prepared. The solution needed to be incubated at 37°C overnight to ensure that the polyHEMA was completely dissolved. Before the next step, the stock solution was centrifuged at 2500rpm for 30 minutes to pellet any un-dissolved polyHEMA. The polyHEMA stock was stored in the dark at room temperature until required. A 1%

(w/v) solution of polyHEMA was prepared freshly by diluting the 12% polyHEMA stock with 95% ethanol. Each coverslip was evenly covered with 40µl of 1% polyHEMA. The coated coverslips were dried for 90 minutes at room temperature and at 60°C for another 90 minutes.

2.2.3 Palladium coating

Palladium was then deposited onto the surface of these polyHEMA-coated coverslips by using an Edwards 12E6 vacuum coating unit (Figure 2, page 56). In this system, palladium wire (0.125mm in diameter and 11mm in length) was first twined around a tungsten filament that could be placed between the two electrodes of the coating unit. The palladium wire could be evaporated using 40 watts for 20-30 seconds (16A at 2.5V). Evaporated palladium deposited on coverslips through photolithographically etched copper foils to form different sizes of islands. Three types of foil islands masks were used. Two could form either large (ø45µm) or small (ø22µm) islands on coverslips, another one could form mixed sizes of islands (from ø10µm to ø45µm) a long with large areas for normal spreading cells on each coverslip.

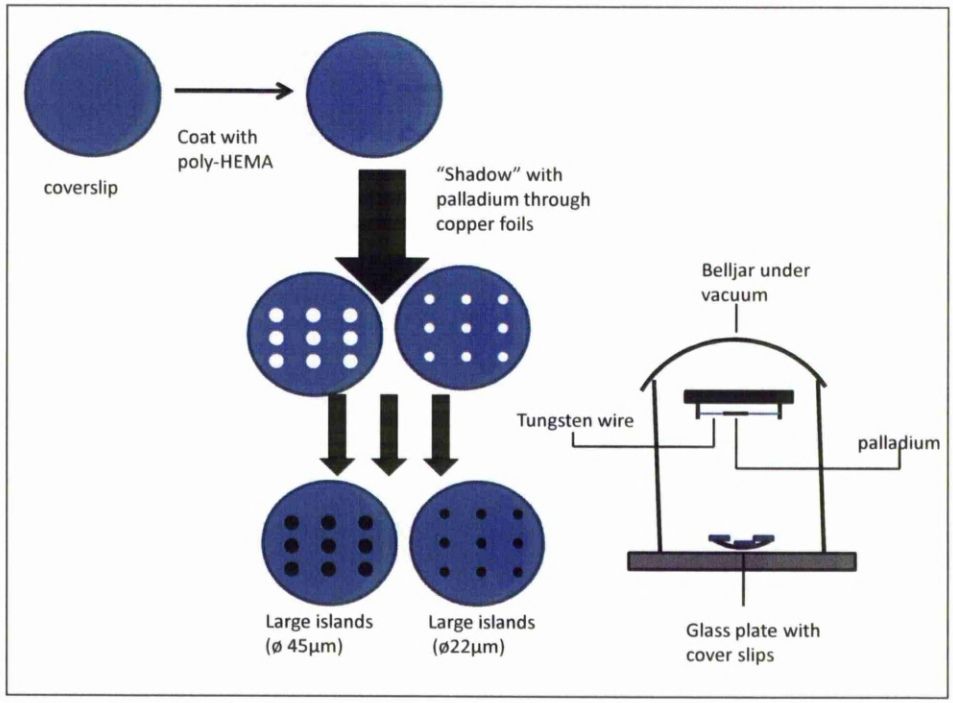

Figure 2-The process of making polyHEMA surrounded palladium coated adhesive islands

The figure shows the process of making adhesive islands. Glass coverslips were first coated with poly-HEMA, and then palladium was deposited onto these coverslips in a vacuum system. The figure is adopted from the Foster's thesis (2005).

2.3 Experiments with a PTI deltascan based imaging system

2.3.1 Prepare the cells for Ca^{2+} imaging

Cells need to be transferred onto glass coverslips (ø22μm) or adhesive islands 1 day before the experiments using PTI Ca^{2+} imaging system. For the normal spreading cells, experiments were performed on both non-confluent and confluent cells. Normally, the non-confluent cells were 1-2 days cultured while the confluent and quiescent cells were 4-5 days cultured before plated onto coverslips. For the restricted cells, 3-day old Swiss 3T3 cells were used and transferred onto islands.

A 6-well plate containing one glass coverslip or a palladium coated coverslip with islands in each well was sterilized under UV light for 30 minutes. After that, cells were transferred onto the sterilized coverslips following the protocol described in section 2.1.2. After 3-4 hours' culture in 10% FCS-DMEM, the cells were changed to SF-DMEM to avoid cell proliferation. They were cultured for 16 hours serum free before the experiments.

2.3.2 Loading cells with fura-2

Fura-2-acetoxymethyl ester (Fura-2 AM) is a membrane-permeable derivative of the ratiometric Ca^{2+} indicator used to measure $[Ca^{2+}]_i$ by fluorescence. After fura-2 diffuses inside the cell, its acetoxymethyl easter group is hydrolyzed by cellular esterases. Removal of the esters regenerates "fura-2", the pentacarboxylate Ca^{2+} indicator. Fura-2 fluorescence was excited at wavelengths of 340nm and 380nm reflecting the excitation peaks in Ca^{2+}-saturated and Ca^{2+}-free conditions, respectively. The emission intensity 510nm from each excitation wavelength (340 and 380nm) was measured and used to generate a ratiometric measure of $[Ca^{2+}]_i$. In addition, 340/380nm ratio can be used to monitor Sr^{2+}, Ba^{2+} fluxes and 340/360nm ratio can be used for Mn^{2+} quench protocol.

HEPES buffered saline (HBS), which contains 145mM NaCl, 5mM KCl, 1mM $MgSO_4$, 1mM NaH_2PO_4 and 10mM Hepes, was prepared and supplemented with 10mM glucose prior to each experiment. Loading buffer was made by preparing HBS containing 2μM fura-2 and 0.012% pluronic F127, 0.1%w/v BSA and 200μM sulphinpyrazone (SPZN). Each coverslip with cells was

immersed with 1ml loading buffer at 37°C for 45-60 minutes in the dark. After loading, the cells were rinsed in Ca^{2+} free HBS to remove excess dye and kept in HBS (Ca^{2+} free or containing 1mM Ca^{2+}) at 37°C until use.

2.3.3 Ca^{2+} measurement

The PTI Ca^{2+} imaging system was coupled to a Nikon Diaphoto inverted microscope. Cells are excited at 340nm and 380nm using a PTI Deltascan light source. The light is then directed to the cells using a Nikon m400 dichronic mirror. The emitted light is able to pass through the dichronic mirror and be detected by a photonic science intensified charge-coupled camera after passing through a 510nm band pass filter. The 340nm and 380nm signals are then converted by a software into 340nm/380nm ratiometric traces and used to indicate the changes in $[Ca^{2+}]_i$.

The coverslip with cells was placed in a purpose built water-jacketed chamber with the cells immersed in a 1ml volume of HBS.

2.3.4 Ca^{2+} calibration

The intracellular Ca^{2+} concentration can be calibrated by converting the ratio (F340/F380) to $[Ca^{2+}]_i$ using an equation derived by Grynkiewicz *et al.* (1985). It requires five parameters including the ratio of the fura-2 fluorescent signals at 340nm/380nm (R), the maximum ratio (R_{max})in saturating Ca^{2+}, the minimum ratio (R_{min}) in zero Ca^{2+}, dissociation constant (Kd) for fura-2 in Ca^{2+} and the ratio of maximum and the fluorescence of the Ca^{2+} free dye at 380nm/fluorescence of the Ca^{2+} bound dye at 380nm (β).

$$[Ca^{2+}]_i=Kd\beta(R-R_{min})/(R_{max}-R)$$

In order to get the R_{max}, ionomycin (3μM) was added to cells in HBS which induced a rise in $[Ca^{2+}]_i$. While the R_{min} was obtain by adding EGTA (10mM) to cells in HBS again in the presence of ionomycin.

2.4 Experiments with the flexstation microplate reader

2.4.1 Flexstation reader

The Molecular Devices Flexstation is a benchtop scanning fluorometer and integrated fluid transfer workstation capable of conducting endpoint, kinetic, lambda scan and well scan experiments in a multi-well plate format (6, 12, 24, 48 and 96-well) and fluidics transfer experiments in 96-well format. The Flexstation Reader was used to monitor the $[Ca^{2+}]_i$ response in Swiss 3T3 cells by measuring fura-2 fluorescence. A set of eight wells of a 96-well plate were read in a single column simultaneously. The machine monitors all the wells in a column over a time course, during which up to three compounds can be added robotically. Multiple columns are read sequentially for additional run times.

2.4.2 Preparing cells for the flexstation

2-3 days old Swiss 3T3 cells were first plated onto 96-well plates with half of the plate 48 wells used. The cell concentration was carefully controlled, from $5x10^4$ to $7.5x10^4$ cells per well. Each well was added with 100µl cells suspension in 10% FCS-DMEM. After cultured at 37°C for 3-4 hours, 10% FCS-DMEM was aspirated and the cells were washed 3X in HBS with 1mM Ca^{2+}. Subsequently, SF-DMEM was added into each well (100µl). Cells were cultured for 6-16 hours before the Flexstation experiment.

2.4.3 Loading cells with fura-2

Fresh Ca^{2+} loading buffer was prepared as described in section 2.3.2. The SF-DMEM was removed from the assay plate of cells with a multichannel pipette and then 100µl loading solution was added into each well instead. The plate was placed in a 37°Cincubator for 45 minutes in the dark. After the cells were loaded with fura-2, the loading buffer was replaced with HBS either with 1mM Ca^{2+} or EGTA or Ca^{2+} free (80µl per well) depending on what the experiment was carried out.

2.4.4 Preparing the compound plate

The compound plate was prepared 30 minutes before starting the Flexstation. All the compounds

were made at 5X the final desired concentration by diluting stock with Ca^{2+} free or 1mM Ca^{2+} contained HBS. Each compound was added into corresponding column, 300µl per well, according to the time point at which it should be added to the assay plate. The prepared the compound plates was kept on ice and transferred into a 37°C incubator to warm up 10 minutes prior the experiment.

2.4.5 Experimentation

The Flexstation plate reader was usually started at least 30 minutes in advance, since the machine needed to warm up to 37°C. Then, both the assay plate and the compound plate were put into the Flexstation microplate reader and reading initiated. The first addition point was always set at 20 seconds after starting a run in order, to record a baseline before additions. Subsequent addition time points varied in different assays. The data was recorded and analyzed by SoftMax Pro software.

2.5 Immunofluorescence

2.5.1 Staining the phospho-cPLA$_2$ in normal spreading cells

3-4 days old Swiss 3T3 cells were plated onto UV sterilized coverslips (ø 22µm) in a 6-well plate in 10% FCS-DMEM as described in section 2.1.2 and allowed to grow as normal till 60% confluent.

Medium was removed from the cells and washed 3X in PBS. In order to fix the cell, 1ml 100% methanol was added to each well of a 6-well plate at room temperature for 10 minutes. After that, cells were washed 3X in PBS. Ten percent chicken serum in PBS was added into each well to block the cells for 1 hour at room temperature.

The primary antibody was diluted 1 in 100 in PBS containing 1% of the same chicken serum that used for blocking and 1% triton X100. Forty microliters of this primary antibody solution was placed on to each of the coverslips and they were incubated overnight at 4°C. Each coverslip was covered with parafilm to prevent the primary antibody solution from drying.

The next day, cells were rinsed 3X in PBS allowing 10 minutes for each wash. The second antibody was diluted 1 in 500 in PBS containing the same 1% chicken serum and 1% triton X100. Then, the cells were incubated with 40µl of secondary antibody solution and each coverslip covered with parafilm for 1 hour at room temperature in dark. Cells were then washed 3X in the same way with PBS to remove the excess second antibody. Finally, coverslips were placed on glass slide and mounted with VECTASHIELD with the edge sealed with nail varnish.

2.5.2 Staining the phospho-cPLA$_2$ in shape restricted cells

Cells were transferred onto coverslips with adhesive islands according to the protocol mentioned in section 2.1.2. After about 16 hours, the cells were washed 3X in PBS. Following that, the cells were fixed with 100% methanol for 5 minutes at room temperature. The fixation time is reduced to 5 minutes in order to protect the polyHEMA from dissolving by methanol. After that, the primary and secondary antibody was used in a same way as described in section 2.5.1. Finally, the stained cells were mounted with VECTASHIELD as before.

2.5.3 Confocal microscopy

Confocal microscopy is an optical imaging technique used to increase micrograph contrast and/or to reconstruct three-dimensional images by using a spatial pinhole to eliminate out-of-focus light in specimens that are thicker than the focal plane.

Images of the stained cells were acquired using an inverted Leica SP2 AOBS laser scanning confocal microscope that allowed 458, 476, 488, 496, 514, 574, 594 and 633 laser line excitation. The FITCwide program was chosen for cells stained with the Alexa Fluor 488 chicken anti-rabbit IgG. The laser line 594 was used to excite the cells stained with the Alexa Fluor 596 chicken anti-rabbit IgG. Emission band width was adjusted to give optimal signal with no overlap into other channels. The scan speed was set as 400Hz per second. A scan format of 1024x1024 was used. The image was obtained from a frame average of 6. The gain and offset settings were always kept the same during each experiment to allow determination of relative intensities. The 63x oil immersion objective was normally used.

2.6 Plasmid transfection

2.6.1 Preparing the plasmid

The plasmids: mCherry-STIM1 and YFP-STIM1 were obtained from the laboratory stock prepared following standard plasmids preparation protocol by colleagues. I have prepared the GFP-cPLA$_2$ plasmid using a similar protocol, which is described in Appendix 1.

Part 2: Materials

name	supplier
Swiss 3T3 fibroblast	A gift from professor Pennington
Dulbecco's modified Eagle's medium (DMEM)	Invitrogen
Trypsin-EDTA	Invitrogen
Fetal Calf Serum	Invitrogen
antibiotics&antimyotics	Invitrogen
Bombesin	CalBiochem
Thapsigargin	Calbiochem
ETYA	CalBiochem
fura-2 AM	Invitrogen
Pluronic F127	Sigma Aldrich Chemical Company
Sulphinpyrazone	Sigma Aldrich Chemical Company
$CaCl_2$ solution	BDH Laboratory Suppliers
$BaCl_2$	Sigma Aldrich Chemical Company
$SrCl_2$	Sigma Aldrich Chemical Company
LOE908	Tocris
SK&F 96365	CalBiochem
$cPLA_2\alpha$ inhibitor	CalBiochem
AACOCF3	CalBiochem
RHC80267	CalBiochem
PolyHEMA	Sigma Aldrich Chemical Company
Ethanol	Sigma Aldrich Chemical Company
phospho-$cPLA_2$ antibody(Ser 505)–R rabbit	Santa Cruz Biotechology
Anti-rabbit immune-globulin 488 or 596	Invitrogen
YFP-STIM1 plasmid	A gift from Professor Bob Burgoyne
mCherry-STIM1 Plasmid	A gift from Professor Bob Burgoyne
JetPRIME	Polyplus
GeneJuice	Novagen

Chicken Serum	Sigma Aldrich Chemical Company
Goat Serum	Sigma Aldrich Chemical Company
Triton 100x	Sigma Aldrich Chemical Company
Methanol	Sigma Aldrich Chemical Company
ERK inhibitor FR180204	CalBiochem
PD98059	CalBiochem
Bromoenol Lactone(BEL)	CalBiochem
Flasks($25cm^3$ and $75cm^3$)	Sarstedt
6-well and 96-well tissue culture plate	Corning
Cover glass	VWR

Chapter 3

Defining the system

Contents:

Figures:

3.1 Introduction

The main aim of the thesis is to investigate cell shape-dependent Ca^{2+} influx induced by the mitogen: bombesin. Swiss 3T3 cells were chosen because cell-shape regulation of Ca^{2+} influx and proliferation was first characterized using this type of cell (Ireland *et al.*, 1987; Pennington *et al.*, 2007). Before undertaking a more detailed investigation of the cell-shape-dependent Ca^{2+} influx, a series of experiments were performed to confirm that the bombesin-evoked $[Ca^{2+}]_i$ responses in Swiss 3T3 cells were consistent with earlier observations. In addition, the influence of cell density on bombesin-evoked $[Ca^{2+}]_i$ responses was studied with both confluent and non-confluent cells, because earlier experiments suggested that cell density might affect the $[Ca^{2+}]_i$ responses (Evans *et al.*, 1984; Otun *et al.*, 1992).

Two additional agonists, ETYA and thapsigargin, were used to test the $[Ca^{2+}]_i$ response. ETYA has been used to induce AA regulated Ca^{2+} entry as it is an analogue of AA. However, the ability of ETYA in inducing ARC influx is less effective than AA itself (Mignen *et al.*, 2008). While ETYA induces a NSOCE, thapsigargin is the typical agonist for inducing SOCEs. Both agonists were used to test the existence of ARC channel and SOCC activity in Swiss 3T3 cells.

In addition, palladium coated islands surrounded by non-adhesive polyHEMA were used to restrict the cell shape. The bombesin-induced $[Ca^{2+}]_i$ response was then examined in shape-restricted cells. Previous studies have reported that the bombesin-induced Ca^{2+} influx was inhibited in cells on small islands (ø22μm) (Pennington et al., 2007). Similar experiments were repeated to confirm the existence of such cell-shape-dependent Ca^{2+} influx.

3.2 Methods

3.2.1 Cell culture

Swiss 3T3 cells were cultured in flasks and then transferred onto glass coverslips according to standard protocol as described in section 2.1. The confluent cells were cultured for 4-5 days until they were closely packed while the non-confluent cells were cultured for 1-2 days in flasks before transferred onto coverslips (Section 2.3.1). For the experiments using shape-restricted cells, cells

were transferred onto either large (ø45μm) or small (ø22μm) islands according to standard protocol as described in section 2.1.2.

Cells on coverslips or islands were grown for 3-4 hours until attached in FCS-DMEM and then kept in SF-DMEM for 16 hours before each experiment.

3.2.2 Ca^{2+} imaging

During the experiment, cells on glass coverslips or islands were loaded with 2μM fura-2 as described in section 2.3.2 and immersed in HBS containing either 1mM Ca^{2+} or 1mM EGTA. Cells were stimulated with agonists: 100nM bombesin, 2μM thapsigargin or 100nM/1μM ETYA to induce $[Ca^{2+}]_i$ responses in different experiments. The changes of fura-2 fluorescence were monitored using the Ca^{2+} imaging system (Section 2.3.3). More details of the each experiment are described in section 3.3.

3.3 Results

3.3.1 Bombesin-induced $[Ca^{2+}]_i$ response

Figure 3.3.1A (a) shows two typical bombesin-induced $[Ca^{2+}]_i$ responses in a normal spreading confluent or non-confluent Swiss 3T3 cell in HBS containing 1mM Ca^{2+}. In total, 4 experiments were carried out using confluent cells while 5 experiments were performed in non-confluent cells. The results indicated that 100nM bombesin could consistently induce a $[Ca^{2+}]_i$ response, although the amount of Ca^{2+} influx varied among cells. All the confluent cells in each experiment showed a $[Ca^{2+}]_i$ response (n=42 cells). However, it is not the case in non-confluent cells. In 2 out of 5 experiments, approximately half of the non-confluent cells failed to response to bombesin, therefore, only 26 out of 31 non-confluent cells showed a bombesin-induced $[Ca^{2+}]_i$ response.

Similarly, figure 3.3.1B (a) shows two typical bombesin-induced $[Ca^{2+}]_i$ responses in a normal spreading confluent or non-confluent Swiss 3T3 cell in HBS containing 1mM EGTA. Results are representative of 22 and 23 experiments for confluent and non-confluent cells respectively. Consistent with what is indicated in figure 3.3.1A, in 8 out of 23 experiments, approximately half

of the non-confluent cells showed a Ca^{2+} release. Therefore, 13 out of 130 non-confluent cells failed to response to bombesin, whereas all the 312 confluent cells showed a Ca^{2+} release. This further confirms that 100nM bombesin is an effective agonist to induce $[Ca^{2+}]_i$ response in Swiss 3T3 cells although it is relatively less efficacious in the non-confluent cells.

The bombesin-evoked Ca^{2+} release and Ca^{2+} influx in either confluent or non-confluent quiescent Swiss 3T3 cells are compared in figure 3.3.1A (b) and figure 3.3.1B (b). The statistical analysis suggested that the stimulation by bombesin caused a significantly bigger Ca^{2+} influx and a much smaller Ca^{2+} release in non-confluent cells than that in the confluent cells.

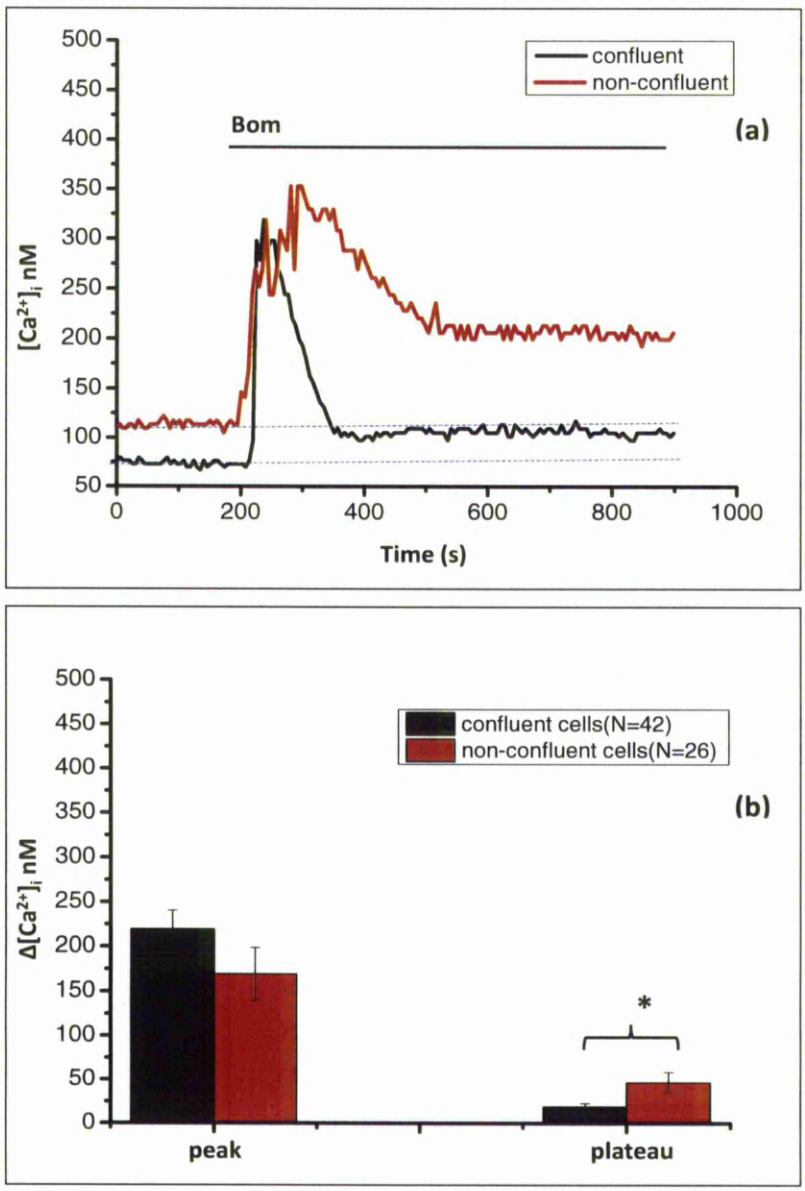

Figure 3.3.1A-Bombesin-induced Ca^{2+} influx

Quiescent Swiss 3T3 cells were cultured, unrestricted on glass coverslips in SF-DMEM for 16 hours before experiments. (a) Typical Ca^{2+} responses to bombesin (100nM) are shown in the presence of 1mM Ca^{2+} in confluent cells (black) or non-confluent cells (red). The $[Ca^{2+}]_i$ was measured using fura-2, at 37°C. (b) Mean data of increased $[Ca^{2+}]_i$ at both the peak and plateau of the responses caused by the addition of bombesin (100nM) were indicated in solid bars. The $\Delta[Ca^{2+}]_i$ is measured as the $[Ca^{2+}]_i$ at the peak or plateau, which is 400 seconds after the peak, minus the baseline $[Ca^{2+}]_i$ before the addition of bombesin. Error bars shown are ± S.E. of (N) number of indicated cells. *$P<0.05$, when $\Delta[Ca^{2+}]_i$ value of (N) number of cells were subjected to t-test.

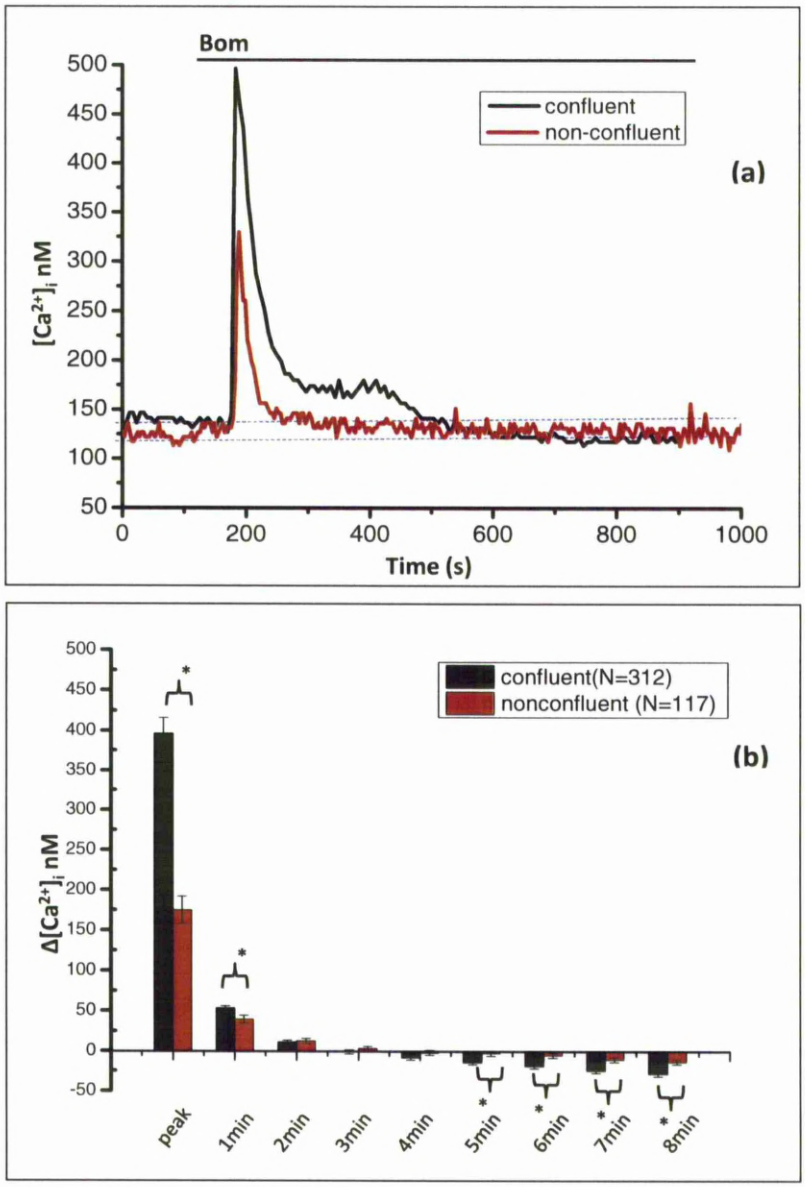

Figure 3.3.1B–Bombesin-induced Ca^{2+} release

Quiescent Swiss 3T3 cells were cultured, unrestricted on glass coverslips in SF-DMEM for 16 hours before experiments. (a) Typical Ca^{2+} responses to 100nM bombesin are shown in the presence of 1mM EGTA in confluent cells (black) or non-confluent cells (red). The $[Ca^{2+}]_i$ was measured using fura-2, at 37°C. (b) Mean changes in $[Ca^{2+}]_i$ at the peak and plateau of the responses caused by the addition of bombesin (100nM) were indicated in solid bars. The black bars represent the data of confluent cells and the red bars show the data of non-confluent cells. The $\Delta[Ca^{2+}]_i$ is measured as the $[Ca^{2+}]_i$ at the peak and series time points of plateau, which are from 1 minute to 8 minutes after the peak, minus the baseline $[Ca^{2+}]_i$ before the addition of bombesin. Error bars shown are ± S.E. of (N) number of indicted cells. *P<0.05, when $\Delta[Ca^{2+}]_i$ value of (N) number of cells were subjected to t-test.

3.3.2 Thapsigargin-induced Ca^{2+} influx

Figure 3.3.2 shows two typical thapsigargin-evoked $[Ca^{2+}]_i$ responses in Swiss 3T3 cells. The results indicate that thapsigargin (2μM) does not induce a consistent $[Ca^{2+}]_i$ response and the responses vary among cells even in the same experiment. In total, 12 separate experiments (n=97 cells) were repeated.

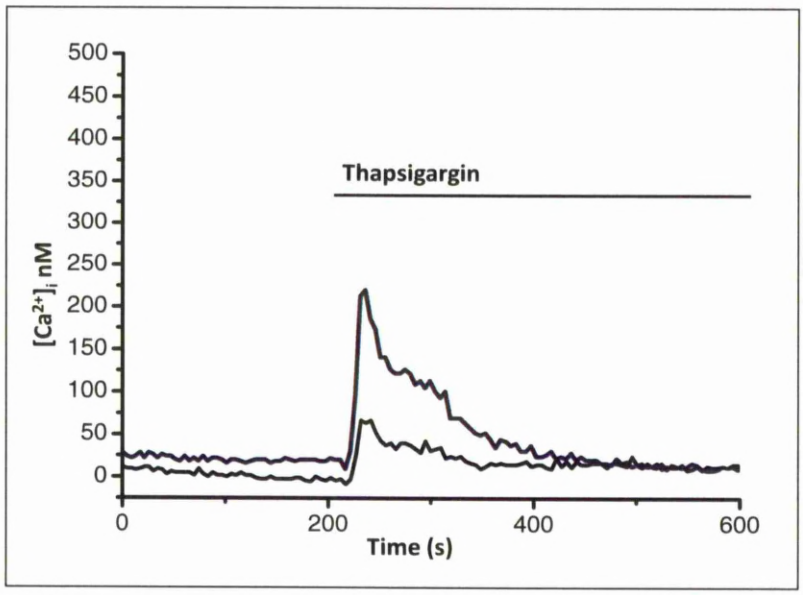

Figure 3.3.2-Thapsigargin-induced Ca^{2+} influx

3-day-old quiescent Swiss 3T3 cells were cultured, unrestricted on glass coverslips in SF-DMEM for 16 hours before experiments. Two $[Ca^{2+}]_i$ responses are shown to thapsigargin (2μM) which was added at 200 seconds in the presence of 1mM Ca^{2+} in HBS. The $[Ca^{2+}]_i$ was measured using fura-2, at 37°C. The figure is representative of the variation seen in 12 separate experiments.

3.3.3 ETYA-induced Ca^{2+} influx

Figure 3.3.3 shows typical ETYA-induced $[Ca^{2+}]_i$ responses in Swiss 3T3 cells. Cells showed an elevation in $[Ca^{2+}]_i$ on addition of 100nM ETYA in 2 (n=17 cells, figure a) out of 13 experiment (n=94 cells). The proportion of responsive cells increased to 10 (n=65 cells, figure b) out of 23 experiments (n=168 cells) when the concentration of ETYA was increased to 1μM. Consequently, ETYA rarely evoked a $[Ca^{2+}]_i$ response at 100nM and elicited a response in about 50% of experiments at 1μM.

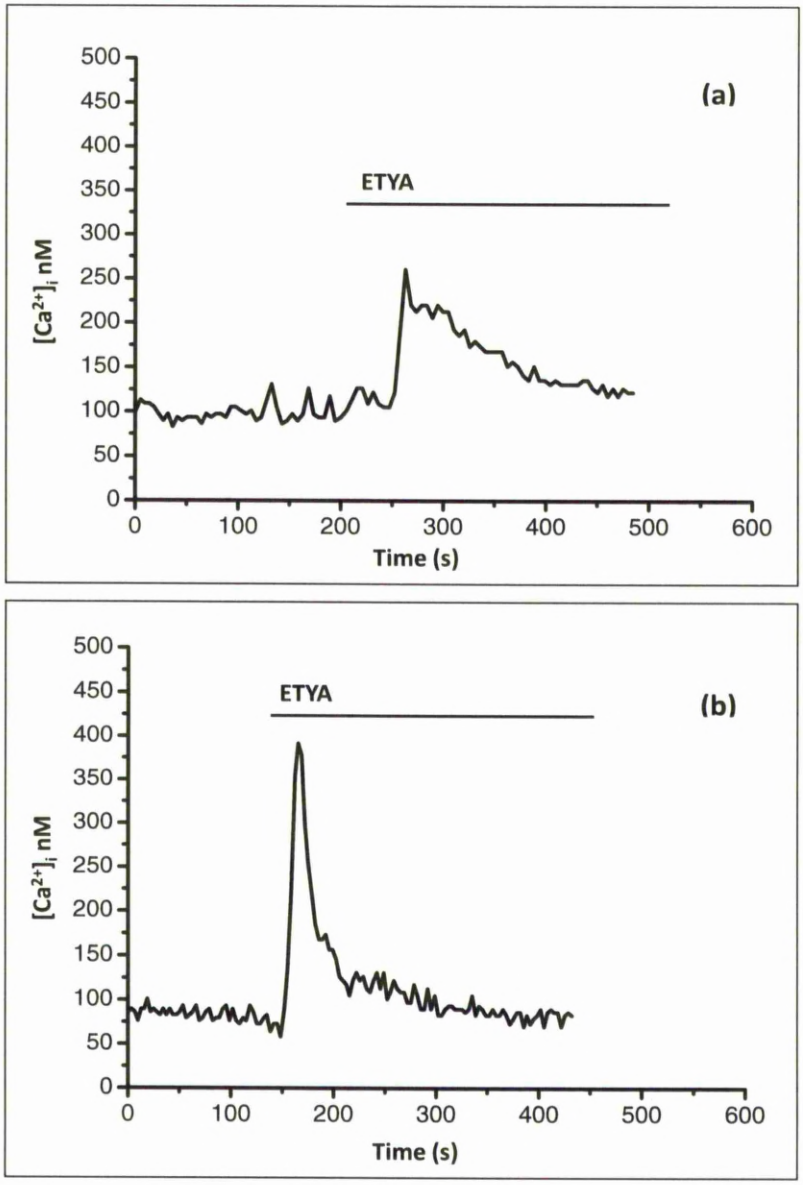

Figure 3.3.3-ETYA-induced Ca^{2+} influx

3-day-old quiescent Swiss 3T3 cells were cultured, unrestricted on glass coverslips in SF-DMEM for 16 hours before experiments. Two $[Ca^{2+}]_i$ responses are shown to 100nM (a) and 1μM (b) ETYA added at 200 and 150 seconds, respectively, in the presence of 1mM Ca^{2+} in HBS. The $[Ca^{2+}]_i$ was measured using fura-2, at 37°C. Figure (a) represents typical $[Ca^{2+}]_i$ responses to 100nM ETYA seen from cells in the 2 experiments when clear responses were seen. In a further 11 experiments, no response to 100nM ETYA was observed. Figure (b) represents typical $[Ca^{2+}]_i$ responses to 1μM ETYA seen from cells in the 10 experiments when clear responses were seen. In a further 13 experiments, no response to 100nM ETYA was observed.

3.3.4 The effect of cell shape on bombesin-induced Ca^{2+} influx

Figure 3.3.4 shows typical $[Ca^{2+}]_i$ responses to 100nM bombesin in a cell on either a small island (a) or a large island (b). In the cell on the small island, the $[Ca^{2+}]_i$ returns to resting level quickly after the initial Ca^{2+} release without a plateau, which indicates that the Ca^{2+} influx is inhibited in shape-restricted cells. In total, 3 separate experiments were performed.

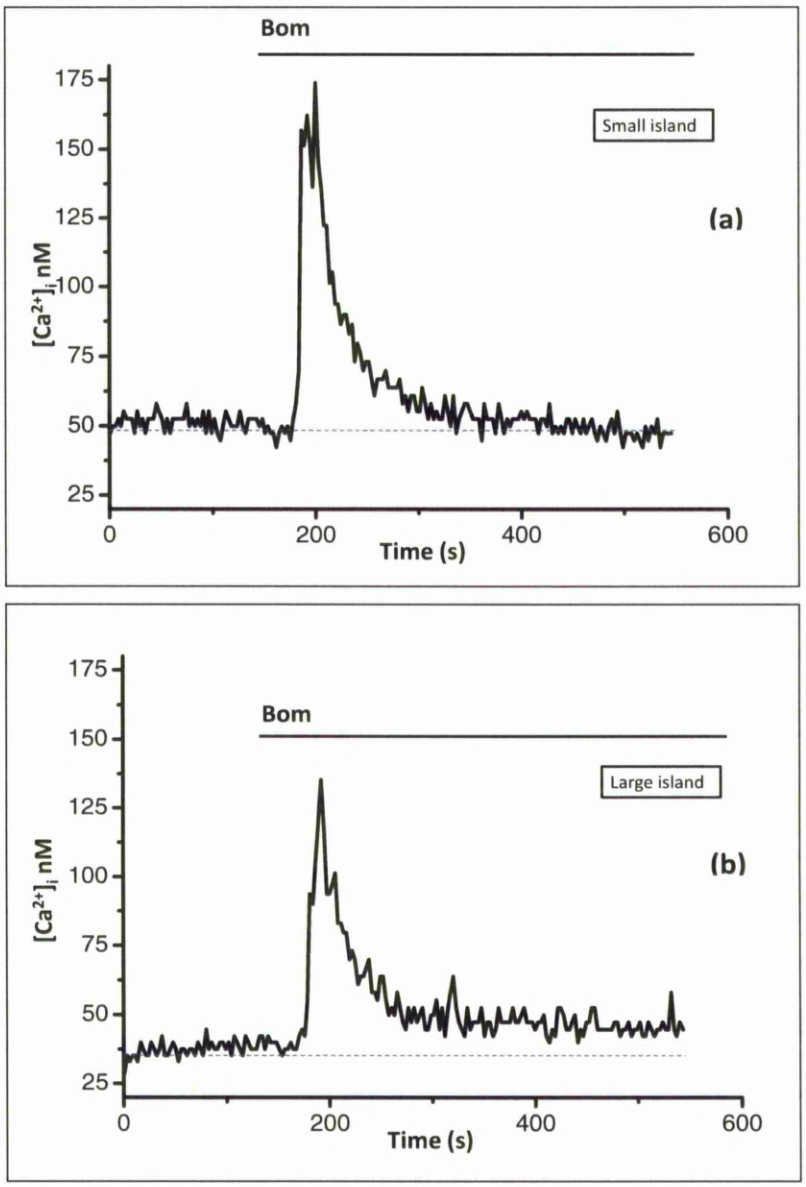

Figure 3.3.4-Cell-shape-dependent Ca^{2+} influx induced by bombesin

3-day-old quiescent Swiss 3T3 cells were cultured and restricted on either small (a) or large (b) islands in SF-DMEM for 16 hours before experiments. A $[Ca^{2+}]_i$ response is shown to bombesin (100nM) added at 180 seconds in the presence of 1mM Ca^{2+} in HBS. The $[Ca^{2+}]_i$ was measured using fura-2, at 37℃. Each figure is representative of 3 separate experiments.

3.4 Discussion

The data presented in this chapter confirms that the $[Ca^{2+}]_i$ responses in Swiss 3T3 cells could be monitored with the indicator, fura-2.

In normal spreading Swiss 3T3 cells, stimulation of 100nM bombesin consistently indicated a $[Ca^{2+}]_i$ response including a transient Ca^{2+} release from the intracellular store and a sustained Ca^{2+} influx. Moreover, the Ca^{2+} responses to both thapsigargin and ETYA were also observed. This is consistent with the existence of SOCCs and ARC-like channels in Swiss 3T3 cells.

In addition, the effect of cell density on bombesin-evoked $[Ca^{2+}]_i$ responses was studied. The results indicate that the sustained Ca^{2+} influx to bombesin is larger in non-confluent cells than that in confluent cells. Also, the confluent cells show a bigger Ca^{2+} release than non-confluent cells whereas the Ca^{2+} sequestration is quicker. Both confluent and non-confluent cells have a similar resting level of fura-2 fluorescence, with the range of ratio 340/380 from 0.45 to 0.55. Hence, the differences in increased $[Ca^{2+}]_i$ between confluent and non-confluent cells due to bombesin (figure 3.1.1 & figure 3.1.2) is convincing. The mechanism of the cell density influence on bombesin-evoked $[Ca^{2+}]_i$ response is unclear. However, it was reported that after 5 days cultured confluent endothelial cells possess significantly lower levels of AA when compared to freshly harvested non-confluent cells (Evans *et al.*, 1984). Since it is known that AA could induce Ca^{2+} influx, if the generation of AA in Swiss 3T3 cells is affected in a similar way to that in endothelial cells as reported, a higher level of AA in non-confluent cells may explain why they show a bigger Ca^{2+} entry. No clear evidence was found to explain whether the SOCE is cell density dependent. However, it is observed that there are no significant differences in thapsigargin-induced Ca^{2+} release and influx in confluent and non-confluent endothelial cells (Otun *et al.*, 1992). On the other hand, it is known that the shape of confluent cells is more restricted than non-confluent, as they are more tightly packed and rounded. Such cell shape differences may be another possible explanation for the different bombesin-evoked $[Ca^{2+}]_i$ responses in confluent and non-confluent cells, although the degree of cell-cell contact and adhesion may also be important.

Furthermore, the study in shape restricted cells confirmed that the bombesin-evoked Ca^{2+} influx is influenced by cell shape, which is consistent with the observation in previous studies (Pennington et al., 2007). In addition, the Bombesin-evoked Ca^{2+} response in cells on islands are more similar to the response in confluent cells than that in non-confluent cells. Therefore, restriction of cell shape may make cells act in a way similar to when they are confluent. This cell shape-dependent bombesin-induced Ca^{2+} influx is discussed in the following chapters.

In summary, the experiment results in this chapter indicate that:

1. Bombesin (100nM) is an effective agonist to evoked $[Ca^{2+}]_i$ responses in Swiss 3T3 cells.
2. Thapsigargin (2μM) and ETYA (100nM) are able to induce $[Ca^{2+}]_i$ responses in Swiss 3T3 cells.
3. The bombesin-induced $[Ca^{2+}]_i$ responses are cell density dependent. The bombesin-evoked Ca^{2+} release is bigger in the confluent cells than that in the non-confluent cells. Bombesin-evoked a bigger Ca^{2+} influx in the non-confluent cells than in the confluent ones.
4. The bombesin-evoked Ca^{2+} influx is inhibited by cell shape restriction using adhesive islands.

Chapter 4

Ba^{2+} and Sr^{2+} influxes in Swiss 3T3 cells

Contents:

Figures:

4.1 Introduction

According to the evidence presented in chapter 3 and earlier studies (Pennington et al., 2007), cell-shape-dependent Ca^{2+} influx induced by bombesin was observed in Swiss 3T3 cells. In order to help characterize which Ca^{2+} entry pathways are involved, extracellular Ca^{2+} can be substituted by other divalent cations.

Ca^{2+} channels have been reported in many types of cells to be permeable to Sr^{2+} and Ba^{2+}, as well as Ca^{2+} (Nachshen and Blaustein, 1982; Hughes and Schachter, 1994; Liu *et al.*, 1995). Moreover, it is known that these divalent cations can enter cells via multiple pathways. For instance, Ca^{2+} and Ba^{2+} enter rat A7r5 smooth muscle cells through either passive pathways or receptor operated pathways (Hughes and Schachter, 1994). It was reported that arginine vasopressin (AVP)-evoked Sr^{2+} entry in A7r5 cells is through a non-capacitative pathway mediated by AA (Broad *et al.*, 1999). In addition, both Sr^{2+} and Ba^{2+} influxes were seen through passive pathways in Ca^{2+} free solution in HEK293 cells without any extracellular stimuli (Zhu *et al.*, 1998). Moreover, further Sr^{2+} and Ba^{2+} influxes were observed when the transient receptor potential 3 (Trp3) protein is expressed in HEK293 cells after stimulation with carbachol (CCh) (Zhu *et al.*, 1998). Besides, IP_3-sensitive intracellular stores can accumulate both Ca^{2+} and Sr^{2+} but not Ba^{2} (Liu *et al.*, 1995).

A previous study in our laboratory has observed that thapsigargin is able to induce the Ba^{2+} and Sr^{2+} influx in Swiss 3T3 cells while ETYA and bombesin only induce the influx of Sr^{2+} (Foster, 2005). Since bombesin acted more like ETYA rather than thapsigargin, it was suggested that AA might participate in the bombesin-induced Ca^{2+} influx (Foster, 2005). In my research, similar experiments were performed in order to confirm this suggestion. In addition to monitoring the Ba^{2+} and Sr^{2+} responses in normal spreading cells, the responses to agonists in shape restricted cells were studied as well. If Ba^{2+} or Sr^{2+} enters cell through a pathway which is shape-dependent, then the influx should be blocked or reduced in cells on small islands.

Mn^{2+} quench has also been widely used to monitor Ca^{2+} influx by recording fluorescence with 340nm excitation, where Mn^{2+} decreased and Ca^{2+} increased the signal (Sage *et al.*, 1989;

Simpson *et al.*, 1995; Du *et al.*, 2000). An excitation wavelength of 360nm allows the selective study of Mn^{2+} entry without interference in the signal caused by changes in $[Ca^{2+}]_i$ (Sage *et al.*, 1989; Simpson *et al.*, 1990). However, Mn^{2+} cannot be used to distinguish different forms of Ca^{2+} entry. Also, as described above, with Mn^{2+} quench, the signal decreases in the presence of agonist following the Mn^{2+} influx. As a result of these limitations, Mn^{2+} is not used in my study.

The experiments presented in this chapter are aimed at studying the cell shape-dependent Ca^{2+} influx by using Ba^{2+} and Sr^{2+} as Ca^{2+} substitutes, with objective of determining if particular influx pathways are affected by cell shape.

4.2 Method

4.2.1 Cell culture

Swiss 3T3 cells were cultured in flasks according to standard protocol as described in section 2.1.1. Cells were transferred onto glass coverslips 1 day before the experiments. For the experiments on Sr^{2+} influx in confluent and non-confluent Swiss 3T3 cells, the same protocol was used as described in section 3.2.1. For the experiments using shape restricted cells, cells were transferred onto either large (ø 45μm) or small (ø 22μm) islands according to standard protocol as described in section 2.1.2.

Cells on coverslips or islands were grown for 3-4 hours until attached in FCS-DMEM and then kept in SF-DMEM for 16 hours before each experiment.

4.2.2 Ca^{2+} imaging

Prior to each experiment, cells were loaded with 2μM fura-2 for 45min at 37°C in the dark as described in section 2.3.2. They were immersed in HBS containing 1mM Ca^{2+} before being placed in the heated chamber on the microscope stage. Ca^{2+} free or 1mM EGTA containing HBS was used as extracellular medium when the cell responses is recorded. During the experiments, agonists including bombesin, thapsigargin or ETYA were added to stimulate the cell following the addition of either Ba^{2+} or Sr^{2+}. The changes of fura-2 fluorescence were monitored using the Ca^{2+} imaging

system. Details of individual experiments are described in section 4.3.

4.3 Results

4.3.1 Bombesin-induced Sr^{2+} and Ba^{2+} influx

Figure 4.3.1A shows the Ba^{2+} or Sr^{2+} responses in Swiss 3T3 cells after stimulation with 100nM bombesin. Ba^{2+} induced a small and slow influx in response to bombesin (a). This occurred in 10 out of 11 experiments. The average increase in ratio340/380 caused by this bombesin-induced Ba^{2+} entry is 0.098 ± 0.007 (n=43 cells). The Sr^{2+} influx to bombesin is much quicker and more pronounced (b), and occurred in 46 out of 47 experiments (n=388 cells). More detailed statistical analysis of bombesin-induced Sr^{2+} influx is indicated in figure 4.3.4. In addition, both Ba^{2+} and Sr^{2+} responses to bombesin in the same cell are displayed (c), which further confirms the difference between Ba^{2+} and Sr^{2+} influxes after the stimulation by bombesin.

Figure 4.3.1.B shows the control experiments. Addition of 1mM Ba^{2+} (a) or 1mM Sr^{2+} (b) did not affect the ratio340/380 in un-stimulated Swiss 3T3 cells.

Figure4.3.1A-Bombesin-induced Ba^{2+} and Sr^{2+} influxes

3-day-old quiescent Swiss 3T3 cells were cultured, unrestricted on glass coverslips in SF-DMEM for 16 hours before experiments. Responses to 100nM bombesin in Ca^{2+} free HBS with subsequent addition of either Ba^{2+} (a) or Sr^{2+} (b) are shown. Bombesin (100nM) was added at 200 seconds and Ba^{2+} (1mM) or Sr^{2+} (1mM) was added at 600 seconds. Both Ba^{2+} and Sr^{2+} influxes were tested in a same cell (c), in which 1mM Ba^{2+} was added at 600 seconds and then at 900 seconds the solution was replaced by a solution containing 1mM Sr^{2+}. Each figure is representative of at least 5 separated experiments.

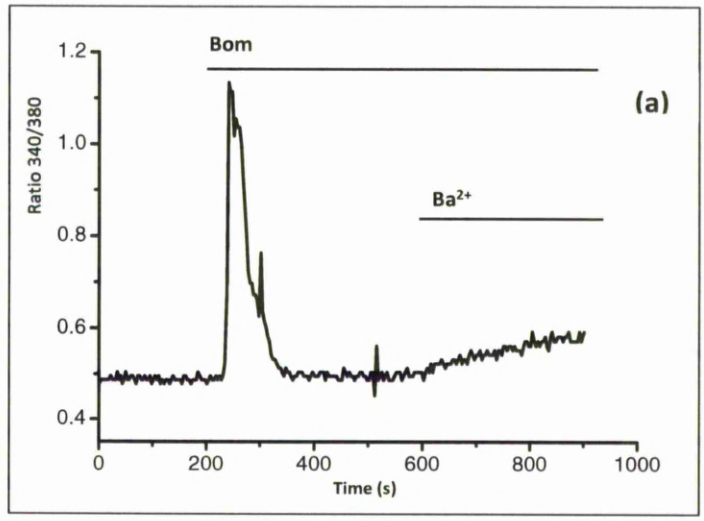

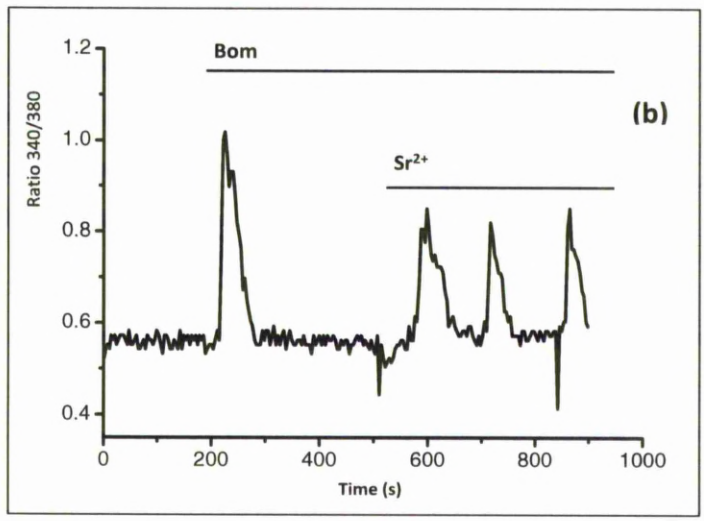

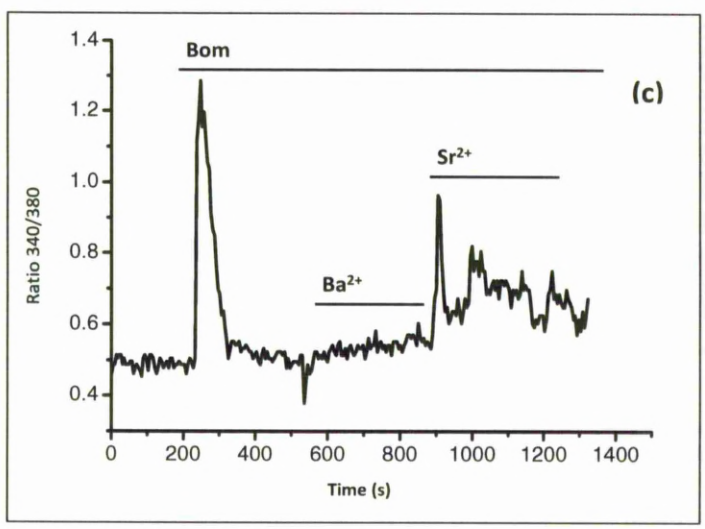

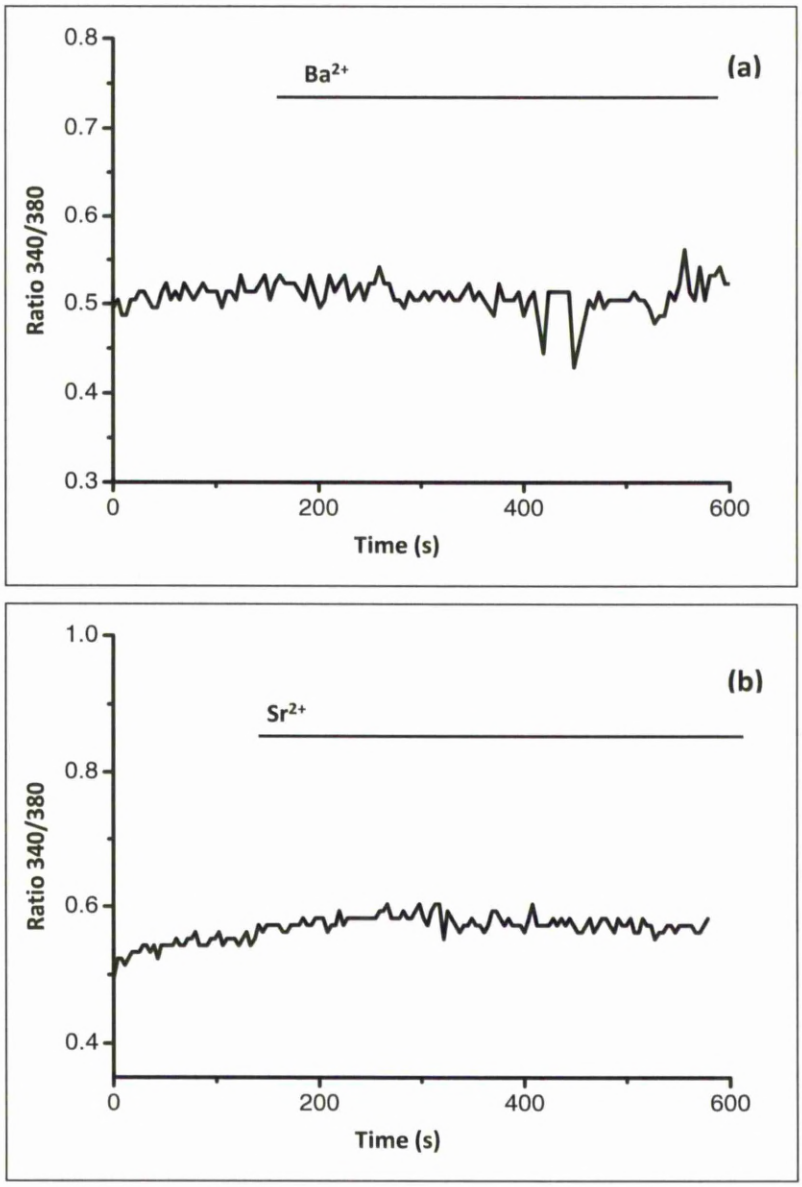

Figure 4.3.1B-Ba^{2+} and Sr^{2+} control

3-day-old quiescent Swiss 3T3 cells were cultured, unrestricted on glass coverslips in SF-DMEM for 16 hours before experiments. Ba^{2+} (a) or Sr^{2+} (b) were added to give a final concentration of 1mM in Ca^{2+} free HBS at 180 seconds. The figure is representative of at least 3 separate experiments.

4.3.2 Thapsigargin-induced Ba^{2+} influx

Figure 4.3.2 (a) shows the typical Ba^{2+} influx observed after the stimulation of thapsigargin (2μM). Thapsigargin consistently induced Ba^{2+} entry, which was seen in 10 out of 11 experiments. The average amplitude of such increased ratio340/380 is 0.237 ± 0.02 (n=66 cells), which is much greater compared to that induced by bombesin (0.098 ± 0.007) (Section 4.3.1). For comparison, two Ba^{2+} responses to either bombesin or thapsigargin in a same cell are shown in figure 4.3.2 (b).

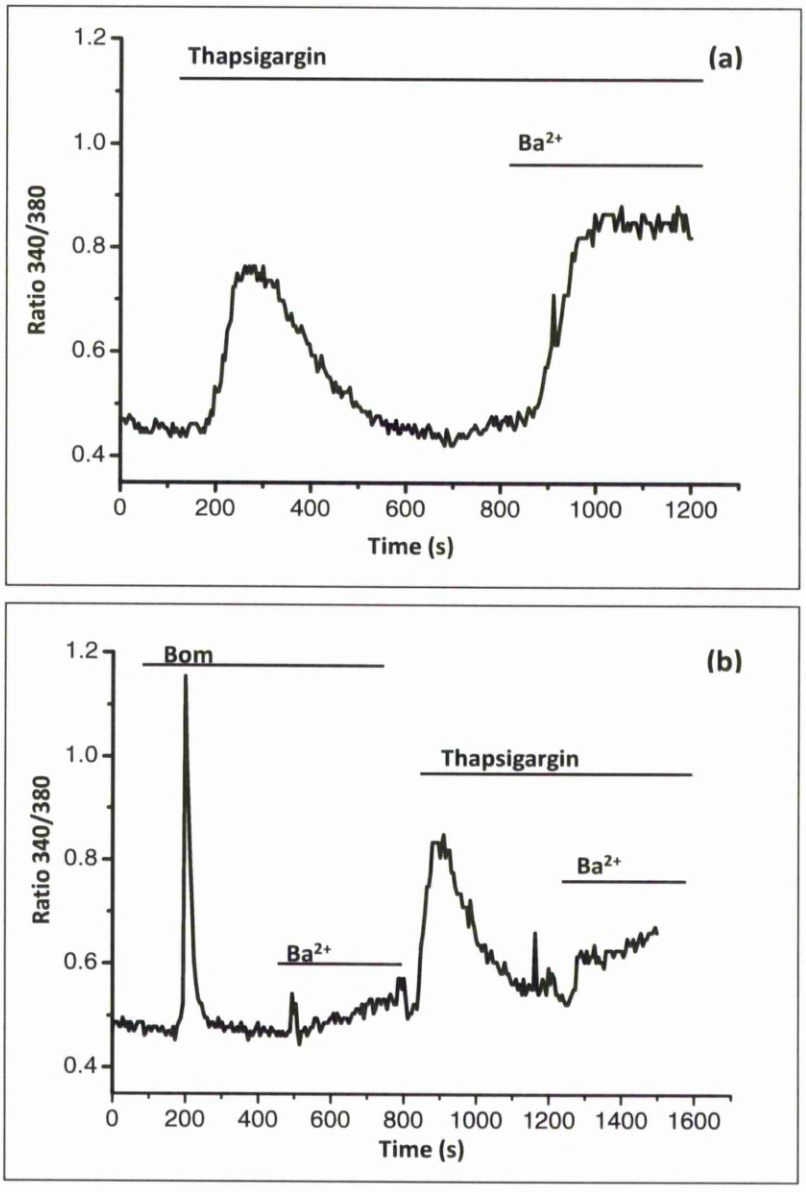

Figure 4.3.2-Thapsigargin-induced Ba^{2+} influx

3-day-old quiescent Swiss 3T3 cells were cultured, unrestricted on glass coverslips in SF-DMEM for 16 hours before experiments. The response in the presence of Ba^{2+} (a) to thapsigargin was shown in Ca^{2+} free HBS. In figure (a), thapsigargin (2μM) was added at 200 seconds and then Ba^{2+} was added to the final concentration at 1mM to the solution at 800 seconds. In figure (b), bombesin (100nM) was first added to stimulate the cell at 200 seconds and Ba^{2+} was added at 500 seconds into the solution in HBS. After that, the solution was replaced with fresh HBS and thapsigargin (2μM) was added at 800 seconds and followed the 1mM Ba^{2+} at 1200 seconds. The figure is representative of 4 (a) and 6 (b) separate experiments.

4.3.3 ETYA-induced Ba^{2+} and Sr^{2+} influx

Figure 4.3.3A (a) shows an ETYA-evoked Ba^{2+} influx and a thapsigargin-induced Ba^{2+} influx that occurred in the same cell. Compared to thapsigargin, in most cases, ETYA (100nM), which is dissolved in ethanol, failed to induce Ba^{2+} influx (8 in 11 experiments, n=61 cells). Figure 4.3.3A (b) shows the ethanol control experiment on the Ba^{2+} response, in which no Ba^{2+} influx is observed (2 experiments, n=17 cells).

However, an apparent Ba^{2+} influx after the stimuli of ETYA was seen several times with a low incidence (3 in 11 experiments, n=22 cells), and is shown in figure 4.3.3B (a). The increased 340/380 ratio caused by the influx of Ba^{2+} after ETYA is 0.418 ± 0.009. At the same period of time, Ba^{2+} passive influxes were observed in 3 of 5 control experiments (n=19 cells), with an increased ratio of 0.2176. As shown in figure 4.3.3B (b), an addition of 1mM Ba^{2+} causes an increase in ratio340/380 with no stimulation by any agonist, which reveals that the passive influx of Ba^{2+} occurs occasionally in Swiss 3T3 cells.

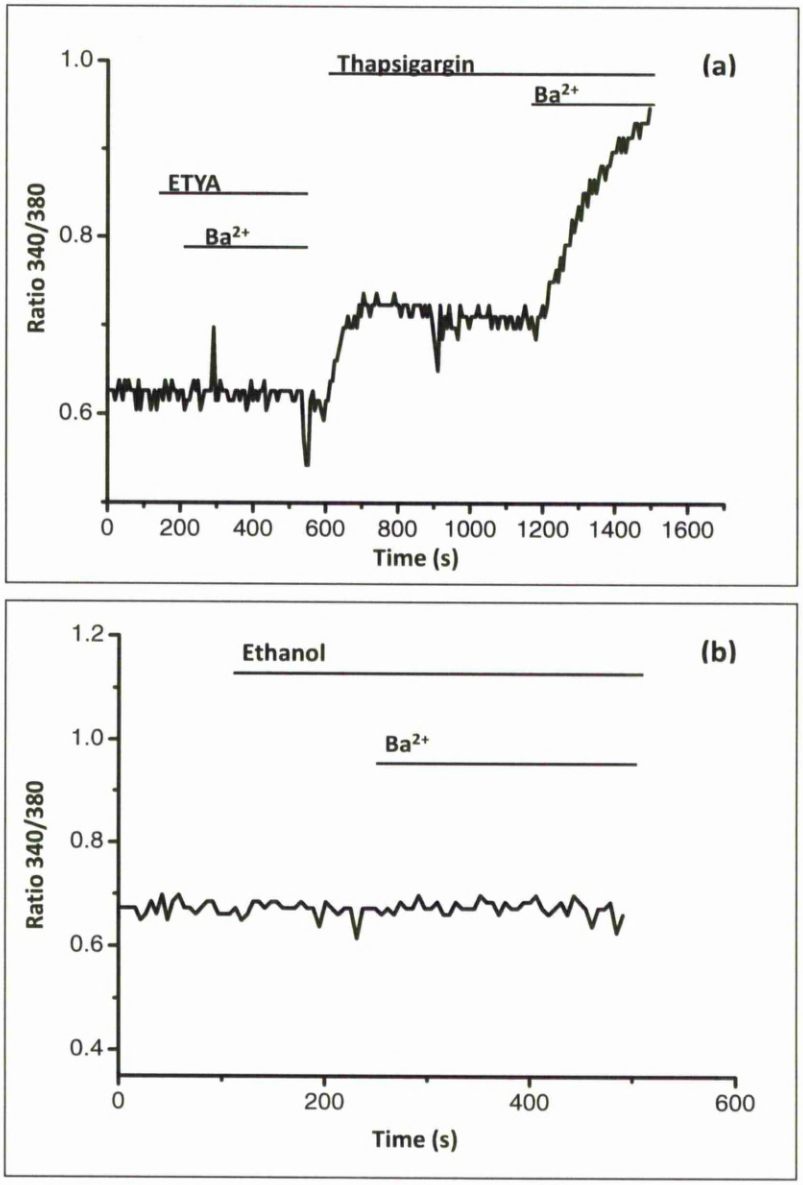

Figure 4.3.3A-ETYA-induce Ba^{2+} response

3-day-old quiescent Swiss 3T3 cells were cultured, unrestricted on glass coverslips in SF-DMEM for 16 hours before experiments. Experiments were initiated in Ca^{2+} free HBS. A typical response of Ba^{2+} (a) to ETYA (100nM) is shown. In figure (a), both ETYA and 1mM Ba^{2+} were added to solution at 200 seconds and then the solution was replaced with fresh HBS containing 1mM EGTA at 600 sec with 2μM thapsigargin added at the same time. A further addition of 1mM Ba^{2+} was made at 1200 seconds. In figure (b), ethanol (1μl) was added to the 1mM EGTA containing HBS at 150 seconds as the control of ETYA stimulation and 1mM Ba^{2+} was added at 300 seconds. Each figure is representative of at least 2 separate experiments.

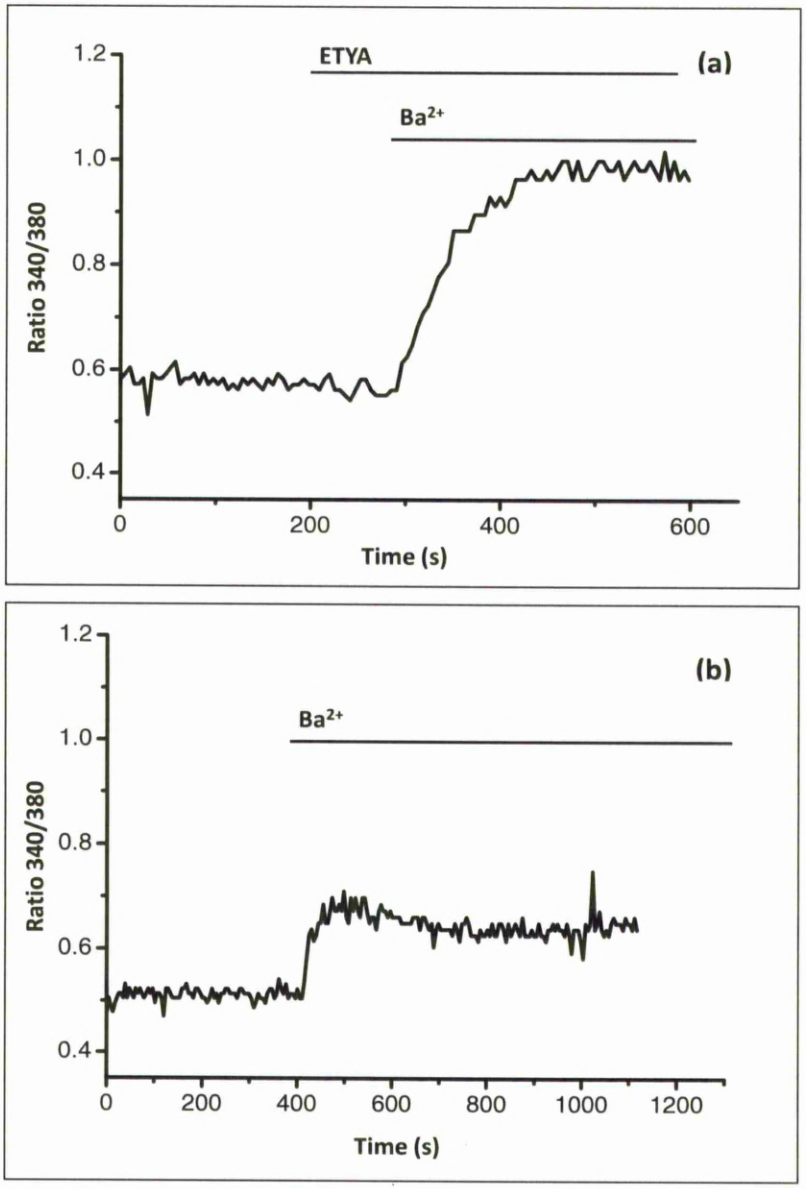

Figure 4.3.3B-ETYA-induced Ba^{2+} response with Ba^{2+} passive influx

3-day-old quiescent Swiss 3T3 cells were cultured, unrestricted on glass coverslips in SF-DMEM for 16 hours before experiments. Experiments were initiated in Ca^{2+} free HBS. In figure (a), Ba^{2+} (1mM) show a large and quick influx to 100nM ETYA at 300 seconds. In figure (b), an addition of Ba^{2+} (1mM) at 400 seconds causes a passive influx. Each figure is representative of at least 3 separate experiments.

4.3.4 Bombesin-induced Sr^{2+} influx in confluent and non-confluent cells

The effect of cell density on bombesin-induced Sr^{2+} influx has been tested. In the experiment, cells were first stimulated with 100nM bombesin. After the initial Ca^{2+} release, 1mM Sr^{2+} was added and this resulted in a Sr^{2+} influx (Figure 4.3.1A). This bombesin-evoked Sr^{2+} influx was seen in all 24 experiments in confluent cells (n=298 cells) and 22 out of 23 experiments in non-confluent cells (n=90 cells). In 2 out of these 22 experiments, there are about half the non-confluent cells failed to show a Sr^{2+} influx (n=5 cells). The result is consistent with the experiments investigating the effect of cell density on bombesin-induced Ca^{2+} influx (Section 3.3.1). Bombesin is more consistent at causing a Sr^{2+} influx in confluent cells compared with non-confluent cells.

The statistical data of the increases of ratio340/380 caused by the bombesin-induced Ca^{2+} release or Sr^{2+} influx are shown in figure 4.3.4. The results suggested that the bombesin-evoked Sr^{2+} influx is significant bigger in non-confluent cells than in the confluent cells according to the t-test ($p<0.05$). This is consistent to the bombesin-induced Ca^{2+} influx in confluent and non-confluent cells (Section 3.3.1). This implies that although the cell density has an effect on the bombesin-evoked Sr^{2+} influx similar to that on Ca^{2+} influx.

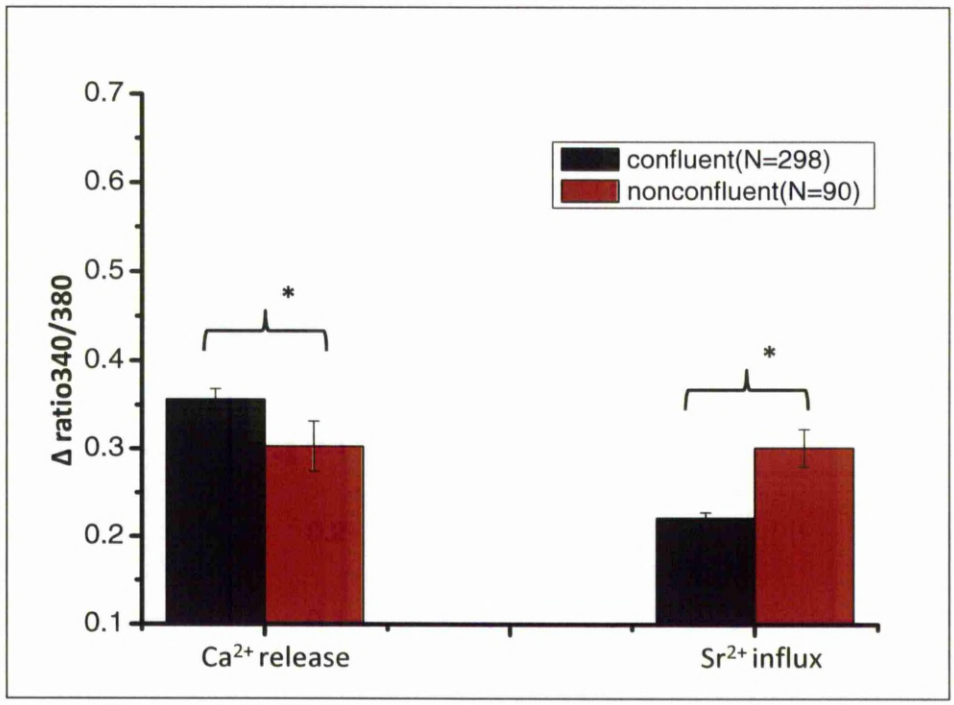

Figure 4.3.4-Bombesin-induced Ca^{2+} release and Sr^{2+} influx in confluent and non-confluent cells

Quiescent Swiss 3T3 cells were cultured, unrestricted on glass coverslips in SF-DMEM for 16 hours before experiments. Mean data showing increased ratio340/380 caused by bombesin-induced Ca^{2+} release and Sr^{2+} influx in either confluent (black) or non-confluent (red) cells. The Δratio340/380 is measured as the ratio340/380 at the peak points of Ca^{2+} release and Sr^{2+} influx minus the baseline value before the addition of bombesin. Error bars shown are ± S.E. of (N) number of indicted cells. $P<0.05$, when Δratio340/380 value of (N) number of cells were subjected to t-test.

4.3.5 Bombesin-induced Ba^{2+} responses in restricted cells

Bombesin-induced Ba^{2+} responses in shape-restricted cells show great variation. Figure 4.3.5A and figure 4.3.5B show three types of Ba^{2+} responses to bombesin (a-c), and two Ba^{2+} control responses (d) in either large and small islands. The results indicate that there is no significant difference between bombesin-evoked Ba^{2+} responses in cells on either large or small islands. In the cells on large islands, a Ba^{2+} influx with the increase of ratio340/380 ranged from 0.1 to 0.2 was observed in 8 of 14 cells. Similarly, there were 9 out of 14 cells showed a Ba^{2+} influx after the stimulation of bombesin in cells on small islands. The remaining of the cells presented no response to bombesin or Ba^{2+}. On the other hand, passive Ba^{2+} influxes were observed in cells on both sizes of island. In cells on large islands, Ba^{2+} passive leak occurred in 3 out of 4 cells, and in cells on small islands, 2 in 3 cells showed such leak.

Figure 4.3.5C shows the statistical data relating to the increase ratio340/380 caused by Ba^{2+} influxes in restricted cells. The results suggested that there are no significant differences of the Ba^{2+} responses including passive influx and bombesin-evoked influx between large and small islands restricted cells.

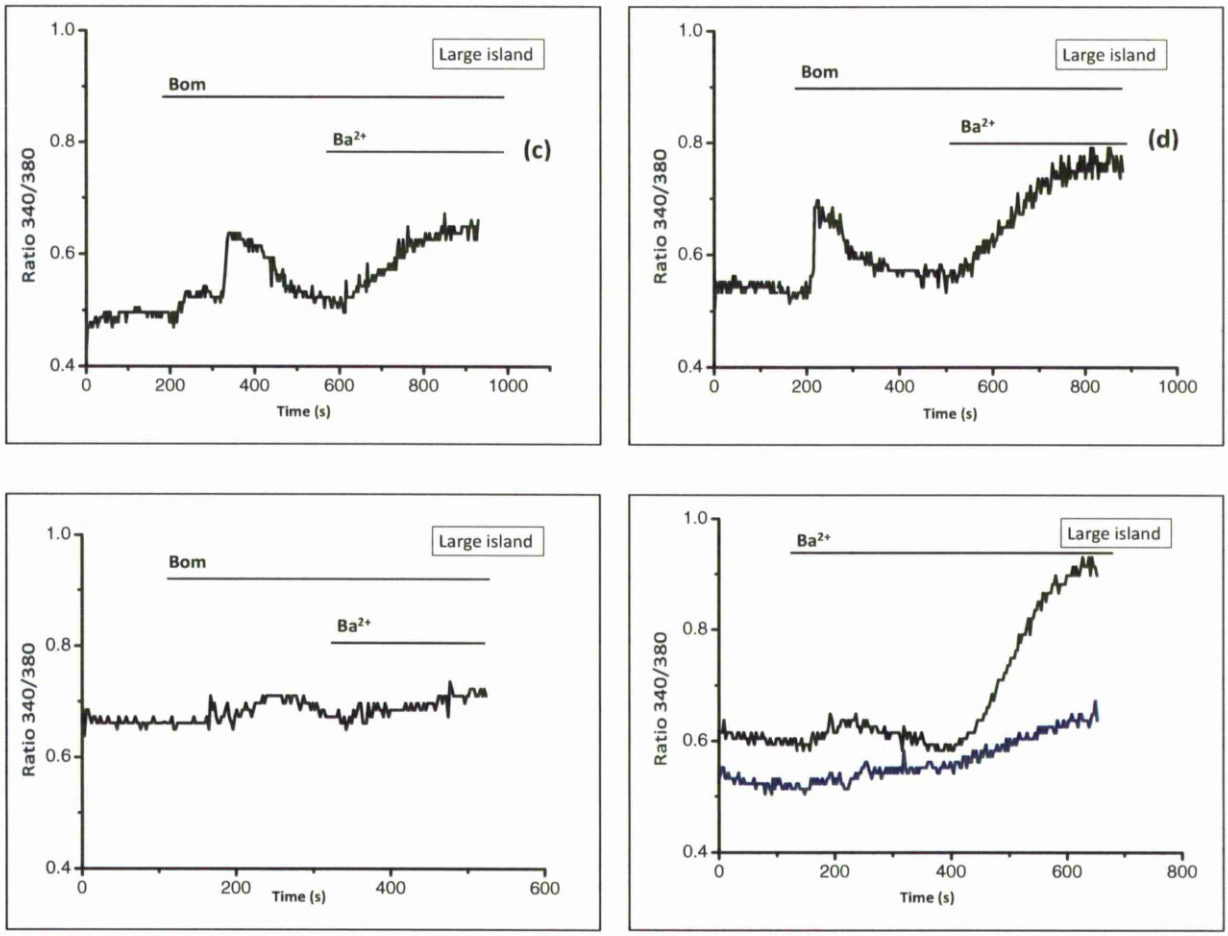

Figure 4.3.5A-Ba^{2+} responses in cells on large islands

3-day-old quiescent Swiss 3T3 cells were cultured and restricted on large islands in SF-DMEM for 16 hours before experiments. Three Ba^{2+} responses to bombesin were shown in figure (a-c). Bombesin (100nM) was added at 180 seconds to Ca^{2+} free HBS. Ba^{2+} (1mM) was then added at 600 seconds in figure (a) & figure (b) and at 400 seconds in figure (c). Figure (d) shows two Ba^{2+} control responses in two single cells, with Ba^{2+} (1mM) added to Ca^{2+} free HBS at 180 seconds. Each figure is representative of at least 2 separate experiments.

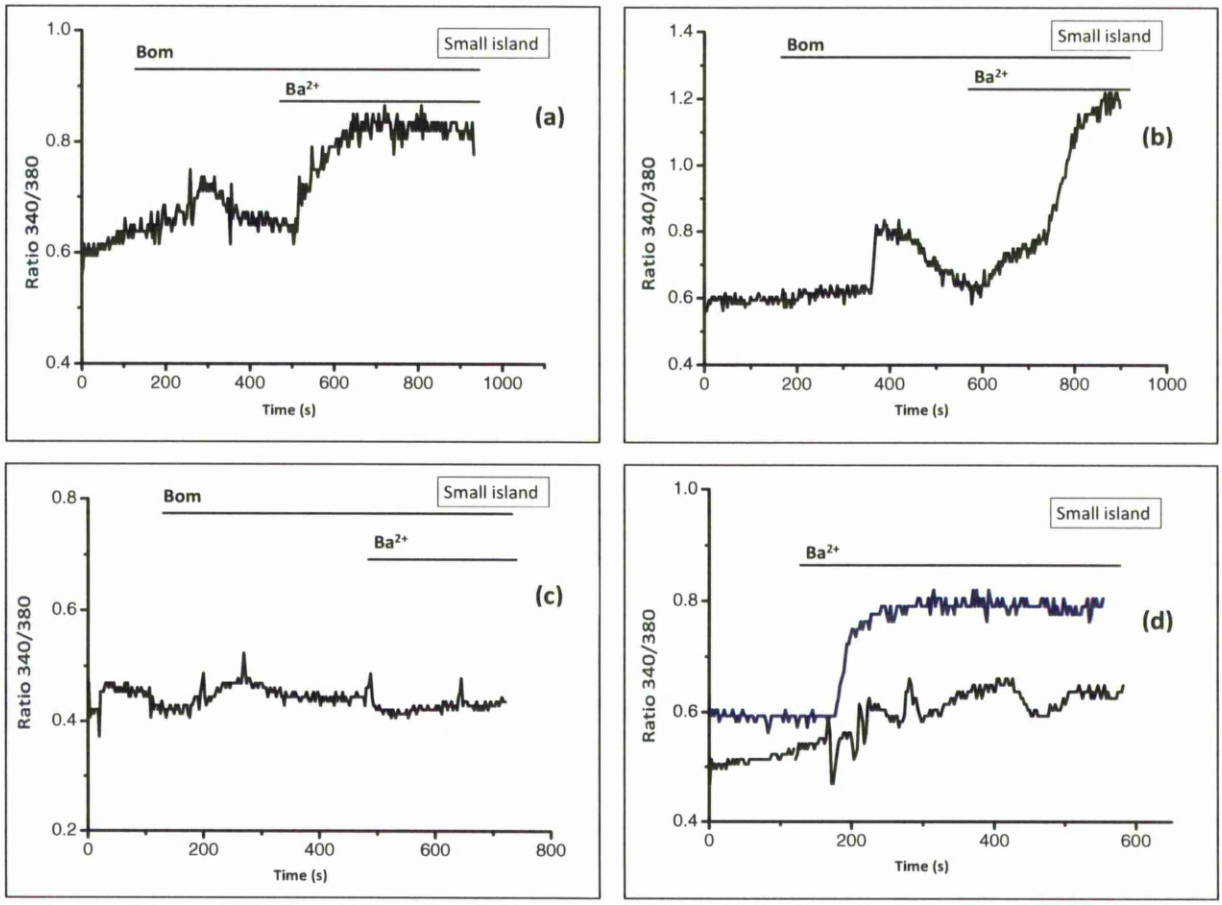

Figure 4.3.5B-Ba^{2+} responses in cells on small islands

3-day-old quiescent Swiss 3T3 cells were cultured and restricted on small islands in SF-DMEM for 16 hours before experiments. Three Ba^{2+} responses to bombesin were shown in figure 3.4.2a-c. Bombesin (100nM) was added at 180 seconds to Ca^{2+} free HBS. Then Ba^{2+} (1mM) was added at 600 seconds in figure 3.4.2a & figure 3.4.2b, and at 500 seconds in figure 3.4.2c. Figure 3.4.2d shows two Ba^{2+} control responses in two single cells, with Ba^{2+} (1mM) added to Ca^{2+} free HBS at 180 seconds. Each figure is representative of at least 2 separate experiments.

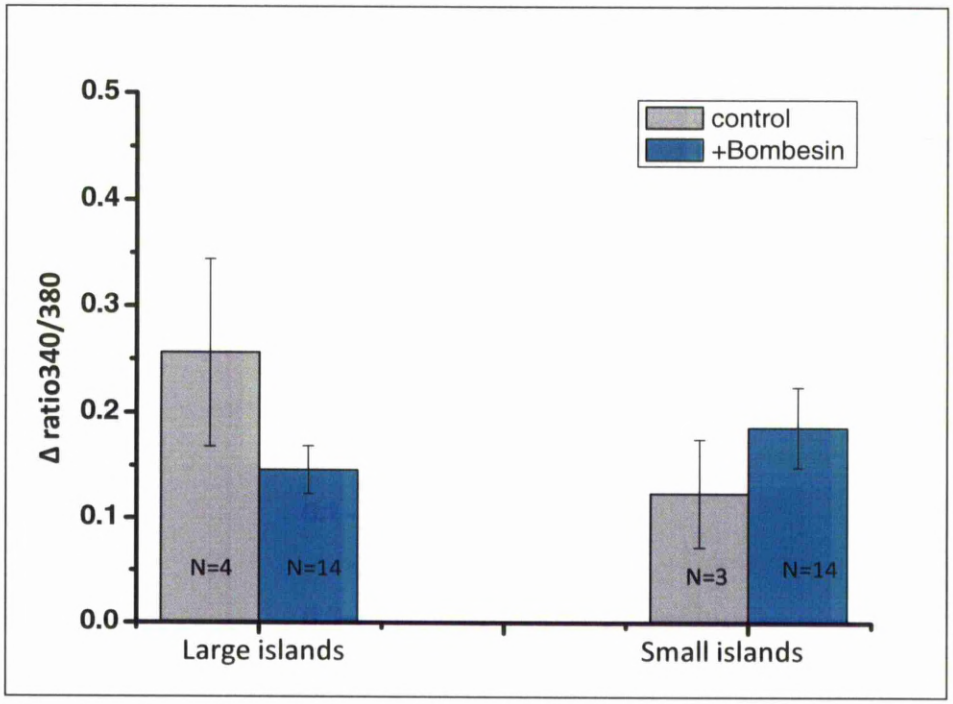

Figure 4.3.5C-Statistical data of Ba^{2+} responses in restricted cells

3-day-old quiescent Swiss 3T3 cells were cultured and restricted on small islands in SF-DMEM for 16 hours before experiments. Mean data of increased ratio340/380 due to Ba^{2+} influx in cells on either large or small islands was indicated in solid bars. The grey bars present the data of Ba^{2+} spontaneous influx with no agonist stimulation whereas the blue bars present the data of Ba^{2+} influx after the stimulation of bombesin. The Δratio340/380 was measure as the maximum ratio340/380 during the sustained Ba^{2+} influx phase minus the baseline ratio340/380 level before the stimulation. "N" represents the number of cells showed a Ba^{2+} influx. Error bars shown are ± S.E. of (N) number of indicted cells. $P>0.05$, when Δratio340/380 value of (N) number of cells were subjected to t-tests.

4.3.6 Bombesin-induced Sr^{2+} responses in restricted cells

Similar to Ba^{2+}, bombesin-induced Sr^{2+} responses in shaped restricted cells various among single cells. Figure 4.3.6A and figure 4.3.6B display three types of Sr^{2+} responses to bombesin (a-c) and Sr^{2+} control responses (d) in cells on either large or small islands. After the stimulation of bombesin, the Sr^{2+} influxes were not consistently observed. In the cells on large islands, 8 cells out of 19 showed a Sr^{2+} influx. With a similar frequency, the Sr^{2+} influx occurred in 9 out of 19 cells on small islands. The Sr^{2+} passive influxes were frequently seen in restricted cells on both sizes of islands. In the cells on large islands, Sr^{2+} entered the cells in 4 out of 5 cells without any stimulation. In the cells on small islands, Sr^{2+} passive influx occurred in 3 out of 5 cells.

Figure 4.3.6C indicates the statistical data of the increase ratio340/380 caused by Sr^{2+} influxes in restricted cells. The results suggested that there are no significant differences of the Sr^{2+} responses including passive influx and bombesin-evoked influx between large and small islands restricted cells.

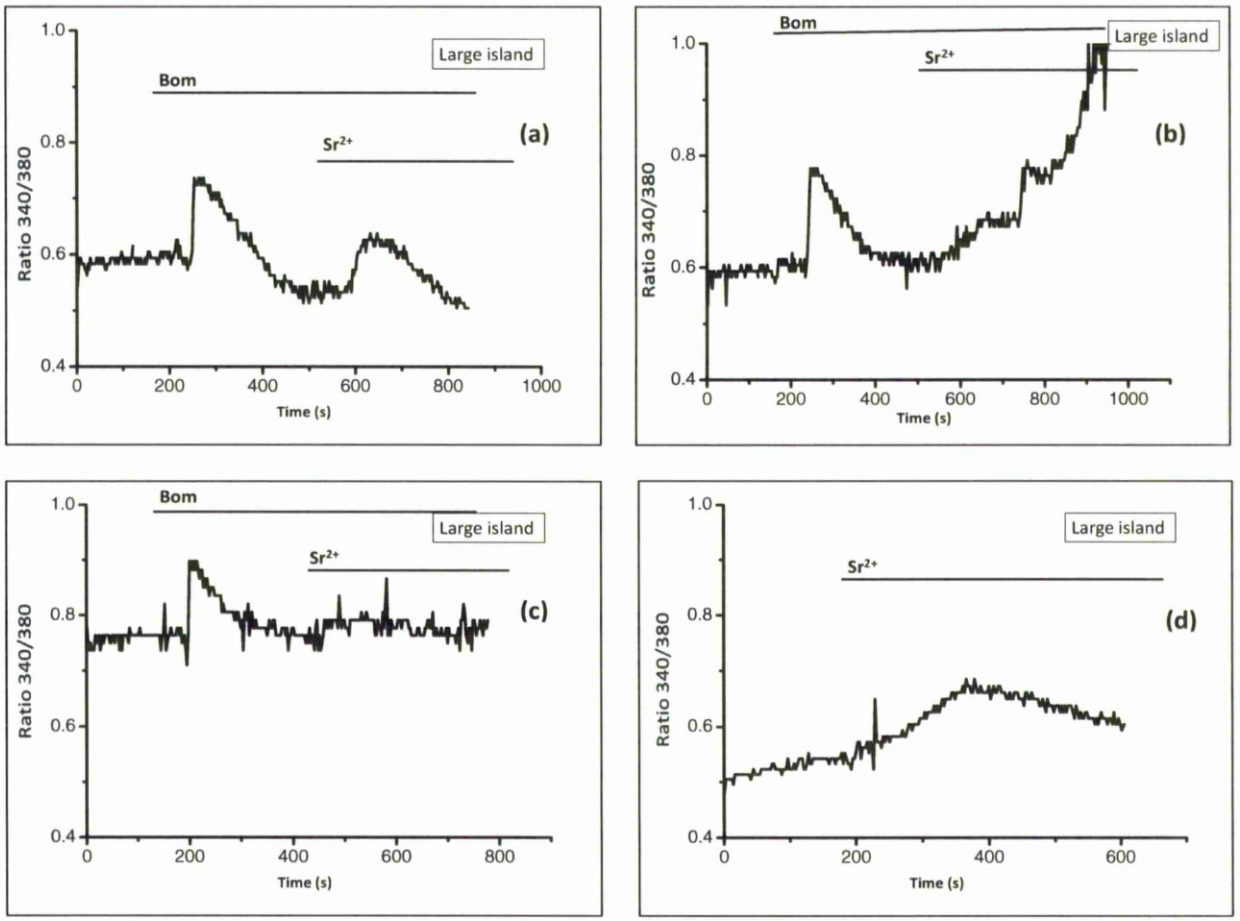

Figure 4.3.6A-Sr^{2+} responses in cells on large islands

3-day-old quiescent Swiss 3T3 cells were cultured and restricted on large islands in SF-DMEM for 16 hours before experiments. Three Sr^{2+} responses to bombesin were shown in figure (a-c). Bombesin (100nM) was added to Ca^{2+} free HBS at 180 seconds. Sr^{2+} (1mM) was then added at 600 seconds in figure (a) & figure (b) and at 500 seconds in figure (c). Figure (d) shows a Sr^{2+} control response in a single cell, with Sr^{2+} (1mM) added to Ca^{2+} free HBS at 180 seconds. Each figure is representative of at least 2 separate experiments.

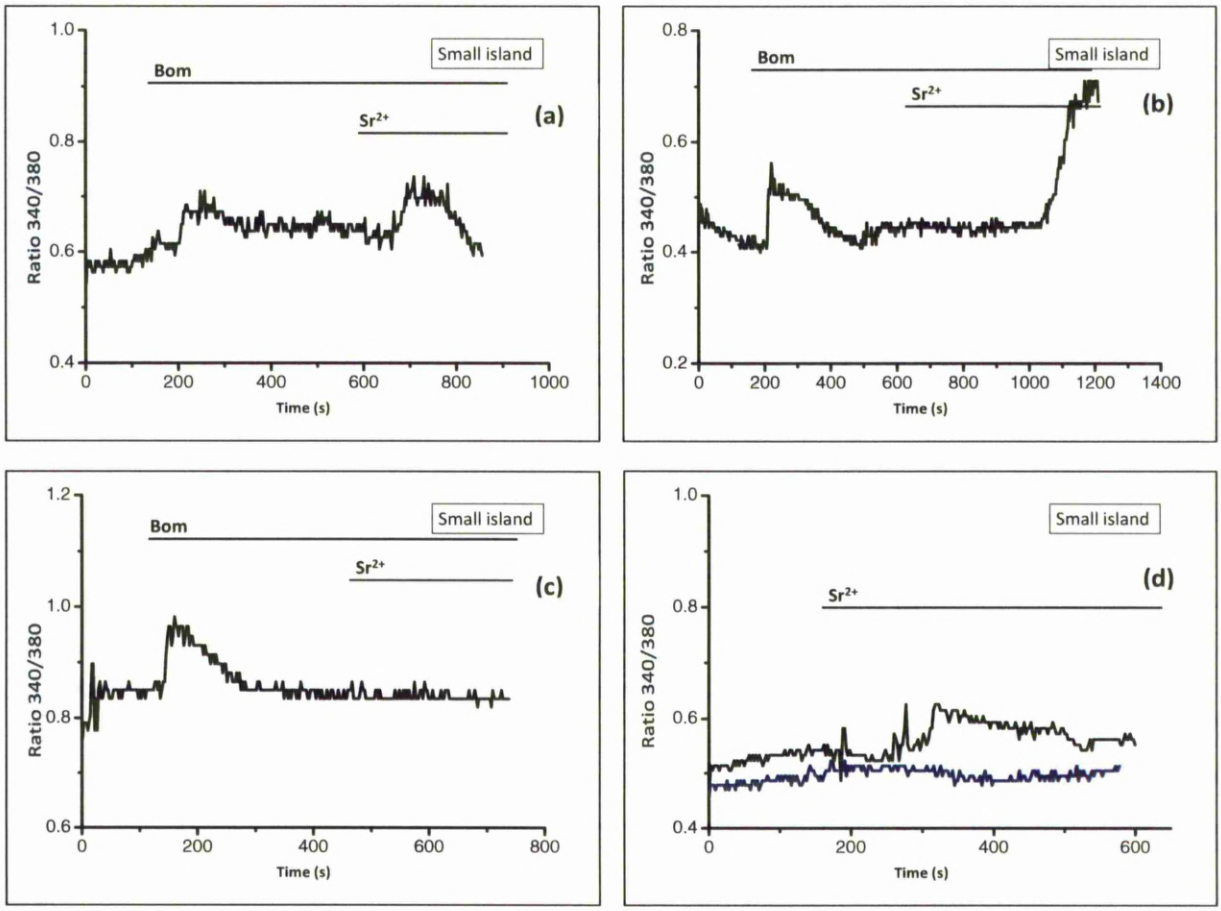

Figure 4.3.6B -Sr^{2+} responses in cells on small islands

3-day-old quiescent Swiss 3T3 cells were cultured and restricted on small islands in SF-DMEM for 16 hours before experiments. Three Sr^{2+} responses to bombesin were shown in figure (a-c). Bombesin (100nM) was added to Ca^{2+} free HBS at 180 seconds. Sr^{2+} (1mM) was then added at 600 seconds in figure (a) & figure (b) and at 500 seconds in figure (c). Figure (d) shows two Sr^{2+} control responses in two single cells, with Sr^{2+} (1mM) added to Ca^{2+} free HBS at 180 seconds. Each figure is representative of at least 2 separate experiments.

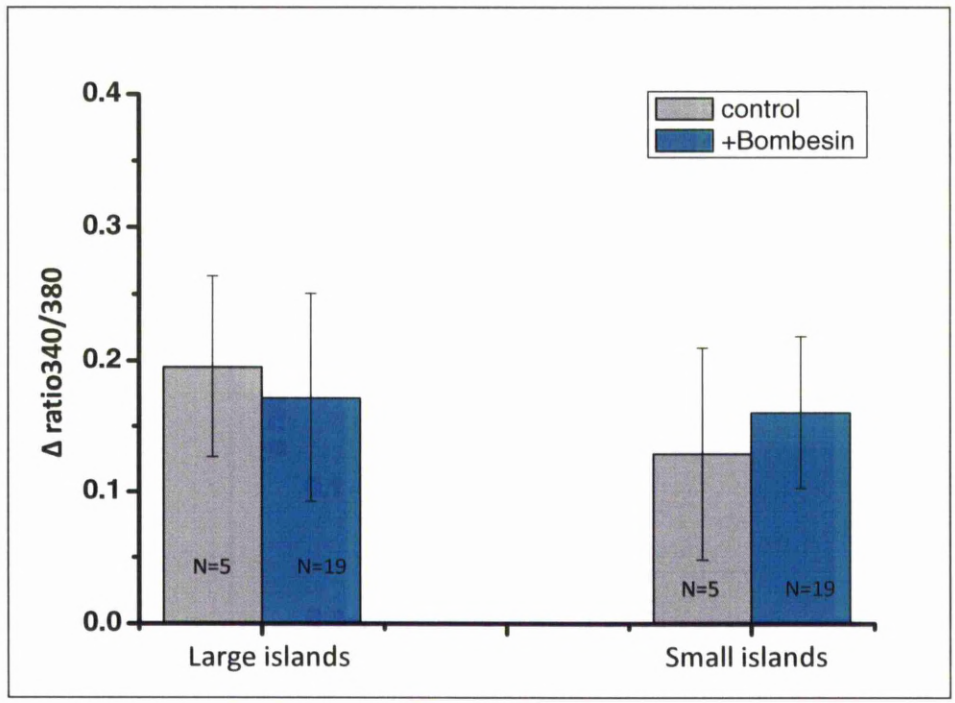

Figure 4.3.6C-Statistical data of Sr^{2+} response in restricted cells

Mean data of increased ratio340/380 due to Sr^{2+} influx in cells on either large or small islands was indicated in solid bars. The grey bars present the data of Sr^{2+} spontaneous influx with no agonist stimulation whereas the blue bars present the data of Sr^{2+} influx after the stimulation of bombesin. The Δratio340/380 was measure as the maximum ratio340/380 during the sustained Sr^{2+} influx phase minus the baseline ratio340/380 level before the stimulation. "N" represents the number of cells showed a Sr^{2+} influx. Error bars shown are ± S.E. of (N) number of indicted cells. $P>0.05$, when Δratio340/380 value of (N) number of cells were subjected to t-test.

4.4 Discussion

In the study where divalent cations were used as substitutes for Ca^{2+}, it was confirmed that both Ba^{2+} and Sr^{2+} are able to permeate into Swiss 3T3 cells. At the beginning of this research, similar experiments on agonists-induced Ba^{2+} and Sr^{2+} responses were performed according to the protocol of Foster's (2005) research in our laboratory. It was observed that, in the same cell, bombesin-induced a slight and slow Ba^{2+} influx while thapsigargin is able to evoke a big and quick Ba^{2+} entry. In a same way, no Ba^{2+} influx occurred after the stimulation of ETYA whereas thapsigargin-induced a quick and significant Ba^{2+} entry response. These observations suggested that bombesin acts like ETYA rather than thapsigargin that it activates channels allowing quite small amount or no Ba^{2+} to pass through. This hypothesis is coherent with the Foster's study implying that ARC channels are involved in bombesin-evoked Ca^{2+} influx pathway.

Nevertheless, this hypothesis is subsequently challenged due to the presence of passive Ba^{2+} and Sr^{2+} influxes in Swiss 3T3 cells observed after further study. For example, Ba^{2+} enters the cell spontaneously when studying the effect of ETYA on Ba^{2+} responses. Such passive influx is difficult to predict or prevent. Besides, it has been argued that both NSOCE and SOCE pathways are permeable to Ba^{2+} while only NSOCE is permeable to Sr^{2+} (Moneer and Taylor, 2002). Consequently, the Ba^{2+} influx observed after the stimuli of agonists may be an agonist-evoked influx or a passive influx or both.

Furthermore, in order to study the effect of cell shape, the Ba^{2+} and Sr^{2+} influxes were examined in cell shape-restricted cells. However, the results were disturbed by high frequency of Ba^{2+} and Sr^{2+} passive influxes as well. Both Ba^{2+} and Sr^{2+} are able to enter cells in either large or small islands spontaneously, which indicates that cell shape has no effect on their passive influx channels. The Ba^{2+} and Sr^{2+} response to bombesin showed great variations among restricted cells. It was observed that after the stimulation by bombesin, some restricted cells showed a slight Ba^{2+} influx with a Δratio340/380 less than 0.1 and some cells showed a significant Ba^{2+} entry with a Δratio340/380 more than 0.2 while rest of the restricted cells showed no Ba^{2+} influx. These three types of responses were seen in either large or small islands restricted cells. The Sr^{2+} responses to bombesin could be categorized into similar three types as well. Since 3 distinct types of response

with either Ba^{2+} or Sr^{2+} were observed in both restricted and spread cells (small and large islands), it appears that cell shape does not have a clear effect on the characteristic of the divalent cation pathway that can be activated.

Compared to the data in normal spreading cells presented in section 4.3.1, significant Ba^{2+} influxes occurred in restricted cells (Figure 4.3.5Ab & Figure 4.3.5Bb). However, the high occurrence of Ba^{2+} passive influx during the same period of experiments could be the main cause of these responses. The role for TRP channels in this effect cannot be ruled out and needs to be further investigated. In addition, as the intracellular Ba^{2+} ($[Ba^{2+}]_i$) concentration is controlled by not only the Ba^{2+} influx but the pumps in plasma membrane and ER should remove Ba^{2+}. The high increased $[Ba^{2+}]_i$ is probably due to the cells' inability to clear Ba^{2+} from the cytoplasm (Liu *et al.*, 1995). This hypothesis needs to be investigated by further research. On the other hand, the frequency of a Sr^{2+} influx to bombesin was reduced in restricted cells compared to that in normal spreading cells. The study on the effect of cell density reveals that bombesin could consistently induce a Sr^{2+} influx in normal spreading cells. However, confluent cells are more likely to show a bombesin-evoked Sr^{2+} influx than non-confluent cells (Figure 4.3.4). These data reconciles with the observation that Ca^{2+} influx appears bigger in non-confluent cells (Section 3.3.1). In the case of Sr^{2+} entry, it could well be that cell density or cell-cell contact influence this cation entry pathway.

The mean data of Δratio340/380 cause by Ba^{2+} or Sr^{2+} influxes exhibited in figure 4.3.5C and figure 4.3.6C suggest that Ba^{2+} showed a smaller influx in cells on large islands than that in the cells on small islands whereas Sr^{2+} acted in a converse way. However, such differences were not as significant as the variation of responses among cells limited the statistical confidence of the results. The sample size of each group is small, so the results are not well representative. Therefore, more experiments need to be carried out to confirm the conclusion.

In summary, the Ba^{2+} and Sr^{2+} responses to bombesin, thapsigargin and ETYA imply a possibility that Ca^{2+} enters cell after bombesin stimulation through the AA activated pathways. However, due to the spontaneous influx of both cations, the involvement of ARC channels cannot be

confirmed. Ba^{2+} and Sr^{2+} investigation contributed less to the study of the cell-shape-dependent Ca^{2+} influx pathway than expected. As a result, alternative ways, which are described in the following chapters, should be applied to carry on the study.

To sum up, the key findings presented in the chapter are:

1. Bombesin induces a slight and slow Ba^{2+} influx in Swiss 3T3 cells. ETYA induces no Ba^{2+} influx while thapsigargin can consistently evoke a Ba^{2+} influx.
2. All the three agonist, bombesin, thapsigargin and ETYA can consistently induce a Sr^{2+} influx.
3. The bombesin-induced Sr^{2+} influx is not cell density dependent.
4. The bombesin-evoked Ba^{2+} and Sr^{2+} responses showed a great variation in adhesive islands restricted cells. There is no significant difference according to the statistic analysis between the Ba^{2+}/Sr^{2+} flux in cells on small islands and that in cells on large islands.
5. The Ba^{2+}/Sr^{2+} spontaneous influxes occurred during the experiment, which disturbed the results. As a result, Ba^{2+} and Sr^{2+} fluxes were not an ideal approach for the study on shape-sensitive Ca^{2+} influx pathway in Swiss 3T3 cells.

Chapter 5

AA-induced Ca^{2+} influx: the activation of $cPLA_2$ after the stimulation by bombesin

Contents:

Figures:

5.1 Introduction

Based on the initial data obtained from the agonist-evoked Ba^{2+} and Sr^{2+} influx experiments, we suspected that the major Ca^{2+} influx during the cell proliferation was more likely through the ARC channels rather than the CRAC channels. Given that AA is an important regulator of Ca^{2+} influx, the effect of bombesin on the process that led to the generation of AA were first studied. As described in section 1.6.3.3, PLA_2 enzyme plays a vital role in regulating the release of AA and $cPLA_2$ possesses a preference for phospholipids containing AA (Leslie, 1997). Previous studies have reported that bombesin increased the activities of $cPLA_2$ and that this was followed by the release of AA in Swiss 3T3 cells (Domin and Rozengurt, 1993). Consequently, it is necessary to determine if $cPLA_2$ plays a role in the activation of Ca^{2+} influx in response to bombesin. Also the translocation of $cPLA_2$ is an important step in its activation. This process may well be susceptible to cell shape restriction that is now known to prevent Ca^{2+} influx.

Cytoplasmic PLA_2 is phosphorylated during its activation. The phosphorylation sites of $cPLA_2$ vary in response to different stimuli and in different cell types. For instance, it is revealed that there are four sites of $cPLA_2$ phosphorylation observed in sf9 cells: Ser^{437}, Ser^{454}, Ser^{505}, and Ser^{727} (de Carvalho *et al.*, 1996). In addition, okadaic acid caused a marked increase in AA release from Sf9 cells and a selective increase in the phosphorylation of $cPLA_2$ at Ser^{727} (de Carvalho *et al.*, 1996). Phosphorylation on Ser^{505} has been shown to be a MAP kinase consensus site in various cell types (reviewed by Lin *et al.*, 1993). Evidence indicates that replacement of Ser^{505} with Ala results in a loss in activity of $cPLA_2$ and the decrease of agonist stimulates arachidonate release (Abdullah *et al.*, 1995). In macrophages, a transient increase in $[Ca^{2+}]_i$ and phosphorylation of $cPLA_2$ on Ser^{505} by MAP kinase can act together to fully activate $cPLA_2$ leading to AA release (Qiu *et al.*, 1998). Phosphorylation of $cPLA_2$ on Ser^{505} also occurs in thrombin- and collagen-stimulated platelets and cytokine-stimulated HeLa cells (Börsch-Haubold *et al.*, 1998).

In my research, the activation of $cPLA_2$ induced by bombesin was investigated by testing the increase of phospho-$cPLA_2$ in the cell. Since bombesin is a mitogen, $cPLA_2$ is more likely to be phosphorylated on Ser^{505}. Therefore, the phospho-$cPLA_2$ (Ser^{505}) antibody was used to monitor the phospho-$cPLA_2$ in both normal spreading and cell shape restricted cells. Confocal microscopy

was used to identify the changes of phospho-cPLA$_2$ in both resting and bombesin stimulated cells.

Further experiments were carried out in order to investigate whether the increase of phospho-cPLA$_2$ in bombesin-stimulated cells is through phosphorylation of MAP kinase. It is known that underlying mechanisms of the cPLA$_2$ phosphorylation are complex (Section 1.6.3.3). ERKs, which are members of the MAP kinase family, are reported to responsible for the phosphorylation of cPLA$_2$ on Ser^{505} and the release of AA in many cell types (Chang *et al.*, 2006). It is conceivable that ERK1/ERK2 or MAP kinase p42/44 is the key regulator of cPLA$_2$ phosphorylation. In this study, two MAP kinase inhibitors were used to block the ERK pathway in Swiss 3T3 cells: ERK Inhibitor II (FR180204) and PD98059. FR180204 selectively inhibits ERK1 and ERK2 (Ohori *et al.*, 2007) while PD98059 inhibits p42/p44 MAP kinase. If the phosphorylation of cPLA$_2$ after stimulation by bombesin is through the ERK/MAPK pathway, no increased phospho-cPLA$_2$ would be observed in bombesin-stimulated cells in the presence of FR180204 or PD98059.

In addition to the cPLA$_2$ pathway, other possible mechanisms that may generate AA were investigated as well. As described in section 1.6.3.3.1, iPLA$_2$ is able to liberate AA (Atsumi *et al.*, 1998; Akiba *et al.*, 1999). Moreover, iPLA$_2$ is reported to play a role in SOCEs as an essential component of signal transduction from the stores to plasma membrane channels (Singaravelu *et al.*, 2006; Boittin *et al.*, 2008). Therefore, the involvement of iPLA$_2$ in the bombesin-evoked Ca^{2+} influx was tested. The inhibitor bromoenol lactone (BEL), which is a widely used iPLA$_2$ inhibitor (Balsinde *et al.*, 1995) was used as BEL substantially reduces SOCEs (Smani *et al.*, 2003).

5.2 Method

5.2.1 Cell culture

Swiss 3T3 cells and cells on either large or small islands cultured according to standard protocol as mentioned in section 2.1. For unrestricted cells, 3 day-confluent cells were transferred to glass coverslips 1 day before the experiment. After an initial 3-4 hours culture in FCS-DMEM on coverslips, the cells were kept in SF-DMEM for 16 hours prior to experimentation.

5.2.2 Stimulation by bombesin

The coverslips containing cells were placed in a 6 well plate containing HBS with 1mM Ca^{2+} at 37°C. Cells were divided into two groups: the control group and the bombesin-stimulated group. For the stimulated group, bombesin (100nM) was added into 3 distinct wells at 2 minutes, 4 minutes and 8 minutes before fixing the cells with 100% methanol. In the control group, a sham addition was made instead of bombesin.

5.2.3 Pre-treatment of cells with inhibitors

For the immunofluorescence experiments, 12 coverslips with Swiss 3T3 cells were divided into 3 groups with 4 coverslips in each group. The first group was used as a control pretreated with DMSO (1:500) in 1ml HBS for 1 hour at 37°C. In the same way, the other two groups are pre-incubated with inhibitors: FR180204 (10μM) or PD98059 (20μM) or BEL (20μM). After that, each group was stimulated with bombesin as described in section 5.2.2.

For the experiments testing the $[Ca^{2+}]_i$ response using Ca^{2+} PTI imaging system, coverslips were incubated with either DMSO as a vehicle control or inhibitors during the fura-2 loading at 37°C for 1 hr. At end of the incubation, the cells were washed with HBS containing 1mM Ca^{2+} and placed into chamber for the Ca^{2+} imaging system.

For the experiments using a Flexstation plate reader, similar protocols to those for the Ca^{2+} imaging system were used. DMSO or inhibitors were added during the fura-2 loading period in order to pre-incubate the cells with these agents. The following steps were the same standard protocol described in section 2.4.

5.2.4 Antibody staining

The cells were stained with primary antibody (phospho-$cPLA_2$ Ser^{505}-R) following the standard protocol described in section 2.5. However, cells on islands were fixed with 100% methanol for 5

min at room temperature rather than 10 min to order to diminish damage to the polyHEMA. In addition, cells on islands were loaded with the secondary antibody for 2 hours instead of 1 hour. In these experiments, Alexa Fluor 488 chicken anti-rabbit IgG was used as the secondary antibody. Antibody dilution was prepared as described in section 2.5.1. In the experiments testing the inhibitors (FR180204, PD98059 and BEL), Alexa Fluor 596 chicken anti-rabbit IgG was used as the secondary antibody.

5.2.5 Confocal microscopy

The distribution of phospho-cPLA$_2$ was examined using a Leica SP2 AOBS scanning confocal microscope. More details were described in section 2.5.3. After optimizing the confocal settings for control slides, the settings were then kept the same during each experiment in order to allow the relative staining intensity to be determined.

5.3 Results

5.3.1 Effect of bombesin on phospho-cPLA$_2$ in normal spreading cells

At least 8 separate experiments have been performed to test the effect of bombesin on phospho-cPLA$_2$ immunofluorescence in normal spreading cells. Figure 5.3.1A shows 4 confocal images of immunofluorescence of phospho-cPLA$_2$ in both resting and bombesin-stimulated cells that were selected from the same experiment. Each image was recorded under identical system settings. Un-restricted cells were grown on glass coverslips and the control group was un-stimulated before fixing with methanol (a). There are three sets of stimulated cells which were fixed at 2 minutes, 4 minutes and 8 minutes after stimulation by 100nM bombesin (c-d).

The immunofluorescence gives an indication of distribution and amount of phospho-cPLA$_2$ in each ser of cells. The images show that phospho-cPLA$_2$ was diffuse in the cytosol in both resting and stimulated cells. It is apparent that the fluorescence of stimulated cells is brighter than that of the resting cells, especially those cells fixed at 2 minutes after bombesin stimulation.

The change of fluorescence intensity of phospho-cPLA$_2$ was examined using the Leica software by calculating the mean and total intensity of each single cell. The total intensity is the sum

fluorescence in the selected area of interest (one single cell). The mean intensity is the average pixel fluorescence in the selected area. In figure 5.3.1B, the statistical data of the fluorescence intensity represented in each column was collected from 24 randomly selected cells from 6 experiments (4 cells from each experiment) using the same system settings. The results indicate that there is a significant increase of the phospho-$cPLA_2$ fluorescence intensity in bombesin-treated un-restricted cells with the maximum amount in the '2 minutes' stimulated group compared to other groups.

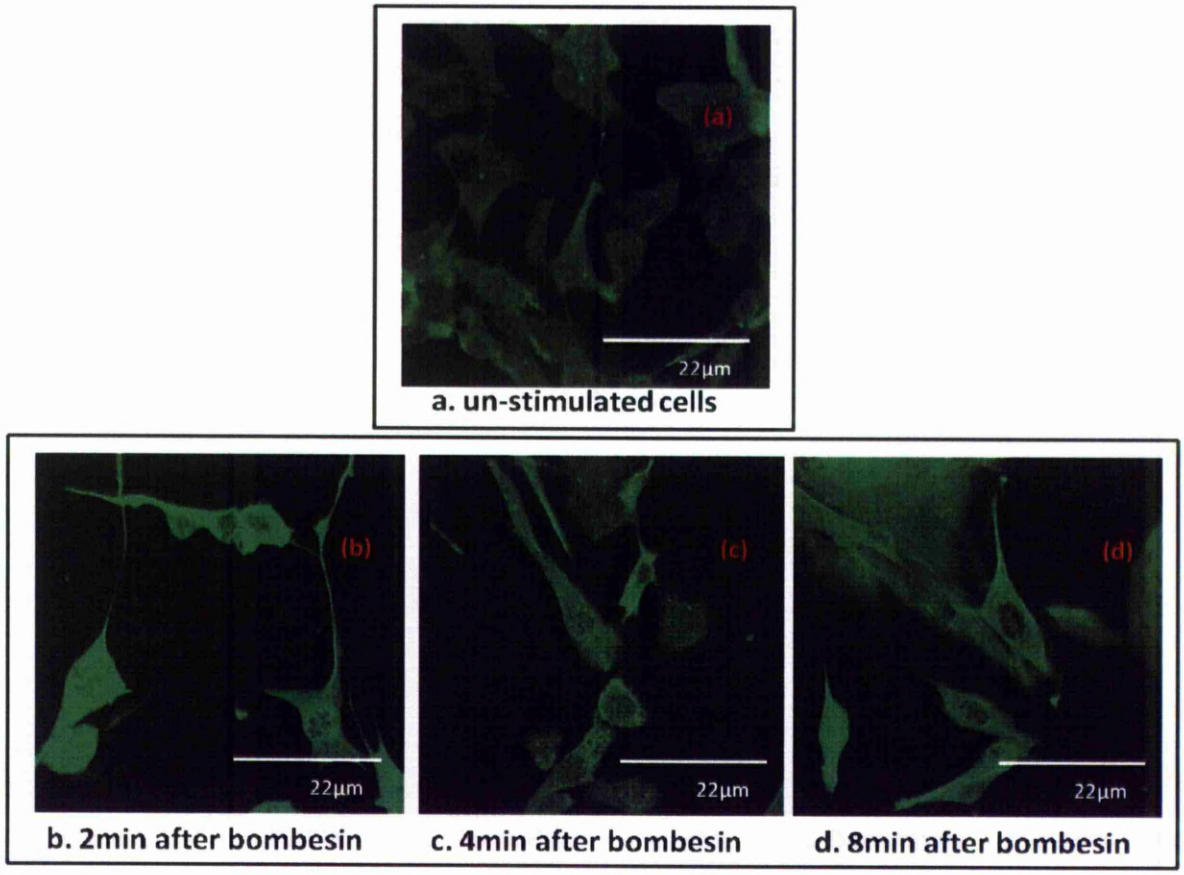

Figure 5.3.1A-The immunofluorescence of phospho-cPLA$_2$ in normal spreading cells

3-day-old quiescent Swiss 3T3 cells were cultured and unrestricted on glass coverslips in SF-DMEM for 16 hours before stained with primary antibody (phospho-cPLA$_2$ Ser^{505}-R) and secondary Alexa Fluor 488 chicken anti-rabbit IgG. Images were visualized with a Leica laser scanning confocal microscope. The images of resting cells are presented in figure a. Figure b-d are three sets of bombesin-stimulated cells that were fixed at 2 min, 4min and 8min respectively after the stimulation. Results shown are representative of 6 separate experiments.

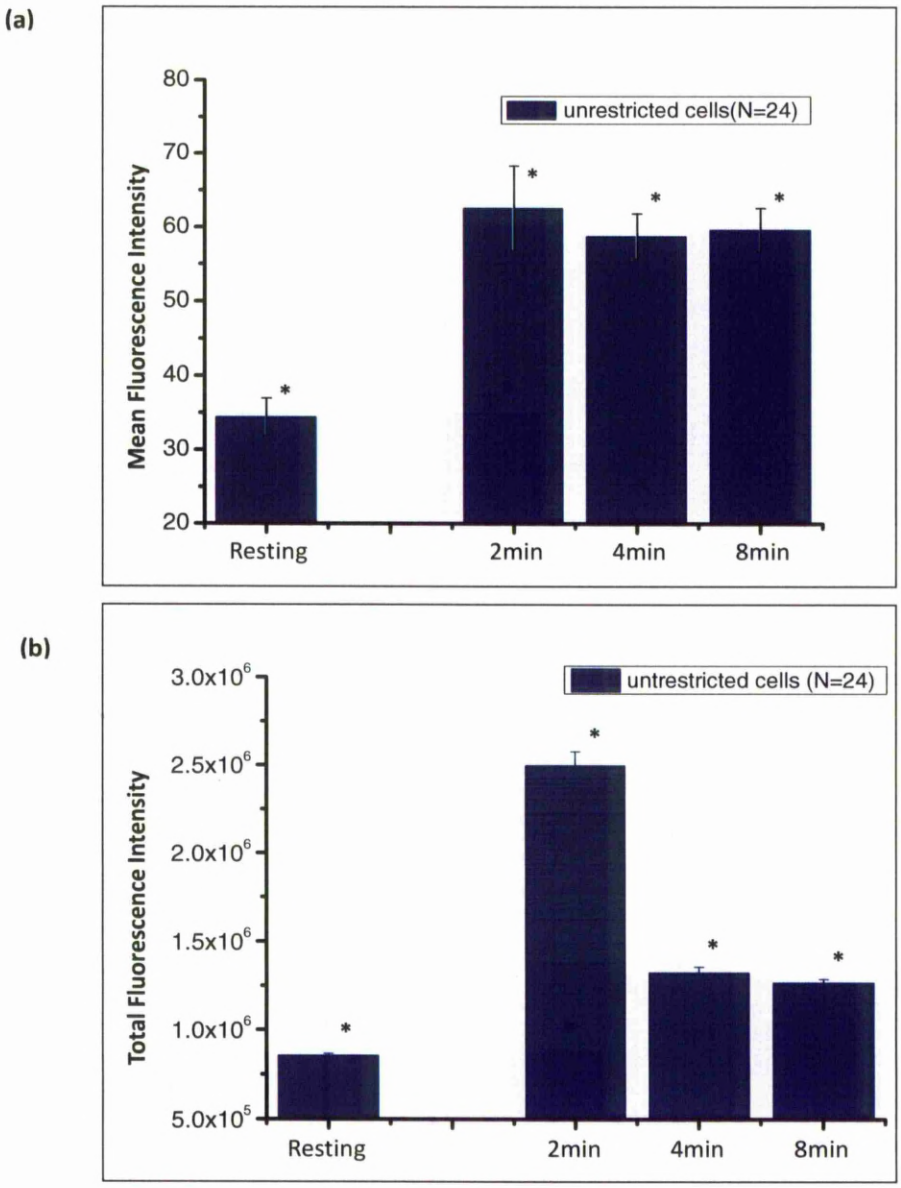

Figure 5.3.1B- The fluorescence intensity of phospho-cPLA$_2$ in normal spreading cells

3-day-old quiescent Swiss 3T3 cells were cultured and unrestricted on glass coverslips in SF-DMEM for 16 hours before stained with primary antibody (phospho-cPLA$_2$ Ser^{505}-R) and secondary Alexa Fluor 488 chicken anti-rabbit IgG. The solid bars represent the mean (a) or total (b) data of phospho-cPLA$_2$ fluorescence intensity in each single cell. Error bars shown are ± S.E. of (N) number of indicted cells. *P<0.05, statistical analysis of fluorescence intensity in (N) number of cells in each group are compared using one-way ANOVA.

5.3.2 Effect of bombesin on phospho-cPLA$_2$ in shape restricted cells

Following the study in normal spreading cells, the effect of cell shape on bombesin-evoked phospho-cPLA$_2$ was examined. In total, 16 separate experiments were conducted to test the influence of cell shape. Figure 5.3.2A shows the confocal image of 4 single cells on the large islands (a), and another 4 on the small islands (b). Both un-stimulated cells and bombesin-stimulated cells at 2, 4 and 8 minutes before fixation are shown. All images were recorded under the same system settings. These data are similar to that seen in un-restricted cells on the glass coverslips.

Figure 5.3.2B shows the statistical data of mean (a) and total (b) phospho-cPLA$_2$ fluorescence intensities from single cells on islands. There is a distinct increase of intensity in bombesin-stimulated cells on the large islands, which is confirmed by the one-way ANOVA test ($p<0.05$). Although there is an apparent increase of intensity in stimulated cells at 2min and 4min time points in cells on the small islands, the differences are not significant according to ANOVA analysis. Figure 5.3.2B also suggests that the resting phospho-cPLA$_2$ immunofluorescence intensity (mean data) is higher in cells on small islands than that in the cells on large islands.

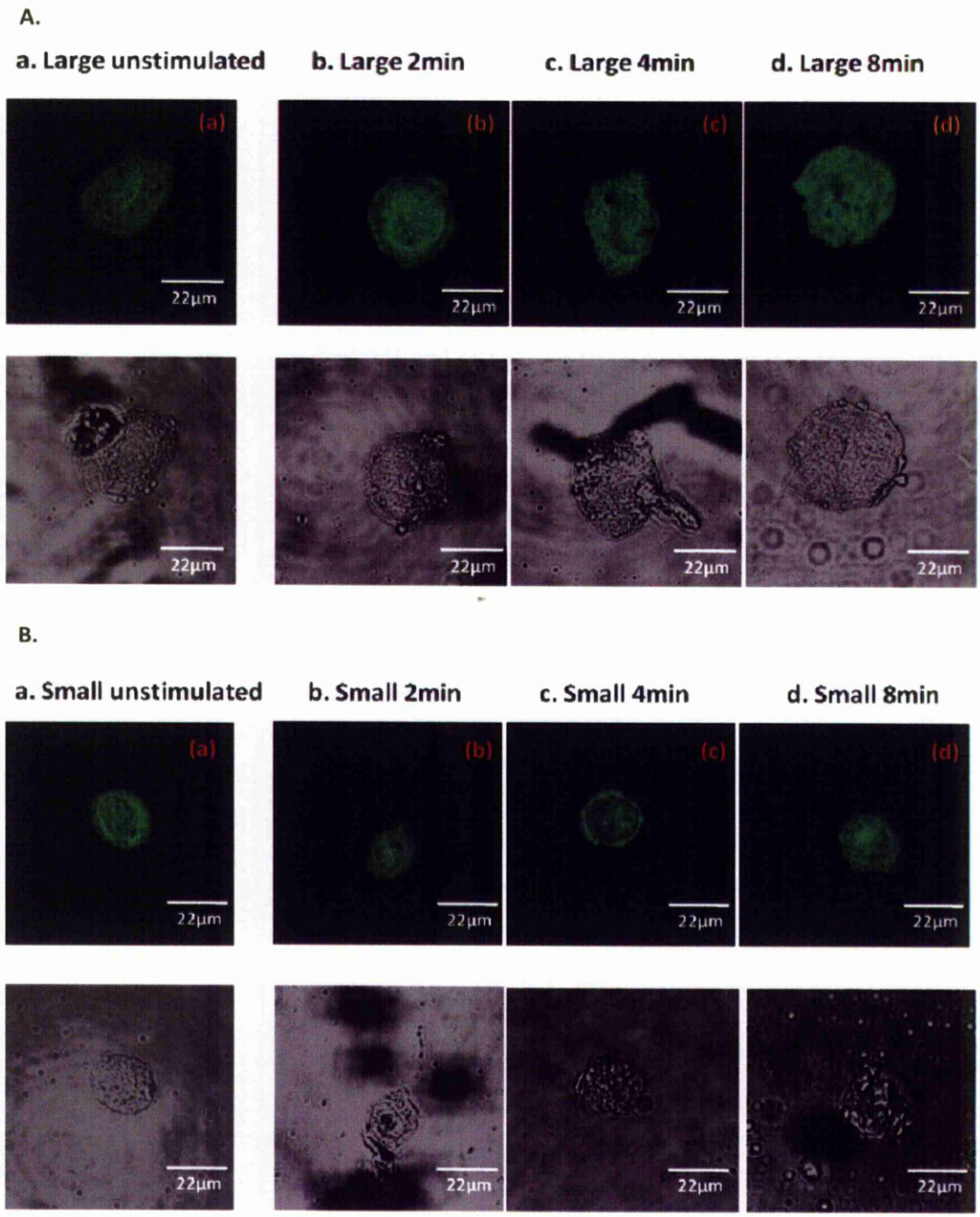

Figure 5.3.2A-The immunofluorescence of phospho-cPLA$_2$ in shape restricted cells

3-day-old quiescent Swiss 3T3 cells were cultured and restricted with either large or small islands in SF-DMEM for 16 hours before stained with primary antibody (phospho-cPLA$_2$ Ser^{505}-R) and secondary Alexa Fluor 488 chicken anti-rabbit IgG. Images were visualized with a Leica laser scanning confocal microscope. The images of resting cells are presented in figure (a). Figure (b-d) show three sets of bombesin-stimulated cells that were fixed at 2 min, 4min and 8min respectively after the stimulation. Results shown are representative of 16 separate experiments.

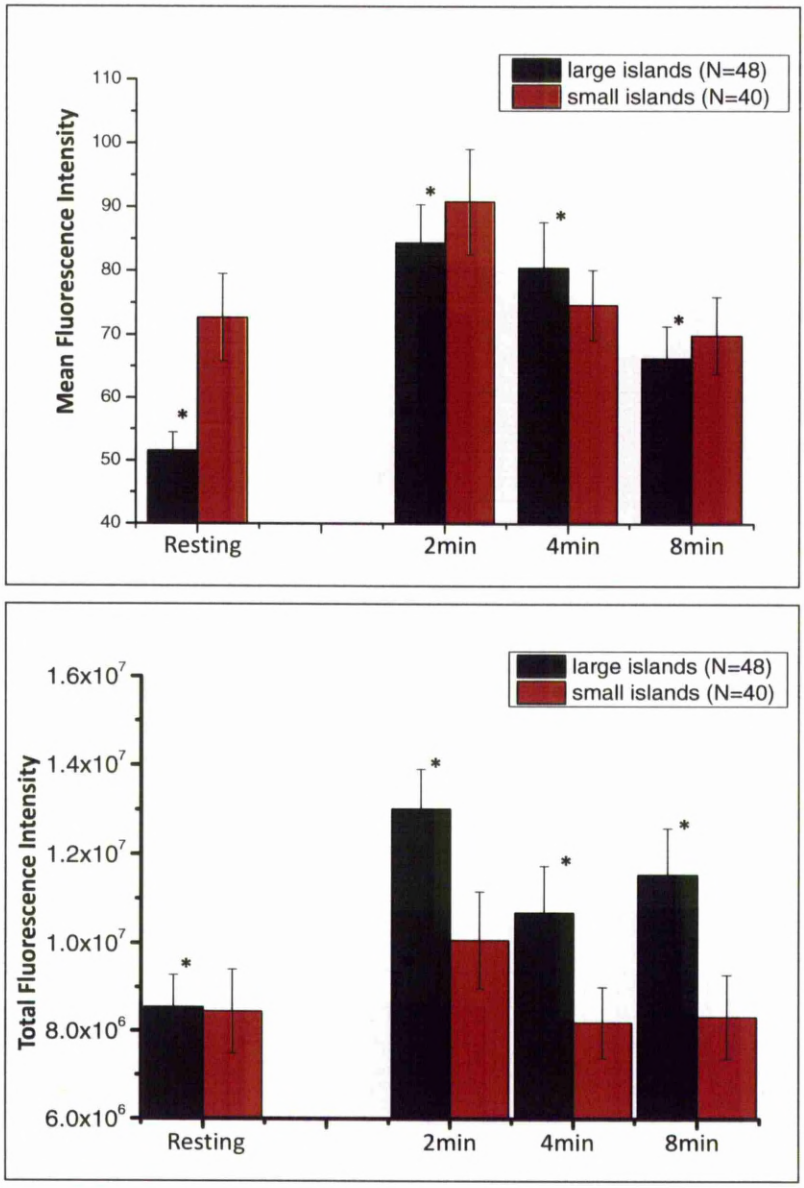

Figure 5.3.2B-The fluorescence intensity of phospho-cPLA$_2$ in shape restricted cells

3-day-old quiescent Swiss 3T3 cells were cultured and restricted with either large or small islands in SF-DMEM for 16 hours before stained with primary antibody (phospho-cPLA$_2$ Ser^{505}-R) and secondary Alexa Fluor 488 chicken anti-rabbit IgG. The solid bars represent the mean (a) or total (b) data of phospho-cPLA$_2$ fluorescence intensity in each single cell. The black bars represent the data in cells on large islands while the red bars are for those on the small islands. Error bars shown are ± S.E. of (N) number of indicated cells. *P<0.05, statistical analysis of fluorescence intensity in (N) number of cells in each group are compared using one-way ANOVA.

5.3.3 The mechanism of bombesin regulated cPLA$_2$ phosphorylation

The data presented in section 5.3.1 indicates that there is a phospho-cPLA$_2$ intensity increase in bombesin-stimulated cells. The mechanism of bombesin-regulated phospho-cPLA$_2$ activation was therefore further examined by testing whether the ERK/MAP kinase pathway was involved in the phosphorylation of cPLA$_2$. Figure 5A shows the two inhibitors, FR180204 and PD98059 could inhibit the phosphorylation of cPLA$_2$ by MAPK. Figure 5.3.3A shows the phospho-cPLA$_2$ immunofluorescence of 3 cell groups treated with DMSO as a control or treated with one of the ERK inhibitors, FR180204 or PD98059. The level of phospho-cPLA$_2$ in either resting or bombesin stimulated cells are compared in each group (A-C).

In total, 3 experiments following the same protocol have been performed. Three of experiments showed that with the presence of FR180204 (10μM) or PD98059 (20μM), the phospho-cPLA$_2$ fluorescence increased in the bombesin stimulated cells, especially in those cells fixed 2 minutes after the bombesin addition.

Figure 5.3.3B shows the statistical data of mean (a) and total (b) phospho-cPLA$_2$ fluorescence intensity in either DMSO-controlled or inhibitor-treated cells. The statistical analysis indicates that the level of phospho-cPLA$_2$ fluorescence intensity in either FR180204- or PD98059- treated cells is lower than that in the DMSO-controlled cells, no matter whether the cells were resting or bombesin-stimulated. However, according to the t-test analysis, such difference is not significant, except difference between control cells and the ones treated by PD98059 at the time point of 8min after bombesin-stimulation. Moreover, a significant increase of phospho-cPLA$_2$ fluorescence intensity was still observed in inhibitor-treated cells according to one-way ANOVA analysis ($p<0.05$). Generally speaking, the ERK inhibitors seem to have no influence on the cPLA$_2$ activation regulated by bombesin, though they showed a trend to suppress the resting level of phospho-cPLA$_2$.

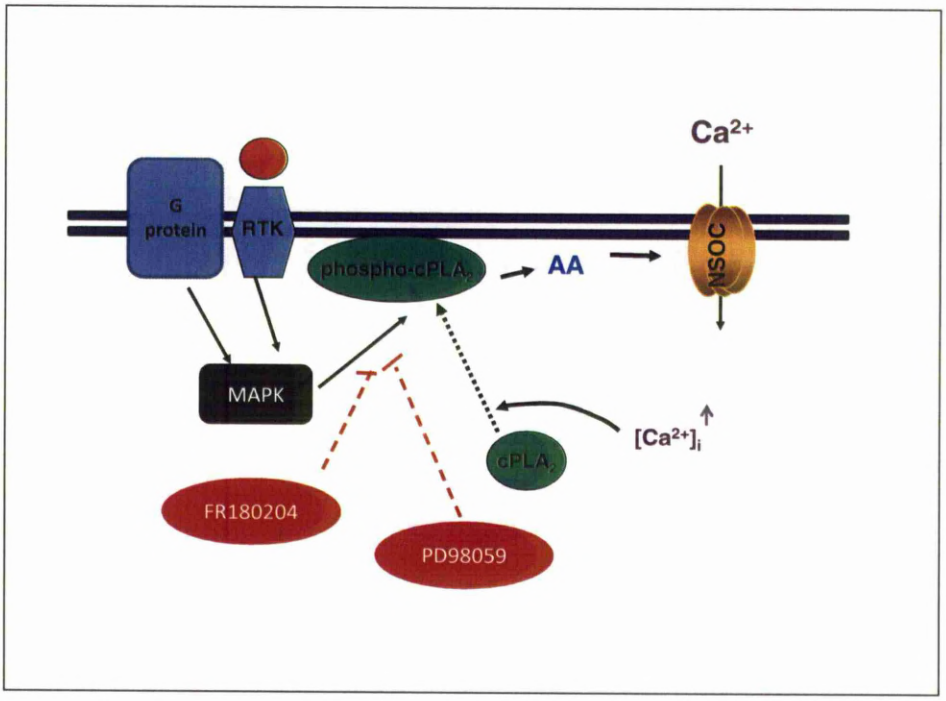

Figure 5A-Inhibition mechanism of ERK FR180204 and PD98059

The figure shows the inhibition mechanism of ERK FR180204 and PD98059 on $cPLA_2$ activation pathway. Both inhibitors could block the phosphorylation of $cPLA_2$ by MAPK.

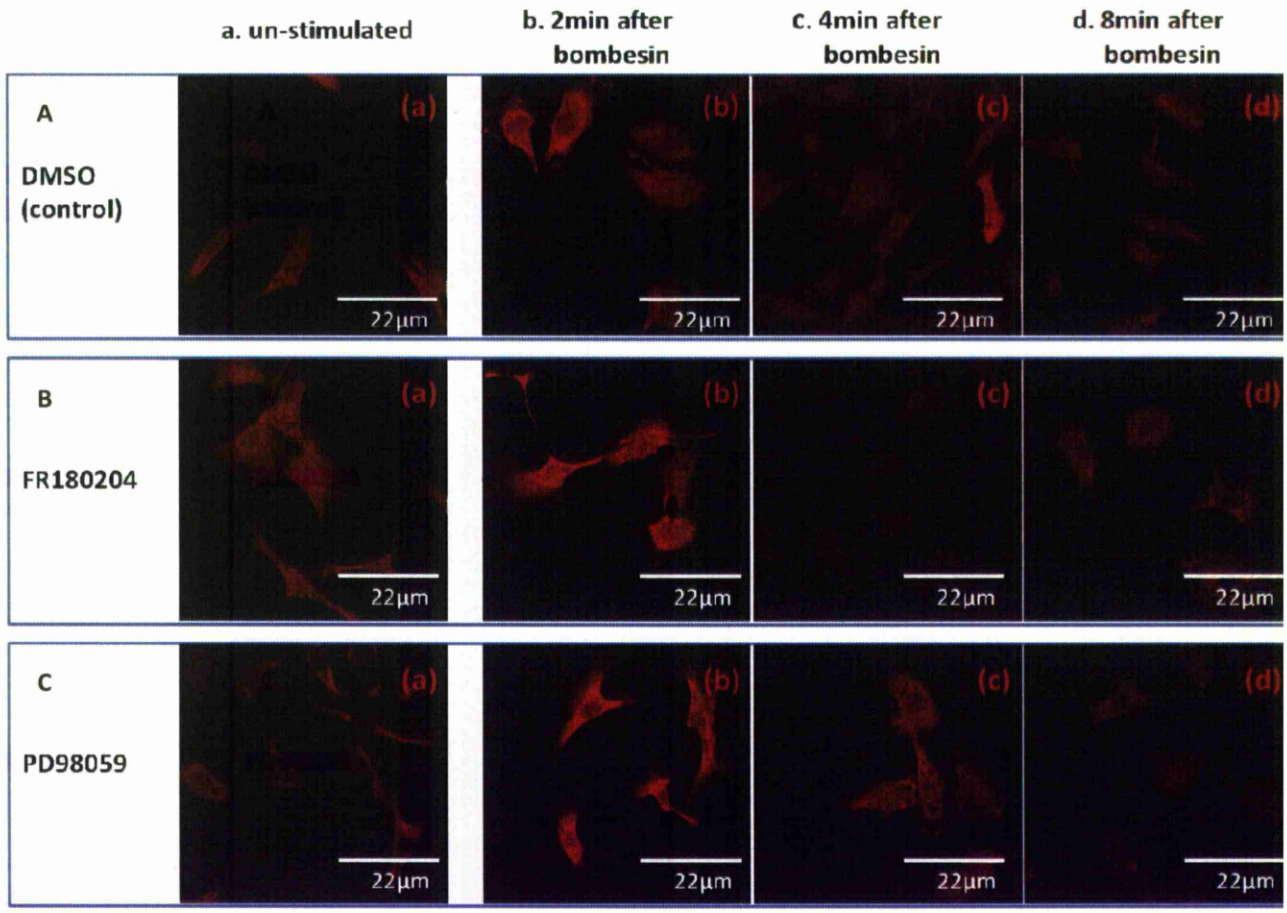

Figure 5.3.3A-The effect of ERK inhibitors in bombesin regulated phospho-cPLA$_2$ activation

3-day-old quiescent Swiss 3T3 cells were cultured and unrestricted on glass coverslips in SF-DMEM for 16 hours before stained with primary antibody (phospho-cPLA$_2$ Ser^{505}-R) and secondary Alexa Fluor 596 chicken anti-rabbit IgG. Images were visualized with a Leica laser scanning confocal microscope. The cells in group A were pre-treated with DMSO for 1 hour while the other two groups (B&C) were pre-treated with FR180204 or PD98059 respectively. The images of resting cells in each group are presented in figure (a). Figure (b-d) show three sets of bombesin-stimulated cells that were fixed at 2 min, 4min and 8min respectively after the stimulation. Results shown are representative of 3 separate experiments.

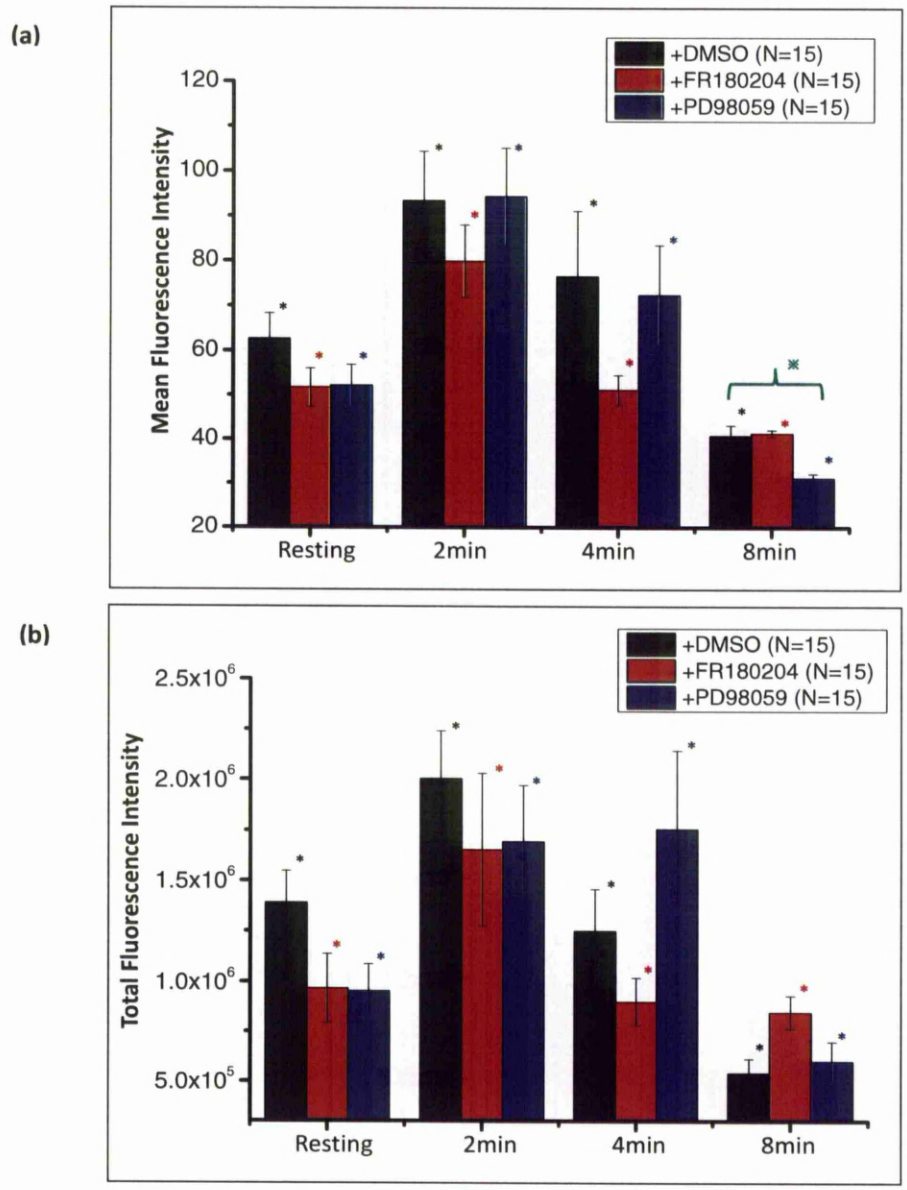

Figure 5.3.3B-The effect of ERK inhibitors in bombesin regulated phospho-cPLA$_2$ activation

3-day-old quiescent Swiss 3T3 cells were cultured and restricted with either large or small islands in SF-DMEM for 16 hours before stained with primary antibody (phospho-cPLA$_2$ Ser^{505}-R) and secondary Alexa Fluor 596 chicken anti-rabbit IgG. The solid bars represent the mean (a) or total (b) data of phospho-cPLA$_2$ fluorescence intensity in each single cell. The black bars represent the data in controlled cells and the red and blue bars represent the data in the FR180204 or PD98059 treated cells. Error bars shown are ± S.E. of (N) number of indicated cells. *P<0.05, statistic analysis of fluorescence intensity in (N) number of cells in each group are compared using one-way ANOVA. ※P<0.05, when statistical analysis of fluorescence intensity in (N) number of cells are subjected to t-test.

5.3.4 The effect of ERK inhibitors and BEL in bombesin-induced $[Ca^{2+}]_i$ response

The ERK inhibitors and BEL were further used to test whether the bombesin-induced $[Ca^{2+}]_i$ response requires either $cPLA_2$ phosphorylation or $iPLA_2$ activity. Figure 5B shows the inhibition mechanism of BEL. Experiments were performed either using a PTI Ca^{2+} imaging system or a Flexstation plate reader.

The figure 5.3.4A shows the bombesin-induced $[Ca^{2+}]_i$ responses in DMSO-treated control cells or inhibitor-treated cells. In figure 5.3.4A (a), the typical $[Ca^{2+}]_i$ response to 100nM bombesin in DMSO-treated cells is seen. In total, 4 control experiments were performed (n=14 cells). Figure 5.3.4A (b) shows the $[Ca^{2+}]_i$ responses in the cells treated with all three inhibitors FR180204 (10μM), PD98059 (20μM) and BEL (20μM) for 1 hr. The bombesin-induced $[Ca^{2+}]_i$ responses were inhibited in the cells treated with all 3 inhibitors, which was observed in all the 5 experiments (n=15 cells). Figure 5.3.4A (c-e) shows the $[Ca^{2+}]_i$ responses in the cells treated with one of the three inhibitors. When the cells were treated with the inhibitors separately, the bombesin-induced $[Ca^{2+}]_i$ response was still seen in FR180204- (n=5 cells) or PD98059- (n=7 cells) treated cells, whereas it was blocked in BEL-treated cells (n=6 cells). This indicates that both ERK inhibitors FR180204 and PD98059 have little effect on the bombesin-evoked $[Ca^{2+}]_i$ responses while BEL is effective to inhibit the response. Earlier studies showed BEL has no inhibition on the thapsigargin-induced Ca^{2+} release (Smani *et al.*, 2003). In this study, BEL suppressed the bombesin-evoked Ca^{2+} release.

To confirm the results, similar experiments were performed with the Flexstation plate readers to monitor the $[Ca^{2+}]_i$ responses with the presence of inhibitors. Figure 5.3.4B shows the Flexstation recorded bombesin-evoked $[Ca^{2+}]_i$ responses traces in either DMSO control or inhibitor-treated cells. The traces present the typical response seen 1 in 5 replicate wells. The results were quite consistent with those obtained from the PTI Ca^{2+} imaging system. The bombesin-induced $[Ca^{2+}]_i$ responses, including Ca^{2+} release and Ca^{2+} influx were completely inhibited in cells-treated with all 3 inhibitors or those treated with BEL alone. The cells incubated with both FR180204 and PD98059 showed similar $[Ca^{2+}]_i$ responses to the control cells.

In summary, the results indicated that these two ERK inhibitors: ERK FR180204 and PD98059 have no inhibition effect on bombesin-induced $[Ca^{2+}]_i$ response in 3T3 cells, which suggests the phosphorylation of $cPLA_2$ is not required for the bombesin to evoke $[Ca^{2+}]_i$ response. On the other hand, since the BEL alone is enough to inhibit such $[Ca^{2+}]_i$ responses, $iPLA_2$ is possibly involved.

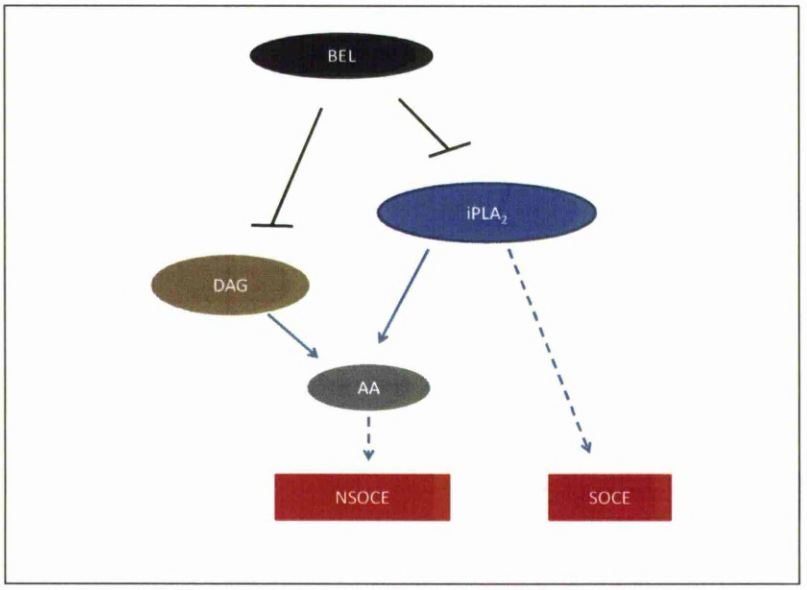

Figure 5B-The inhibition mechanism of BEL in Ca^{2+} related responses

This figure shows the inhibition mechanism of BEL in Ca^{2+} entry pathways. BEL could inhibit the activity of $iPLA_2$ and the generation of DAG.

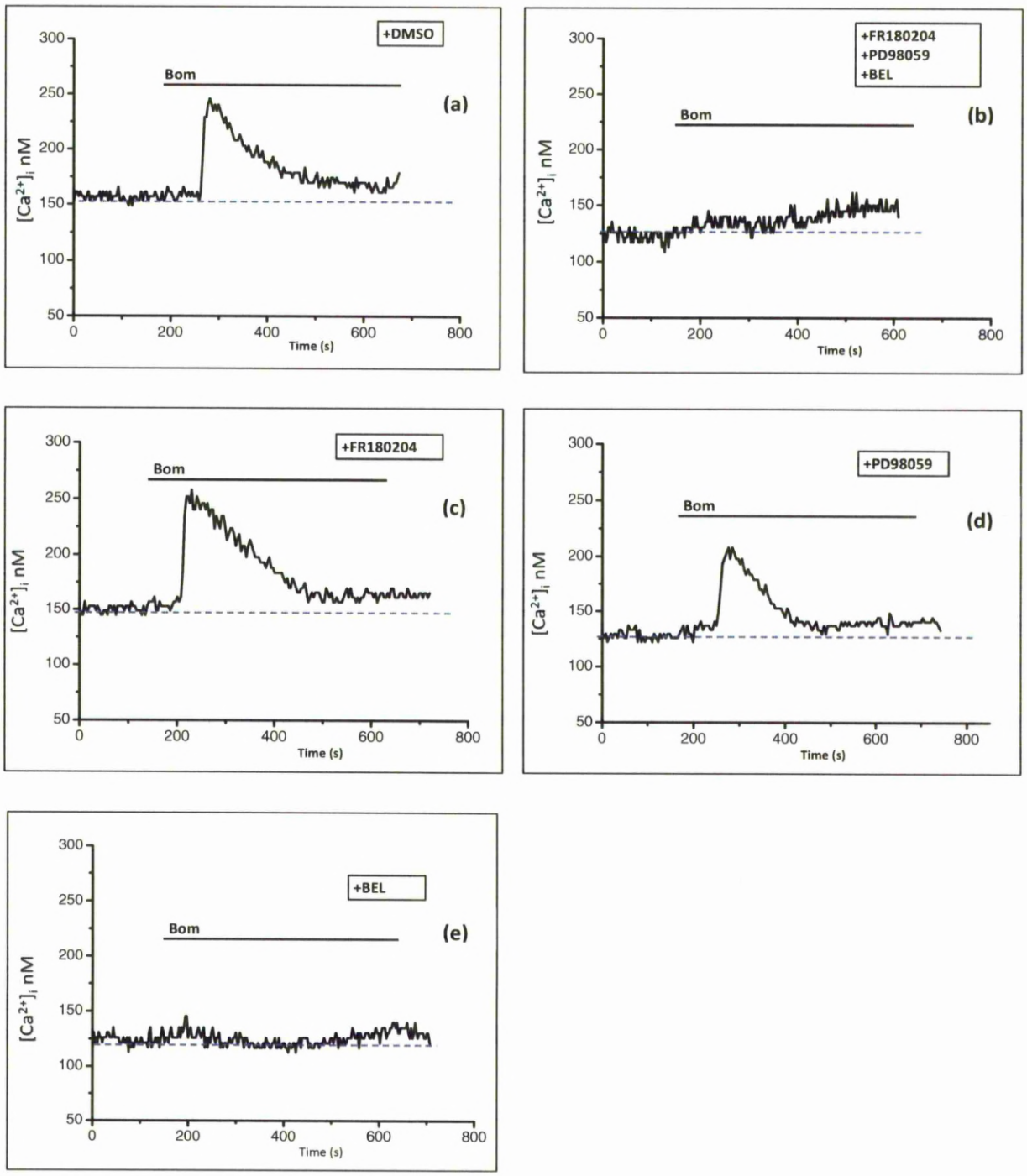

Figure 5.3.4A-The effect of ERK inhibitors and BEL in bombesin-induced $[Ca^{2+}]_i$ response

3-day-old quiescent Swiss 3T3 cells were cultured on coverslips in SF-DMEM for 16 hours before experiments. A $[Ca^{2+}]_i$ response is shown to bombesin (100nM) added at 180 seconds in the

presence of 1mM Ca^{2+} in HBS. The $[Ca^{2+}]_i$ was measured using fura-2, at 37°C, using a Ca^{2+} imaging system. Figure (a) shows a typical $[Ca^{2+}]_i$ response in a DMSO control cell. Figure (b) shows a typical $[Ca^{2+}]_i$ response in cells treated with all 3 inhibitors (FR & PD & BEL). Figures (c-e) show three $[Ca^{2+}]_i$ responses to bombesin in cells treated with either FR180204 or PD98059 or BEL respectively. Each figure is representative of at least 2 separate experiments.

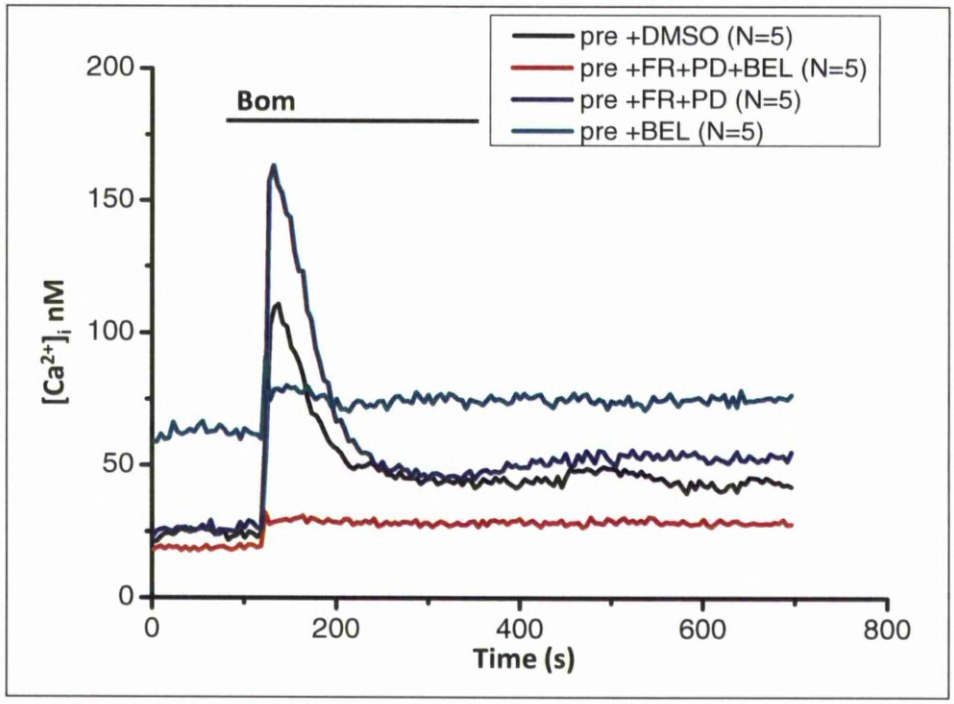

Figure 5.3.4B-The effect of ERK inhibitors and BEL in bombesin-induced $[Ca^{2+}]_i$ response

3-day-old quiescent Swiss 3T3 cells were cultured in 96-well plates in SF-DMEM for 16 hours before experiments. Each line represents a $[Ca^{2+}]_i$ response to bombesin (100nM) added at 120 seconds in the presence of 1mM Ca^{2+} in HBS in each well. The $[Ca^{2+}]_i$ was measured using fura-2, at 37°C, using a Flexstation reader. The cells were pretreated with either DMSO or inhibitors for 1 hr before reading the $[Ca^{2+}]_i$ responses to bombesin. Individual traces are typical of 5 similar replicates from a single plate.

5.4 Discussion

The data presented in this chapter suggests that there is an increase of phospho-$cPLA_2$ following the stimulation by bombesin in normal spreading Swiss 3T3 cells. Since the activation of $cPLA_2$ requires phosphorylation to form phospho-$cPLA_2$, this finding is consistent with the hypothesis that the bombesin leads to the generation of AA through $cPLA_2$ resulting in AA-induced Ca^{2+} influx. Another prediction is that activation of $cPLA_2$ requires its translocation to intracellular membrane. However, because the distribution of phosphorylated $cPLA_2$ was measured, the location of $cPLA_2$ before its phosphorylation is unclear. The $cPLA_2$ has been found to target Golgi, ER and the perinuclear membrane (Evans *et al.*, 2001). Due to the abundant immunofluorescence signal of phospho-$cPLA_2$ in Swiss 3T3 cells, it was difficult to identify the exact location of phospho-$cPLA_2$. It has also been suggested that the $cPLA_2$ is already localized within the membrane during the activation of I_{ARC}, since no significant Ca^{2+} dependent $cPLA_2$ translocation is detected at low agonist concentration (Osterhout and Shuttleworth, 2000). Therefore, whether the $cPLA_2$ has been translocated and fully activated after the bombesin-stimulation needs to be verified.

The application of two ERK inhibitors: FR180204 and PD98059 suggests that the ERK pathway, which is known to be the main pathway for $cPLA_2$ phosphorylation (Chang *et al.*, 2006), has no role in the increase of phospho-$cPLA_2$ after bombesin-stimulation. Furthermore, these two inhibitors showed little effect on bombesin-induced $[Ca^{2+}]_i$ responses as well, which implies that the phosphorylation of $cPLA_2$ by ERKs is not involved this Ca^{2+} entry pathway. These findings challenge our hypothesis. One explanation is that the bombesin-induced $cPLA_2$ phosphorylation is not mediated by ERKs but by other kinases. Similar results have been reported which underpin such possibility. For example, it was observed that PD98059 failed to inhibit the phosphorylation of $cPLA_2$ stimulated by thrombin or collagen. As a result, it is believed that the ERKs are not involved in the process of AA release from platelets (de Carvalho *et al.*, 1996). It was also found that phosphorylation of $cPLA_2$ in lipopolysaccharide- or TNFa-treated neutrophils and thrombin-stimulated platelets occurred independently on p42/p44 MAP kinase activation (Leslie, 1997). Moreover, PKC and PKA have been reported to phosphorylate $cPLA_2$ *in vitro*, though the increase of $cPLA_2$ activity is slight (Qiu and Leslie, 1994). Nevertheless, another possibility is that

the phosphorylated $cPLA_2$ is the consequence of the bombesin-evoked $[Ca^{2+}]_i$ response rather than the cause. As described in section 1.6.3.3, a relevant change of $[Ca^{2+}]_i$ plays an important role in promoting the translocation of $cPLA_2$ to associate with its substrate and become activated (Clark *et al.*, 1991; Leslie, 1997). In another words, the $cPLA_2$ is not required for the $[Ca^{2+}]_i$ response caused by bombesin.

Although the importance of $cPLA_2$ in the bombesin-evoked $[Ca^{2+}]_i$ response is questioned, the involvement of AA which could be generated through other pathways cannot be ruled out. Since BEL is a typical $iPLA_2$ inhibitor which inhibits the bombesin-induced $[Ca^{2+}]_i$ response. It is suspected that it is $iPLA_2$ and not $cPLA_2$ that is responsible for the $[Ca^{2+}]_i$ response activated by bombesin. Evidence has shown that $iPLA_2$ is capable of liberating AA (Balsinde and Dennis, 1997). The inhibition of $[Ca^{2+}]_i$ response by BEL (Figure 5.3.4A) may block the elevation of $[Ca^{2+}]_i$ required by $cPLA_2$ activation, since it was observed that BEL prevented the increase of phospho-$cPLA_2$ after bombesin stimulation (preliminary data not shown). If this is true, it confirms that the increase of phospho-$cPLA_2$ after the bombesin-induced $[Ca^{2+}]_i$ elevation is the consequence but not the cause of the process. It was also argued that BEL cannot be used as a selective $iPLA_2$ inhibitor in whole cell studies since it indirectly inhibits the DAG activation as well (Balsinde and Dennis, 1997). It was found that BEL inhibits the activity of Mg^{2+}-dependent PA phosphohydrolase (PAP-1) which can convert PA into DAG in the PLD-DAG pathway (Section 1.6.3.4) (Balsinde and Dennis, 1996) DAG, however, has also been proved demonstrated to produce AA (Kennerly *et al.*, 1979). Hence, no matter whether BEL blocks either the activation of $iPLA_2$ or DAG, it is capable of hindering the generation of AA after all.

In addition to the function in AA generation, $iPLA_2$ has been reported to be involved in the SOCEs. For example, it was observed that the impairment of $iPLA_2$ function with BEL leads to irreversible inhibition of thapsigargin-induced SOCEs in wide variety of cell types (Smani *et al.*, 2003; Martínez and Moreno, 2005; Singaravelu *et al.*, 2008). The crucial role of $iPLA_2$ in SOCE activation was recently confirmed by the observation that molecular knockdown of the CG6718 gene which is a *Drosophila* homologue of human $iPLA_2\beta$ significantly affected SOCE (Vig *et al.*, 2006). A relationship among STIM1, Orai, CIF and $iPLA_2\beta$ was reviewed and it was argued that CIF-induced

activation of $iPLA_2\beta$ can promote the signal transduction between STIM1 and Orai1, leading to Ca^{2+} entry (reviewed by Bolotina, 2008). Therefore, although I believe $iPLA_2$ is necessary for the bombesin to induce a $[Ca^{2+}]_i$ response, which Ca^{2+} entry pathway is involved is still uncertain.

In this chapter, the influence of cell shape on the $cPLA_2$ phosphorylation was tested. According to the results, the increase of the phospho-$cPLA_2$ in the cells on small islands seemed to be partially inhibited compared to the increase seen in cells on large islands and the normal unrestricted cells. However, since the results of the phospho-$cPLA_2$ immunofluorescence in the restricted cells showed a great variation, this conclusion needs to be verified. Based on the speculation mentioned above, the augmentation of phospho-$cPLA_2$ as a consequence of bombesin-evoked $[Ca^{2+}]_i$ response may be restrained due to the inhibition of Ca^{2+} influx in shape restricted cells.

The key evidence presented in this chapter is listed in following:

1. There is a significant increase of phospho-$cPLA_2$ after the stimulation of bombesin in normal spreading Swiss 3T3 cells.
2. The significant increase of phospho-$cPLA_2$ intensity was observed in cells on the large islands but not the ones on the small islands.
3. Two ERK inhibitors, FR180204 and PD98059 showed little effect on the increase of phospho-$cPLA_2$ intensity and bombesin-evoked $[Ca^{2+}]_i$ response in Swiss 3T3 cells.
4. The inhibitor BEL effectively blocked the bombesin-evoked $[Ca^{2+}]_i$ response in Swiss 3T3 cells.

In order to confirm which Ca^{2+} entry pathway is responsible for the bombesin-evoked $[Ca^{2+}]_i$ elevation, I decided to use inhibitor to distinguish SOCE from NSOCE. The results were presented in chapter 6.

Chapter 6

The effect of diverse inhibitors on bombesin-induced Ca^{2+} influx

Contents:

Figures:

6.1 Introduction

The last chapter provided evidence that the activation of $cPLA_2$ may not be a pre-requisition for Ca^{2+} influx as was expected in the bombesin-induced $[Ca^{2+}]_i$ response in Swiss 3T3 cells. In order to find out which Ca^{2+} entry pathway is involved in bombesin-evoked Ca^{2+} influx, a number of inhibitors more specific to the generation of AA were utilized.

A $cPLA_2\alpha$ inhibitor was first used to block the activation of $cPLA_2\alpha$, which is the only PLA_2 enzyme that shows significant selectivity toward phospholipids bearing AA at the sn-2 position (Murakami and Kudo, 2002). AACOCF3, a potent slow inhibitor of $cPLA_2$, was applied as well. In addition to the $cPLA_2$ pathway, the involvement of DAG pathway was further tested with a DAG lipase inhibitor, RHC80267 (Sutherland and Amin, 1982; Trimble *et al.*, 1993). It has been demonstrated that DAG lipase pathway is an important alternative way to release AA (Canonico *et al.*, 1985; Chuang and Severson, 1990).

In addition, activating influx downstream of AA generation was tested using a non selective cation channel blocker LOE908, which has frequently been used to examine the activation of NSCCs. It was reported that the non-selective cationic channels (NSCCs) are distinguished from SOCCs in terms of their sensitivity to LOE908 but not SK&F96365 (Kawanabe *et al.*, 2001; Niger *et al.*, 2004). The participation of SOCCs has been tested with the inhibitor SK&F96365 which is widely used to block the thapsigargin-induced store-operated Ca^{2+} influx (Yoshida *et al.*, 2003).

Generally speaking, in this chapter, the involvement of AA and the mechanism of its generation in the shape-dependent Ca^{2+} influx pathway are studied using various inhibitors.

6.2 Method

6.2.1 Cell culture

Swiss 3T3 cells were cultured as described in section 2.1. Cells were plated onto glass coverslips and culture in FCS-DMEM for 3-4 hours. Subsequently, cells were kept in SF-DMEM for 16 hours before the experiments.

6.2.2 Addition of $cPLA_2$ and Ca^{2+} influx inhibitors

In order to test the effect of $cPLA_2\alpha$ inhibitor (6μM), RHC80267 (20μM) and AACOCF3 (10μM), cells on coverslips were incubated with either DMSO as control or inhibitors in SF-DMEM at 37°C overnight. After that, cells were loaded with fura-2 as described in section 2.3.2. Inhibitors were again added into the HBS containing 1mM Ca^{2+} when cells were placed in the chamber for PTI Ca^{2+} imaging system expect for those controlled cells. LOE908 (30μM) and SK&F96365 (30μM) were added instantly during the experiment.

6.2.3 Ca^{2+} imaging

Prior to the experiment, cells on glass coverslips were loaded with 2μM fura-2 and immersed in HBS containing 1mM Ca^{2+} or Ca^{2+} free HBS. The photometric traces showing the changes of fura-2 fluorescence that were monitored from individual cells using PTI Ca^{2+} imaging system (see section 2.3 for more details).

6.2.4 Flexstation microplate reader

The cells were loaded with fura-2 following the standard protocol described in section 2.4. During the reading, inhibitors and bombesin were added sequentially. In the experiments testing the Ca^{2+} influx, the compounds were diluted with 1mM Ca^{2+} containing HSB. In the compound plate, the first column was added with control vehicle or one of the inhibitors and the second column was added with bombesin. In the experiments testing the Ba^{2+} or Sr^{2+} influx, compounds were diluted with Ca^{2+} free HBS. In the compound plate, the first two columns were prepared as described above while the third column contained Ba^{2+} or Sr^{2+}.

6.3 Results

6.3.1 The effect of AA inhibitors on bombesin-induced $[Ca^{2+}]_i$ responses

Three inhibitors were used (cPLA$_2\alpha$ inhibitor, RHC80267 and AACOCF3) to test the involvement of AA in bombesin-induced $[Ca^{2+}]_i$ responses. Figure 6 shows the inhibition mechanism of these three inhibitors on the AA generation. When the inhibitors were added to cells instantly before the bombesin, there was no apparent inhibition (data not presented). As a result and following previous studies, cells were then pre-incubated with each of these inhibitors overnight or with DMSO as a control. Then during the experiments, the same concentration of each inhibitor was added to the HBS.

Figure 6.3.1A shows a typical $[Ca^{2+}]_i$ response evoked by 100nM bombesin in either control or inhibitor-treated cells. In total, 6 similar experiments were performed to confirm the results. Figure 6.3.1B exhibits the statistical data relating to the increase of $[Ca^{2+}]_i$ caused by bombesin at both the peak and plateau points of the response in either control and inhibitor treated cells. A t-test was used to compare the responses and small but significant changes were recorded ($p<0.05$). Compared to the response in control cell (n=45 cells), 6μM cPLA$_2\alpha$ inhibitor (n=58 cells) and 20μM RHC80267 (n=37 cells) show some inhibition at the $[Ca^{2+}]_i$ response induced by bombesin while 10μM AACOCF3 (n=22 cells) was not very effective. The results indicate that the cPLA$_2\alpha$ inhibitor somehow increases the $\Delta[Ca^{2+}]_i$ at the peak points but that it significantly inhibits the Ca^{2+} influx. The RHC80267 compound inhibits both the bombesin-evoked Ca^{2+} release and influx. However, AACOCF3 showed no significant influence on the $[Ca^{2+}]_i$ response.

In addition, the effect of these inhibitors was tested with a Flexstation plate reader. Figure 6.3.1C shows the typical bombesin-evoked $[Ca^{2+}]_i$ responses in either vehicle control or inhibitor-treated cells monitor by Flexstation in each 96-well plate. "N" represents the number of replicate wells that were recorded from 2 plates. Cells were treated with inhibitor at the beginning of the experiments followed with the stimulation of 100nM bombesin. Figure 6.3.1C (a) which shows the $[Ca^{2+}]_i$ response in control (red) and cPLA$_2\alpha$ inhibitor treated cells (black) indicated that cPLA$_2\alpha$ inhibitor increases the overall $[Ca^{2+}]_i$ response. Figure 6.3.1C (b) shows the response in control or RHC80267-treated cells which suggest that RHC80267 suppresses the

bombesin-induced Ca^{2+} influx. Figure 6.3.1C (c) indicates that AACOCF3 has little effect on bombesin-evoked $[Ca^{2+}]_i$ response. Generally, the results obtained from Flexstation reader are consistent with that obtained from the PTI Ca^{2+} imaging system.

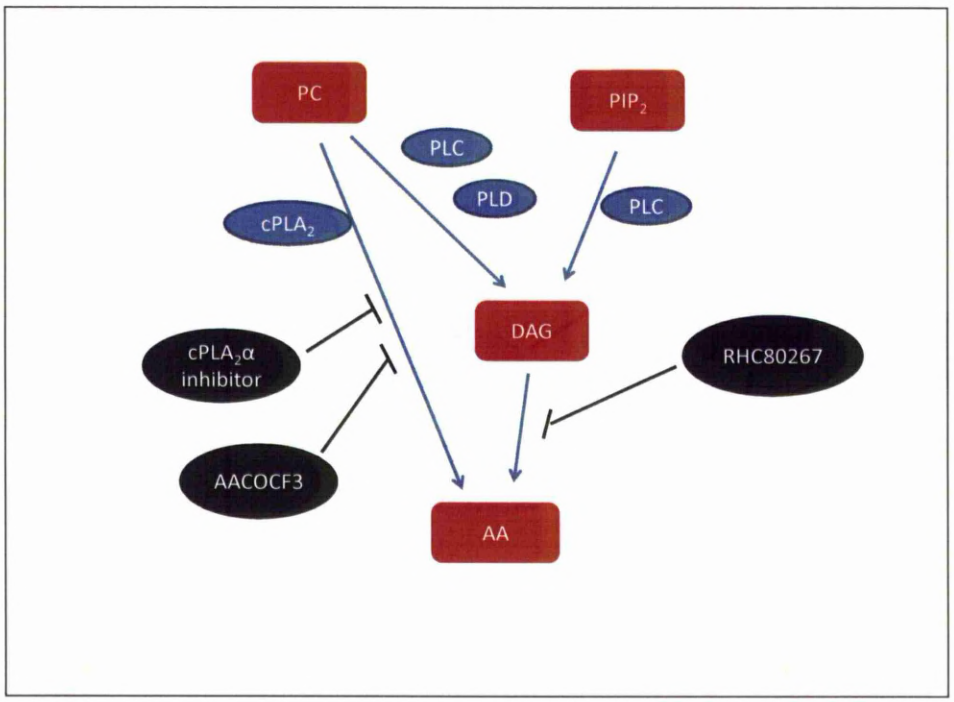

Figure 6-The inhibition mechanisms of three AA generation inhibitors

This figure shows the inhibition mechanisms of three inhibitors on the AA generation pathways. The $cPLA_2\alpha$ inhibitor and AACOCF3 inhibit the PLA pathway that produces AA. RHC80267 inhibits the DAG pathway for AA generation.

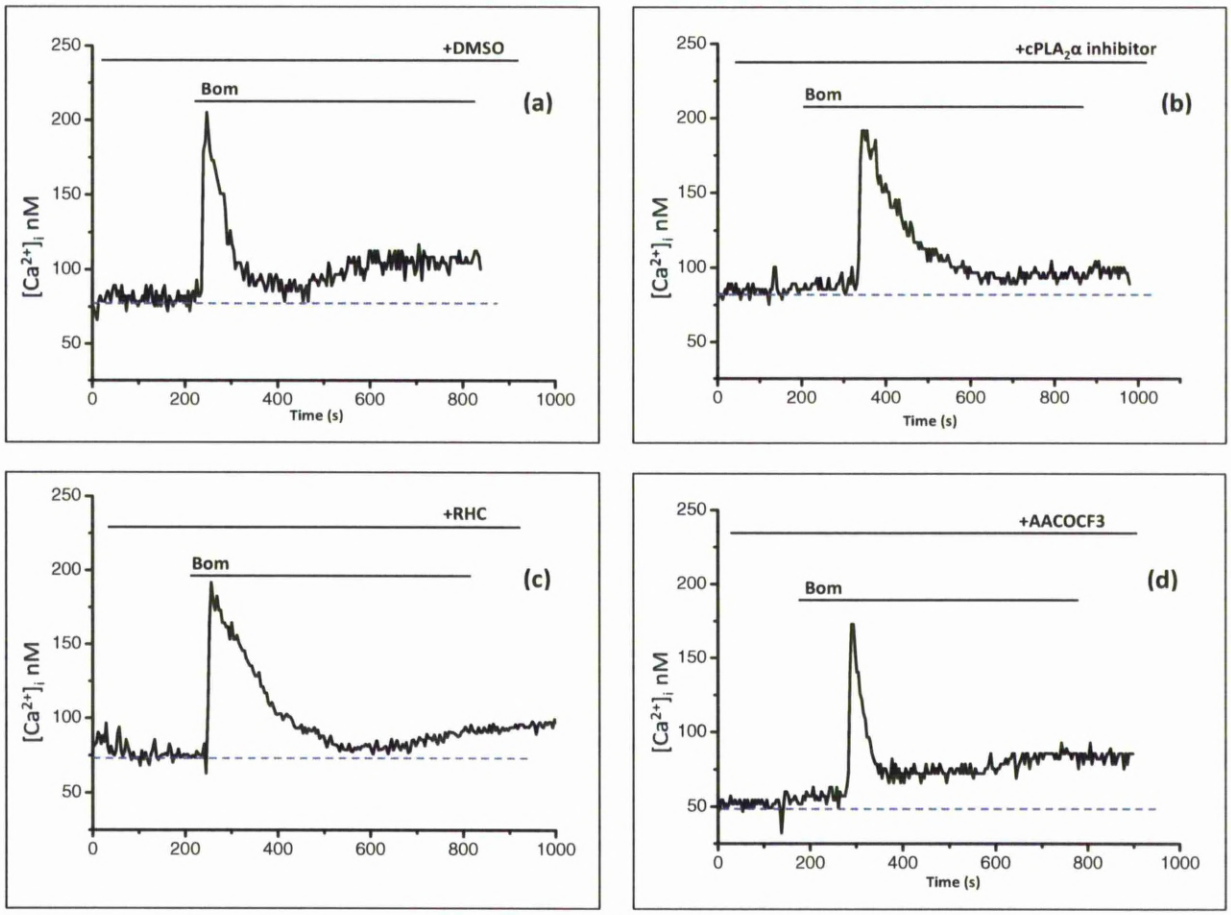

Figure 6.3.1A-The effect of AA inhibitors on bombesin-induced $[Ca^{2+}]_i$ responses monitored by Ca^{2+} imaging system

3-day-old quiescent Swiss 3T3 cells were cultured on coverslips in SF-DMEM with either DMSO or inhibitors pretreated for 16 hours before experiments. A $[Ca^{2+}]_i$ response is shown to bombesin (100nM) added at 200 seconds in the presence of 1mM Ca^{2+} in HBS. The $[Ca^{2+}]_i$ was measured using fura-2, at 37℃, using a Ca^{2+} imaging system. Figure (a) shows the $[Ca^{2+}]_i$ response in a DMSO control cell. Figure (b) presents a $[Ca^{2+}]_i$ response in cells treated with 6μM $cPLA_2\alpha$ inhibitor. Figure (c) presents a $[Ca^{2+}]_i$ response in cells treated with 20μM RHC80267 while figure (d) is a $[Ca^{2+}]_i$ response to bombesin in cells treated with 10μM AACOCF3. Each figure is representative of 6 experiments.

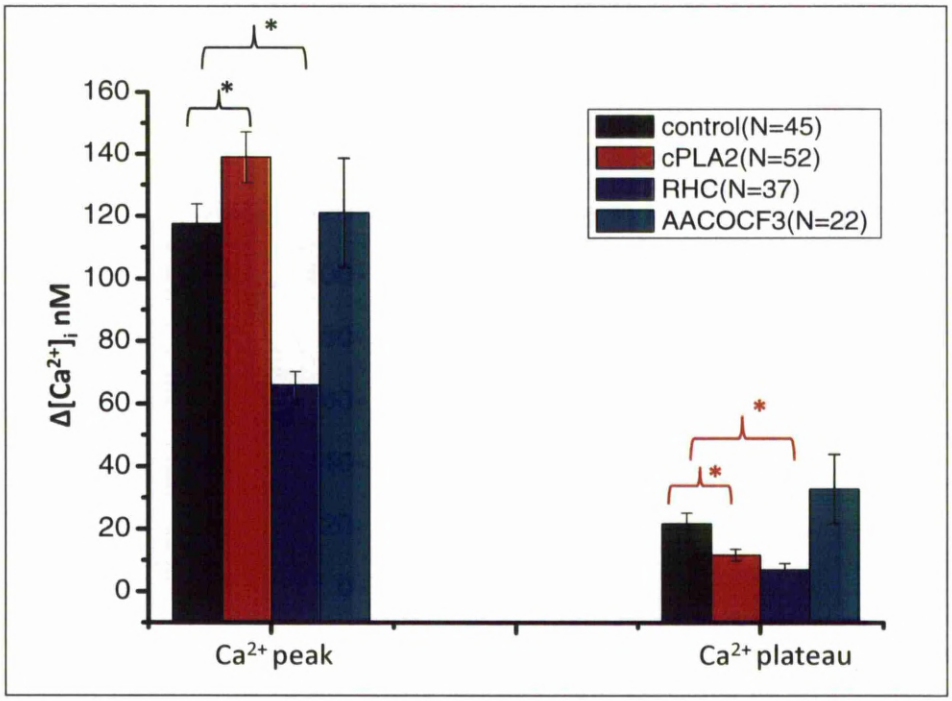

Figure 6.3.1B-The effect of AA inhibitors on bombesin-induced $[Ca^{2+}]_i$ responses monitored by Ca^{2+} imaging system

Quiescent Swiss 3T3 cells were cultured, unrestricted on glass coverslips in SF-DMEM for 16 hours before experiments. Mean data of increased $[Ca^{2+}]_i$ at both the peak and plateau points of the responses caused by the addition of bombesin (100nM) are indicated in solid columns. The columns in black represent the data in control cells and the columns with other colours show the data in cells which were treated with 6μM $cPLA_2\alpha$ inhibitor (red) or 20μM RHC80267 (blue) or 10μM AACOCF3 (green). The $\Delta[Ca^{2+}]_i$ is measured as $[Ca^{2+}]_i$ at the peak or plateau, which is 300 seconds after the peak, minus the baseline Ca^{2+} concentration before the addition of bombesin. Error columns shown are ± S.E. of (N) number of indicted cells. *$P<0.05$, when $\Delta[Ca^{2+}]_i$ value of (N) number of cells were subjected to t-test comparing to the control group.

Figure 6.3.1C-The effect of AA inhibitors on bombesin-induced $[Ca^{2+}]_i$ responses monitored by Flexstation plate reader

3-day-old quiescent Swiss 3T3 cells were cultured in a 96-well plate in SF-DMEM for 16 hours before experiments. Cells were first stimulated with DMSO as vehicle control or inhibitors at 20 seconds. A $[Ca^{2+}]_i$ response is shown to bombesin (100nM) added at 120 seconds in the presence of 1mM Ca^{2+} in HBS. The $[Ca^{2+}]_i$ was measured using Fura-2, at 37℃, through a Flexstation reader. Figure (a) shows two $[Ca^{2+}]_i$ responses in either DMSO control (black) and 6μM $cPLA_2\alpha$ inhibitor treated cells (red). Figure (b) presents two $[Ca^{2+}]_i$ responses with or without the presence of RHC80267 at a final concentration of 20μM. Figure (c) shows the $[Ca^{2+}]_i$ responses in control and 10μM AACOCF3 treated cells. "N" represents the number of similar replicate wells read by the Flexstation reader from 2 plates.

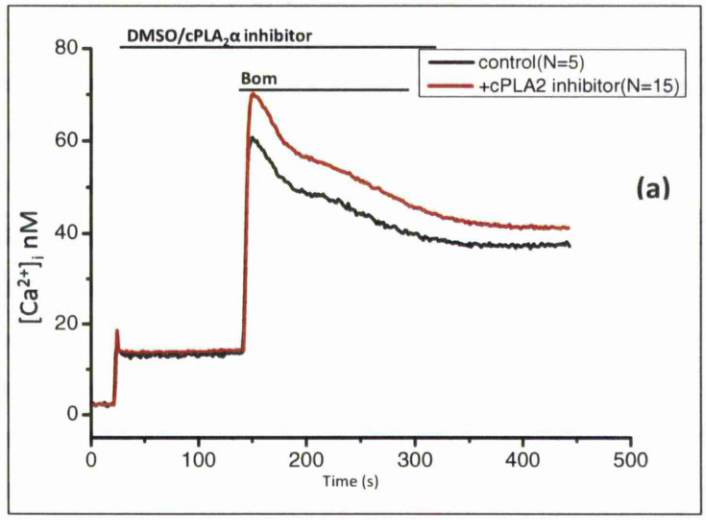

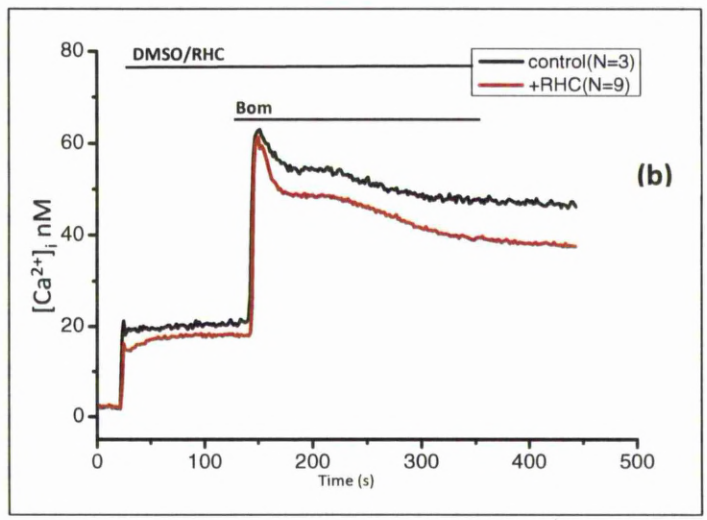

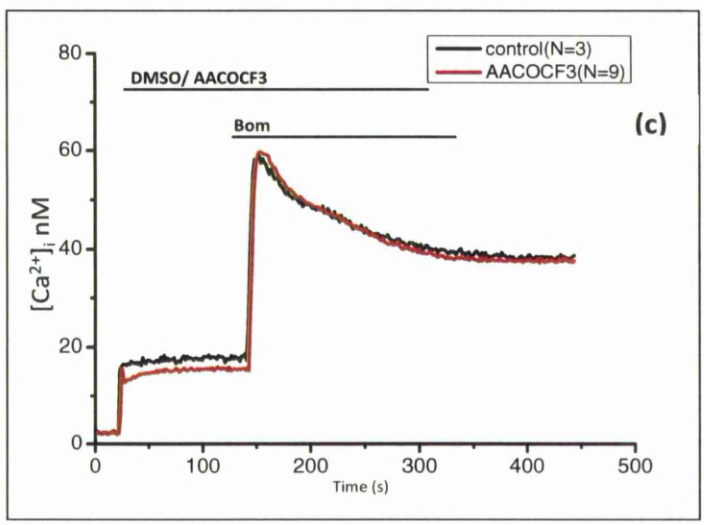

6.3.2 The effect of $cPLA_2$ inhibitors on $[Ca^{2+}]_i$ responses and Sr^{2+} influx

Sr^{2+} was further used to mimic the Ca^{2+} influx in order to test the effect of these AA inhibitors on both Ca^{2+} release and influx. The same protocol was applied to examine the function of inhibitors.

Figure 6.3.2A shows the typical bombesin-evoked Ca^{2+} release and Sr^{2+} influx in either control or inhibitor treated cells. In total, more than 10 similar experiments were performed to confirm the results. Figure 6.3.2B shows the statistical data of the increase in ratio340/380 caused by bombesin at both the peak of Ca^{2+} release and Sr^{2+} influx points of the response in either control or inhibitor-treated cells. A t-test was used to compare the responses ($p<0.05$). Compared to the response in control cell (n=87 cells), 6μM $cPLA_2\alpha$ inhibitor (n=42 cells) showed a significant influence on bombesin-evoked Ca^{2+} release and Sr^{2+} influx. However, rather than showing an inhibition function, the $cPLA_2\alpha$ inhibitor enhanced both the Ca^{2+} release and Sr^{2+} influx. Similarly, 10μM AACOCF3 (n=15 cells) significantly increased Sr^{2+} influx. AACOCF3 showed no influence on the bombesin-induced Ca^{2+} release. The results indicate that 20μM RHC80267 (n=84 cells) has little inhibition on both Ca^{2+} release and Sr^{2+} influx induced by bombesin (100nM).

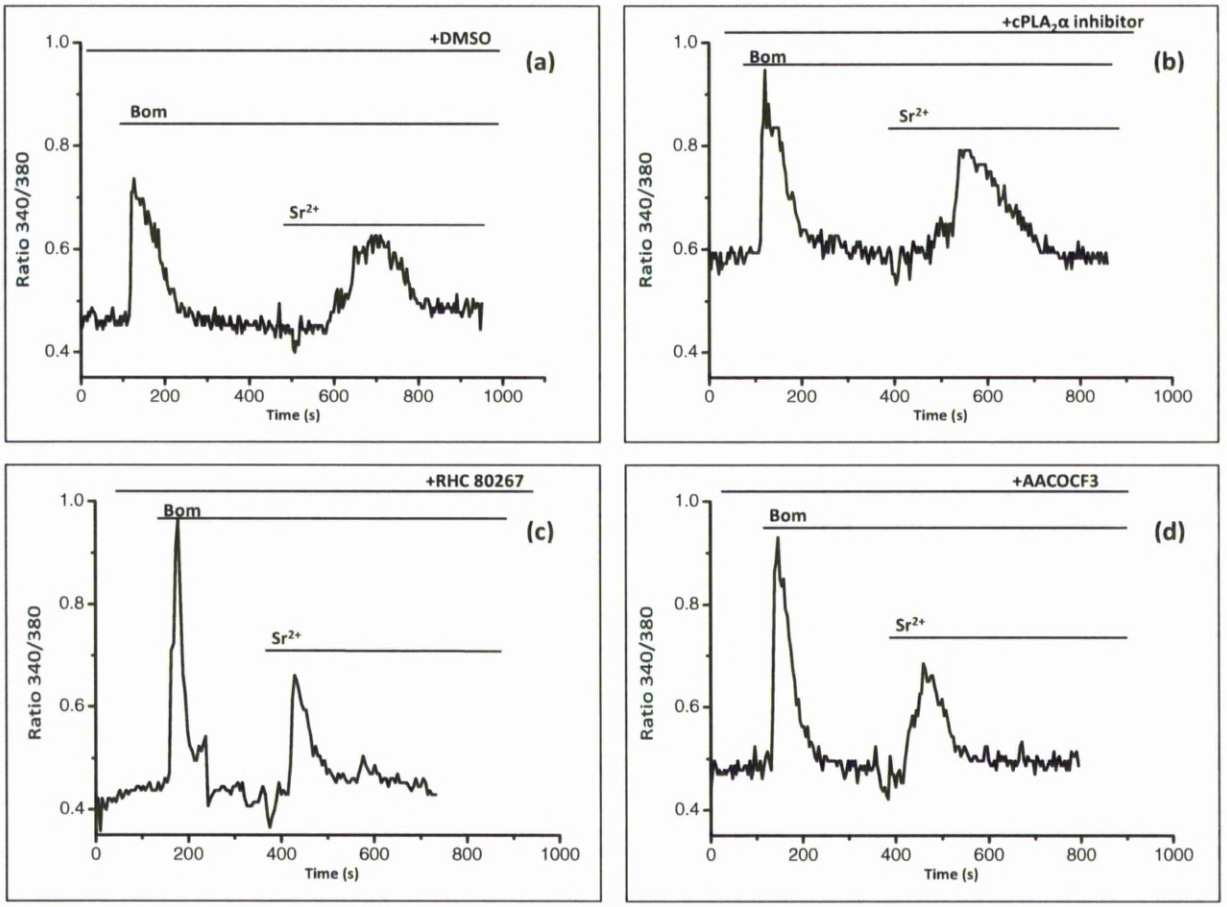

Figure 6.3.2A-The effect of AA inhibitors on bombesin-induced Ca^{2+} release and Sr^{2+} influx

3-day-old quiescent Swiss 3T3 cells were cultured on coverslips in SF-DMEM with either DMSO or inhibitors pretreated for 16 hours before experiments. A Ca^{2+} release is shown to bombesin (100nM) added at 120 seconds in Ca^{2+} free HBS. Sr^{2+} (1mM) was added at 400 seconds which results in a Sr^{2+} influx. The $[Ca^{2+}]_i$ and Sr^{2+} concentration was measured using fura-2, at 37°C, using a Ca^{2+} imaging system. Figure (a) shows the Ca^{2+} release and Sr^{2+} influx to bombesin in a DMSO control cell. Figure (b) presents the response in cells treated with 6μM $cPLA_2\alpha$ inhibitor. Figure (c) presents the response in cells treated with 20μM RHC80267 while figure (d) is the response in cells treated with 10μM AACOCF3. Each figure is representative of 10 experiments.

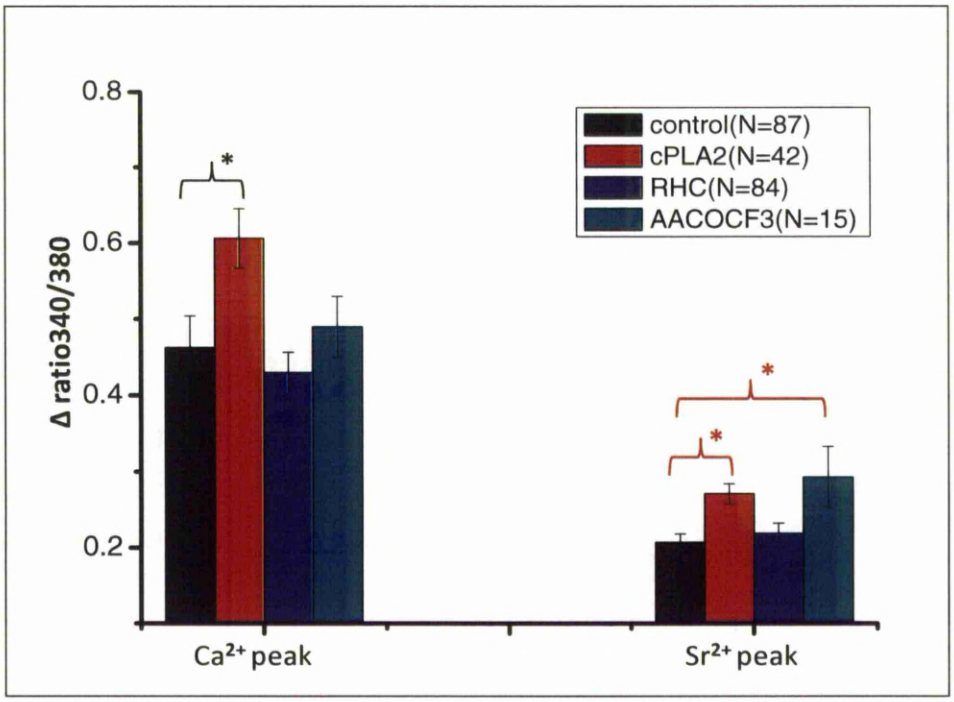

Figure 6.3.2B-The effect of AA inhibitors on bombesin-induced Ca^{2+} release and Sr^{2+} influx

Quiescent Swiss 3T3 cells were cultured, unrestricted on glass coverslips in SF-DMEM for 16 hours before experiments. Mean data of the change in ratio340/380 at both the Ca^{2+} release and Sr^{2+} influx peak points of the responses caused by the addition of bombesin (100nM) are indicated in solid columns. The columns in black represent the data in control cells and the columns with other colours show the data in cells which were treated with 6μM $cPLA_2\alpha$ inhibitor (red) or 20μM RHC80267 (blue) or 10μM AACOCF3 (green). The Δratio340/380 is measured as the ratio340/380 at the peak points minus the baseline ratio340/380 before the addition of bombesin. Error columns shown are ± S.E. of (N) number of indicted cells. *P<0.05, when Δratio340/380 value of (N) number of cells were subjected to t-test.

6.3.3 The effect of inhibitor LOE908 on the bombesin-induced $[Ca^{2+}]_i$ responses

The inhibitor LOE908 was used to test the participation of NSSCs in bombesin-evoked Ca^{2+} influx. The effect of LOE908 was first examined with the PTI Ca^{2+} imaging system. In each experiment, the cells were treated with DMSO as vehicle control or 30μM LOE908 before stimulation with 100nM bombesin.

Figure 6.3.3A shows the typical bombesin-evoked $[Ca^{2+}]_i$ responses in either control or LOE908 treated cells (n>34 cells). The responses in both confluent (n=102 cells) and non-confluent cells (n=54 cells) were presented in either (a & b) or (c & d) respectively. There were little differences in the effect of LOE908 on either confluent or non-confluent cells. However, the Ca^{2+} influx was suppressed in LOE908-treated cells compared to that in the control cells. In addition, it was found that the $[Ca^{2+}]_i$ baseline consistently dropped immediately after the addition of LOE908 (Figure d). LOE908 also efficiently ceased the Ca^{2+} oscillations (Figure b).

Figure 6.3.3B shows the statistical data of the increase $[Ca^{2+}]_i$ caused by bombesin at both the peak and plateau points of the response in either control and LOE908-treated cells. The data is collected from 17 control experiments and 17 LOE908-treated experiments in both confluent and non-confluent cells. From each experiment, the responses in 2 individual cells were randomly selected for the statistical analysis (n=34 cells). T-tests were used to compare the responses. The results indicated that the LOE908 significantly decreased the $\Delta[Ca^{2+}]_i$ during the plateau compared with the control ($p<0.05$), especially from 5min after the peak. However, the suppression at the peak point is not significant.

The Flexstation plate reader was then utilized to confirm the results obtained from the PTI Ca^{2+} imaging system. Figure 6.3.3C shows two representative bombesin-induced $[Ca^{2+}]_i$ response traces in either DMSO control or LOE908-treated cells. It was confirmed that the bombesin-evoked Ca^{2+} influx is suppressed in LOE908-treated cells. Both Ba^{2+} and Sr^{2+} were used to test whether LOE908 is able to inhibit the channels that are permeable to Ba^{2+} or Sr^{2+}. Figure 6.3.3D shows the bombesin-induced Ba^{2+} or Sr^{2+} influx in either controlled (black) or LOE908-treated cells (red). The figure represents a typical response read from 1 of 6 replicate

wells in 1 plate. The results indicate that LOE908 can block the Ba^{2+} and Sr^{2+} entry channels.

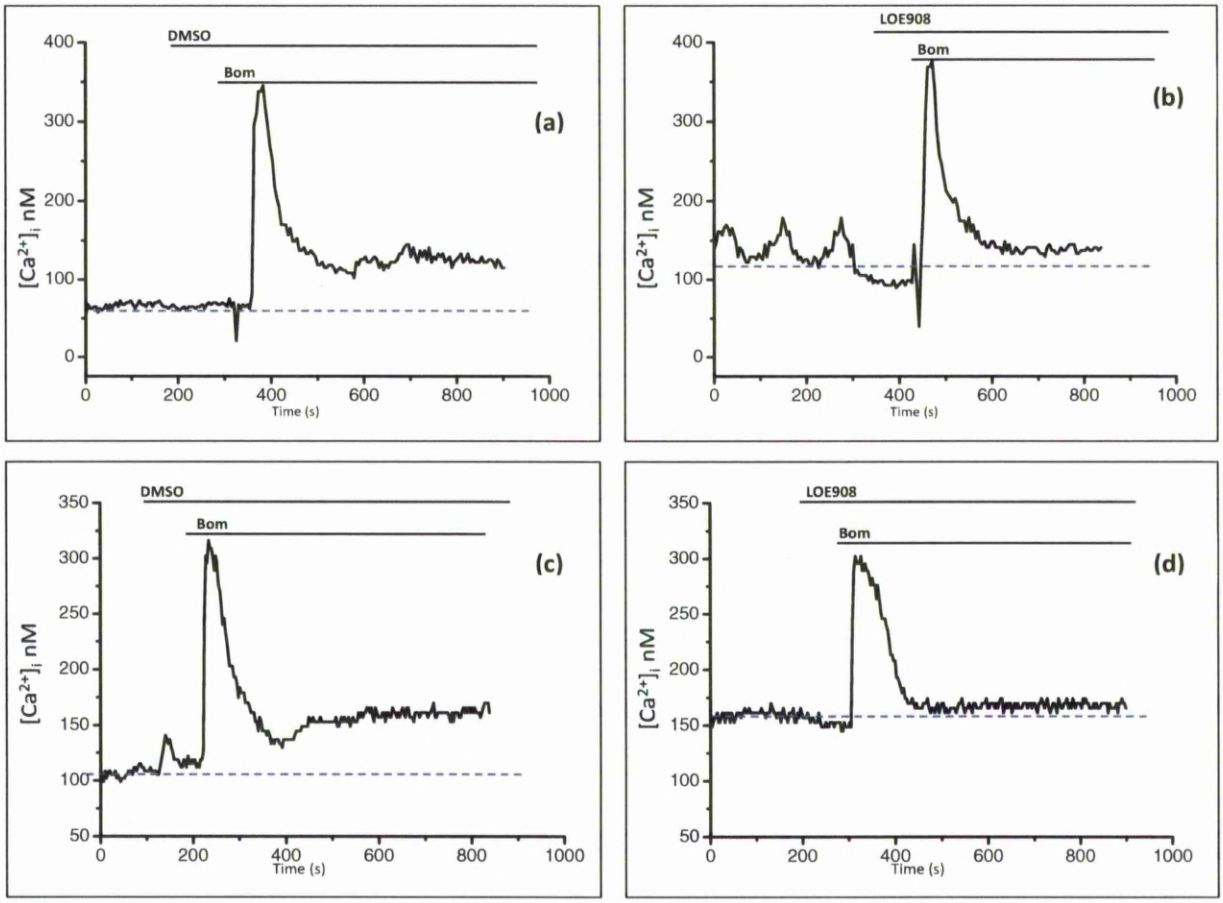

Figure 6.3.3A-The effect of inhibitor LOE908 on the bombesin-induced $[Ca^{2+}]_i$ responses

Quiescent Swiss 3T3 cells were cultured on coverslips in SF-DMEM. Cells were pretreated with either DMSO or inhibitors for 16 hours before experiments. A Ca^{2+} release is shown to bombesin (100nM) in HBS containing 1mM Ca^{2+}. Figures (a) & (b) present two bombesin-induced $[Ca^{2+}]_i$ responses in confluent cells with or without the addition of LOE908 (30μM) before the bombesin. Similarly, figures (c) & (d) show the $[Ca^{2+}]_i$ response in non-confluent cells. At least 17 similar experiments were performed.

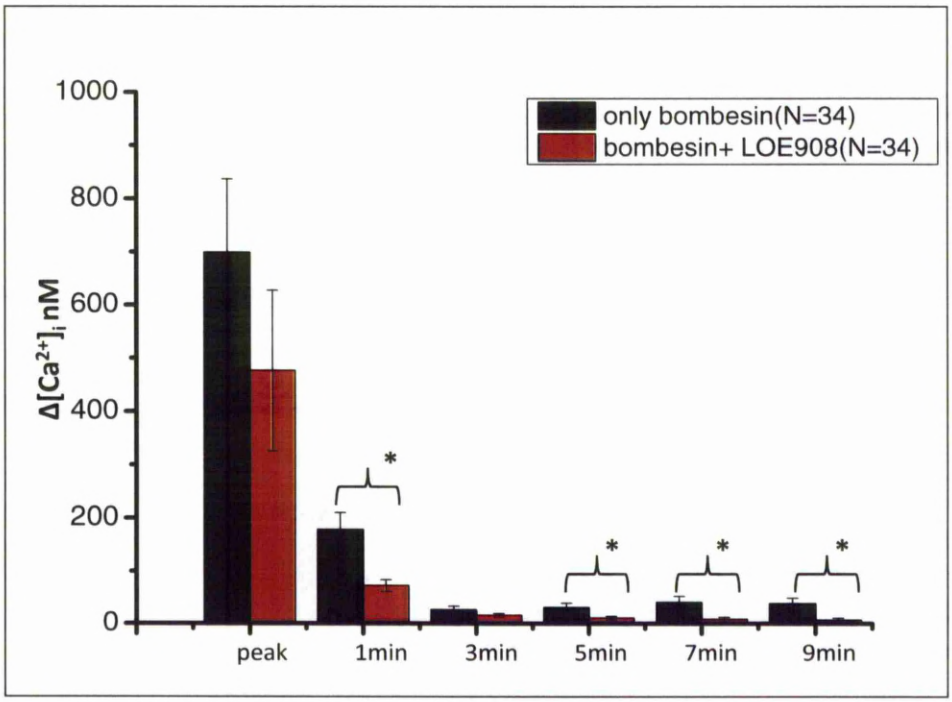

Figure 6.3.3B-The effect of LOE908 on bombesin-induced $[Ca^{2+}]_i$ response

Quiescent Swiss 3T3 cells were cultured, unrestricted on glass coverslips in SF-DMEM for 16 hours before experiments. Mean data of increased $[Ca^{2+}]_i$ at the peak and plateau of the responses caused by the addition of bombesin (100nM) are indicated in solid columns. The black columns represent the data of controlled cells and the red columns show the data of LOE908 (30μM) treated cells. The $\Delta[Ca^{2+}]_i$ is measured as $[Ca^{2+}]_i$ at the peak or a series time points of plateau, which are from 1 minute to 9 minutes after the peak, minus the baseline $[Ca^{2+}]_i$ before the addition of bombesin. Error columns shown are ± S.E. of (N) number of indicated cells. *$P<0.05$, when $\Delta[Ca^{2+}]_i$ value of (N) number of cells were subjected to t-test.

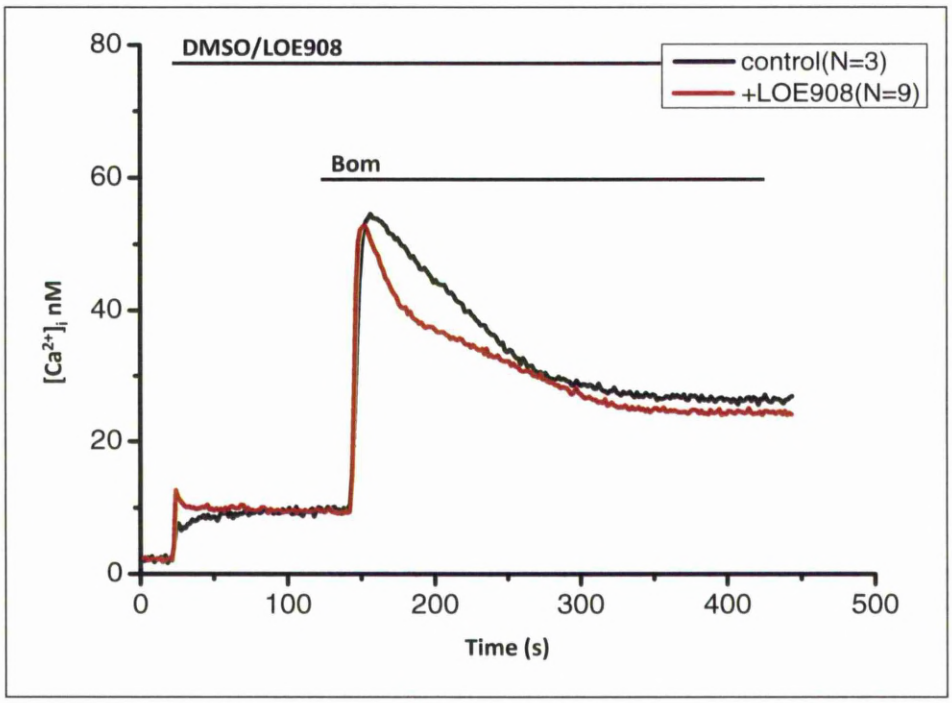

Figure 6.3.3C-The effect of LOE908 on the bombesin-induced $[Ca^{2+}]_i$ response as monitored by the Flexstation plate reader

3-day-old quiescent Swiss 3T3 cells were cultured in a 96-well plate in SF-DMEM for 16 hours before experiments. Cells were first stimulated with DMSO (black) as vehicle control or 30μM LOE908 (red) at 20 seconds. A $[Ca^{2+}]_i$ response is shown to bombesin (100nM) added at 100 seconds in the presence of 1mM Ca^{2+} in HBS. The $[Ca^{2+}]_i$ was measured using fura-2, at 37°C, through a Flexstation reader. "N" represents the number of similar replicate wells read by the Flexstation reader from 2 plates.

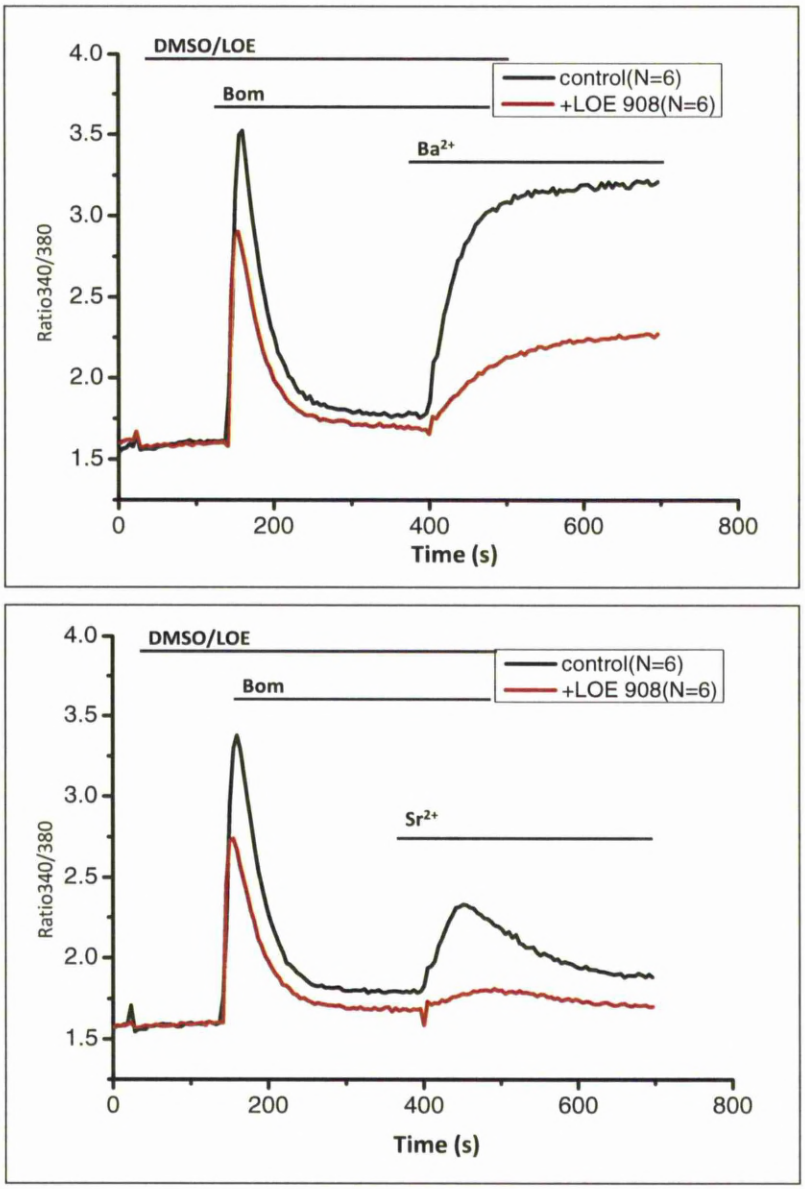

Figure 6.3.3D-The effect of LOE908 on bombesin-induced Ba^{2+} and Sr^{2+} as monitored by the Flexstation plate reader

3-day-old quiescent Swiss 3T3 cells were cultured in a 96-well plate in SF-DMEM for 16 hours before experiments. Cells were first stimulated with DMSO (black) as vehicle control or 30μM LOE908 (red) at 20 seconds. A Ca^{2+} release is shown to bombesin (100nM) added at 100 seconds in the presence of Ca^{2+} free HBS. Either 1mM Ba^{2+} (a) or 1mM Sr^{2+} (b) was then added at 400 seconds. The ratio340/380 was measured using fura-2, at 37°C, through a Flexstation plate reader. "N" represents the number of similar replicate wells read by the Flexstation reader from 1 plate.

6.3.4 The effect of the inhibitor SK&F 96365 on the bombesin-induced $[Ca^{2+}]_i$ responses

Since SOCE is a very important and widely spread Ca^{2+} entry pathway, its involvement in the bombesin-evoked $[Ca^{2+}]_i$ responses was tested. In addition, according to the data presented in chapter 5, $iPLA_2$ which is believed to be important to SOCEs may play a role in the bombesin-evoked $[Ca^{2+}]_i$ response. Therefore, the role of SOCEs needed to be tested. A widely used SOCE inhibitor, SK&F96365, was used to investigate the Ca^{2+} entry pathway.

Figure 6.3.4A presents two typical $[Ca^{2+}]_i$ responses evoked by bombesin in either control (n=48 cells) or 30μM SK&F96365 treated (n=57 cells) cells. In total 10 similar experiments were conducted. The bombesin-induced $[Ca^{2+}]_i$ response was reduced by SK&F96365. Figure 6.3.4B shows the statistical data of the $[Ca^{2+}]_i$ increase caused by bombesin at both the peak and plateau points of the response in either control or SK&F96365-treated cells. A t-test was used to compare the responses. The results indicate that the SK&F96365 significantly decreases the $\Delta[Ca^{2+}]_i$ during the plateau.

In addition to the PTI Ca^{2+} imaging system, the Flexstation plate reader was used to confirm the results. Figure 6.3.4C shows two representative bombesin-induced $[Ca^{2+}]_i$ response traces in either DMSO controlled or SK&F96365-treated cells. It was confirmed that the bombesin-evoked Ca^{2+} influx is suppressed by SK&F96365. Both Ba^{2+} and Sr^{2+} were used to test the whether SK&F96365 is able to inhibit the channels that are permeable to Ba^{2+} or Sr^{2+}. Figure 6.3.3D shows the bombesin-induced Ba^{2+} or Sr^{2+} influx in either control (black) or SK&F96365-treated cells (red). The figure represents a typical response read from 1 of 6 replicate wells in 1 plate. The results indicate that SK&F96365 could block the Ba^{2+} and Sr^{2+} entry channels.

The function of SK&F96365 was also tested on thapsigargin-evoked $[Ca^{2+}]_i$ responses in Swiss 3T3 cells. Figure 6.3.4E shows two typical $[Ca^{2+}]_i$ responses after the stimulation of 2μM thapsigargin in either control (n=22 cells) or 30μM SK&F96365-treated (n=16 cells) cells. More than 3 experiments were conducted. The results were consistent showing that SK&F96365 strongly abolishes the thapsigargin-evoked $[Ca^{2+}]_i$ response. After the addition of SK&F96365, thapsigargin only induced very slow and sluggish increase in $[Ca^{2+}]_i$, which indicates a small Ca^{2+} release from

stores. This is in contrast with some other cell types where a substantial Ca^{2+} release can still be seen in the presence of SK&F96365 (Merritt et al., 1990).

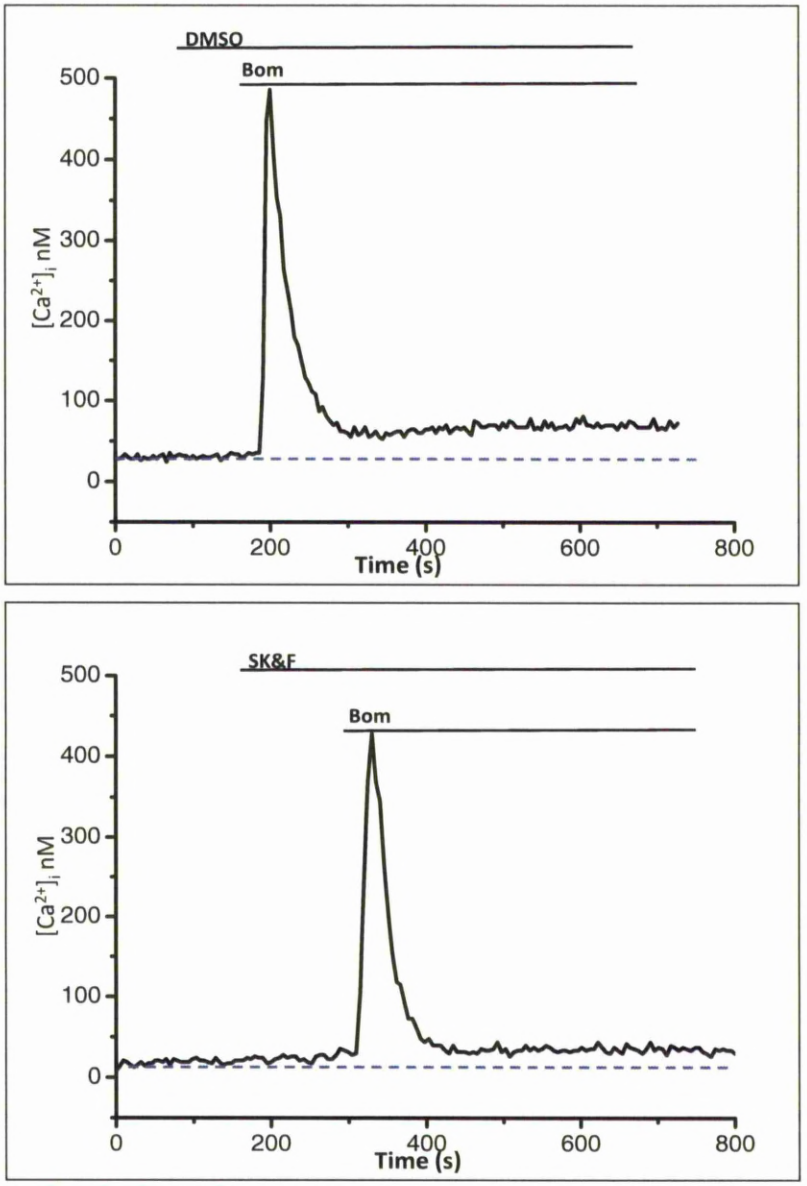

Figure 6.3.4A- The effect of the inhibitor SK&F96365 on the bombesin-induced $[Ca^{2+}]_i$ responses monitored with the PTI Ca^{2+} imaging system

3-day old quiescent Swiss 3T3 cells were cultured on coverslips in SF-DMEM with either DMSO or inhibitors pretreated for 16 hours before experiments. A Ca^{2+} release is shown to bombesin (100nM) in HBS containing 1mM Ca^{2+}. Figure (a) shows a bombesin-induced $[Ca^{2+}]_i$ response in control cells. Figure (b) shows a bombesin-evoked $[Ca^{2+}]_i$ response with the addition of SK&F96365 (30μM) before the bombesin. At least 10 experiments were performed.

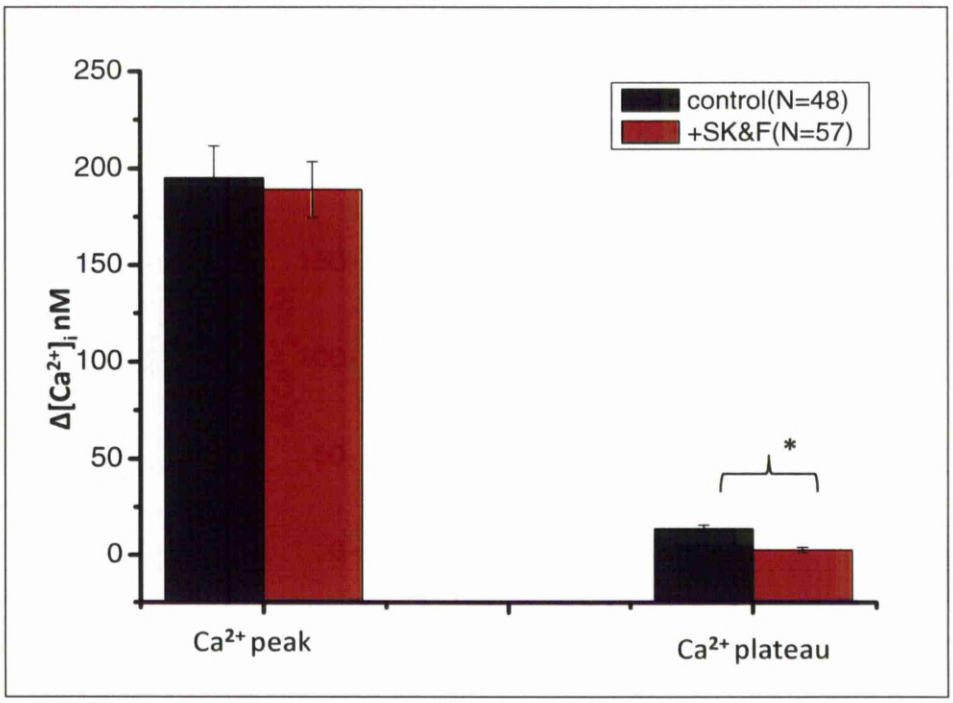

Figure 6.3.4B- The effect of the inhibitor SK&F96365 on the bombesin-induced $[Ca^{2+}]_i$ responses monitored with the Ca^{2+} imaging system

Quiescent Swiss 3T3 cells were cultured, unrestricted on glass coverslips in SF-DMEM for 16 hours before experiments. Mean data of increased $[Ca^{2+}]_i$ at the peak and plateau of the responses caused by the addition of bombesin (100nM) are indicated in solid columns. The black columns represent the data of controlled cells and the red columns show the data of SK&F96365 (30μM) treated cells. The $\Delta[Ca^{2+}]_i$ is measured as the $[Ca^{2+}]_i$ at the peak and plateau, which is 300 seconds after the peak, minus the baseline $[Ca^{2+}]_i$ before the addition of bombesin. Error bars shown are ± S.E. of (N) number of indicated cells. *$P<0.05$, when $\Delta[Ca^{2+}]_i$ value of (N) number of cells were subjected to t-test. At least 10 experiments were performed.

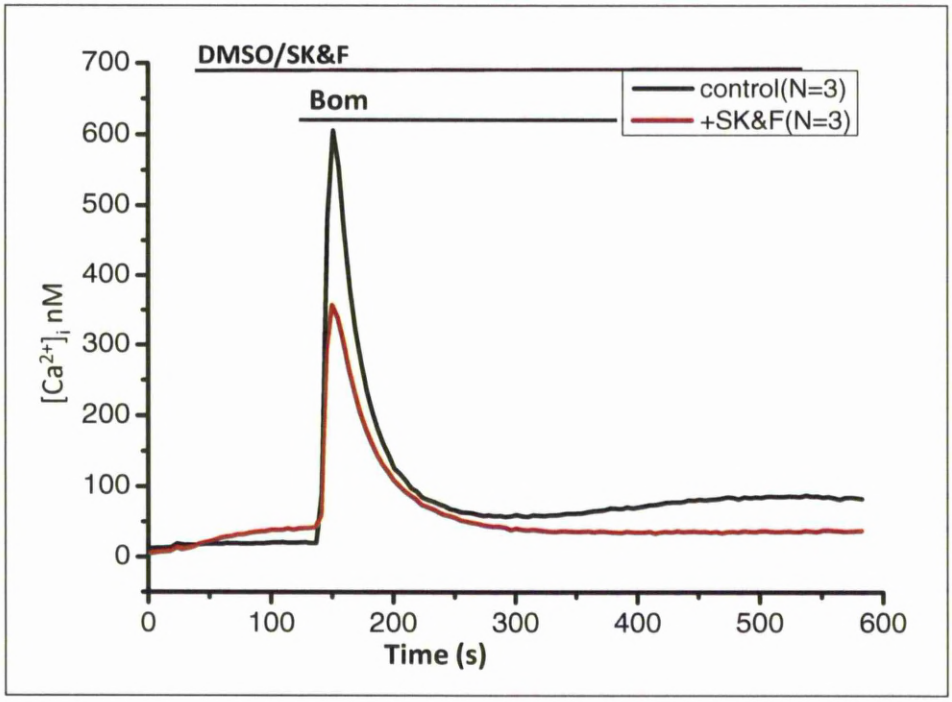

Figure 6.3.4C- The effect of inhibitor SK&F96365 on the bombesin-induced $[Ca^{2+}]_i$ responses as monitored by the Flexstation plate reader

3-day-old quiescent Swiss 3T3 cells were cultured in a 96-well plate in SF-DMEM for 16 hours before experiments. Cells were first stimulated with DMSO (black) as vehicle control or 30μM SK&F96365 (red) at 20 seconds. A $[Ca^{2+}]_i$ response is shown to bombesin (100nM) added at 120 seconds in the presence of 1mM Ca^{2+} in HBS. The $[Ca^{2+}]_i$ was measured using Fura-2, at 37°C, through a Flexstation reader. "N" represents the number of similar replicate wells read by the Flexstation reader from 1 plate.

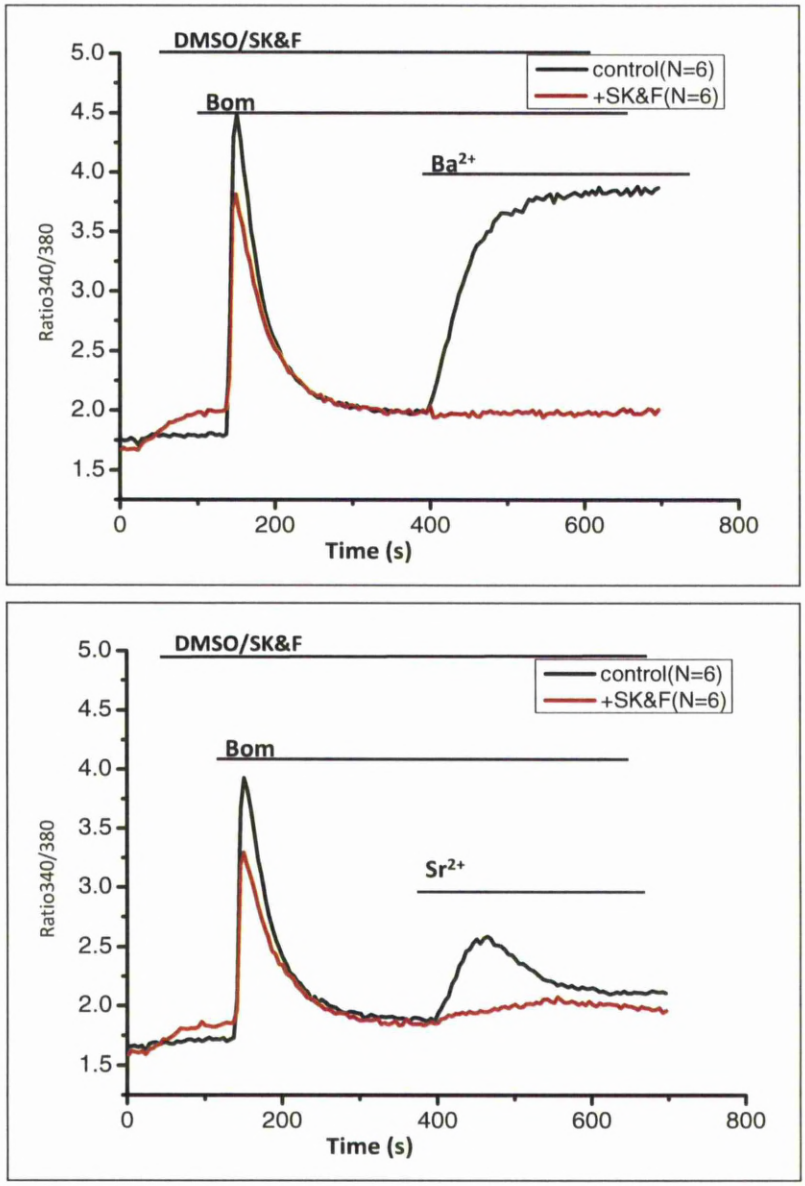

Figure 6.3.4D-The effect of SK&F96365 on bombesin-induced Ba^{2+} and Sr^{2+} responses as monitored by the Flexstation plate reader

3-day-old quiescent Swiss 3T3 cells were cultured in a 96-well plate in SF-DMEM for 16 hours before experiments. Cells were first stimulated with DMSO (black) as vehicle control or 30μM SK&F96365 (red) at 20 seconds. A Ca^{2+} release is shown to bombesin (100nM) added at 100 seconds in the presence of in Ca^{2+} free HBS. Then either 1mM Ba^{2+} (a) or 1mM Sr^{2+} (b) was added at 400 seconds. The ratio340/380 was measured using Fura-2, at 37°C, through a Flexstation reader. "N" represents the number of wells read by the Flexstation reader. "N" represents the number of similar replicate wells read by the Flexstation reader from 1 plate.

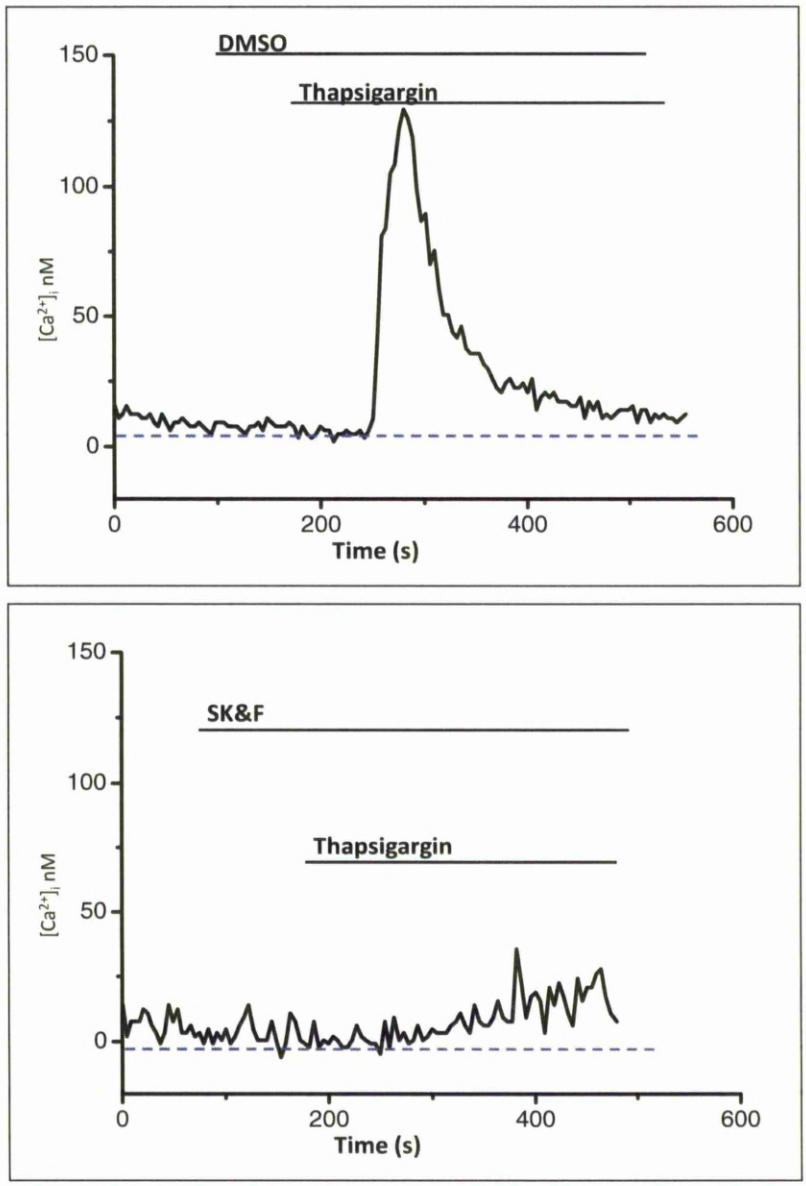

Figure 6.3.4E- The effect of inhibitor SK&F96365 on the thapsigargin-induced $[Ca^{2+}]_i$ responses

3-day old quiescent Swiss 3T3 cells were cultured on coverslips in SF-DMEM with either DMSO or inhibitors pretreated for 16 hours before experiments. A Ca^{2+} release is shown to thapsigargin (2μM) in HBS containing 1mM Ca^{2+}. Figure (a) represents a typical thapsigargin-induced $[Ca^{2+}]_i$ response in control cells. Figure (b) shows a bombesin-evoked $[Ca^{2+}]_i$ response with the addition of SK&F96365 (30μM) before the bombesin. At least 3 experiments were performed.

6.4 Discussion

In this chapter, the effect of Ca^{2+} influx inhibitors on the bombesin-induced Ca^{2+} influx was investigated. The results gained by either using a PTI Ca^{2+} imaging system when the cells were pre-treated with inhibitor or a Flexstation plate reader when the cell were treated with inhibitors instantly turned out to be similar. This increases the confidence of the data presented in this chapter.

According to the statistical analysis, it was suggested that the $cPLA_2\alpha$ inhibitor was more influential than AACOCF3 on the bombesin-evoked $[Ca^{2+}]_i$ response. The results indicate that $cPLA_2\alpha$ inhibitor suppressed the Ca^{2+} influx, which in turn suggests that the $cPLA_2\alpha$ may be involved in the bombesin-induced Ca^{2+} influx pathway. However, it was found that the $cPLA_2\alpha$ inhibitor caused a significant increase in the Ca^{2+} release and Sr^{2+} influx, which questions the effectiveness of this inhibitor. AACOCF3 also tends to cause a bigger bombesin-evoked $[Ca^{2+}]_i$ response and it significantly increased Sr^{2+} influx compared to that in the control cells. Such a side effect of AACOCF3 has been observed by others, and is attributed to the property of AACOCF3 acting as an analogue of AA (Riendeau *et al.*, 1994). This finding could reinforce the notion that AA is important in the bombesin-induced $[Ca^{2+}]_i$ response.

According to the results obtained from the experiments using the PTI Ca^{2+} imaging system, it was revealed that the RHC80267 significantly decreases the bombesin-evoked $[Ca^{2+}]_i$ response, especially the Ca^{2+} entry (Figure 6.3.1B). However, the bombesin-evoked Ca^{2+} release was not suppressed by the RHC80267 when the responses were monitored using a Flexstation plate reader. This might because the cells were treated with RHC80267 for a longer time in experiments with the Ca^{2+} imaging system compared with the cell used in the Flexstation microplate reader.

RHC80267 is a potent and specific *in vitro* DAG lipase inhibitor (Canonico *et al.*, 1985). As described in section1.6.3.4, the DAG pathway is an important alternative to release AA (Watanabe-Tomita *et al.*, 1997). Therefore, the inhibition by RHC80267 suggests that DAG may be required for the bombesin-evoked Ca^{2+} influx, and this supports the supposition described in

chapter 5. However, some caution must be applied to this interpretation since RHC80267 did not appear to affect Sr^{2+} influx (Figure 6.3.2B). It was observed that RHC80267 failed to inhibit AVP-evoked Sr^{2+} entry in A7r5 cells, which was suggested to be mediated through DAG-AA pathway (Broad *et al.*, 1999). On the other hand, results confirmed that both LOE908 and SK&F96365 are able to suppress the bombesin-induced Ca^{2+} influx. Since LOE908 is regarded to block the NSCCs while the SK&F96365 is well known for its function on SOCCs (Kawanabe *et al.*, 2001), it is believed that both the NSCCs and SOCCs have been activated by bombesin in order to conduct Ca^{2+} entry in the Swiss 3T3 cells. However, neither of the inhibitors could fully abolish the bombesin-evoked $[Ca^{2+}]_i$ response, although both of them are able to block most of the Ba^{2+} or Sr^{2+} influx. These finding suggests that other Ca^{2+} channels which are neither sensitive to LOE908 and SK&F96365 nor selective to Ba^{2+} and Sr^{2+} participate in the bombesin-evoked Ca^{2+} entry pathway. However, this conclusion is challenged by several observations. The first problem is the specificity of both inhibitors. Although LOE908 and SK&F96365 are widely used to inhibit NSCCs or SOCCs respectively, both inhibitors were found to block a variety of ion channels. It has been shown that LOE908 (10μm or 30μm) has no effect on thapsigargin-induced SOCEs in A7r5 cell and that LOE908 and SK&F96365 can be used to distinguish NSCCEs and SOCEs (Miwa *et al.*, 2000; Moneer and Taylor, 2002). However, another study found that LOE908 (~2μM) is a potent blocker of a Ca^{2+} conductance activated by thapsigargin-induced depletion of intracellular Ca^{2+} stores in endothelial cells (Encabo *et al.*, 1996). Based on this evidence, the specificity of LOE908 seems to be concentration- and cell type-dependent. Therefore, despite the fact that LOE908 was reported to inhibit endothelin-1-induced AA release in Chinese hamster ovary (CHO) cells (Kawanabe *et al.*, 2003), it remains questionable whether the reduced bombesin-induced Ca^{2+} influx by LOE908 observed in this thesis is due to the inhibition of the NSCCEs, such as I_{ARC}.

Another explanation for the observation that neither LOE908 or SK&F96365 fully blocked the bombesin-evoked Ca^{2+} influx while Ba^{2+} and Sr^{2+} influxes were inhibited may be related to the reciprocal regulation between I_{SOC} and I_{ARC} (Mignen *et al.*, 2001). ARC channels are indeed specifically activated by low agonist concentrations and provide the predominant route of Ca^{2+} entry under these conditions while SOCCs provides the predominant route of Ca^{2+} entry at high agonist concentrations. It was reported that at high concentrations of agonist, the prolonged

depletion of intracellular Ca^{2+} stores and following activation of SOCCs that cause a sustained elevation of $[Ca^{2+}]_i$ could, in turn, inhibit the activity of the ARC channels (Mignen *et al.*, 2001). Therefore, when the SOCEs have already been fully activated in cells, the I_{ARC} is likely to be under suppression. In this thesis, when the SOCEs were inhibited by SK&F96365, it might in turn remove such reciprocal inhibition of I_{SOC} on I_{ARC}. This consequently may result in the activation of ARC channels conducting the Ca^{2+} influx. The reciprocal regulation is believed to be dependent on the global $[Ca^{2+}]_i$, rather than a local effect of the Ca^{2+} actually entering through the channels. AA has also been reported to inhibit SOCEs in some cells (Moneer and Taylor, 2002). Hence, such switch in the predominant mode of Ca^{2+} entry from I_{ARC} to I_{SOC} might occur when LOE908 was applied in order to avoid the change in global $[Ca^{2+}]_i$. However, since there is no reciprocal regulation in the Ba^{2+} or Sr^{2+} influx, when either LOE908 or SK&F96365 was added, no alternative entry pathways was activated. Therefore, the Ba^{2+} or Sr^{2+} entry is more likely to be fully blocked by these inhibitors.

In summary, these experiments showed that:

1. The $cPLA_2\alpha$ inhibitor suppressed the bombesin-evoked Ca^{2+} influx. However, it appears to increase the Ca^{2+} release and Sr^{2+} influx by a mechanism that remains unclear.
2. The inhibitor AACOCF3 has little influence on the bombesin-induced $[Ca^{2+}]_i$ responses. However, the Ca^{2+} influx tends to be bigger in the cells with the presence of AACOCF3 than that in the control cells. AACOCF3 significantly increased bombesin-evoked Sr^{2+} influx.
3. The inhibitor RHC80267 significantly reduced bombesin-evoked Ca^{2+} influx. The bombesin-evoked Ca^{2+} release is seen to be suppressed in the RHC80267 pre-treated cells using a PTI Ca^{2+} imaging system while no such suppression is seen in cells treated with RHC80267 instantly using a Flexstation plate reader. In addition, RHC80267 has little effect on the Sr^{2+} influx.
4. Both LOE908 and SK&F96365 significantly blocked the bombesin-evoked Ca^{2+} influx. They are very effective at inhibiting the Ba^{2+} and Sr^{2+} fluxes.
5. The involvement of the SOCEs in the bombesin-evoked $[Ca^{2+}]_i$ response is confirmed, although a role of AA in this $[Ca^{2+}]_i$ response cannot be ruled out.

Chapter 7

The activation of STIM1 in bombesin-evoked Ca^{2+} influx

Contents:

Figures:

7.1 Introduction

Based on the findings from the previous chapters, the SOCEs appear to be involved in the bombesin-induced $[Ca^{2+}]_i$ responses in Swiss 3T3 cells. The role of SOCE in bombesin-evoked Ca^{2+} influx and its relation to cell shape was therefore examined. In particular, it was decided to focus on the translocation of STIM1, since this represents a key step in SOCE activation and may be sensitive to alterations in the cytoskeleton.

As mentioned in section 1.6.2.2, it is now clear that STIM1 is a necessary component for the activation of SOCCs (Liou *et al.*, 2005). Although the precise mechanism of how STIM1 acts in SOCE is still not fully understood, a widely accepted model is that STIM1 proteins need to form puncta for the activation of SOCCs (Wu *et al.*, 2006; Smyth *et al.*, 2007). Based on this theory, the STIM1 oligomerization and translocation for puncta formation have become two criteria to identify the activation of SOCEs.

It is difficult to examine STIM1 by immunofluorescence due to its relative low level of expression, though they were observed in Swiss 3T3 cells in a previous study in our laboratory. For a similar reason, it is difficult to investigate STIM1 using western blotting. Although blots can be obtained from cells expressing endogenous STIM1, no spatial information can be obtained relating to the location of STIM1 and puncta formation. Consequently, it was decided to investigate STIM1 activation by transfection with yellow fluorescent protein (YFP)-chimeric STIM1 plasmids (Burgoyne *et al.*, 2010). However, Swiss 3T3 cells were found to be difficult to transfect (transfection rate < 10%) with the YFP-STIM1. Therefore, it was decided initially to use HeLa cells as an alternative. HeLa cells have been widely used for the study of STIM1, where STIM1 oligomerization and the formation of puncta were observed (Liou *et al.*, 2007).

The activation of STIM1 in response to the stimulation by either bombesin or thapsigargin in normal spreading HeLa cells on coverslips was investigated first. It has been widely observed that thapsigargin can lead to STIM1 puncta formation in HeLa cells (Liou *et al.*, 2007). Therefore, thapsigargin was used as a standard positive control to compare with bombesin.

The influence of cell shape on STIM1 was examined using large and small adhesive islands. The cell cytoskeleton including actin, microtubules, intermediate filaments are required for maintenance of the cell shape (reviewed by Hay, 2005). The localization and movements of intracellular signaling proteins are often controlled by the cytoskeleton, especially the actin filaments and microtubules (reviewed by Smyth *et al.*, 2007). When the cell shape is restricted by islands, the distribution of the cytoskeleton is altered. It has been observed in our laboratory that the actin cytoskeleton was re-organized in the cells on small islands and formed a ring of actin which is reminiscent of that induced by jasplakinolide (Foster, 2005). Jasplakinolide is also known to block Ca^{2+} entry as it was observed to inhibit the SOCEs in both DDT1MF-2 cells and A7r5 cells (Patterson *et al.*, 1999). Based on all these findings, the hypothesis is that STIM1 puncta formation may be inhibited due to the re-organization of actin cytoskeleton in cells on small islands. This then may account for the absence of bombesin-induced Ca^{2+} influx in shape-restricted cells.

In summary, the primary aim is to exam the activation of STIM1 in experiments by transfecting HeLa cells with YFP-STIM1 in order to establish STIM1 localization using confocal microscopy. In addition, a fluorescence-activated cell sorter (FACS) was used to enrich the transfected cell population. Another objective is to determine the localization of STIM1 in cells on large and small islands.

In the experiments, HeLa cells expressing YFP-STIM1 were restricted from spreading by plating onto adhesive islands as described in previous chapters. They were then stimulated with either bombesin or thapsigargin. As with previous experiments, there was a loss of cells when transferring cells onto islands. In order to obtain a good occupancy of YFP-STIM1 expressing cells, the population needed to be enriched. To achieve this, a FACS was applied to sort the YFP expressing cells.

Although Swiss 3T3 cells were difficult to transfect, if Jet Prime transfection reagent along with mCherry-STIM1 was used, the transfection rate was enhanced to 30%-50%. Consequently, the distribution of STIM1 in normal spreading Swiss 3T3 cells could be investigated. Since the FACS

increased the density of transfected cells, the STIM1 distribution in the shape restricted Swiss 3T3 cells could also be examined.

7.2 Method

7.2.1 Cell culture

HeLa cells were cultured according to standard protocol for Swiss 3T3 cells as described in section 2.1. The shape-restricted cells were transferred to coverslips containing either large or small islands using the same protocol described for Swiss 3T3 cells.

7.2.2 Transfection

HeLa cells were grown to 50% confluent for YFP-STIM1 transfection in a 10cm^2 cell culture dish. For each dish, 6μg DNA was added into 500μl Optimem and incubated for 5min. Following that, 24μl reagent Gene juice was added allowing 20min before transferring the mixture onto the cells. Cells were then cultured for at least 24 hrs before the experiments at 37℃.

Swiss 3T3 cells were grown to 50% confluency for mCherry-STIM1 and YFP-STIM1 transfection. For a 6-well plate, 2μg DNA was first added into 200μl Jet prime buffer, mixed and incubated for 5min. After that, 4μl Jet prime reagent was added and incubated for 10min. Then the mixed complex was added into each well where cells were cultured in 2ml FCS-DMEM. The media needed to be replaced with fresh FCS-DMEM after 4 hours culture at 37℃. Cells were then cultured for at least 24 hrs before the experiments.

7.2.3 FACS analysis

Transfected cells were first washed with PBS and resuspended with Trypsin-EDTA following the standard protocol described in section 2.1. They were then centrifuged for 5min at 400xg. After that, cells were suspended in 0.1%BSA in PBS with a density of 1x10^6 cells/ml for sorting by FACS. Meanwhile, untransfected cells were suspended in the same way and used as a control group. Approximately, 10% of the transfected cells can be sorted.

7.2.4 Stimulation of transfected cells

Unstimulated transfected cells were kept in HBS containing 1mM Ca^{2+} before being fixed with 3% paraformaldehyde (PFA). For the stimulated cells, they were treated with 100nM bombesin in HBS containing 1 mM Ca^{2+} or with 2μM thapsigargin in Ca^{2+} free HBS. The agonist-treated HeLa cells were incubated at 37°C for 2min, 4min and 8min before being fixed with 3% PFA. The Swiss 3T3 cells were treated with bombesin in the same way, however those cells on adhesive islands were only incubated for 4min before fixation.

7.2.5 Confocal microscopy

The distribution of STIM1 was examined using a Leica AOBS scanning confocal microscope as described in section2.5.3. Images of YFP- and mCherry-STIM1 were acquired using 488nm and 561nm laser line excitation, respectively.

7.3 Results

7.3.1 The effect of bombesin and thapsigargin on STIM1 in normal spreading HeLa cells

The results show the distribution and density of STIM1 in the YFP-STIM1 expressing normal spreading HeLa cells, which were either stimulated with bombesin or thapsigargin. Figure 7.3.1a shows the confocal microscope images for a single un-stimulated cell scanned at 2 different planes. The figure 7.3.1b-d show the confocal images of 3 single cells which were treated with 100nM bombesin at 2min, 4min and 8min before fixation. For each cell, 4 scanned images at different planes from the bottom to the top of the cell are presented. In a same way, figure 7.3.1e-g show the images of 3 thapsigargin-treated (2μM) cells.

From this figure, puncta can be clearly seen in thapsigargin-stimulated cells. There was no distinct increase of puncta formation in the bombesin-treated cells, compared to the un-stimulated cells. Most of the puncta are located at the base of the cell, especially in those that have been bombesin-treated. Both bombesin- and thapsigargin-stimulated cells show most puncta at the 4 minute time point.

a. control

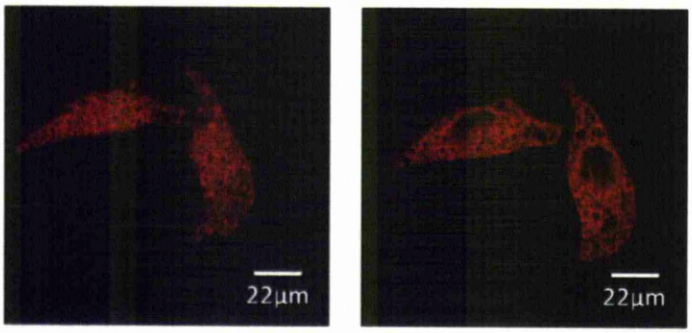

b. +bombesin 2min

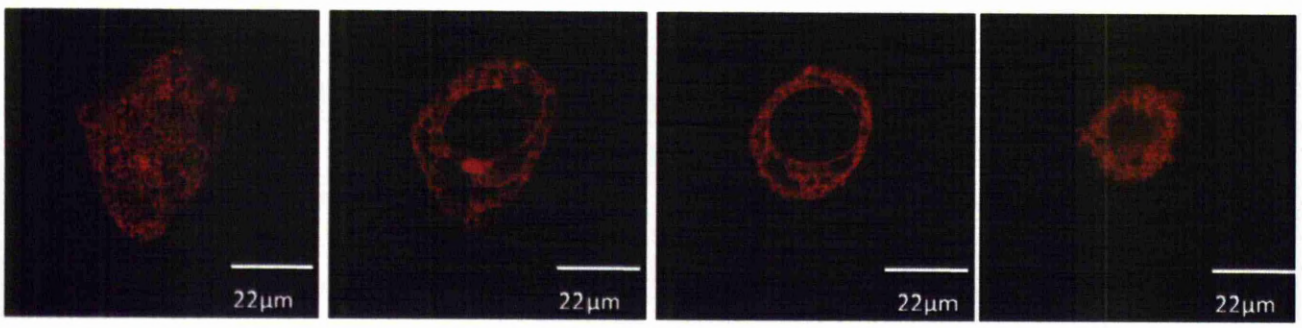

c. +bombesin 4min

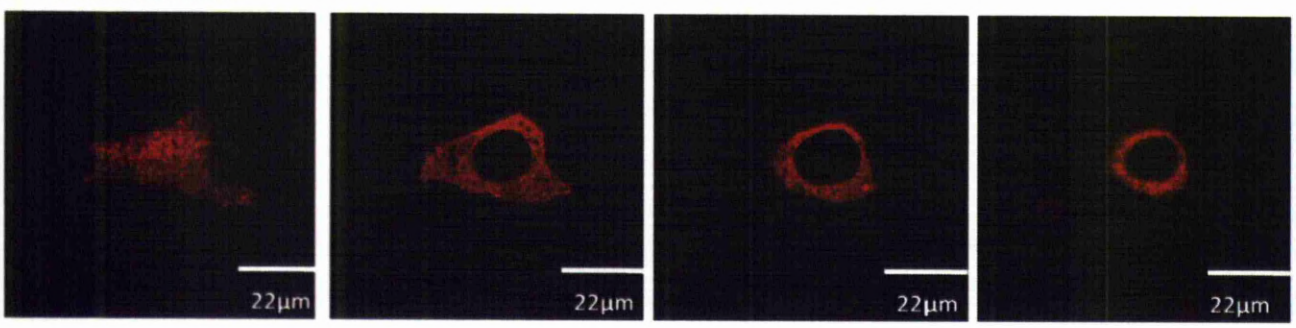

d. +bombesin 8min

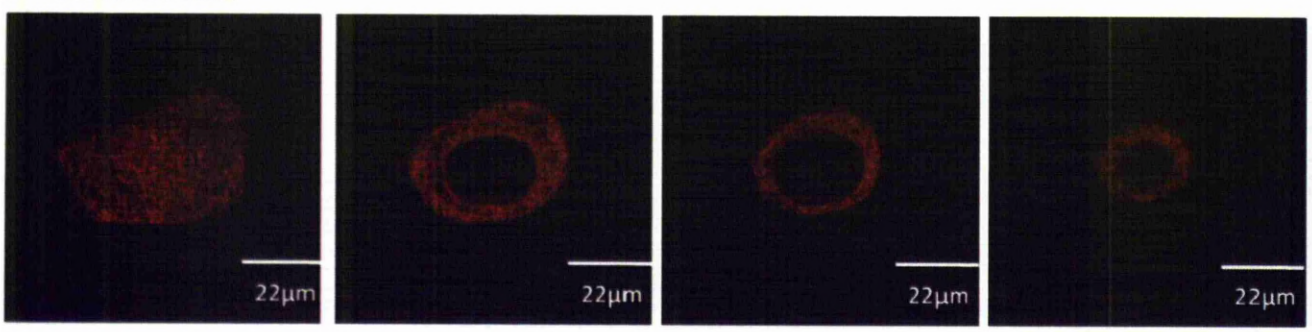

e. +Tg 2min

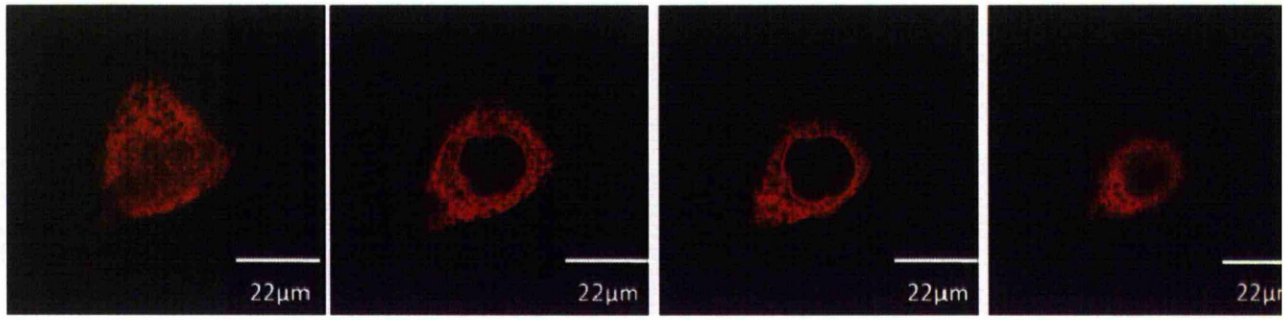

f. +Tg 4min

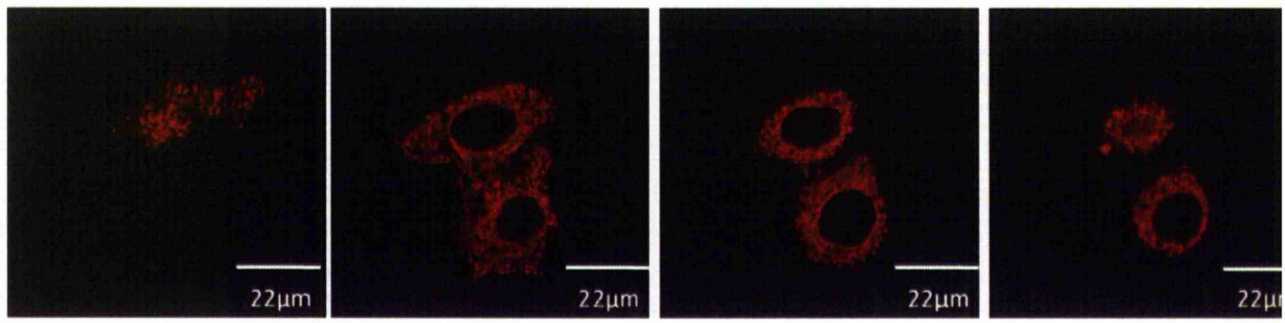

g. +Tg 8min

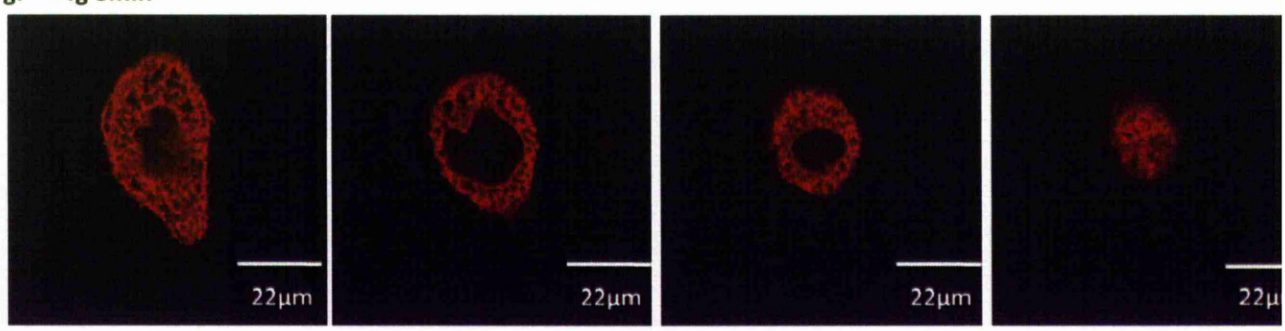

Figure 7.3.1-The effect of bombesin and thapsigargin on STIM1 distribution in normal spreading HeLa cells

YFP-STIM1 over expressing HeLa cells were cultured, unrestricted on glass coverslips. Images were visualized with a Leica SP2 AOBS laser scanning confocal microscope. The images of one single cell scanned in different planes, from the bottom (left) to the top (right), are presented in each figure from (a)-(g). The two images in figure (a) shows the distribution of STIM1 in an un-stimulated cell in 1mM Ca^{2+} containing HBS. Figure (b)-(d) show the distribution of STIM1 in three 100nM bombesin treated cells in 1mM Ca^{2+} containing HBS for 2min (b), 4min (c) and 8min (d) respectively. Figure (e)-(g) present the distribution of STIM1 in three cells treated with 2μM thapsigargin for 2min (e), 4min (f) and 8min (g) consequently. Results shown are representative of 3 separate experiments.

7.3.2 The effect of bombesin and thapsigargin on STIM1 in cell shape restricted HeLa cells

Since it was observed that the STIM1 can be at least partially activated by bombesin in HeLa cells, the effect of cell shape on activation was investigated. Both large (ø45μm) and small (ø22μm) islands were utilized to restrict the HeLa cell shape.

Figure 7.3.2A and figure 7.3.2B show the distribution of STIM1 in cells on either large or small adhesive islands. The confocal images for two un-stimulated cells are presented in figure 7.3.2A (a) and figure 7.3.2B (a). Figure 7.3.2A (b)-(d) and figure 7.3.2B (b)-(d) are confocal images for 100nM bombesin-treated cells on large and small islands at different time points (2min & 4min & 8min), in which four confocal images scanned at different planes are presented for each single cell.

Thapsigargin (2μM) was also used to stimulate the shape restricted HeLa cells. In the same way, figure 7.3.2C and figure 7.3.2D show the distribution of STIM1 in control and thapsigargin-treated restricted cells. In total, 3 similar experiments were performed to confirm the results. Each cell in the figure is representative at least 3 different cells.

Both bombesin and thapsigargin are able to induce the STIM1 puncta formation in the shape restricted cells, whether they were on the large or small islands. As a result, it appears that the formation of STIM1 puncta is not affected by the cell shape in the HeLa cells.

a. large island: control

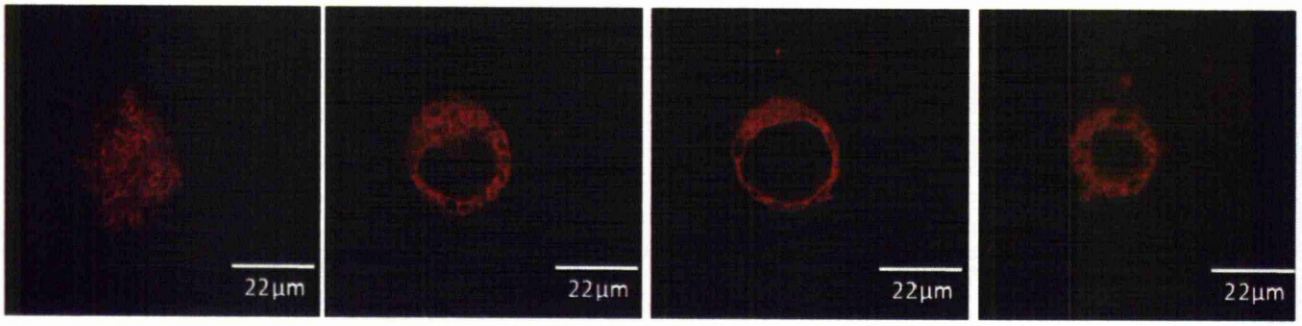

b. large island: +bombesin 2min

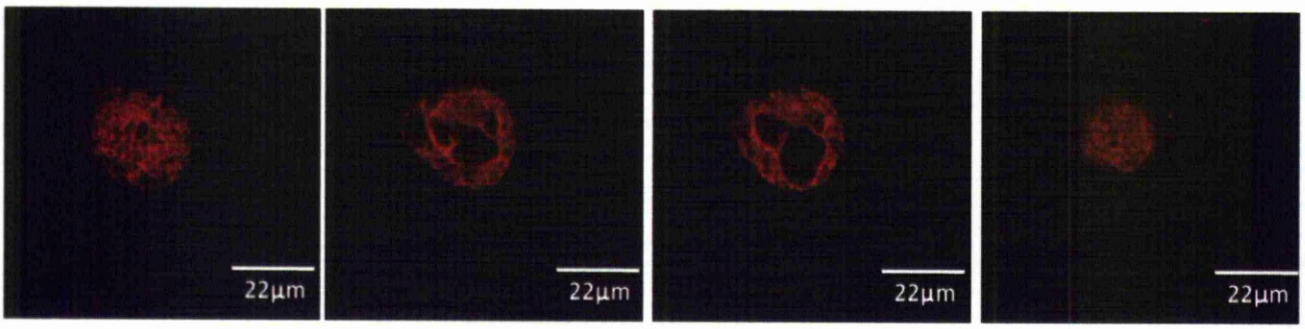

c. large island: +bombesin 4min

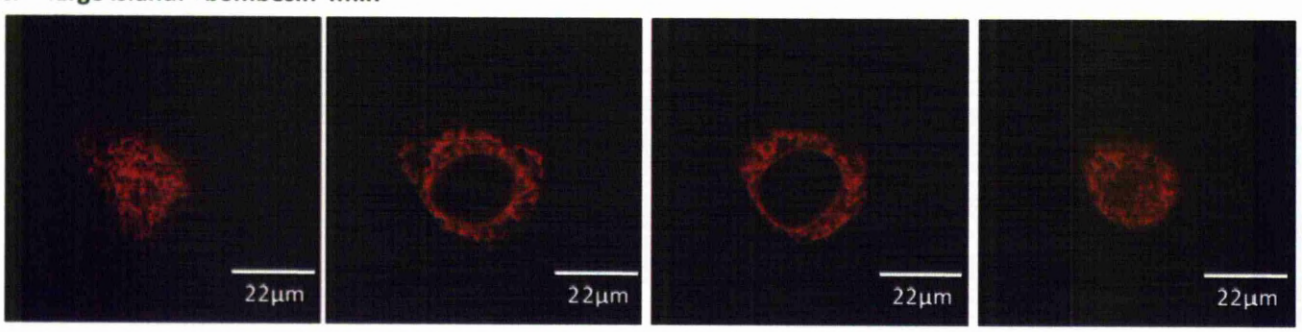

d. large island: +bombesin 8min

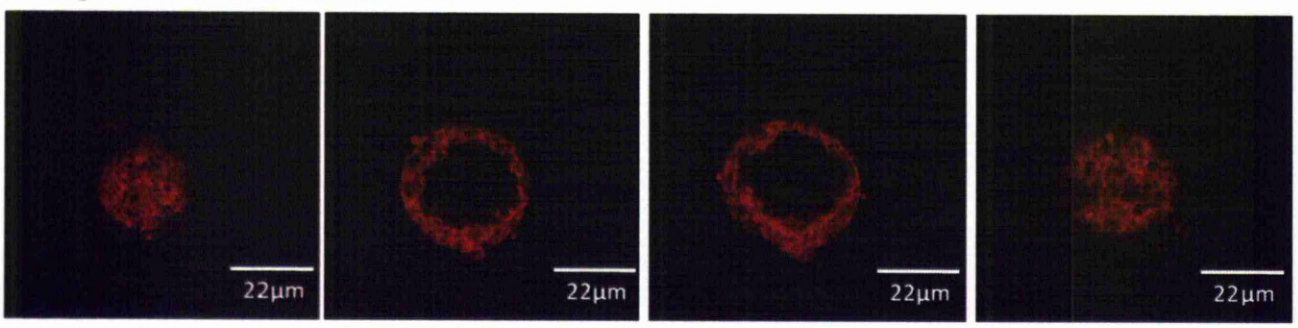

Figure 7.3.2A-The effect of bombesin on STIM1 in the HeLa cells on large islands

YFP-STIM1 over expressing HeLa cells were cultured and restricted with large islands. Images

were visualized with a Leica SP2 ABOS laser scanning confocal microscope. The images of one single cell scanned at different planes, from the bottom (left) to the top (right), are presented in each figure from (a)-(d). Figure (a) shows the distribution of STIM1 in an un-stimulated cell in 1mM Ca^{2+} containing HBS. Figure (b)-(d) show the distribution of STIM1 in three 100nM bombesin-treated cells in 1mM Ca^{2+} containing HBS for 2min (b), 4min(c) and 8min(d) respectively. Results shown are representative of 3 separate experiments.

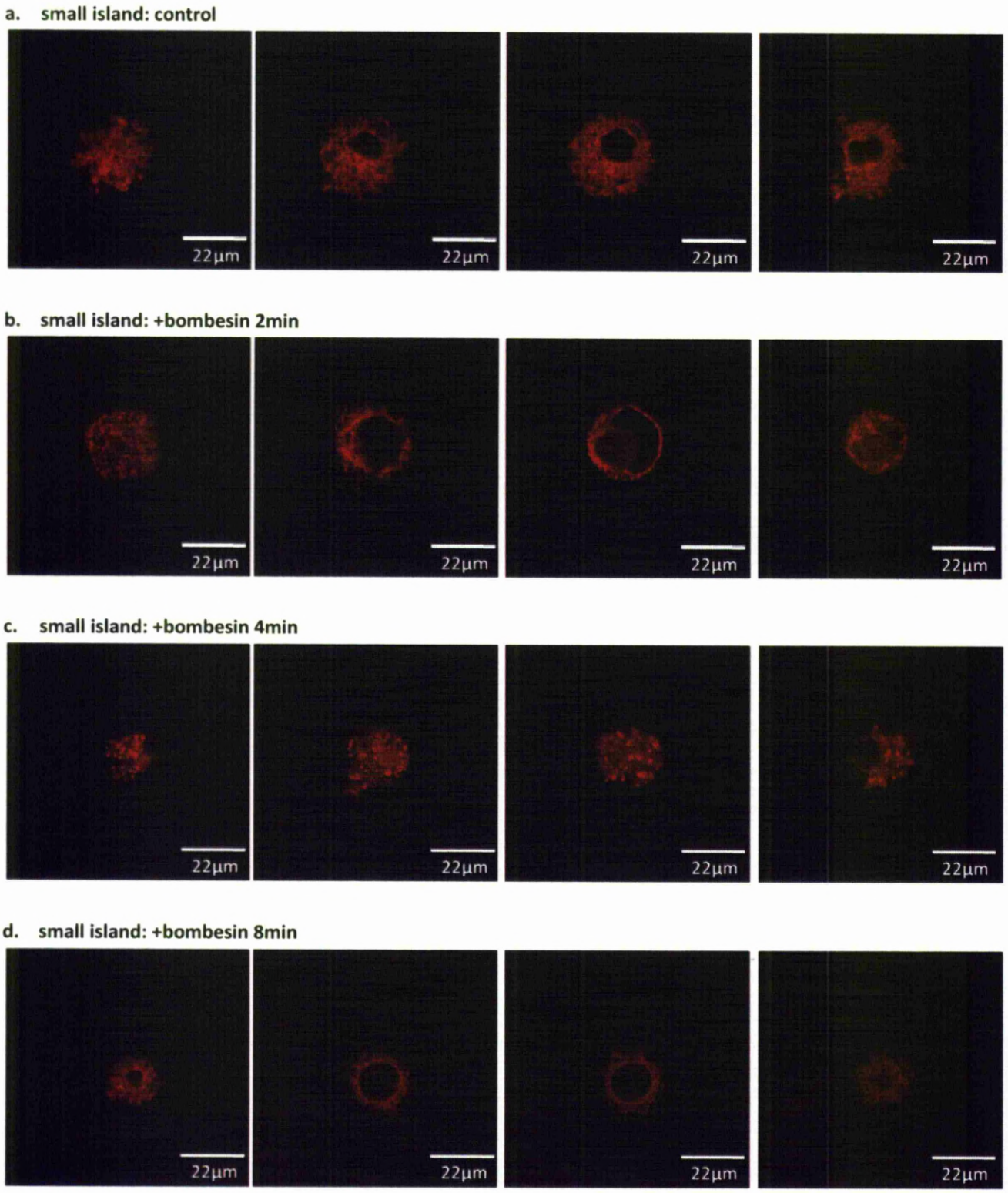

Figure 7.3.2B-The effect of bombesin on STIM1 in the HeLa cells on small islands

YFP-STIM1 over expressing HeLa cells were cultured and cell spreading restricted using small

adhesive islands. Images were visualized with a Leica SP2 ABOS laser scanning confocal microscope. The images of one single cell scanned at different planes, from the bottom (left) to the top (right), are presented in each figure from (a)-(d). Figure (a) shows the distribution of STIM1 in an un-stimulated cell in 1mM Ca^{2+} containing HBS. Figure (b)-(d) show the distribution of STIM1 in three 100nM bombesin-treated cells in 1mM Ca^{2+} containing HBS for 2min (b), 4min(c) and 8min(d) respectively. Results shown are representative of 3 separate experiments.

a. large island: control

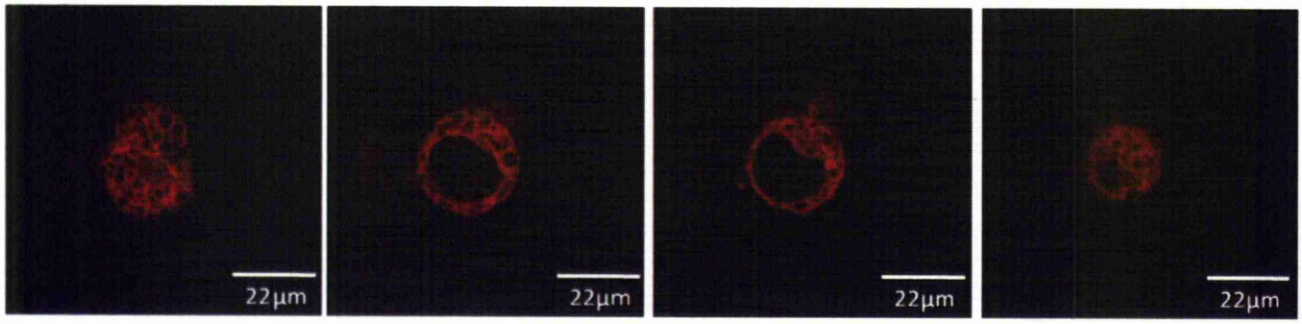

b. large island: +Tg 2min

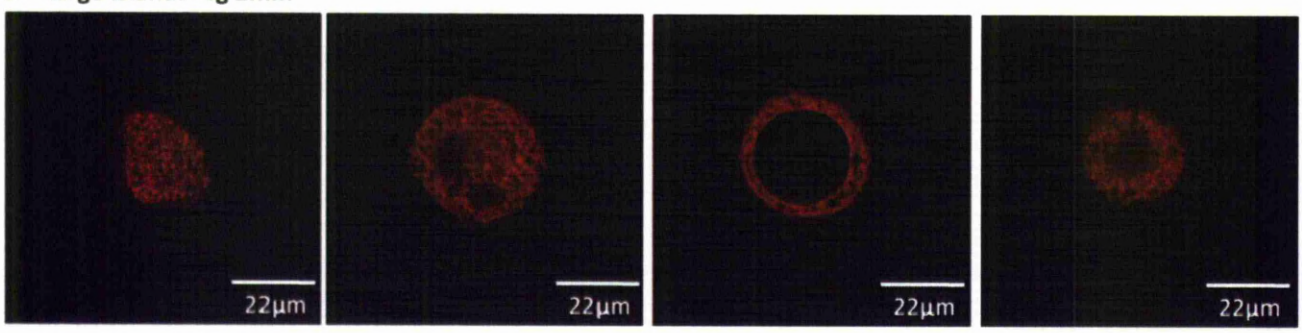

c. large island: +Tg 4min

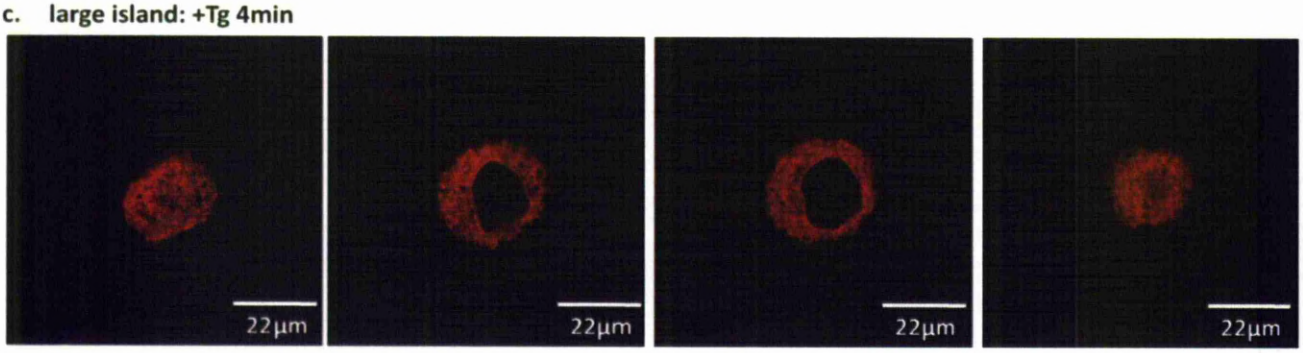

d. large island: +Tg 8min

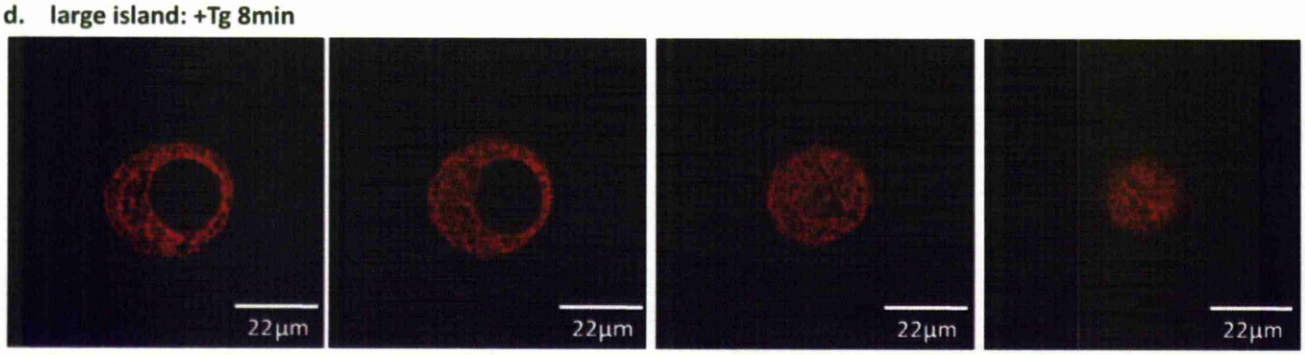

Figure 7.3.2C-The effect of thapsigargin on STIM1 in the HeLa cells on large islands

YFP-STIM1 over expressing HeLa cells were cultured and placed on large adhesive islands. Images were visualized with a Leica SP2 ABOS laser scanning confocal microscope. The images of one

single cell scanned at different planes, from the bottom (left) to the top (right), are presented in each figure from (a)-(d). Figure (a) shows the distribution of STIM1 in an un-stimulated cell in Ca^{2+} free HBS. Figure (b)-(d) show the distribution of STIM1 in three 2μM thapsigargin-treated cells in Ca^{2+} free HBS for 2min (b), 4min(c) and 8min(d) respectively. Results shown are representative of 3 separate experiments.

a. small island: control

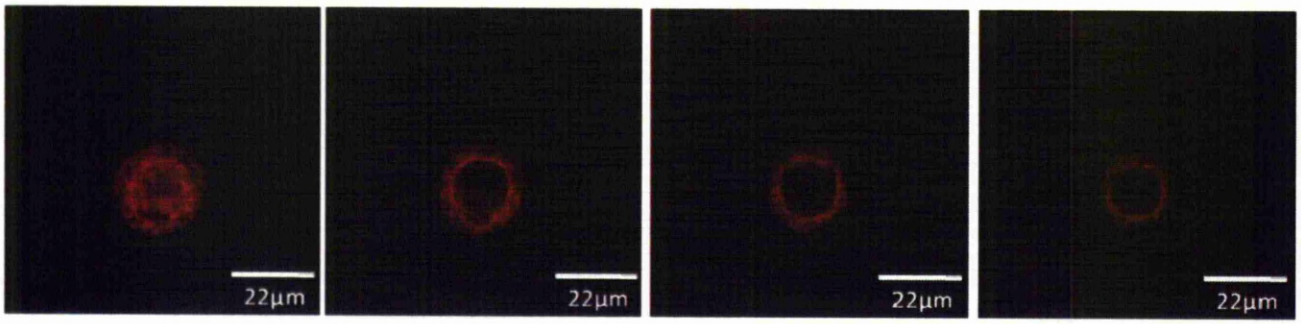

b. small island: +Tg 2min

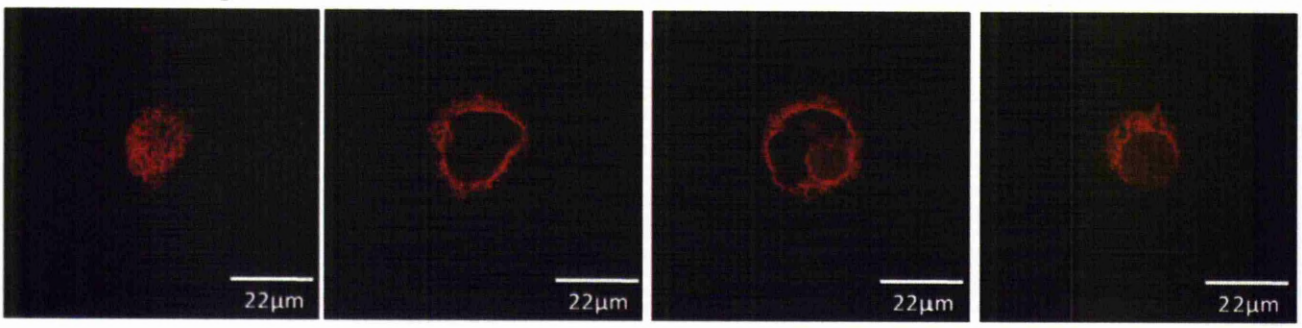

c. small island: +Tg 4min

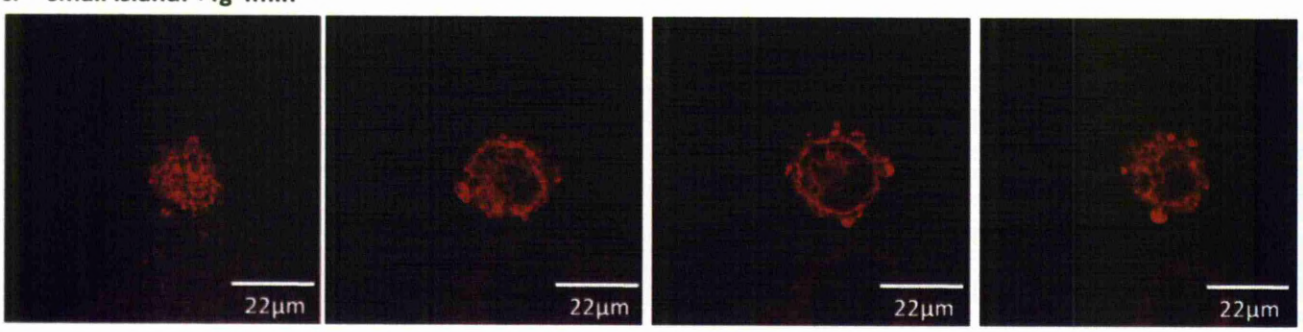

d. small island: +Tg 8min

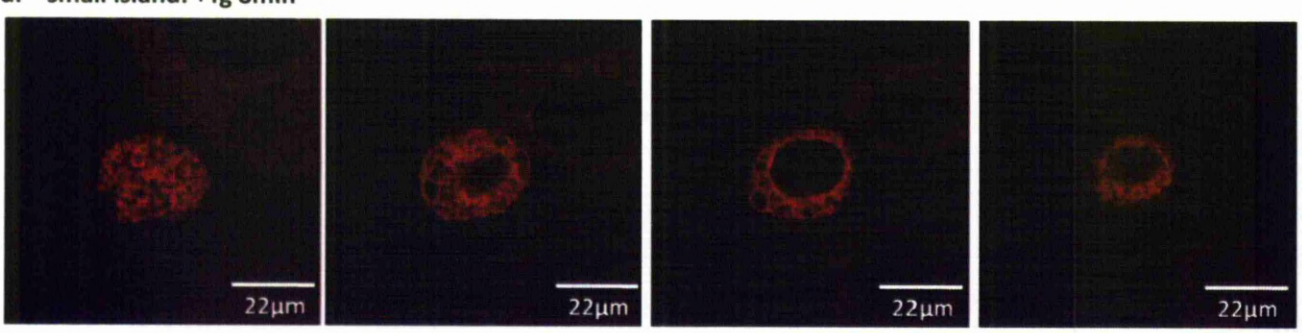

Figure 7.3.2D-The effect of thapsigargin on STIM1 in the HeLa cells on small islands

YFP-STIM1 over expressing HeLa cells were cultured and placed on small adhesive islands. Images were visualized with a Leica SP2 ABOS laser scanning confocal microscope. The images of one

single cell scanned at different planes, from the bottom (left) to the top (right), are presented in each figure from (a)-(d). Figure (a) shows the distribution of STIM1 in an un-stimulated cell in Ca^{2+} free HBS. Figure (b)-(d) show the distribution of STIM1 in three 2μM thapsigargin-treated cells in Ca^{2+} free HBS for 2min (b), 4min(c) and 8min(d) respectively. Results shown are representative of 3 separate experiments.

7.3.3 The effect of bombesin and thapsigargin on STIM1 in normal spreading Swiss 3T3 cells

With a new transfection reagent Jet prime, the mCherry- or YPF-STIM1 transfection rate was increased up to 30% in Swiss 3T3 cells (GeneJuice showed a transfection rate at 1-2%). As a result, the activation of STIM1 to either bombesin or thapsigargin was first examined in normal spreading cells.

Figure 7.3.3A shows the distribution of mCherry-STIM1 in either control or stimulated cells. Two un-stimulated cells (left) in 1mM Ca^{2+} HBS are presented in figure 7.3.3A (a), which are representative of 17 out of 25 investigated un-stimulated cells shown no puncta formation. In the remaining cells, some degree of puncta formation was observed as shown in the image (right) in figure 7.3.3A (a). In other words, 8 out of 25 cells (32%) un-stimulated cells show STIM1 puncta. Figure 7.3.3A (b)-(d) show bombesin (100nM) treated cells at 2min, 4min and 8min after the stimulation. Two different cells are presented in each figure (b)-(d). For the stimulated cells at the 2 minute time point (b), 17 out of 21 cells (81%) clearly show STIM1 puncta. At the 4 minute time point (c), there are 14 out of 18 (78%) bombesin-treated cells showing STIM1 puncta. Similarly, the proportion of cells that possess STIM1 puncta in stimulated cells at the 8 minute (d) time point was 3 out of 4 (75%). The results indicate that bombesin is able to cause STIM1 puncta formation in most cases. In a same way, figure 7.3.3A (e)-(g) shows 2μM thapsigargin-stimulated cells at different time points. At the 2 minute time point, there are 12 out of 14 (86%) thapsigargin-treated cells with STIM1 puncta (e). Similarly, STIM1 puncta were observed in 5 out of 7 (71%) cells stimulated with thapsigargin at 4min (f) after the stimulation. All the thapsigargin-treated cells (n=2 cells) at the 8 minute time point showed the STIM1 puncta (g).

Followed the above, the STIM1 formation in cell shape restricted Swiss 3T3 cells was investigated. In order to sort the cells by FACS, YFP-STIM1 was transfected into Swiss 3T3 cells. The transfected cells were sorted before being placed onto islands. Figure 7.3.3B shows 3 YFP-STIM1 expressing Swiss 3T3 cells that are either normal spreading (a) or restricted by islands (b) & (c). These data show that YFP-STIM1 expressing Swiss 3T3 can be sorted and cultured on islands for analysis of STIM1 puncta formation.

Furthermore, the activation of STIM1 by either bombesin or thapsigargin in restricted Swiss 3T3

cells was examined. All the stimulated cells were treated with either bombesin in 1mM Ca^{2+} containing HBS or thapsigargin in Ca^{2+} free HBS for 4min before the fixation. Figure 7.3.3C shows the distribution of STIM1 in either control (a) or agonist treated (b & c) normal spreading Swiss 3T3 cells. Clear STIM1 puncta can be seen in the thapsigargin-treated cells but not in the bombesin-stimulated ones. Figure 7.3.3D & figure 7.3.3E show the distribution of STIM1 in either large or small islands restricted cells. Similarly, the STIM1 puncta is only observed in thapsigargin-stimulated cells.

a. **Control**

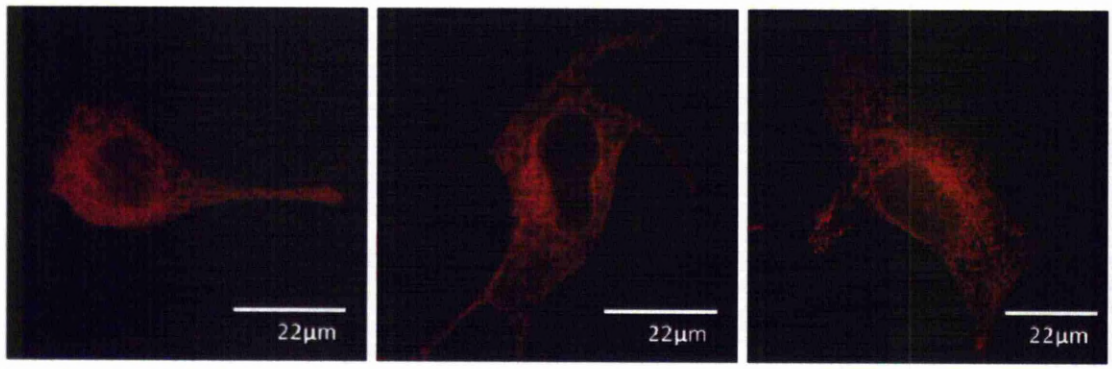

b. **+bombesin 2min**

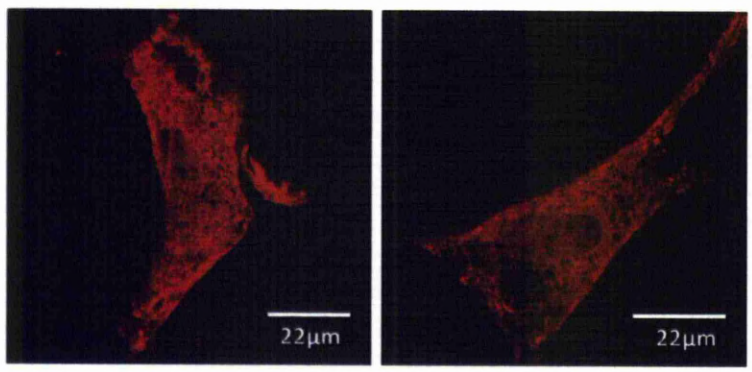

c. **+bombesin 4min**

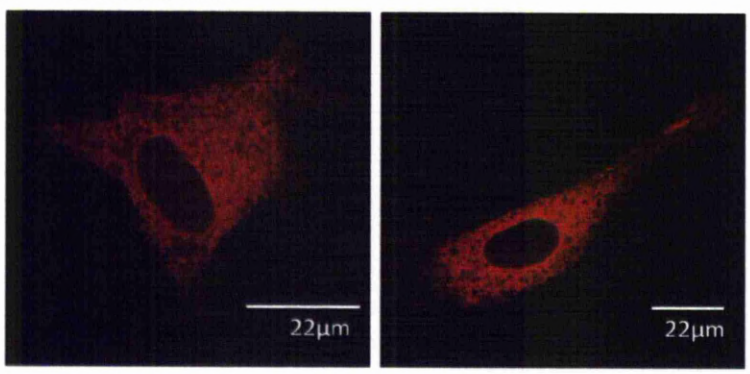

d. **+bombesin 8min**

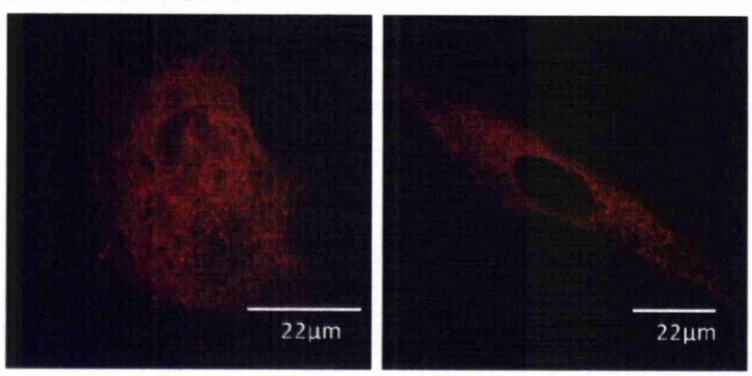

e. +Tg 2min

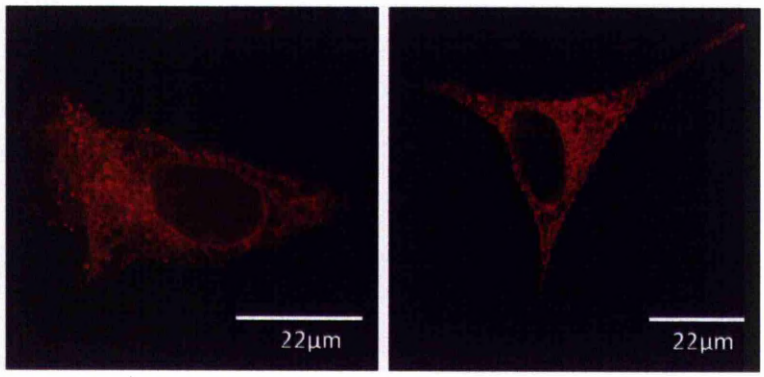

f. +Tg 4min

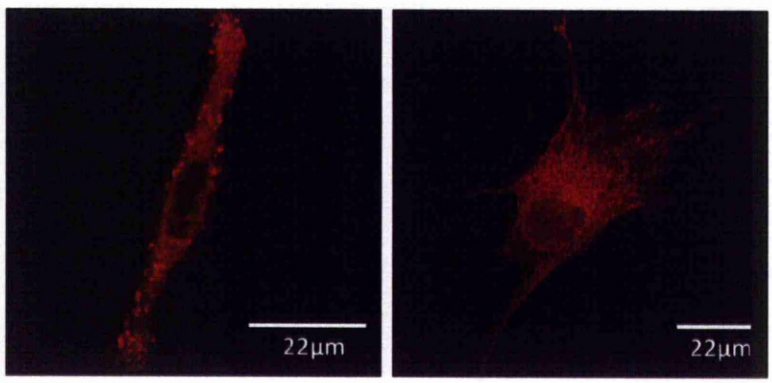

g. +Tg 8min

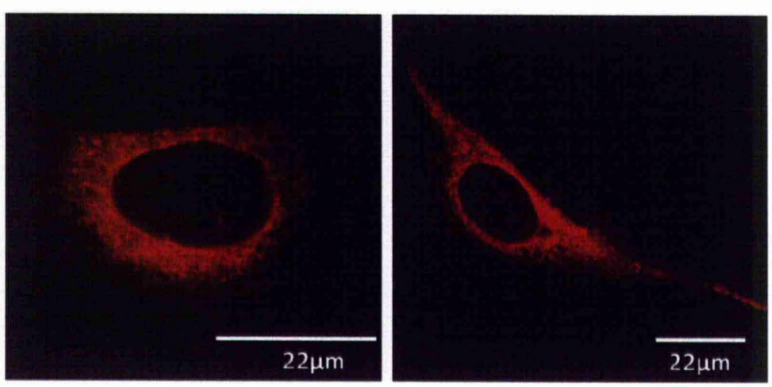

Figure 7.3.3A- The effect of bombesin and thapsigargin on STIM1 in normal spreading Swiss 3T3 cells

The mCherry-STIM1 expressing Swiss 3T3 cells were cultured, unrestricted on glass coverslips. Images were visualized with a Leica SP2 ABOS laser scanning confocal microscope. The images of two different single cells are presented in each figure from (a)-(g). Figure (a) shows the distribution of STIM1 in the un-stimulated cells in 1mM Ca^{2+} containing HBS. Figure (b)-(d) show the distribution of STIM1 in 100nM bombesin treated cells in 1mM Ca^{2+} containing HBS for 2min (b), 4min(c) and 8min(d) respectively. Figure (e)-(g) present the distribution of STIM1 in cells treated with 2μM thapsigargin for 2min(e), 4min(f) and 8min(g) consequently. Results shown are representative of 3 separate experiments.

a. **Control: normal spreading**

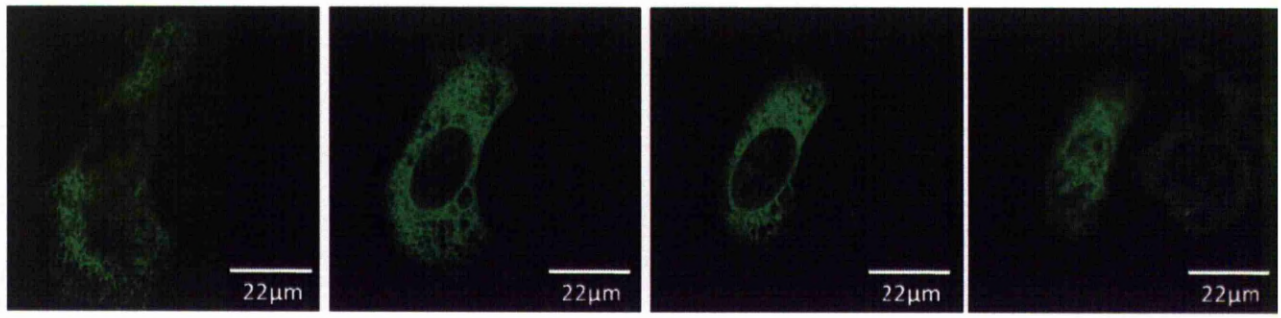

b. **Control: large islands**

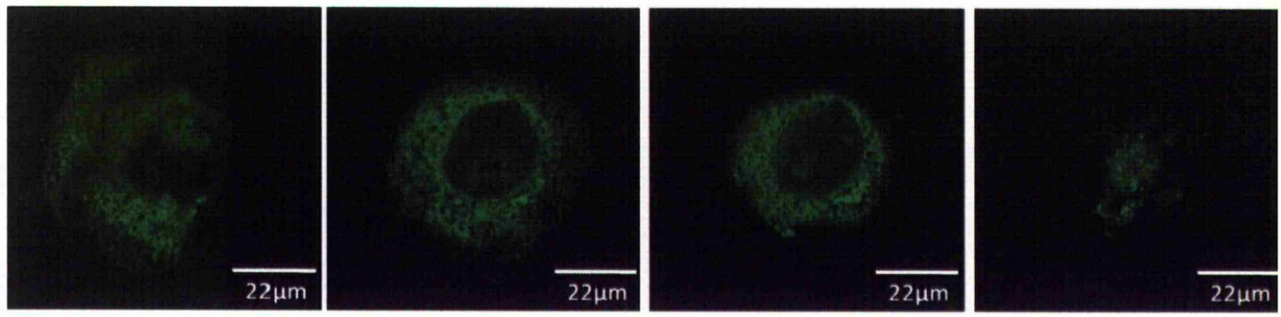

c. **Control: small islands**

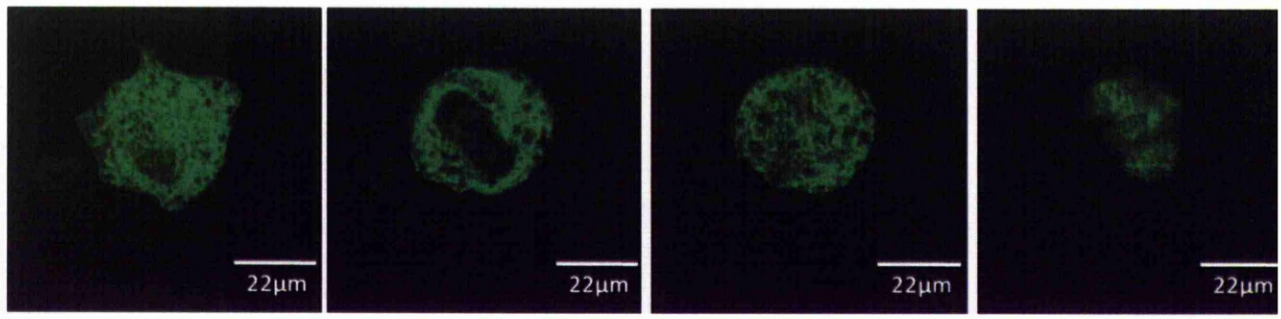

Figure 7.3.3B-The distribution in normal spreading and shape restricted Swiss 3T3 cells

YFP-STIM1 expressing Swiss 3T3 cells were cultured unrestricted on the glass coverslips (a) or on the large (b) and small (c) islands. Cells were cultured in FCS-DMEM before fixation. The images were visualized with a Leica SP2 ABOS laser scanning confocal microscope. Images of one single cell scanned at different planes, from the bottom (left) to the top (right), are presented in each figure from (a)-(c). The result is 5 experiments. These data were obtained in collaboration with Dr Alex Laude.

a. **Normal spreading: control**

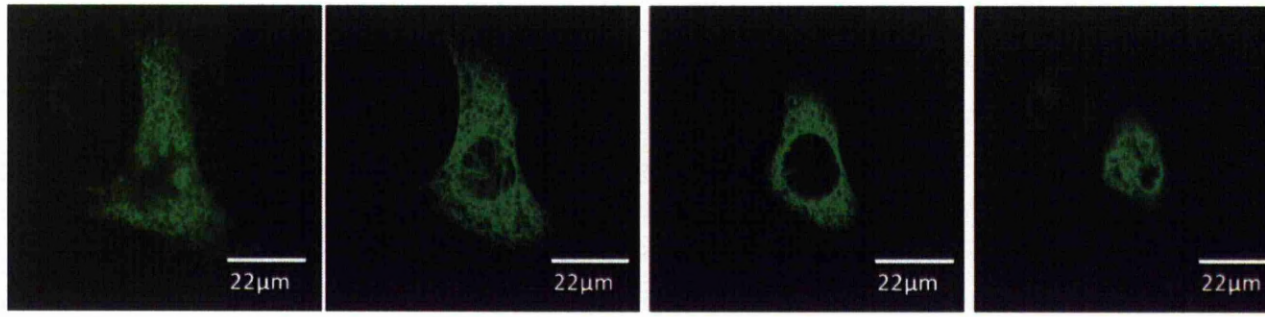

b. **Normal spreading: +bombesin**

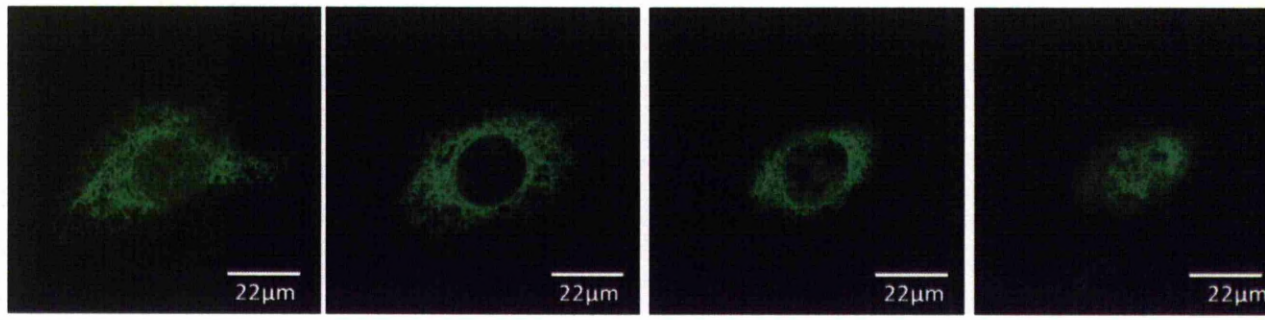

c. **Normal spreading: +Tg**

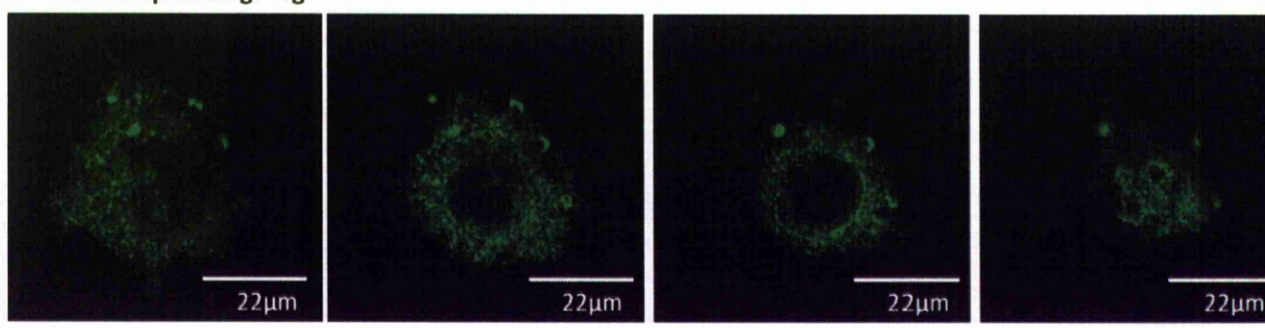

Figure 7.3.3C- The effect of bombesin and thapsigargin on STIM1 in normal spreading Swiss 3T3 cells

YFP-STIM1 expressing Swiss 3T3 cells were cultured unrestricted on the glass coverslips. Cells were sorted by FACS and then cultured in FCS-DMEM for 16 hrs before fixation. The images were visualized with a Leica SP2 ABOS laser scanning confocal microscope. Images of one single cell scanned at different levels, from the bottom (left) to the top (right), are presented in each figure from (a)-(c). Figure (a) presents an un-stimulated cell while figure (b) & (c) present cells stimulated by bombesin (100nM) and thapsigargin (2µM) for 4min, respectively. The result is representative of 5 experiments. These data were obtained in collaboration with Dr Alex Laude.

a. Large islands: control

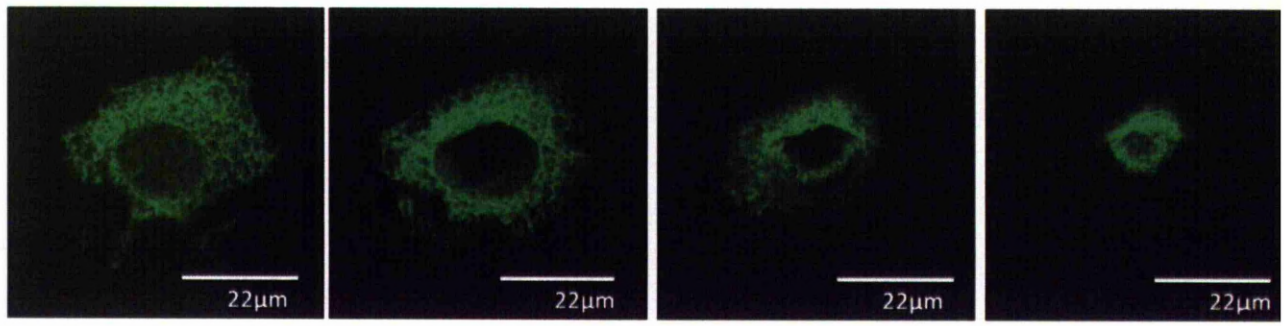

b. Large islands: + bombesin

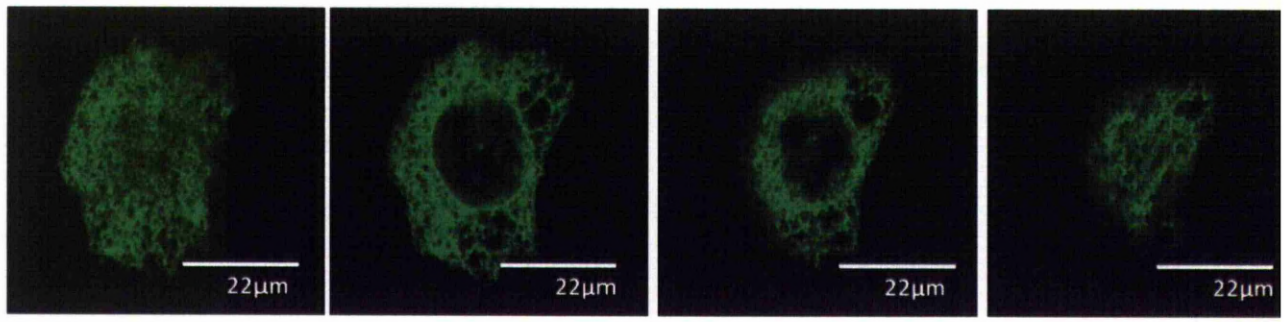

c. Large islands: +Tg

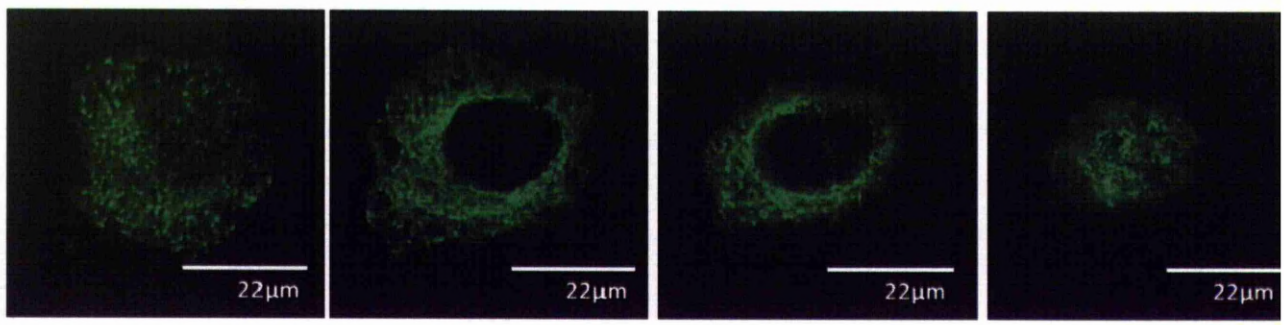

Figure 7.3.3D- The effect of bombesin and thapsigargin on STIM1 in Swiss 3T3 cells on the large islands

YFP-STIM1 expressing Swiss 3T3 cells were cultured unrestricted on the large islands. Cells were sorted by FACS and then cultured in FCS-DMEM for 16 hrs before fixation. The images were visualized with a Leica SP2 ABOS laser scanning confocal microscope. Images of one single cell scanned at different levels, from the bottom (left) to the top (right), are presented in each figure from (a)-(c). Figure (a) presents an un-stimulated cell while figure (b) & (c) present cells stimulated by bombesin (100nM) and thapsigargin (2μM) for 4min, respectively. The result is representative of 5 experiments. These data were obtained in collaboration with Dr Alex Laude.

a. Small islands: control

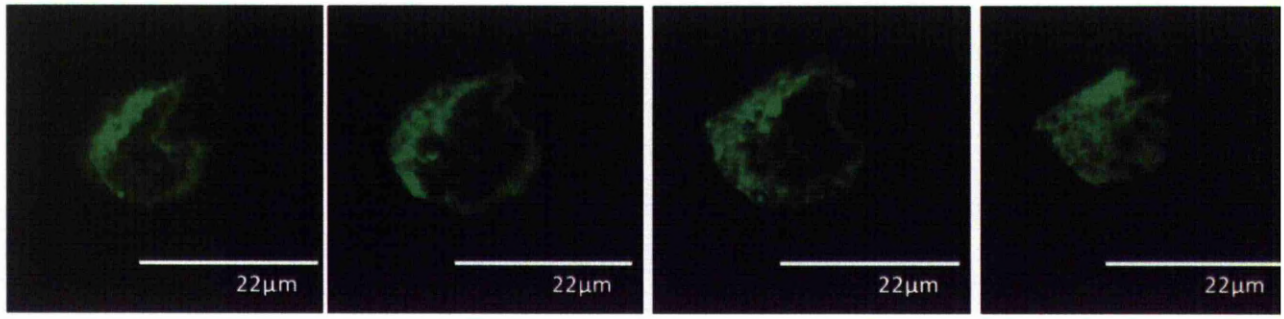

b. Small islands: +bombesin

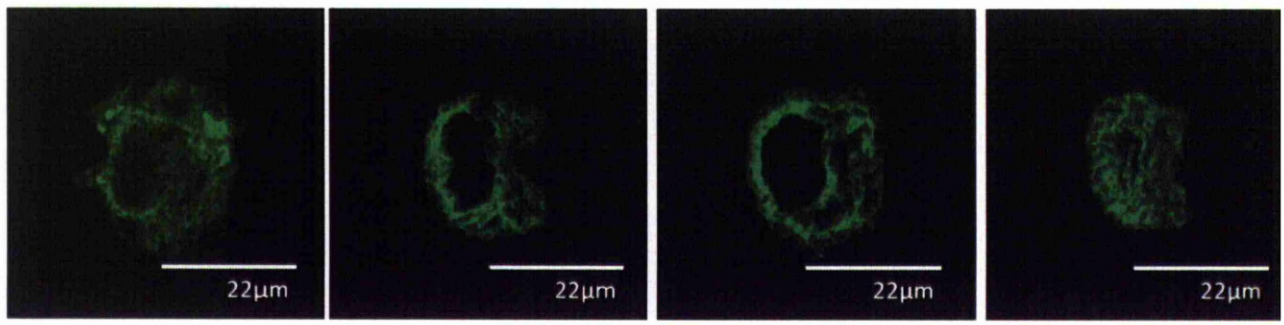

c. Small islands: +Tg

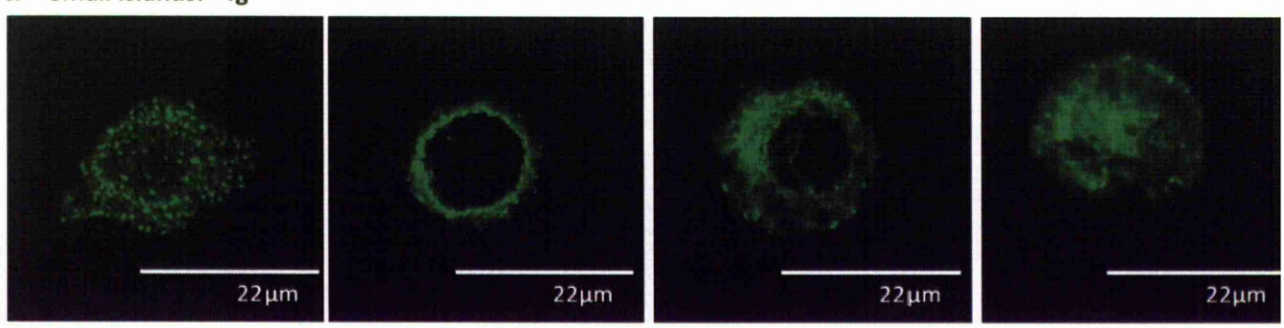

Figure 7.3.3E-The effect of bombesin and thapsigargin on STIM1 in Swiss 3T3 cells on the small islands

YFP-STIM1 expressing Swiss 3T3 cells were cultured unrestricted on the small islands. Cells were sorted by FACS and then cultured in FCS-DMEM for 16 hrs before fixation. The images were visualized with a Leica SP2 ABOS laser scanning confocal microscope. Images of one single cell scanned at different levels, from the bottom (left) to the top (right), are presented in each figure from (a)-(c). Figure (a) presents an un-stimulated cell while figure (b) & (c) present cells stimulated by bombesin (100nM) and thapsigargin (2μM) for 4min, respectively. The result is representative of 5 experiments. These data were obtained in collaboration with Dr Alex Laude.

7.4 Discussion

It is agreed that STIM1 puncta formation always precedes the induction of SOCE, and this is consistent with a causal role for STIM1 redistribution in activating SOCCs (Baba *et al.*, 2006). In this chapter, the location of STIM1 redistribution in response to the stimulation by bombesin or thapsigargin in normal spreading HeLa cells and Swiss 3T3 cells was investigated using confocal microscopy.

Some STIM1 puncta were occasionally observed in un-stimulated cells (Figure 7.3.3Aa & 7.3.3Ba). Similar findings were reported by Baba *et al.* (2006), and they argued that at any one time at least a small fraction of STIM1 distributions in the ER occur as small puncta.

The results demonstrate that thapsigargin is very effective at inducing the formation of STIM1 puncta in both HeLa and Swiss 3T3 cells. This is entirely consistent with its property to deplete Ca^{2+} stores and trigger SOCE. The result shows that: in HeLa cells, STIM1 puncta formed as early as 2 min after addition of thapsigargin, and the amount of puncta increased at 4min followed by a decrease at 8min. The time course corresponds with the time dependence of SOCE after thapsigargin-stimulated release from stores in this cell type (Gamberucci *et al.*, 1994; Missiaen *et al.*, 1994). Similarly, the thapsigargin-treated Swiss 3T3 cells when treated for 4min possess more puncta than the cells at other two time points.

Fewer STIM1 puncta were seen in the bombesin-treated HeLa or Swiss 3T3 cells compared to the thapsigargin-treated ones (Figure 7.3.1 &7.3.3A). Since STIM1 puncta was also seen in resting cells, whether the stimulation by bombesin facilitates the formation of STIM1 puncta is difficult to confirm without quantitative analysis. However, in this case, it is quite likely that the limited amount of STIM1 puncta is insufficient to fully active SOCCs and lead to a large Ca^{2+} influx. In other words, the partially activated SOCCs may not be fully responsible for the bombesin-induced Ca^{2+} influx although they certainly participate. This conclusion explains the observation that SK&F96365, rather than fully blocking, merely reduced the amount of bombesin-induced Ca^{2+} influx, which is presented in chapter 6.

An interesting observation in the experiments is that most of the puncta were based or adjacent to the bottom of the cells. Since cells were attached to the coverslips, shaped as a "bell", the bottom is where the most area of plasma membrane can be seen under confocal microscope. Therefore, the accumulation of puncta at the base of the cells suggest that most of them are close to or even located at the plasma membrane, which agrees with the common definition of puncta that it is a structure near or within the plasma membrane (Liou *et al.*, 2005; Zhang *et al.*, 2006).

Following the examination in normal spreading cells, the dependence of the redistribution of STIM1 on the cell shape was investigated. The result indicated that the thapsigargin-induced formation of STIM1 puncta is not impaired by the restriction of cell shape in either HeLa or Swiss 3T3 cells (Figure 7.3.2C-D & 7.3.3D-E). This is consistent with the observation in our laboratory that the thapsigargin-evoked Ca^{2+} influx can be activated in the Swiss 3T3 cell on the small islands (Foster, 2005). In addition, this finding supports the conclusion that the actin cytoskeleton does not play an obligate role in the SOCE pathway as argued by other researchers. For example, it was reported that depolymerization of the actin cytoskeleton with cytochalasin D does not negatively impact SOCEs in NIH 3T3 cells (Ribeiro *et al.*, 1997).

However, the formation of STIM1 puncta evoked by bombesin in restricted cells seemed to be different from that induced by thapsigargin. Although the STIM1 puncta was seen in the restricted HeLa cells, STIM1 puncta were not observed in the restricted Swiss 3T3 cells. The differences between HeLa and Swiss 3T3 cells may due to the difference of their original cell sizes. The original size of HeLa cell is much smaller than that of the Swiss 3T3 cell. As a result, the ø22μm small adhesive island may not be small enough to have the HeLa cell shape intensively restricted. The bombesin-evoked $[Ca^{2+}]_i$ response in HeLa cells was not measured, therefore it is not known whether bombesin is able to evoke a cell shape-dependent Ca^{2+} influx in this cell line. For the Swiss 3T3 cells, as long as the absence of bombesin-induced STIM1 puncta in restricted cells can be confirmed, it may account for the loss of the bombesin-evoked Ca^{2+} influx in cells on small islands (Figure 3.3.4).

Although the actin cytoskeleton may have little effect on the thapsigargin-induced SOCEs, it was found that disruption of the actin cytoskeleton with cytochalasin D inhibits agonist-evoked Ca^{2+} influx (Ribeiro *et al.*, 1997). The relationship between PLC and IP_3 receptors might be altered when the skeleton was disrupted. This may further impair PLC-dependent Ca^{2+} signaling (Ribeiro *et al.*, 1997). We know that activated PLC stimulates hydrolysis of PIP_2 into DAG and IP_3 (Lee and Rhee, 1995). The latter triggers Ca^{2+} release via IP_3Rs on the ER (Berridge *et al.*, 2003). STIM1 as an ER depletion sensor is translocated and formed the puncta at the ER-PM junction as consequence of IP_3-induced ER depletion. Based on this evidence, it may be suspected that the bombesin-induced STIM1 puncta formation observed in normal spreading Swiss 3T3 cells is through the PLC-IP_3 pathway. As a result, when the actin cytoskeleton is disrupted by restriction the cell shape using adhesive islands, this might alter the activation of PLC and IP_3, and the bombesin-induced STIM1 puncta formation is prevented. However, such hypothesis is challenged by a observation that the Ca^{2+} release from ER which is normally controlled by IP_3 is not inhibited by the restriction of cell shape by islands in Swiss 3T3 cells (Pennington et al., 2007). This finding suggests that the activity of IP_3 is not cell shape dependent.

Another possible explanation for the absence of bombesin-induced STIM1 formation in the restricted Swiss 3T3 cells is the effect of microtubular cytoskeleton on STIM1. The microtubular cytoskeleton is known to be a major regulator of ER structure and function (Terasaki *et al.*, 1986). Some evidence has suggested that microtubules might play a facilitative role in organizing STIM1 to communicate with Orai channels (Smyth *et al.*, 2007). Restriction of the cell shape with islands might cause a re-arrangement of the microtubular structure which consequently alters the activation of STIM1. According to a previous finding in our laboratory, microtubular structure was observed in small adhesive islands restricted Swiss 3T3 cells (Foster, 2005). However, the distribution of microtubules in shape restricted-cells differs from that in the normal spreading cells (see Appendix 2). Therefore, microtubules are possible to affect the distribution and translocation of STIM1 in restricted cells. Although no clear STIM1 puncta was observed in bombesin-stimulated Swiss 3T3 cells, the distribution of STIM1 tended to be more condensed than that in un-stimulated cells. The condensed distribution of STIM1 is similar to an observation

in a study measuring the structure of ER microtubule network during cell division. It is found that the ER displays a reticular network of convolved cisternae linked to tubules in the interphase while it undergoes a transformation and is organized as extended cisternae from prometaphase to telophase (Lu *et al.*, 2009). Hence, the condensed STIM1 seen in bombesin-stimulated cells might be due to the change of ER microtubule structure. Furthermore, because Swiss 3T3 cells are difficult to be transfect with mCherry- or YFP-STIM1, limited data were obtained from the experiments.

In conclusion, the study clearly indicates STIM1 puncta can form in shape-restricted cells. In addition to STIM1, STIM2 should be studied. It was reported that STIM2 may already be partially active at basal ER Ca^{2+} concentrations and be fully activated by small reductions of ER Ca^{2+} concentration, while STIM1 may require much larger receptor-triggered reductions in ER Ca^{2+} to be activated (Brandman *et al.*, 2007). Since the result in my research imply that the $[Ca^{2+}]_i$ response in restricted cells is smaller than that in normal spreading cells, STIM2 which is more sensitive to smaller Ca^{2+} release might play a more important role in this bombesin-induced Ca^{2+} influx than STIM1. More studies on STIM2 in Swiss 3T3 cells are therefore needed.

In summary, the key findings presented in this chapter are:

1. Thapsigargin is effective at inducing STIM1 puncta formation in normal spreading HeLa and Swiss 3T3 cells.
2. The thapsigargin-induced STIM1 puncta formation in HeLa and Swiss 3T3 cells is not affected by cell restriction using adhesive islands.
3. Bombesin is not very effective in generating STIM1 puncta and there was not a noticeable increase in STIM1 puncta compared with control cells. Less STIM1 puncta were observed in bombesin-stimulated cells than in thapsigargin-stimulated cells.
4. STIM1 puncta were observed in bombesin-stimulated cell shape-restricted HeLa cells. However, no bombesin-evoked STIM1 puncta was seen in restricted Swiss 3T3 cells.

Chapter 8

General discussion

Contents:

8.1 General discussion

It has been demonstrated that restricting cell shape leads to inhibition of cell cycle progression. (Folkman and Moscona, 1978; Ireland *et al.*, 1987; Watt *et al.*, 1988; Huang *et al.*, 1998) In particular, Swiss 3T3 cells failed to enter S phase under the stimulation of FCS when they are cultured on small (ø22μm) adhesive islands (Ireland *et al.*, 1987; Pennington *et al.*, 2007). More recently, it has been demonstrated that bombesin-induced Ca^{2+} influx was inhibited in such small island restricted cells (Pennington et al., 2007). Similar results are presented here in chapter 3, which confirms the existence of this cell-shape-dependent Ca^{2+} influx. It is known that Ca^{2+} signals, derived from mitogen-evoked signaling pathways, play a critical role in regulating the cell cycle. Ca^{2+} and various Ca^{2+} binding proteins regulate a number of cell cycle regulatory factors, such as cyclinD-CDK4 complex, p21 and p27 to control the cell cycle (Kahl and Means, 2003). Consequently, the absence of the bombesin-induced Ca^{2+} influx would be expected to inhibit cell cycle progression in Swiss 3T3 cells restricted by small adhesive islands. The main aim of this research is to investigate the mechanisms underlying bombesin-induced cell shape-dependent Ca^{2+} influx.

Previous work in our laboratory proposed a possibility that AA may be involved in this bombesin-induced Ca^{2+} influx. It has been seen that bombesin acts like the AA analogue ETYA that stimulates Ca^{2+} and Sr^{2+} entry but not Ba^{2+} entry. Nevertheless, thapsigargin evokes both Sr^{2+} and Ba^{2+} influx (Foster, 2005). As a result, the role of AA in the bombesin-evoked Ca^{2+} influx was first examined.

Following the same protocol, I tested the effect of agonists, bombesin, ETYA and thapsigargin, on the influx of Ba^{2+} and Sr^{2+}. The data is presented in chapter 4. Although similar results, that are consistent to Foster's study, were obtained, the reliability of the effects is questioned due to the occurrence of spontaneous Ba^{2+} and Sr^{2+} influxes. Whether the influx of Ba^{2+} or Sr^{2+} is due to the stimulation of agonists or a passive leaking is unclear. Ba^{2+} influxes were seen after the addition of ETYA, with a bigger amplitude of Δratio340/380 than the spontaneous influx observed during the same period of time (Figure 4.3.3B). This observation implied that ETYA is able to evoke a Ba^{2+} influx, which is in agreement with the model proposed by Foster (Foster, 2005). However, rather

than no response, bombesin showed a tendency to evoked a slight Ba^{2+} influx according to my data (Figure 4.3.1A). Whether ETYA as well as bombesin induce a small Ba^{2+} influx and a big Sr^{2+} entry is still an issue to be resolved. Furthermore, the experiments in shape restricted cells indicated that, in more than half the cases, cells showed a Ba^{2+} influx with or without the stimulation of bombesin. In addition, no significant difference was seen in either Ba^{2+} or Sr^{2+} influx in the cells on large or small adhesive islands. Collectively speaking, the model based on the specific responses of Ba^{2+} and Sr^{2+} to agonists is challenged since a Ba^{2+} influx was seen after the stimulation of bombesin or ETYA. Due to the occasional spontaneous influx of Ba^{2+} and Sr^{2+}, both cations were not able to distinguish particular activation by either SOCE or NSOCE. Consequently, other approaches to determine the nature of the bombesin-evoked influx were adopted.

In order to characterize the involvement of AA in this shape-dependent Ca^{2+} influx, the $cPLA_2$ pathway which is primarily responsible for the liberation of AA was examined. The immunofluorescence experiments presented in chapter 5 indicate that there was an increase of phospho-$cPLA_2$ after the addition of bombesin in normal spreading Swiss 3T3 cells. This bombesin-induced phospho-$cPLA_2$ expression was suppressed in small island-restricted cells according to the data, although there were increases of immunofluorescence intensity of phospho-$cPLA_2$ occasionally seen in those restricted cells (Section 5.3.2). However, whether the bombesin-regulated phospho-$cPLA_2$ increase occurred in the upstream or downstream of the $cPLA_2$-AA pathway is questionable, since the ERK/MAPK inhibitors, ERK FR182040 and PD98059 failed to inhibit the Ca^{2+} influx evoked by bombesin (Figure 5.3.5 A & B). In addition, the increase of phospho-$cPLA_2$ intensity was still seen in ERK FR182040 and PD98059 treated cells. All these findings suggested that the ERK/MAPK pathway is not participating in the pathway that activates the Ca^{2+} influx after the stimulation of bombesin. Therefore, the $cPLA_2$, which is activated through the phosphorylation by ERK/MAPK, may be not required for the bombesin-evoked Ca^{2+} influx.

The importance of $cPLA_2$ to the bombesin-evoked $[Ca^{2+}]_i$ responses was further questioned when two $cPLA_2$ inhibitors were utilized. Although the $cPLA_2\alpha$ inhibitor caused a moderate suppression on Ca^{2+} influx, it somehow increased the bombesin-evoked Ca^{2+} release and also Sr^{2+} influx.

Another inhibitor AACOCF3 showed no inhibition but rather slightly increased both bombesin-induced Ca^{2+} release and influx (Section 6.3.1 & 6.3.2). These data are not consistent with $cPLA_2$ playing a major role in controlling bombesin-induced Ca^{2+} entry. Although the involvement of $cPLA_2$ is challenged, the importance of AA in this Ca^{2+} entry pathway cannot be ruled out. One piece of evidence is that the inhibitor AACOCF3, as an analogue of AA, (Riendeau *et al.*, 1994) increased the bombesin-induced Ca^{2+} release and Ca^{2+} influx (Section 6.3.1&6.3.2). In addition to $cPLA_2$, AA is generated through other phospholipases, such as $iPLA_2$ or PLC/PLD-DAG pathway.

The data in chapter 5 indicate that an $iPLA_2$ inhibitor BEL blocks the bombesin-evoked $[Ca^{2+}]_i$ response. This suggests that $iPLA_2$ rather than $cPLA_2$ is more likely to contribute to the activation of Ca^{2+} entry. Ca^{2+}-independent phospholipase A_2 is able to generate AA along with other fatty acids and lysophospholipids. In addition, it is regarded as an essential component of signal transduction from the stores to plasma membrane in SOCEs (reviewed by Bolotina, 2008). Besides, no increase of phospho-$cPLA_2$ intensity in bombesin-stimulated cells was observed when the cells were treated with BEL together with ERK FR182040 and PD98059 (preliminary data not shown) which might be due to the absence of Ca^{2+} responses inhibited by BEL. This observation implies that the activation of $cPLA_2$ requires the bombesin-evoked $[Ca^{2+}]_i$ responses, which means it occurs downstream rather than upstream of this Ca^{2+} influx.

Other than $iPLA_2$, BEL has been reported to inhibit the action of DAG by suppressing the generation of DAG from PA in the PLD-DAG pathway (Balsinde and Dennis, 1997). Therefore, the DAG pathway might account for the generation of AA in this bombesin-evoked Ca^{2+} influx. This possibility is supported by the application of a DAG lipase inhibitor RHC80267. It significantly inhibits the bombesin-induced $[Ca^{2+}]_i$ responses, especially the influx, which indicated that DAG is necessary for the bombesin to induce $[Ca^{2+}]_i$ responses (Section 6.3.1 & 6.3.2).

Although the data has not ruled out a role of AA in bombesin-evoked Ca^{2+} influx, the involvement of SOCE is supported by other data. It was observed that a widely used SOCE inhibitor SK&F96365 suppressed this bombesin-induced Ca^{2+} influx (Section 6.3.4). At the same time, another inhibitor

LOE 908 showed a similar inhibition effect on the Ca^{2+} influx (Section 6.3.3). However, whether LOE 908 inhibits a SOCE or a NSCCE is still controversial. Its actions seem to be cell type and concentration dependent (Encabo *et al.*, 1996; Miwa *et al.*, 2000; Moneer and Taylor, 2002). In addition, both inhibitors failed to fully block the Ca^{2+} influx but partially suppressed although they are able to inhibit most of the Ba^{2+} or Sr^{2+} influxes. Such difference between Ca^{2+} and Ba^{2+} or Sr^{2+} might be explained by the reciprocal regulation between I_{SOC} and I_{ARC} theory (Mignen *et al.*, 2001). Based on these findings and the ability of thapsigargin to evoke $[Ca^{2+}]_i$ responses, the involvement of SOCEs in this bombesin-induced Ca^{2+} influx is convincing. However, whether it co-exists with other Ca^{2+} entry pathways or is fully responsible for bombesin-evoked Ca^{2+} influx is unclear. Also, it is unclear as to whether SOCE can be regulated by cell shape.

In order to answer these questions, the activation of STIM1 was studied in both HeLa and Swiss 3T3 cells. The STIM1 puncta was seen in either bombesin or thapsigargin stimulated HeLa and Swiss 3T3 cells (Section 7.3.1 & 7.3.3). However, the amount of bombesin-induced STIM1 puncta is less than that induced by thapsigargin. This limited amount of STIM1 puncta in bombesin-treated cells implies that the SOCCs might not be fully activated. Consequently, SOCEs may not fully account for the bombesin-induced Ca^{2+} influx.

In addition, the data in chapter 7 show that restricting the cell shape with adhesive islands has little effect on the formation of STIM1 induced by thapsigargin in either HeLa or Swiss 3T3 cells. These observations indicate that the thapsigargin-evoked STIM1 puncta formation is not cell shape dependent which is consistent with the finding that the thapsigargin-evoked Ca^{2+} influx is not inhibited in cells restricted with small islands (Foster, 2005). A recent study in epithelial cells, in which cells are plated in hard and soft substrate, suggested that it is the substrate but not the cell size that affects the STIM1 translocation (Chiu *et al.*, 2007), which is in general agreement with my observation that STIM1 can translocate in shape-restricted cells.

Bombesin-induced STIM1 puncta formation seems to be absent when restricting cell shape with islands in Swiss 3T3 cells. No clear STIM1 puncta was seen in bombesin stimulated Swiss 3T3 cells on small islands (Figure 7.3.3E). Such inhibition might due to the re-arrange of cytoskeleton

caused by cell shape restriction. It was reported that disruption of actin cytoskeleton with cytochalasin D alters the PLC-IP_3 pathway (Ribeiro *et al.*, 1997). Such altered PLC-IP_3 pathway may lead to an absence of STIM1 puncta. The actin cytoskeleton was seen be re-arranged into a ring shape in small island restricted cells (Foster, 2005). However, it was found that low concentration of cytochalasin D could disrupt the ring shape actin cytoskeleton without inhibiting the Ca^{2+} entry (Foster, 2005). In addition, there was no difference between the Ca^{2+} release induced by IP_3 in the cells on either large or small islands (Foster, 2005), which suggests the PLC-IP_3 pathway is not affected when the actin cytoskeleton is altered by small islands. Another possible link between actin cytoskeleton and SOCE is a plasma membrane anchored protein, annexin A6. Annexin A6 was found to be a key player linking the actin cytoskeleton with SOCEs, and its interaction with plasma membrane and subsequent stabilization of cortical actin might contribute to attenuation of Ca^{2+} entry in HEK293 cells (Monastyrskaya *et al.*, 2009). Whether the localization of annexin A6 is altered in small adhesive island-restricted Swiss 3T3 cells need to examined.

Rather than the actin cytoskeleton, microtubules are more likely to affect the distribution of STIM1 (Smyth *et al.*, 2007). According to previous research in our laboratory, restricting the cell shape with islands changed the distribution of microtubules (Foster, 2005; Appendix 2). Therefore, there is a possibility that microtubule re-arrangement is responsible for the absence of STIM1 puncta in islands restricted cells.

Consequently, the mechanism that leads to the apparent absence of STIM1 puncta in shape-restricted bombesin-stimulated cells is still unclear. Due to the limited data obtained from the experiments on STIM1, whether STIM1 forms puncta in bombesin-stimulated shape-restricted cells needs to be confirmed by further research.

8.2 Conclusion

In my research, the bombesin-induced cell-shape-dependent Ca^{2+} influx is confirmed by the utilization of small and large adhesive islands. The mechanism of such influx was investigated. Previous studies pointed out the possibility of ARC channels involved in this cell-shape-dependent Ca^{2+} influx based on experiments on Ba^{2+} and Sr^{2+}. However these two

divalent cations proved not to be useful in studying the Ca^{2+} entry pathways due to the presence of spontaneous influxes. The presence of spontaneous fluxes means that characterization of the influx pathway by divalent cations permeability is difficult to achieve. Consequently, other approaches were adopted.

The experiments on the activity of $cPLA_2$ showed that although the $cPLA_2$ is phosphorylated after the stimulation of bombesin, such phosphorylation is not necessary for the activation of bombesin-evoked Ca^{2+} influx. Since in the cells on small islands, there is increased phospho-$cPLA_2$, but under the condition there was no Ca^{2+} influx. In addition, the ERK inhibitors failed to prevent the increase of phospho-$cPLA_2$ or bombesin-evoked Ca^{2+} influx. On the other hand, the application of inhibitors BEL and RHC80267 indicates that, rather than $cPLA_2$, the DAG or $iPLA_2$ pathways which are able to generate AA may still participate in the bombesin-evoked Ca^{2+} influx.

In addition to the participation of ARC channels, the SOCCs may account for this cell-shape-dependent Ca^{2+} influx as well. The most convincing evidence is that the SK&F96365 suppressed the bombesin-evoked Ca^{2+} influx. In addition, it was observed that the STIM1 forms puncta in bombesin treated Swiss 3T3 cells. However, the amount of puncta is much less than that formed after the stimulation of thapsigargin. Whether the limited amount of STIM1 puncta is sufficient to fully activate the SOCCs and generate a Ca^{2+} influx is doubtful. In addition, no bombesin-induced STIM1 puncta was seen in adhesive islands restricted Swiss 3T3 cells.

Collectively, data in my research show that both ARC entry pathway and the SOCE pathway are likely to account for the bombesin-induced Ca^{2+} influx. Cytosolic phospholipase A_2 does not appear to be important in the regulation of cell-shape-dependent Ca^{2+} influx. The analysis of STIM1 localization proved interesting, since STIM1 puncta were seen in HeLa and Swiss 3T3 cells even when the cells spreading was restricted with small islands.

8.3 Future research

Based on the data presented here, there are several aspects that require further research to identify the mechanism that underlies the bombesin-induced cell-shape-dependent Ca^{2+} influx.

Whether these two entry pathways: the ARC entry pathway and the SOCE pathway co-exist or only one of them participates in this process still needs to be studied in more detail. Besides, the mechanism that leads to the inhibition of this bombesin-evoked Ca^{2+} influx in small island restricted cells also requires more investigations.

In order to confirm the involvement of AA, the DAG pathway should be studied. Whether cell shape restriction has any effect on the DAG pathway could be investigated. The liberation of AA after the stimulation by bombesin could be examined by labeling with [^{3}H] AA.

The activation of $iPLA_2$ is another interesting aspect to study. Is $iPLA_2$ able to generate AA to induce an ARC entry or another fatty acid to cause a SOCE that result in the bombesin-evoked Ca^{2+} entry?

Whether the SOCE is responsible for the shape-dependent Ca^{2+} influx needs to be confirmed. If the bombesin-induced STIM1 puncta formation does not occur in the shape restricted cells, this may explain how cell shape influences Ca^{2+} influx. In addition, rather than STIM1, STIM2 which is sensitive to a small amount of Ca^{2+} release, might play an important role in this Ca^{2+} influx (Brandman et al., 2007). Therefore, it is worth studying the activation of STIM2 in Swiss 3T3 cells. Moreover, recent reports suggest that STIM puncta formation may be influenced by processes other than Ca^{2+} store depletion. For example, it is found that Golli-BG21, a member of the MBP (myelin basic protein) family of proteins, regulates SOCE in T-cells and oligodendrocyte precursor cells (Burgoyne *et al.*, 2010). A novel EF-hand protein, CRAC regulator 2A, regulates SOCEs by interacting directly with Orai1 and STIM1, forming a ternary complex that dissociates at elevated $[Ca^{2+}]_i$ (Srikanth *et al.*, 2010). Therefore, cell shape may exert an effect on puncta formation and Ca^{2+} entry by one of these routes.

References

Aarhus, R., D. M. Dickey, *et al.* (1996). "Activation and inactivation of Ca^{2+} release by NAADP+." J Biol Chem **271**(15): 8513-6.

Abdullah, K., W. Cromlish, *et al.* (1995). "Human cytosolic phospholipase A2 expressed in insect cells is extensively phosphorylated on Ser-505." BBA-General Subjects **1244**(1): 157-164.

Adkins, C. and C. Taylor (1999). "Lateral inhibition of inositol 1, 4, 5-trisphosphate receptors by cytosolic Ca^{2+}." Current Biology **9**(19): 1115-1118.

Akiba, S., S. Mizunaga, *et al.* (1999). "Involvement of group VI Ca^{2+}-independent phospholipase A2 in protein kinase C-dependent arachidonic acid liberation in zymosan-stimulated macrophage-like P388D1 cells." Journal of Biological Chemistry **274**(28): 19906.

Alcón, S., S. Morales, *et al.* (2002). "Contribution of different phospholipases and arachidonic acid metabolites in the response of gallbladder smooth muscle to cholecystokinin." Biochemical Pharmacology **64**(7): 1157-1167.

Alicia, S., Z. Angelica, *et al.* (2008). "STIM1 converts TRPC1 from a receptor-operated to a store-operated channel: moving TRPC1 in and out of lipid rafts." Cell Calcium **44**(5): 479-91.

Ambudkar, I. S., H. L. Ong, *et al.* (2007). "TRPC1: the link between functionally distinct store-operated calcium channels." Cell Calcium **42**(2): 213-23.

Anastasi, A., V. Erspamer, *et al.* (1971). "Isolation and structure of bombesin and alytesin, two analogous active peptides from the skin of the European amphibiansBombina andAlytes." Cellular and Molecular Life Sciences **27**(2): 166-167.

Arnaudeau, S., W. Kelley, *et al.* (2001). "Mitochondria recycle Ca^{2+} to the endoplasmic reticulum and prevent the depletion of neighboring endoplasmic reticulum regions." Journal of Biological Chemistry **276**(31): 29430.

Atsumi, G., M. Tajima, *et al.* (1998). "Fas-induced arachidonic acid release is mediated by Ca^{2+}-independent phospholipase A2 but not cytosolic phospholipase A2, which undergoes proteolytic inactivation." Journal of Biological Chemistry **273**(22): 13870.

Avruch, J., A. Khokhlatchev, *et al.* (2001). "Ras activation of the Raf kinase: tyrosine kinase recruitment of the MAP kinase cascade." Recent Prog Horm Res **56**: 127-55.

Börsch-Haubold, A., F. Bartoli, *et al.* (1998). "Identification of the phosphorylation sites of cytosolic phospholipase A2 in agonist-stimulated human platelets and HeLa cells." Journal of Biological Chemistry **273**(8): 4449.

Baba, Y., K. Hayashi, *et al.* (2006). "Coupling of STIM1 to store-operated Ca^{2+} entry through its constitutive and inducible movement in the endoplasmic reticulum." Proceedings of the National Academy of Sciences **103**(45): 16704.

Bakowski, D., M. Glitsch, *et al.* (2001). "An examination of the secretion like coupling model for the activation of the Ca^{2+} release activated Ca^{2+} current ICRAC in RBL 1 cells." The Journal of Physiology **532**(1): 55-71.

Baksh, S., H. R. Widlund, *et al.* (2002). "NFATc2-mediated repression of cyclin-dependent kinase 4 expression." Mol Cell **10**(5): 1071-81.

Balsinde, J., M. Balboa, *et al.* (1999). "Regulation and inhibition of phospholipase A2." Annual Review of Pharmacology and Toxicology **39**(1): 175-189.

Balsinde, J., I. Bianco, *et al.* (1995). "Inhibition of calcium-independent phospholipase A2 prevents arachidonic acid incorporation and phospholipid remodeling in P388D1 macrophages."

Proceedings of the National Academy of Sciences **92**(18): 8527.

Balsinde, J. and E. Dennis (1996). "Bromoenol lactone inhibits magnesium-dependent phosphatidate phosphohydrolase and blocks triacylglycerol biosynthesis in mouse P388D1 macrophages." Journal of Biological Chemistry **271**(50): 31937.

Balsinde, J. and E. Dennis (1997). "Function and inhibition of intracellular calcium-independent phospholipase A2." Journal of Biological Chemistry **272**(26): 16069.

Barbiero, G., L. Munaron, *et al.* (1995). "Role of mitogen-induced calcium influx in the control of the cell cycle in Balb-c 3T3 fibroblasts." Cell Calcium **18**(6): 542-56.

Battey, J., J. Way, *et al.* (1991). "Molecular cloning of the bombesin/gastrin-releasing peptide receptor from Swiss 3T3 cells." Proceedings of the National Academy of Sciences of the United States of America **88**(2): 395.

Belkacemi, L., I. Bedard, *et al.* (2005). "Calcium channels, transporters and exchangers in placenta: a review." Cell Calcium **37**(1): 1-8.

Berridge, M. J. (1990). "Calcium oscillations." J Biol Chem **265**(17): 9583-6.

Berridge, M. J., M. D. Bootman, *et al.* (2003). "Calcium signalling: dynamics, homeostasis and remodelling." Nat Rev Mol Cell Biol **4**(7): 517-29.

Bhakta, N., D. Oh, *et al.* (2005). "Calcium oscillations regulate thymocyte motility during positive selection in the three-dimensional thymic environment." Nature immunology **6**(2): 143-151.

Bodding, M. (2001). "Reduced store-operated Ca($^{2+}$) currents in rat basophilic leukaemia cells cultured under serum-free conditions." Cell Calcium **30**(2): 141-50.

Boittin, F.-X., N. Macrez, *et al.* (1999). "Norepinephrine-induced Ca^{2+} waves depend on InsP3 and ryanodine receptor activation in vascular myocytes." Am J Physiol Cell Physiol **277**(1): C139-151.

Boittin, F., F. Gribi, *et al.* (2008). "Ca^{2+}-independent PLA2 controls endothelial store-operated Ca^{2+} entry and vascular tone in intact aorta." American Journal of Physiology- Heart and Circulatory Physiology **295**(6): H2466.

Bolotina, V. (2008). "Orai, STIM1 and iPLA2 : a view from a different perspective." The Journal of Physiology **586**(13): 3035.

Bolotina, V. M. and P. Csutora (2005). "CIF and other mysteries of the store-operated Ca^{2+}-entry pathway." Trends Biochem Sci **30**(7): 378-87.

Bootman, M., E. Niggli, *et al.* (1997). "Imaging the hierarchical Ca^{2+} signalling system in HeLa cells." The Journal of Physiology **499**(Pt 2): 307.

Bootman, M. D., P. Lipp, *et al.* (2001). "The organisation and functions of local Ca^{2+} signals." J Cell Sci **114**(12): 2213-2222.

Brandman, O., J. Liou, *et al.* (2007). "STIM2 is a feedback regulator that stabilizes basal cytosolic and endoplasmic reticulum Ca^{2+} levels." Cell **131**(7): 1327-1339.

Broad, L., T. Cannon, *et al.* (1999). "A non-capacitative pathway activated by arachidonic acid is the major Ca^{2+} entry mechanism in rat A7r5 smooth muscle cells stimulated with low concentrations of vasopressin." The Journal of Physiology **517**(1): 121.

Brooks, G. (2005). "Cyclins, cyclin-dependent kinases, and cyclin-dependent kinase inhibitors: detection methods and activity measurements." Methods Mol Biol **296**: 291-8.

Burdakov, D., J. Cancela, *et al.* (2001). "Bombesin-induced cytosolic Ca^{2+} spiking in pancreatic acinar cells depends on cyclic ADP-ribose and ryanodine receptors." Cell Calcium **29**(3): 211-216.

Burgoyne, R., C. Walsh, *et al.* (2010). "Evidence for an interaction between Golli AND STIM1 in

store-operated calcium entry."

Burke, J. and E. Dennis (2009). "Phospholipase A2 structure/function, mechanism, and signaling." The Journal of Lipid Research **50**(Supplement): S237.

Burke, J. E. and E. A. Dennis (2009). "Phospholipase A2 biochemistry." Cardiovasc Drugs Ther **23**(1): 49-59.

Caetano, M. S., A. Vieira-de-Abreu, *et al.* (2002). "NFATC2 transcription factor regulates cell cycle progression during lymphocyte activation: evidence of its involvement in the control of cyclin gene expression." FASEB J **16**(14): 1940-2.

Calcraft, P., M. Ruas, *et al.* (2009). "NAADP mobilizes calcium from acidic organelles through two-pore channels." Nature **459**(7246): 596-600.

Cancela, J. M., O. V. Gerasimenko, *et al.* (2000). "Two different but converging messenger pathways to intracellular Ca($^{2+}$) release: the roles of nicotinic acid adenine dinucleotide phosphate, cyclic ADP-ribose and inositol trisphosphate." EMBO J **19**(11): 2549-57.

Cancela, J. M., F. Van Coppenolle, *et al.* (2002). "Transformation of local Ca^{2+} spikes to global Ca^{2+} transients: the combinatorial roles of multiple Ca^{2+} releasing messengers." EMBO J **21**(5): 909-19.

Canonico, P. L., M. J. Cronin, *et al.* (1985). "Diacylglcerol lipase and pituitary prolactin release : Studies employing RHC 80267." Life Sciences **36**(10): 997-1002.

Carafoli, E. and M. Brini (2000). "Calcium pumps: structural basis for and mechanism of calcium transmembrane transport." Current opinion in chemical biology **4**(2): 152-161.

Chafouleas, J. G., W. E. Bolton, *et al.* (1982). "Calmodulin and the cell cycle: involvement in regulation of cell-cycle progression." Cell **28**(1): 41-50.

Chang, W.-C., C. Nelson, *et al.* (2006). "Ca^{2+} influx through CRAC channels activates cytosolic phospholipase A2, leukotriene C4 secretion, and expression of c-fos through ERK-dependent and -independent pathways in mast cells." FASEB J. **20**(13): 2381-2383.

Charlesworth, A. and E. Rozengurt (1997). "Bombesin and neuromedin B stimulate the activation of p42 (mapk) and p74 (raf-1) via a protein kinase C-independent pathway in Rat-1 cells." Oncogene **14**(19): 2323.

Chen, C. S., J. L. Alonso, *et al.* (2003). "Cell shape provides global control of focal adhesion assembly." Biochem Biophys Res Commun **307**(2): 355-61.

Chen, S. R., L. Zhang, *et al.* (1992). "Characterization of a Ca^{2+} binding and regulatory site in the Ca^{2+} release channel (ryanodine receptor) of rabbit skeletal muscle sarcoplasmic reticulum." J Biol Chem **267**(32): 23318-26.

Chini, E., K. Beers, *et al.* (1995). "Nicotinate adenine dinucleotide phosphate (NAADP) triggers a specific calcium release system in sea urchin eggs." Journal of Biological Chemistry **270**(7): 3216.

Chiu, W., Y. Wang, *et al.* (2007). "Soft substrate induces apoptosis by the disturbance of Ca^{2+} homeostasis in renal epithelial LLC PK1 cells." Journal of cellular physiology **212**(2): 401-410.

Chuang, M. and D. L. Severson (1990). "Inhibition of diacylglycerol metabolism in isolated cardiac myocytes by U-57 908 (RHC 80267), a diacylglycerol lipase inhibitor." Journal of Molecular and Cellular Cardiology **22**(9): 1009-1016.

Churchill, G. C. and A. Galione (2001). "NAADP induces Ca^{2+} oscillations via a two-pool mechanism by priming IP3- and cADPR-sensitive Ca^{2+} stores." EMBO J **20**(11): 2666-71.

Churchill, G. C., Y. Okada, *et al.* (2002). "NAADP mobilizes Ca($^{2+}$) from reserve granules,

lysosome-related organelles, in sea urchin eggs." Cell **111**(5): 703-8.

Clark, E. and R. Hynes (1996). "Ras activation is necessary for integrin-mediated activation of extracellular signal-regulated kinase 2 and cytosolic phospholipase A2 but not for cytoskeletal organization." Journal of Biological Chemistry **271**(25): 14814.

Clark, J., L. Lin, *et al.* (1991). "A novel arachidonic acid-selective cytosolic PLA2 contains a Ca^{2+}-dependent translocation domain with homology to PKC and GAP." Cell **65**(6): 1043-1051.

Coats, S., W. Flanagan, *et al.* (1996). "Requirement of p27Kip1 for restriction point control of the fibroblast cell cycle." Science **272**(5263): 877.

Collins, T., P. Lipp, *et al.* (2001). "Mitochondrial Ca^{2+} uptake depends on the spatial and temporal profile of cytosolic Ca^{2+} signals." Journal of Biological Chemistry **276**(28): 26411.

Cybulsky, A., T. Takano, *et al.* (2004). "The actin cytoskeleton facilitates complement-mediated activation of cytosolic phospholipase A2." American Journal of Physiology- Renal Physiology **286**(3): 466.

da Silva, C. P. and A. H. Guse (2000). "Intracellular Ca($^{2+}$) release mechanisms: multiple pathways having multiple functions within the same cell type?" Biochim Biophys Acta **1498**(2-3): 122-33.

Dajee, M., M. Lazarov, *et al.* (2003). "NF- B blockade and oncogenic Ras trigger invasive human epidermal neoplasia." Nature **421**(6923): 639-643.

Dammermann, W. and A. H. Guse (2005). "Functional ryanodine receptor expression is required for NAADP-mediated local Ca^{2+} signaling in T-lymphocytes." J Biol Chem **280**(22): 21394-9.

Dawson, A. P. (1997). "Calcium signalling: how do IP3 receptors work?" Curr Biol **7**(9): R544-7.

de Carvalho, M., A. McCormack, *et al.* (1996). "Identification of Phosphorylation Sites of Human 85-kDa Cytosolic Phospholipase A Expressed in Insect Cells and Present in Human Monocytes." Journal of Biological Chemistry **271**(12): 6987.

DeHaven, W., J. Smyth, *et al.* (2007). "Calcium inhibition and calcium potentiation of Orai1, Orai2, and Orai3 calcium release-activated calcium channels." Journal of Biological Chemistry **282**(24): 17548.

DeHaven, W. I., B. F. Jones, *et al.* (2009). "TRPC channels function independently of STIM1 and Orai1." J Physiol **587**(Pt 10): 2275-98.

Delphin, C., M. Ronjat, *et al.* (1999). "Calcium-dependent interaction of S100B with the C-terminal domain of the tumor suppressor p53." J Biol Chem **274**(15): 10539-44.

Di Leva, F., T. Domi, *et al.* (2008). "The plasma membrane Ca^{2+} ATPase of animal cells: Structure, function and regulation." Archives of Biochemistry and Biophysics **476**(1): 65-74.

Domin, J. and E. Rozengurt (1993). "Platelet-derived growth factor stimulates a biphasic mobilization of arachidonic acid in Swiss 3T3 cells. The role of phospholipase A2." Journal of Biological Chemistry **268**(12): 8927.

Du, C., G. MacGowan, *et al.* (2000). Calibration of Ca^{2+} dissociation constant of Rhod-2 In vivo in perfused mouse heart using Mn^{2+} quenching, Optical Society of America.

Dumollard, R., J. Carroll, *et al.* (2002). "Calcium wave pacemakers in eggs." J Cell Sci **115**(18): 3557-3564.

Dyson, N. (1998). "The regulation of E2F by pRB-family proteins." Genes & development **12**(15): 2245.

Encabo, A., C. Romanin, *et al.* (1996). "Inhibition of a store-operated Ca^{2+} entry pathway in human endothelial cells by the isoquinoline derivative LOE 908." British journal of pharmacology **119**(4): 702.

Endo, M. (1977). "Calcium release from the sarcoplasmic reticulum." Physiological reviews **57**(1): 71.

Evans, C. E., D. Billington, *et al.* (1984). "Prostacyclin production by confluent and non-confluent human endothelial cells in culture." Prostaglandins, Leukotrienes and Medicine **14**(2): 255-266.

Evans, J., D. Spencer, *et al.* (2001). "Intracellular calcium signals regulating cytosolic phospholipase A2 translocation to internal membranes." Journal of Biological Chemistry **276**(32): 30150.

Farooqui, A. and L. Horrocks (2005). "Signaling and interplay mediated by phospholipases A2, C, and D in LA-N-1 cell nuclei." Reproduction Nutrition Development **45**(5): 613-631.

Fewtrell, C. (1993). "Ca^{2+} Oscillations in Non-Excitable Cells." Annual Review of Physiology **55**(1): 427-454.

Fill, M. and J. Copello (2002). "Ryanodine receptor calcium release channels." Physiological reviews **82**(4): 893.

Fill, M. and J. A. Copello (2002). "Ryanodine receptor calcium release channels." Physiol Rev **82**(4): 893-922.

Folkman, J. and A. Moscona (1978). "Role of cell shape in growth control." Nature **273**(5661): 345-9.

Foskett, J., C. White, *et al.* (2007). "Inositol trisphosphate receptor Ca^{2+} release channels." Physiological reviews **87**(2): 593.

Foster, B. J. (2005). "The Regulation of Mitogen-Evoked Ca^{2+} signalling by Cell Shape." PhD thesis, university of liverpool

Frischauf, I., M. Muik, *et al.* (2009). "Molecular determinants of the coupling between STIM1 and Orai channels: Differential activation of Orai1,2,3 channels by a STIM1 coiled-coil mutant." J Biol Chem.

Gajate, C., F. Gonzalez-Camacho, *et al.* (2009). "Lipid raft connection between extrinsic and intrinsic apoptotic pathways." Biochem Biophys Res Commun **380**(4): 780-4.

Galione, A. and G. C. Churchill (2002). "Interactions between calcium release pathways: multiple messengers and multiple stores." Cell Calcium **32**(5-6): 343-54.

Galione, A., H. C. Lee, *et al.* (1991). "$Ca(^{2+})$-induced Ca^{2+} release in sea urchin egg homogenates: modulation by cyclic ADP-ribose." Science **253**(5024): 1143-6.

Galione, A. and M. Ruas (2005). "NAADP receptors." Cell Calcium **38**(3-4): 273-80.

Gamberucci, A., B. Innocenti, *et al.* (1994). "Modulation of Ca^{2+} influx dependent on store depletion by intracellular adenine-guanine nucleotide levels." Journal of Biological Chemistry **269**(38): 23597.

Gartel, A. L. and A. L. Tyner (1999). "Transcriptional regulation of the p21((WAF1/CIP1)) gene." Exp Cell Res **246**(2): 280-9.

Genazzani, A. A. and A. Galione (1996). "Nicotinic acid-adenine dinucleotide phosphate mobilizes Ca^{2+} from a thapsigargin-insensitive pool." Biochem J **315 (Pt 3)**: 721-5.

Gijon, M. and C. Leslie (1999). "Regulation of arachidonic acid release and cytosolic phospholipase A2 activation." Journal of leukocyte biology **65**(3): 330.

Girard, F., U. Strausfeld, *et al.* (1991). "Cyclin A is required for the onset of DNA replication in mammalian fibroblasts." Cell **67**(6): 1169-79.

Grynkiewicz, G., M. Poenie, *et al.* (1985). "A new generation of Ca^{2+} indicators with greatly improved fluorescence properties." Journal of Biological Chemistry **260**(6): 3440.

Gwack, Y., S. Srikanth, *et al.* (2007). "Biochemical and functional characterization of Orai proteins." J

Biol Chem **282**(22): 16232-43.

Harbour, J. W., R. X. Luo, *et al.* (1999). "Cdk phosphorylation triggers sequential intramolecular interactions that progressively block Rb functions as cells move through G1." Cell **98**(6): 859-69.

Hay, E. (2005). "Extracellular matrix, cell skeletons, and embryonic development." American journal of medical genetics **34**(1): 14-29.

Hayashi, T., J. Mo, *et al.* (2007). "3-Hydroxyanthranilic acid inhibits PDK1 activation and suppresses experimental asthma by inducing T cell apoptosis." Proceedings of the National Academy of Sciences **104**(47): 18619.

Hess, P. and R. W. Tsien (1984). "Mechanism of ion permeation through calcium channels." Nature **309**(5967): 453-6.

Higgins, E. R., M. B. Cannell, *et al.* (2006). "A buffering SERCA pump in models of calcium dynamics." Biophys J **91**(1): 151-63.

Higgins, E. R., M. B. Cannell, *et al.* (2006). "A Buffering SERCA Pump in Models of Calcium Dynamics." Biophysical Journal **91**(1): 151-163.

Hoth, M. and R. Penner (1992). "Depletion of intracellular calcium stores activates a calcium current in mast cells." Nature **355**(6358): 353-6.

Huang, G. N., W. Zeng, *et al.* (2006). "STIM1 carboxyl-terminus activates native SOC, I(crac) and TRPC1 channels." Nat Cell Biol **8**(9): 1003-10.

Huang, S., C. S. Chen, *et al.* (1998). "Control of cyclin D1, p27(Kip1), and cell cycle progression in human capillary endothelial cells by cell shape and cytoskeletal tension." Mol Biol Cell **9**(11): 3179-93.

Huang, S. and D. Ingber (1999). "The structural and mechanical complexity of cell-growth control." Nature Cell Biology **1**(5): E131-E138.

Huang, S. and D. Ingber (2002). "A discrete cell cycle checkpoint in late G1 that is cytoskeleton-dependent and MAP kinase (Erk)-independent." Experimental Cell Research **275**(2): 255-264.

Hughes, A. and M. Schachter (1994). "Multiple pathways for entry of calcium and other divalent cations in a vasculr smooth muscle cell line (A7r5)." Cell Calcium **15**(4): 317-330.

Huser, J. and L. Blatter (1997). "Elementary events of agonist-induced Ca^{2+} release in vascular endothelial cells." American Journal of Physiology- Cell Physiology **273**(5): C1775.

Hyde, C. and S. Missailidis (2009). "Inhibition of arachidonic acid metabolism and its implication on cell proliferation and tumour-angiogenesis." International immunopharmacology **9**(6): 701-715.

Igishi, T. and J. Gutkind (1998). "Tyrosine Kinases of the Src Family Participate in Signaling to MAP Kinase from both Gqand Gi-Coupled Receptors." Biochemical and Biophysical Research Communications **244**(1): 5-10.

Ikura, M., M. Osawa, *et al.* (2002). "The role of calcium-binding proteins in the control of transcription: structure to function." Bioessays **24**(7): 625-36.

Ingber, D. E. (1990). "Fibronectin controls capillary endothelial cell growth by modulating cell shape." Proc Natl Acad Sci U S A **87**(9): 3579-83.

Ireland, G., P. Dopping-Hepenstal, *et al.* (1987). "Effect of patterned surfaces of adhesive islands on the shape, cytoskeleton, adhesion and behaviour of Swiss mouse 3T3 fibroblasts." Journal of cell science. Supplement **8**: 19.

Irvine, R. F. (1990). "[`]Quanta' Ca^{2+} release and the control of Ca^{2+} entry by inositol phosphates - a

possible mechanism." FEBS Letters **263**(1): 5-9.

Jagannathan, S., S. Publicover, *et al.* (2002). "Voltage-operated calcium channels in male germ cells." Reproduction **123**(2): 203.

Ji, W., P. Xu, *et al.* (2008). "Functional stoichiometry of the unitary calcium-release-activated calcium channel." Proc Natl Acad Sci U S A **105**(36): 13668-73.

Kahl, C. R. and A. R. Means (2003). "Regulation of cell cycle progression by calcium/calmodulin-dependent pathways." Endocr Rev **24**(6): 719-36.

Karlsson-Rosenthal, C. and J. B. Millar (2006). "Cdc25: mechanisms of checkpoint inhibition and recovery." Trends Cell Biol **16**(6): 285-92.

Kawanabe, Y., K. Nozaki, *et al.* (2003). "Characterization of Ca^{2+} channels and G proteins involved in arachidonic acid release by endothelin-1/endothelinA receptor." Molecular pharmacology **64**(3): 689.

Kawanabe, Y., Y. Okamoto, *et al.* (2001). "Ca^{2+} channels activated by endothelin-1 in CHO cells expressing endothelin-A or endothelin-B receptors." American Journal of Physiology- Cell Physiology **281**(5): C1676.

Kennerly, D., T. Sullivan, *et al.* (1979). "Diacylglycerol metabolism in mast cells: a potential role in membrane fusion and arachidonic acid release." Journal of Experimental Medicine **150**(4): 1039.

King, R. W., P. K. Jackson, *et al.* (1994). "Mitosis in transition." Cell **79**(4): 563-71.

Kudo, I. and M. Murakami (2002). "Phospholipase A2 enzymes." Prostaglandins & Other Lipid Mediators **68**: 3-58.

Lacinova, L. (2005). "Voltage-dependent calcium channels." Gen Physiol Biophys **24 Suppl 1**: 1-78.

Lambeau, G. and M. Gelb (2008). "Biochemistry and physiology of mammalian secreted phospholipases A2."

Laude, A. and A. Simpson (2009). "Compartmentalized signalling: Ca^{2+} compartments, microdomains and the many facets of Ca^{2+} signalling." FEBS Journal **276**(7): 1800-1816.

Lee, H. C. and R. Aarhus (2000). "Functional visualization of the separate but interacting calcium stores sensitive to NAADP and cyclic ADP-ribose." J Cell Sci **113 Pt 24**: 4413-20.

Lee, S. and S. Rhee (1995). "Significance of PIP2 hydrolysis and regulation of phospholipase C isozymes." Current opinion in cell biology **7**(2): 183-189.

Lenormand, P., C. Sardet, *et al.* (1993). "Growth factors induce nuclear translocation of MAP kinases (p42mapk and p44mapk) but not of their activator MAP kinase kinase (p45mapkk) in fibroblasts." J Cell Biol **122**(5): 1079-88.

Leslie, C. (1997). "Properties and regulation of cytosolic phospholipase A2." Journal of Biological Chemistry **272**(27): 16709.

Lewis, R. and M. Cahalan (1989). "Mitogen-induced oscillations of cytosolic Ca^{2+} and transmembrane Ca^{2+} current in human leukemic T cells." Cell Regulation **1**(1): 99.

Liao, Y., N. W. Plummer, *et al.* (2009). "A role for Orai in TRPC-mediated Ca^{2+} entry suggests that a TRPC:Orai complex may mediate store and receptor operated Ca^{2+} entry." Proc Natl Acad Sci U S A **106**(9): 3202-6.

Lin, L.-L., M. Wartmann, *et al.* (1993). "cPLA2 is phosphorylated and activated by MAP kinase." Cell **72**(2): 269-278.

Lin, T., Q. Chen, *et al.* (1997). "Cell anchorage permits efficient signal transduction between ras and its downstream kinases." Journal of Biological Chemistry **272**(14): 8849.

Liou, J., M. Fivaz, *et al.* (2007). "Live-cell imaging reveals sequential oligomerization and local plasma membrane targeting of stromal interaction molecule 1 after Ca^{2+} store depletion." Proceedings of the National Academy of Sciences **104**(22): 9301.

Liou, J., M. Kim, *et al.* (2005). "STIM is a Ca2?sensor essential for Ca2?store-depletion-triggered Ca2?influx." Curr Biol **15**: 1235-1241.

Liou, J., M. L. Kim, *et al.* (2005). "STIM is a Ca^{2+} sensor essential for Ca^{2+}-store-depletion-triggered Ca^{2+} influx." Curr Biol **15**(13): 1235-41.

Lipskaia, L. and A. M. Lompre (2004). "Alteration in temporal kinetics of Ca^{2+} signaling and control of growth and proliferation." Biol Cell **96**(1): 55-68.

Lis, A., C. Peinelt, *et al.* (2007). "CRACM1, CRACM2, and CRACM3 are store-operated Ca^{2+} channels with distinct functional properties." Curr Biol **17**(9): 794-800.

Liu, X., B. Singh, *et al.* (2003). "TRPC1 is required for functional store-operated Ca^{2+} channels." Journal of Biological Chemistry **278**(13): 11337.

Liu, Y., E. Grapengiesser, *et al.* (1995). "Glucose induces oscillations of cytoplasmic Ca^{2+}, Sr^{2+} and Ba^{2+} in pancreatic [beta]-cells without participation of the thapsigargin-sensitive store." Cell Calcium **18**(2): 165-173.

Lu, L., M. Ladinsky, *et al.* (2009). "Cisternal organization of the endoplasmic reticulum during mitosis." Molecular Biology of the Cell **20**(15): 3471.

Madrid, L., M. Mayo, *et al.* (2001). "Akt stimulates the transactivation potential of the RelA/p65 subunit of NF- B through utilization of the I B kinase and activation of the mitogen-activated protein kinase p38." Journal of Biological Chemistry **276**(22): 18934.

Manji, S. S., N. J. Parker, *et al.* (2000). "STIM1: a novel phosphoprotein located at the cell surface." Biochim Biophys Acta **1481**(1): 147-55.

Martínez, J. and J. Moreno (2005). "Role of Ca^{2+}-independent phospholipase A2 and cytochrome P-450 in store-operated calcium entry in 3T6 fibroblasts." Biochemical Pharmacology **70**(5): 733-739.

Massague, J. (2004). "G1 cell-cycle control and cancer." Nature **432**(7015): 298-306.

McConnell, B., F. Gregory, *et al.* (1999). "Induced expression of p16INK4a inhibits both CDK4-and CDK2-associated kinase activity by reassortment of cyclin-CDK-inhibitor complexes." Molecular and cellular biology **19**(3): 1981.

McFadzean, I. and A. Gibson (2002). "The developing relationship between receptor-operated and store-operated calcium channels in smooth muscle." Br J Pharmacol **135**(1): 1-13.

Means, A. R. (1994). "Calcium, calmodulin and cell cycle regulation." FEBS Lett **347**(1): 1-4.

Mellström, B. and J. Naranjo (2001). "Mechanisms of Ca^{2+}-dependent transcription." Current Opinion in Neurobiology **11**(3): 312-319.

Merritt, J., W. Armstrong, *et al.* (1990). "SK&F 96365, a novel inhibitor of receptor-mediated calcium entry." Biochemical Journal **271**(2): 515.

Meves, H. (2008). "Arachidonic acid and ion channels: an update." Br J Pharmacol **155**(1): 4-16.

Mignen, O. and T. J. Shuttleworth (2000). "I(ARC), a novel arachidonate-regulated, noncapacitative Ca($^{2+}$) entry channel." J Biol Chem **275**(13): 9114-9.

Mignen, O., J. Thompson, *et al.* (2001). "Reciprocal regulation of capacitative and arachidonate-regulated noncapacitative Ca^{2+} entry pathways." Journal of Biological Chemistry **276**(38): 35676.

Mignen, O., J. Thompson, *et al.* (2003). "Ca^{2+} selectivity and fatty acid specificity of the noncapacitative,

arachidonate-regulated Ca^{2+} (ARC) channels." Journal of Biological Chemistry **278**(12): 10174.

Mignen, O., J. Thompson, *et al.* (2008). "Both Orai1 and Orai3 are essential components of the arachidonate-regulated Ca^{2+}-selective (ARC) channels." The Journal of Physiology **586**(1): 185.

Mignen, O., J. L. Thompson, *et al.* (2007). "STIM1 regulates Ca^{2+} entry via arachidonate-regulated Ca^{2+}-selective (ARC) channels without store depletion or translocation to the plasma membrane." J Physiol **579**(Pt 3): 703-15.

Mignen, O., J. L. Thompson, *et al.* (2008). "Both Orai1 and Orai3 are essential components of the arachidonate-regulated Ca^{2+}-selective (ARC) channels." J Physiol **586**(1): 185-95.

Missiaen, L., H. De Smedt, *et al.* (1994). "Kinetics of empty store-activated Ca^{2+} influx in HeLa cells." Journal of Biological Chemistry **269**(8): 5817.

Miwa, S., Y. Iwamuro, *et al.* (2000). "LOE 908: A Specific Blocker of Nonselective Cation Channel." Cardiovascular Drug Reviews **18**(1): 61-72.

Monastyrskaya, K., E. Babiychuk, *et al.* (2009). "Plasma membrane-associated annexin A6 reduces CA^{2+} entry by stabilizing the cortical actin cytoskeleton." Journal of Biological Chemistry **284**(25): 17227.

Moneer, Z. and C. Taylor (2002). "Reciprocal regulation of capacitative and non-capacitative Ca^{2+} entry in A7r5 vascular smooth muscle cells: only the latter operates during receptor activation." Biochemical Journal **362**(Pt 1): 13.

Monteith, G. R., Y. Wanigasekara, *et al.* (1998). "The plasma membrane calcium pump, its role and regulation: new complexities and possibilities." Journal of Pharmacological and Toxicological Methods **40**(4): 183-190.

Morgan, D. O. (1995). "Principles of CDK regulation." Nature **374**(6518): 131-4.

Morino, N., T. Mimura, *et al.* (1995). "Matrix/Integrin Interaction Activates the Mitogen-activated Protein Kinase, p44 and p42." Journal of Biological Chemistry **270**(1): 269.

Mosior, M., D. Six, *et al.* (1998). "Group IV cytosolic phospholipase A2 binds with high affinity and specificity to phosphatidylinositol 4, 5-bisphosphate resulting in dramatic increases in activity." Journal of Biological Chemistry **273**(4): 2184.

Muik, M., M. Fahrner, *et al.* (2009). "A Cytosolic Homomerization and a Modulatory Domain within STIM1 C Terminus Determine Coupling to ORAI1 Channels." J Biol Chem **284**(13): 8421-6.

Muik, M., I. Frischauf, *et al.* (2008). "Dynamic coupling of the putative coiled-coil domain of ORAI1 with STIM1 mediates ORAI1 channel activation." J Biol Chem **283**(12): 8014-22.

Munaron, L., S. Antoniotti, *et al.* (2004). "Intracellular calcium signals and control of cell proliferation: how many mechanisms?" J Cell Mol Med **8**(2): 161-8.

Murakami, M., T. Kambe, *et al.* (1999). "Functional association of type IIA secretory phospholipase A2 with the glycosylphosphatidylinositol-anchored heparan sulfate proteoglycan in the cyclooxygenase-2-mediated delayed prostanoid-biosynthetic pathway." Journal of Biological Chemistry **274**(42): 29927.

Murakami, M. and I. Kudo (2002). "Phospholipase A2." Journal of biochemistry **131**(3): 285.

Murray, A. W. (2004). "Recycling the cell cycle: cyclins revisited." Cell **116**(2): 221-34.

Musacchio, A. and K. Hardwick (2002). "The spindle checkpoint: structural insights into dynamic signalling." Nature Reviews Molecular Cell Biology **3**(10): 731-741.

Nachshen, D. and M. Blaustein (1982). "Influx of calcium, strontium, and barium in presynaptic nerve endings." Journal of General Physiology **79**(6): 1065.

Nakanishi, M. and D. Rosenberg (2006). "Roles of cPLA2 [alpha] and arachidonic acid in cancer."

Biochimica et Biophysica Acta (BBA)-Molecular and Cell Biology of Lipids **1761**(11): 1335-1343.

Neal, J. W. and N. A. Clipstone (2003). "A constitutively active NFATc1 mutant induces a transformed phenotype in 3T3-L1 fibroblasts." J Biol Chem **278**(19): 17246-54.

Niger, C., A. Malassine, *et al.* (2004). "Calcium channels activated by endothelin-1 in human trophoblast." The Journal of Physiology **561**(2): 449.

Nigg, E. A. (1995). "Cyclin-dependent protein kinases: key regulators of the eukaryotic cell cycle." Bioessays **17**(6): 471-80.

Norbury, C. and P. Nurse (1992). "Animal cell cycles and their control." Annu Rev Biochem **61**: 441-70.

Ohori, M., M. Takeuchi, *et al.* (2007). "FR180204, a novel and selective inhibitor of extracellular signal-regulated kinase, ameliorates collagen-induced arthritis in mice." Naunyn-Schmiedeberg's archives of pharmacology **374**(4): 311-316.

Ohtani, K., J. DeGregori, *et al.* (1995). "Regulation of the cyclin E gene by transcription factor E2F1." Proc Natl Acad Sci U S A **92**(26): 12146-50.

Ong, H. L., K. T. Cheng, *et al.* (2007). "Dynamic assembly of TRPC1-STIM1-Orai1 ternary complex is involved in store-operated calcium influx. Evidence for similarities in store-operated and calcium release-activated calcium channel components." J Biol Chem **282**(12): 9105-16.

Osterhout, J. and T. Shuttleworth (2000). "A Ca^{2+}-independent activation of a type IV cytosolic phospholipase A2 underlies the receptor stimulation of arachidonic acid-dependent noncapacitative calcium entry." Journal of Biological Chemistry **275**(11): 8248.

Otun, H., J. Gillespie, *et al.* (1992). "Transients in intracellular free calcium in subconfluent and confluent cultures of a rat smooth muscle cell line." Experimental Physiology **77**(5): 749.

Pages, G., P. Lenormand, *et al.* (1993). "Mitogen-activated protein kinases p42mapk and p44mapk are required for fibroblast proliferation." Proc Natl Acad Sci U S A **90**(18): 8319-23.

Pan, Z., S. Christiansen, *et al.* (1999). "Requirement of phosphatidylinositol 3-kinase activity for bradykinin stimulation of NF- B activation in cultured human epithelial cells." Journal of Biological Chemistry **274**(15): 9918.

Pang, L., S. Decker, *et al.* (1993). "Bombesin and epidermal growth factor stimulate the mitogen-activated protein kinase through different pathways in Swiss 3T3 cells." Biochemical Journal **289**(Pt 1): 283.

Parekh, A. B. and J. W. Putney, Jr. (2005). "Store-operated calcium channels." Physiol Rev **85**(2): 757-810.

Park, C. Y., P. J. Hoover, *et al.* (2009). "STIM1 clusters and activates CRAC channels via direct binding of a cytosolic domain to Orai1." Cell **136**(5): 876-90.

Parvez, S., A. Beck, *et al.* (2008). "STIM2 protein mediates distinct store-dependent and store-independent modes of CRAC channel activation." FASEB J **22**(3): 752-61.

Patterson, R., D. van Rossum, *et al.* (1999). "Store-Operated Ca^{2+} Entry:: Evidence for a Secretion-like Coupling Model." Cell **98**(4): 487-499.

Patterson, R., D. van Rossum, *et al.* (1999). "Store-Operated Ca Entry." Cell **98**(4): 487-499.

Peinelt, C., M. Vig, *et al.* (2006). "Amplification of CRAC current by STIM1 and CRACM1 (Orai1)." Nat Cell Biol **8**(7): 771-3.

Penna, A., A. Demuro, *et al.* (2008). "The CRAC channel consists of a tetramer formed by Stim-induced dimerization of Orai dimers." Nature **456**(7218): 116-20.

Pennington, S. R., B. J. Foster, *et al.* (2007). "Cell shape-dependent Control of Ca^{2+} influx and cell cycle

progression in Swiss 3T3 fibroblasts." J Biol Chem **282**(44): 32112-20.

Pinton, P., T. Pozzan, *et al.* (1998). "The Golgi apparatus is an inositol 1, 4, 5-trisphosphate-sensitive Ca^{2+} store, with functional properties distinct from those of the endoplasmic reticulum." The EMBO Journal **17**(18): 5298-5308.

Potier, M. and M. Trebak (2008). "New developments in the signaling mechanisms of the store-operated calcium entry pathway." Pflugers Arch **457**(2): 405-15.

Pozzan, T., R. Rizzuto, *et al.* (1994). "Molecular and cellular physiology of intracellular calcium stores." Physiol. Rev. **74**(3): 595-636.

Prakriya, M., S. Feske, *et al.* (2006). "Orai1 is an essential pore subunit of the CRAC channel." Nature **443**(7108): 230-3.

Putney, J. W., Jr. (1986). "A model for receptor-regulated calcium entry." Cell Calcium **7**(1): 1-12.

Putney, J. W., Jr. (2001). "Pharmacology of capacitative calcium entry." Mol Interv **1**(2): 84-94.

Putney, J. W., Jr., L. M. Broad, *et al.* (2001). "Mechanisms of capacitative calcium entry." J Cell Sci **114**(Pt 12): 2223-9.

Qiu, Z., M. Gijón, *et al.* (1998). "The role of calcium and phosphorylation of cytosolic phospholipase A2 in regulating arachidonic acid release in macrophages." Journal of Biological Chemistry **273**(14): 8203.

Qiu, Z. and C. Leslie (1994). "Protein kinase C-dependent and-independent pathways of mitogen-activated protein kinase activation in macrophages by stimuli that activate phospholipase A2." Journal of Biological Chemistry **269**(30): 19480.

Randriamampita, C. and R. Y. Tsien (1993). "Emptying of intracellular Ca^{2+} stores releases a novel small messenger that stimulates Ca^{2+} influx." Nature **364**(6440): 809-14.

Rasmussen, C. D. and A. R. Means (1987). "Calmodulin is involved in regulation of cell proliferation." EMBO J **6**(13): 3961-8.

Resnitzky, D. (1997). "Ectopic expression of cyclin D1 but not cyclin E induces anchorage-independent cell cycle progression." Molecular and cellular biology **17**(9): 5640.

Ribeiro, C., J. Reece, *et al.* (1997). "Role of the cytoskeleton in calcium signaling in NIH 3T3 cells." Journal of Biological Chemistry **272**(42): 26555.

Ribeiro, C. M., J. Reece, *et al.* (1997). "Role of the cytoskeleton in calcium signaling in NIH 3T3 cells. An intact cytoskeleton is required for agonist-induced $[Ca^{2+}]i$ signaling, but not for capacitative calcium entry." J Biol Chem **272**(42): 26555-61.

Riendeau, D., J. Guay, *et al.* (1994). "Arachidonyl trifluoromethyl ketone, a potent inhibitor of 85-kDa phospholipase A2, blocks production of arachidonate and 12-hydroxyeicosatetraenoic acid by calcium ionophore-challenged platelets." Journal of Biological Chemistry **269**(22): 15619.

Rizzuto, R. and T. Pozzan (2006). "Microdomains of intracellular Ca^{2+}: molecular determinants and functional consequences." Physiological reviews **86**(1): 369.

Roos, J., P. J. DiGregorio, *et al.* (2005). "STIM1, an essential and conserved component of store-operated Ca^{2+} channel function." J Cell Biol **169**(3): 435-45.

Rossi, D. and V. Sorrentino (2002). "Molecular genetics of ryanodine receptors Ca^{2+}-release channels." Cell Calcium **32**(5-6): 307-19.

Rozengurt, E. (2007). "Mitogenic signaling pathways induced by G protein coupled receptors." Journal of cellular physiology **213**(3): 589-602.

Rozengurt, E. and J. Sinnett-Smith (1983). "Bombesin stimulation of DNA synthesis and cell division in cultures of Swiss 3T3 cells." Proceedings of the National Academy of Sciences of the United

States of America **80**(10): 2936.

Rozengurt, E. and J. Sinnett Smith (1987). "Bombesin induction of c fos and c myc proto oncogenes in Swiss 3T3 cells: Significance for the mitogenic response." Journal of cellular physiology **131**(2): 218-225.

Ruoslahti, E. (1991). "Integrins." J Clin Invest **87**(1): 1-5.

Sage, S., J. Merritt, *et al.* (1989). "Receptor-mediated calcium entry in fura-2-loaded human platelets stimulated with ADP and thrombin. Dual-wavelengths studies with Mn^{2+}." Biochemical Journal **258**(3): 923.

Salido, G. M., S. O. Sage, *et al.* (2009). "TRPC channels and store-operated $Ca(^{2+})$ entry." Biochim Biophys Acta **1793**(2): 223-30.

Santella, L., E. Ercolano, *et al.* (2005). "The cell cycle: a new entry in the field of Ca^{2+} signaling." Cell Mol Life Sci **62**(21): 2405-13.

Santiskulvong, C., J. Sinnett-Smith, *et al.* (2001). "EGF receptor function is required in late G1 for cell cycle progression induced by bombesin and bradykinin." American Journal of Physiology- Cell Physiology **281**(3): C886.

Schaloske, R. and E. Dennis (2006). "The phospholipase A2 superfamily and its group numbering system." Biochimica et Biophysica Acta (BBA)-Molecular and Cell Biology of Lipids **1761**(11): 1246-1259.

Schievella, A., M. Regier, *et al.* (1995). "Calcium-mediated Translocation of Cytosolic Phospholipase A to the Nuclear Envelope and Endoplasmic Reticulum." Journal of Biological Chemistry **270**(51): 30749.

Schwartz, M. A. and D. E. Ingber (1994). "Integrating with integrins." Mol Biol Cell **5**(4): 389-93.

See, V., N. K. Rajala, *et al.* (2004). "Calcium-dependent regulation of the cell cycle via a novel MAPK--NF-kappaB pathway in Swiss 3T3 cells." J Cell Biol **166**(5): 661-72.

Sherr, C. J. (1994). "G1 phase progression: cycling on cue." Cell **79**(4): 551-5.

Sherr, C. J. and J. M. Roberts (1995). "Inhibitors of mammalian G1 cyclin-dependent kinases." Genes Dev **9**(10): 1149-63.

Sherr, C. J. and J. M. Roberts (1999). "CDK inhibitors: positive and negative regulators of G1-phase progression." Genes Dev **13**(12): 1501-12.

Shimizu, M., H. Nakamura, *et al.* (2008). "Ser515 phosphorylation-independent regulation of cytosolic phospholipase A2 [alpha](cPLA2 [alpha]) by calmodulin-dependent protein kinase: Possible interaction with catalytic domain A of cPLA2 [alpha]." Cellular signalling **20**(5): 815-824.

Shirakawa, F. and S. Mizel (1989). "In vitro activation and nuclear translocation of NF-kappa B catalyzed by cyclic AMP-dependent protein kinase and protein kinase C." Molecular and cellular biology **9**(6): 2424.

Shuttleworth, T. J. (1996). "Arachidonic acid activates the noncapacitative entry of Ca^{2+} during $[Ca^{2+}]i$ oscillations." J Biol Chem **271**(36): 21720-5.

Shuttleworth, T. J. (2009). "Arachidonic acid, ARC channels, and Orai proteins." Cell Calcium.

Shuttleworth, T. J. and J. L. Thompson (1996). "Evidence for a non-capacitative Ca^{2+} entry during $[Ca^{2+}]$ oscillations." Biochem J **316 (Pt 3)**: 819-24.

Shuttleworth, T. J., J. L. Thompson, *et al.* (2007). "STIM1 and the noncapacitative ARC channels." Cell Calcium **42**(2): 183-91.

Sigal, E. (1991). "The molecular biology of mammalian arachidonic acid metabolism." American Journal of Physiology- Lung Cellular and Molecular Physiology **260**(2): 13.

Siliciano, J. D., C. E. Canman, *et al.* (1997). "DNA damage induces phosphorylation of the amino terminus of p53." Genes Dev **11**(24): 3471-81.

Simpson, A., A. Stampfl, *et al.* (1990). "Evidence for receptor-mediated bivalent-cation entry in A10 vascular smooth-muscle cells." Biochemical Journal **267**(1): 277.

Simpson, P., R. Challiss, *et al.* (1995). "Divalent cation entry in cultured rat cerebellar granule cells measured using Mn^{2+} quench of fura 2 fluorescence." European Journal of Neuroscience **7**(5): 831-840.

Singaravelu, K., C. Lohr, *et al.* (2006). "Regulation of store-operated calcium entry by calcium-independent phospholipase A2 in rat cerebellar astrocytes." Journal of Neuroscience **26**(37): 9579.

Singaravelu, K., C. Lohr, *et al.* (2008). "Calcium-independent phospholipase A 2 mediates store-operated calcium entry in rat cerebellar granule cells." The Cerebellum **7**(3): 467-481.

Smani, T., S. Zakharov, *et al.* (2003). "Ca^{2+}-independent phospholipase A2 is a novel determinant of store-operated Ca^{2+} entry." Journal of Biological Chemistry **278**(14): 11909.

Smani, T., S. I. Zakharov, *et al.* (2003). "Ca^{2+}-independent Phospholipase A2 Is a Novel Determinant of Store-operated Ca^{2+} Entry." J. Biol. Chem. **278**(14): 11909-11915.

Smrcka, A., J. Hepler, *et al.* (1991). "Regulation of polyphosphoinositide-specific phospholipase C activity by purified Gq." Science **251**(4995): 804.

Smyth, J., W. DeHaven, *et al.* (2007). "Role of the microtubule cytoskeleton in the function of the store-operated Ca^{2+} channel activator STIM1." Journal of cell science **120**(21): 3762.

Smyth, J., W. DeHaven, *et al.* (2007). "Role of the microtubule cytoskeleton in the function of the store-operated Ca^{2+} channel activator, Stim1." Journal of cell science **120**(Pt 21): 3762.

Smyth, J. T., W. I. DeHaven, *et al.* (2007). "Role of the microtubule cytoskeleton in the function of the store-operated Ca^{2+} channel activator STIM1." J Cell Sci **120**(Pt 21): 3762-71.

Smyth, J. T., W. I. Dehaven, *et al.* (2006). "Emerging perspectives in store-operated Ca^{2+} entry: roles of Orai, Stim and TRP." Biochim Biophys Acta **1763**(11): 1147-60.

Srikanth, S., H. Jung, *et al.* (2010). "A novel EF-hand protein, CRACR2A, is a cytosolic Ca^{2+} sensor that stabilizes CRAC channels in T cells." Nature Cell Biology **12**(5): 436-446.

Stevaux, O. and N. J. Dyson (2002). "A revised picture of the E2F transcriptional network and RB function." Curr Opin Cell Biol **14**(6): 684-91.

Stewart, Z., M. Westfall, *et al.* (2003). "Cell-cycle dysregulation and anticancer therapy." Trends in pharmacological sciences **24**(3): 139-145.

Streb, H., R. F. Irvine, *et al.* (1983). "Release of Ca^{2+} from a nonmitochondrial intracellular store in pancreatic acinar cells by inositol-1,4,5-trisphosphate." Nature **306**(5938): 67-69.

Sugawara, H., M. Kurosaki, *et al.* (1997). "Genetic evidence for involvement of type 1, type 2 and type 3 inositol 1,4,5-trisphosphate receptors in signal transduction through the B-cell antigen receptor." EMBO J **16**(11): 3078-88.

Sutherland, C. and D. Amin (1982). "Relative activities of rat and dog platelet phospholipase A2 and diglyceride lipase. Selective inhibition of diglyceride lipase by RHC 80267." Journal of Biological Chemistry **257**(23): 14006.

Takahashi, A., S. Tanaka, *et al.* (2000). "Involvement of calmodulin and protein kinase C in cholecystokinin release by bombesin from STC-1 cells." Pancreas **21**(3): 231.

Takemura, H., A. R. Hughes, *et al.* (1989). "Activation of calcium entry by the tumor promoter thapsigargin in parotid acinar cells. Evidence that an intracellular calcium pool and not an

inositol phosphate regulates calcium fluxes at the plasma membrane." J Biol Chem **264**(21): 12266-71.

Takuwa, N., W. Zhou, *et al.* (1995). "Involvement of intact inositol-1,4,5-trisphosphate-sensitive Ca^{2+} stores in cell cycle progression at the G1/S boundary in serum-stimulated human fibroblasts." FEBS Lett **360**(2): 173-6.

Takuwa, N., W. Zhou, *et al.* (1995). "Calcium, calmodulin and cell cycle progression." Cell Signal **7**(2): 93-104.

Taylor, C. and A. Laude (2002). "IP3 receptors and their regulation by calmodulin and cytosolic Ca^{2+}." Cell Calcium **32**(5-6): 321-334.

Taylor, C. W., D. L. Prole, *et al.* (2009). "Ca($^{2+}$) channels on the move." Biochemistry **48**(51): 12062-80.

Terasaki, M., L. Chen, *et al.* (1986). "Microtubules and the endoplasmic reticulum are highly interdependent structures." Journal of Cell Biology **103**(4): 1557.

Thastrup, O., P. Cullen, *et al.* (1990). "Thapsigargin, a tumor promoter, discharges intracellular Ca^{2+} stores by specific inhibition of the endoplasmic reticulum Ca2 (+)-ATPase." Proceedings of the National Academy of Sciences of the United States of America **87**(7): 2466.

Thullberg, M., J. Bartkova, *et al.* (2000). "Distinct versus redundant properties among members of the INK4 family of cyclin-dependent kinase inhibitors." FEBS Letters **470**(2): 161-166.

Treinys, R. and J. Jurevicius (2008). "L-type Ca^{2+} channels in the heart: structure and regulation." Medicina (Kaunas) **44**(7): 491-9.

Trimble, L., I. Street, *et al.* (1993). "NMR structural studies of the tight complex between a trifluoromethyl ketone inhibitor and the 85-kDa human phospholipase A2." Biochemistry **32**(47): 12560.

Tsien, R. W. and R. Y. Tsien (1990). "Calcium channels, stores, and oscillations." Annu Rev Cell Biol **6**: 715-60.

Tucker, D., M. Ghosh, *et al.* (2009). "Role of phosphorylation and basic residues in the catalytic domain of cytosolic phospholipase A2 in regulating interfacial kinetics and binding and cellular function." Journal of Biological Chemistry **284**(14): 9596.

Ueno, N., M. Murakami, *et al.* (2000). "Functional crosstalk between phospholipase D2 and signaling phospholipase A2/cyclooxygenase-2-mediated prostaglandin biosynthetic pathways." FEBS Letters **475**(3): 242-246.

Venkatachalam, K. and C. Montell (2007). "TRP channels." Annu Rev Biochem **76**: 387-417.

Vermeulen, K., D. R. Van Bockstaele, *et al.* (2003). "The cell cycle: a review of regulation, deregulation and therapeutic targets in cancer." Cell Prolif **36**(3): 131-49.

Vig, M., C. Peinelt, *et al.* (2006). "CRACM1 is a plasma membrane protein essential for store-operated Ca^{2+} entry." Science **312**(5777): 1220.

Wang, J., S. Kalyanaraman, *et al.* (1996). "Bombesin and thrombin affect discrete pools of intracellular calcium through different G-proteins." Biochemical Journal **320**(Pt 1): 87.

Watanabe-Tomita, Y., A. Suzuki, *et al.* (1997). "Arachidonic acid release induced by extracellular ATP in osteoblasts: role of phospholipase D." Prostaglandins, Leukotrienes and Essential Fatty Acids **57**(3): 335-339.

Watanabe, H., J. Vriens, *et al.* (2003). "Anandamide and arachidonic acid use epoxyeicosatrienoic acids to activate TRPV4 channels." Nature **424**(6947): 434-438.

Watt, F., P. Jordan, *et al.* (1988). "Cell shape controls terminal differentiation of human epidermal keratinocytes." Proceedings of the National Academy of Sciences of the United States of

America **85**(15): 5576.

Webb, S. E. and A. L. Miller (2003). "Calcium signalling during embryonic development." Nat Rev Mol Cell Biol **4**(7): 539-551.

Wheeler, L. W., N. H. Lents, *et al.* (2008). "Cyclin A-CDK activity during G1 phase impairs MCM chromatin loading and inhibits DNA synthesis in mammalian cells." Cell Cycle **7**(14): 2179-88.

Whitaker, M. and M. G. Larman (2001). "Calcium and mitosis." Semin Cell Dev Biol **12**(1): 53-8.

Withers, D., S. Bloom, *et al.* (1995). "Dissociation of cAMP-stimulated mitogenesis from activation of the mitogen-activated protein kinase cascade in Swiss 3T3 cells." Journal of Biological Chemistry **270**(36): 21411.

Woolfson, D. N. (2005). "The design of coiled-coil structures and assemblies." Adv Protein Chem **70**: 79-112.

Wu, M. M., J. Buchanan, *et al.* (2006). "Ca^{2+} store depletion causes STIM1 to accumulate in ER regions closely associated with the plasma membrane." J Cell Biol **174**(6): 803-13.

Xu, P., J. Lu, *et al.* (2006). "Aggregation of STIM1 underneath the plasma membrane induces clustering of Orai1." Biochem Biophys Res Commun **350**(4): 969-76.

Yamasaki, M., G. C. Churchill, *et al.* (2005). "Calcium signalling by nicotinic acid adenine dinucleotide phosphate (NAADP)." FEBS Journal **272**(18): 4598-4606.

Yeromin, A. V., S. L. Zhang, *et al.* (2006). "Molecular identification of the CRAC channel by altered ion selectivity in a mutant of Orai." Nature **443**(7108): 226-9.

Yoshida, M., M. Ishikawa, *et al.* (2003). "Store-operated calcium channel regulates the chemotactic behavior of ascidian sperm." Proceedings of the National Academy of Sciences of the United States of America **100**(1): 149.

Yuan, J. P., W. Zeng, *et al.* (2009). "SOAR and the polybasic STIM1 domains gate and regulate Orai channels." Nat Cell Biol **11**(3): 337-43.

Yuan, J. P., W. Zeng, *et al.* (2007). "STIM1 heteromultimerizes TRPC channels to determine their function as store-operated channels." Nat Cell Biol **9**(6): 636-45.

Zeng, W., J. P. Yuan, *et al.* (2008). "STIM1 gates TRPC channels, but not Orai1, by electrostatic interaction." Mol Cell **32**(3): 439-48.

Zhang, S., A. Yeromin, *et al.* (2006). "Genome-wide RNAi screen of Ca^{2+} influx identifies genes that regulate Ca^{2+} release-activated Ca^{2+} channel activity." Proceedings of the National Academy of Sciences **103**(24): 9357.

Zhang, S. L., J. A. Kozak, *et al.* (2008). "Store-dependent and -independent modes regulating Ca^{2+} release-activated Ca^{2+} channel activity of human Orai1 and Orai3." J Biol Chem **283**(25): 17662-71.

Zhang, S. L., Y. Yu, *et al.* (2005). "STIM1 is a Ca^{2+} sensor that activates CRAC channels and migrates from the Ca^{2+} store to the plasma membrane." Nature **437**(7060): 902-5.

Zhao, X., E. Bey, *et al.* (2002). "Cytosolic phospholipase A2 (cPLA2) regulation of human monocyte NADPH oxidase activity. cPLA2 affects translocation but not phosphorylation of p67phox and p47phox." Journal of Biological Chemistry **277**(28): 25385.

Zhu, X. and R. K. Assoian (1995). "Integrin-dependent activation of MAP kinase: a link to shape-dependent cell proliferation." Mol Biol Cell **6**(3): 273-82.

Zhu, X., M. Jiang, *et al.* (1998). "Receptor-activated Ca^{2+} influx via human Trp3 stably expressed in human embryonic kidney (HEK) 293 cells." Journal of Biological Chemistry **273**(1): 133.

Zhu, X., M. Ohtsubo, *et al.* (1996). "Adhesion-dependent cell cycle progression linked to the

expression of cyclin D1, activation of cyclin E-cdk2, and phosphorylation of the retinoblastoma protein." J Cell Biol **133**(2): 391-403.

Zucchi, R. and S. Ronca-Testoni (1997). "The sarcoplasmic reticulum Ca^{2+} channel/ryanodine receptor: modulation by endogenous effectors, drugs and disease states." Pharmacological reviews **49**(1): 1.

Appendix 1

Plasmid preparation

1.1 Transformation of Bacteria E.coli with the Plasmid

To transform E.coli with the GFP-cPLA$_2$ plasmid, 3μl plasmid was mixed with 50μl E.coli, incubated on ice for 5 minutes, heated at 42℃ for 40 seconds and then incubated on ice for another 2 minutes. The transformation mixture was then added with 300μl SOC medium (provided with the kit) and shaked for 1 hour at 37℃. The mixture was plated onto LB agar containing 100mg/L kanamycin. The transformation mixture was allowed to absorb into LB agar on room temperature for 20 minutes before incubated at 37℃ overnight. The colonies containing plasmid DNA were subsequently seen after 1 night growing.

1.2 Preparation of Plasmid DNA

Six colonies of bacteria that contained plasmid DNA were picked by sterile techniques and grown in 6 tubes with 6ml LB medium containing 0.25% kanamycin at 37℃ with shaking system overnight under sterile conditions. The bacteria were then pelleted by centrifuged at 4000xg for 10min. Subsequently, the bacteria were kept in a -20℃ freezer before used.

The GFP-cPLA$_2$ plasmid was isolated from bacteria following the QIAgen minipreparation protocol. The bacteria were thoroughly re-suspended with 250μl Buffer P1 containing RNase by pipetting. Then 250μl Buffer P2 was added and gently mixed by inversion of the tube 4-6 times. Subsequently, 350μl Buffer N3 was added and gently mixed by inversion of the tube 4-6 times and then pelleted by centrifuged at 3000xg for 10 minutes. The supernatant containing plasmid DNA was transferred to QIAprep spin column sitting in a clean collecting tube, then centrifuged at 3000xg for 1 minute. The pin column, which contained plasmid DNA, was then added with 750μl Buffer PE and centrifuged twice at 3000xg. Finally, place the QIAprep column in a clean 1.5 ml microcentrifuge tube. To elute DNA, add 50μl Buffer EB to the center of each QIAprep spin column, let stand for 1 minute, and centrifuge at 6000xg for 1 minute to elute plasmid DNA containing cPLA$_2$.

Appendix 2

The effect of restricting cell spreading on microtubule distribution

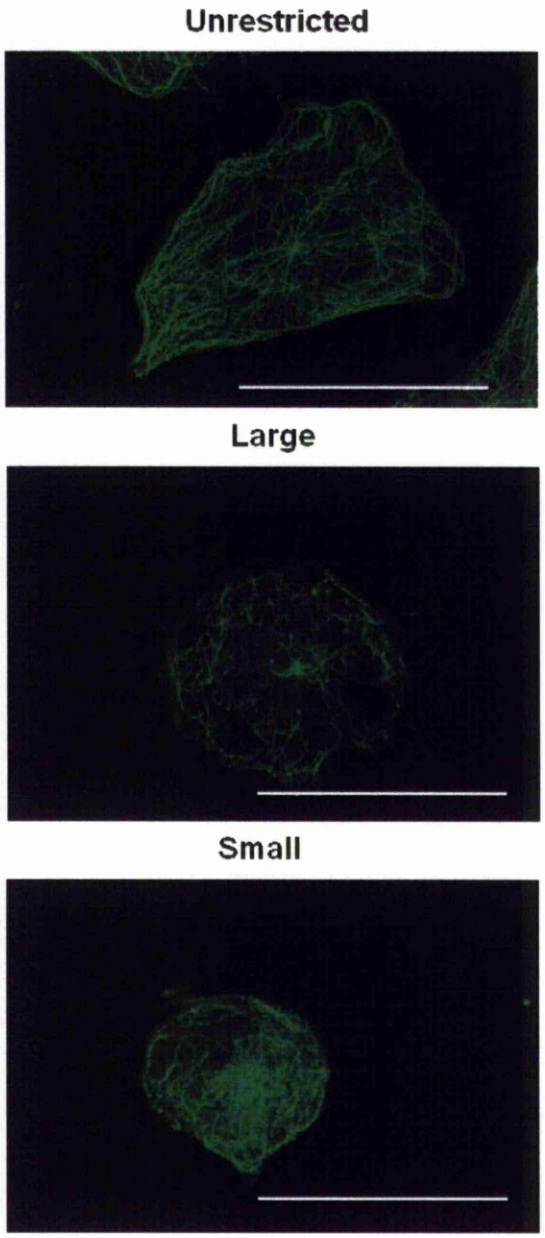

Figure appendix 2- The effect of restricting cell spreading on microtubule distribution

5-dya-old quiescent Swiss 3T3 cells were maintained either unrestricted on glass or restricted on palladium islands in SF-DMEM then stained using primary anti-tubulin and secondary FITC antibodies. Images were visualized using a Leica SP2 AOBS laser scanning confocal microscope. Scale bars represent 50μm (Foster, 2005).